Synthesis and Coordination Chemistry of Multidentate Phosphine Ligands

Mark Peter Driver

A thesis submitted to Cardiff University in candidature for the degree of

Doctor of Philosophy

Department of Chemistry, Cardiff University

September 2016

Declaration

This work has not been submitted in substance for any other degree or award at this or any other university or place of learning, nor is being submitted concurrently in candidature for any degree or other award.

Signed ……(candidate) Date ……

STATEMENT 1

This thesis is being submitted in partial fulfillment of the requirements for the degree of PhD

Signed ……(candidate) Date ……

STATEMENT 2

This thesis is the result of my own independent work/investigation, except where otherwise stated, and the thesis has not been edited by a third party beyond what is permitted by Cardiff University's Policy on the Use of Third Party Editors by Research Degree Students. Other sources are acknowledged by explicit references. The views expressed are my own.

Signed ……(candidate) Date ……

STATEMENT 3

I hereby give consent for my thesis, if accepted, to be available online in the University's Open Access repository and for inter-library loan, and for the title and summary to be made available to outside organisations.

Signed ……(candidate) Date ……

STATEMENT 4: PREVIOUSLY APPROVED BAR ON ACCESS

I hereby give consent for my thesis, if accepted, to be available online in the University's Open Access repository and for inter-library loans **after expiry of a bar on access previously approved by the Academic Standards & Quality Committee.**

Signed ……(candidate) Date ……

Abstract

The work presented herein is concerned with the design, synthesis and characterisation of novel phosphorus containing ligands and the metal complexes thereof. Chapter 1 will provide an introduction to the field and present an overview of recent developments in the literature.

Chapter 2 deals with the development of a synthetic route towards triphosphine macrocycles. The synthesis of *bis*(2-(phosphino)ethyl)phosphines is presented and their coordination chemistry with first row transition metals (Cr, Fe, Ni, Cu) is described. The ability of these complexes to act as templates in the formation of macrocyclic ligands is assessed.

Chapter 3 explores the synthesis of novel chiral multidentate phosphine ligands derived from glycidyl phosphine synthons. The reaction of diphenylglycidyl phosphine with P, N and S based nucleophiles results in the rapid construction of chiral heterodonor ligand frameworks. Preliminary studies of the reactivity of these ligands with metal centres will be presented.

Chapter 4 investigates the synthesis of chiral-at-aluminium complexes based upon a novel γ-amino-β-hydroxyphosphine oxide ligand. Two discreet aluminium alkyl complexes were identified and the interconversion of these species was studied by spectroscopic and computational means.

Chapter 5 concerns the coordination chemistry of bicyclic multidentate ER-NHCs with Pd(0), Pt(0) and Au(I) metal centres. The M(0) complexes display an unexpected proclivity towards the κ^1-*C* coordination mode. This further informs the discussion of the factors controlling the variable coordination chemistry of such ligands in the design of novel catalytic systems.

Acknowledgments

I am very grateful to my supervisors Professor Peter G. Edwards for giving me this opportunity and to Dr Ian Fallis for your continued advice and guidance. Thanks must also be given to Dr Paul Newman; your support and friendship have been invaluable to me, I would never have achieved this without your help. I give thanks also to Dr Ben Ward for your advice and assistance with DFT calculations.

My gratitudes are also due to all of the professional services staff at Cardiff University; especially Dr Rob Jenkins, Robin Hicks, Simon Waller, Tom Williams, Jamie Cross, Simon James and Gaz Coleman. This work would not have been possible without your hard work, dedication and professionalism.

To all the members of the Edwards group, particularly Mauro, Brendan, Lenali and Tom, Thank you for everything. I'd also like to mention the students who have helped immensely in the production of this work, Axel, Owain and Jamie.

On a personal note, I am eternally indebted to my family for their unfailing support throughout everything I do. You give me the strength and encouragement to achieve my dreams. I have been lucky enough to make many wonderful friends (and one "powerful enemy") during my time in Cardiff. My best memories and experiences of the last few years are of times spent with you. I can't thank you all enough for your support and friendship.

To everyone else who has contributed in so many ways, thank you.

Contents

List of Abbreviations

[9]aneP$_3$	1,4,7-triphosphacyclononane
[12]aneP$_3$	1,5,9-triphosphacyclododecane
[15]aneP$_3$	1,6,11-triphosphacyclopentadecane
18-crown-6	1,4,7,10,13,16-hexaoxacyclooctadecane
ABCN	1,1'-Azobis(cyclohexanecarbonitrile)
B3LYP	An exchange-correlation functional
BINAP	2,2'-Bis(diphenylphosphino)-1,1'-binaphthyl
BISBI	2,2'-bis((diphenylphosphanyl)methyl)-1,1'-biphenyl
Bn	Benzyl
Boc	tertbutyloxycarbonyl
bpy	Bipyridine
cod	Cyclooctadiene
Cp	cyclopentadienylide
Cy	Cyclohexyl
cyclam	1,4,8,11-tetraazacyclotetradecane
cyclen	1,4,7,10-tetrazacyclododecane
d	Doublet
dba	dibenzylideneacetone
DCM	dichloromethane
DFT	Density functional theory
Dimsyl	methylsulfinylmethylide
DIOP	*O*-isopropylidene-2,3-dihydroxy-1,4-bis(diphenylphosphino)butane
dipp	2,6-Di(isopropyl)phenyl
DMSO	Dimethyl sulfoxide
dppe	1,2-(diphenylphosphino)ethane
dppp	1,3-(diphenylphosphino)propane
dvtmds	Divinyltetramethyldisiloxane
EDTA	Ethylenediamine tetraacetic acid
ee	Enantiomeric excess
en	ethylene diamine
ER-NHC	Expanded ring N-Heterocyclic carbene
Et	Ethyl
HOMO	highest occupied molecular orbital
^{i}Bu	Iso-butyl
^{i}Pr	Iso-propyl
IR	Infrared
KHMDS	Potassium hexamethyldisilazide
KO^{t}Bu	Potassium tert-butoxide
LDA	Lithium diisopropylamide
L-DOPA	L-3,4-dihydroxyphenylalanine
LUMO	lowest unoccupied molecular orbital
Lys	Lysine
m	Multiplet
MALDI	Matrix assisted laser desorption ionisation

MAO	Methylaluminium oxide
Me	Methyl
MeCN	Acetonitrile
mes	Mesityl
^{n}Bu	n-butyl
NHC	N-Heterocyclic carbene
NMR	Nuclear magnetic resonance
Nu	Nucleophile
ORTEP	Oak Ridge Thermal Ellipsoid Plot Program
OTf	Triflate
***o*-tol**	Ortho-tolyl
PEPPSI	pyridine-enhanced precatalyst preparation stabilization and initiation
Ph	Phenyl
Phe	Phenylalanine
Pr	Propyl
q	Quartet
R,R-DIPAMP	*R,R*-ethane-1,2-diylbis[(2-methoxyphenyl)phenylphosphane]
***R,R*-Tsdpen**	*N*-[(1*S*,2*S*)-2-(amino)-1,2-diphenylethyl]-4-tosylamidate
RCM	Ring-closing metathesis
ROMP	Ring-opening metathesis polymerisation
s	Singlet
Ser	Serine
t	Triplet
TACN	Triazacyclononane
^{t}Bu	Tert-butyl
THF	Tetrahydrofuran
tht	tetrahydrothiophene
TMS	Trimethylsilyl
UFF	Universal force field
UV	Ultraviolet
Val	Valine
VSEPR	Valence shell electron pair repulsion
Xantphos	4,5-bis(diphenylphosphino)-9,9-dimethylxanthene
β_n	Natural bite angle
δ	Chemical shift

Chapter 1

Introduction

Phosphorus(III) ligands: An overview

Phosphines and other trivalent phosphorus compounds (Figure 1) are amongst the most widespread and effective ancillary ligands for transition metal coordination chemistry. Complexes of P(III) ligands have been found with all transition metals as well as many main group and f-block metals.[1] Complexes of the late transition metals are particularly favourable and such complexes have long been fundamental to the development of new homogeneous catalysts.[2]

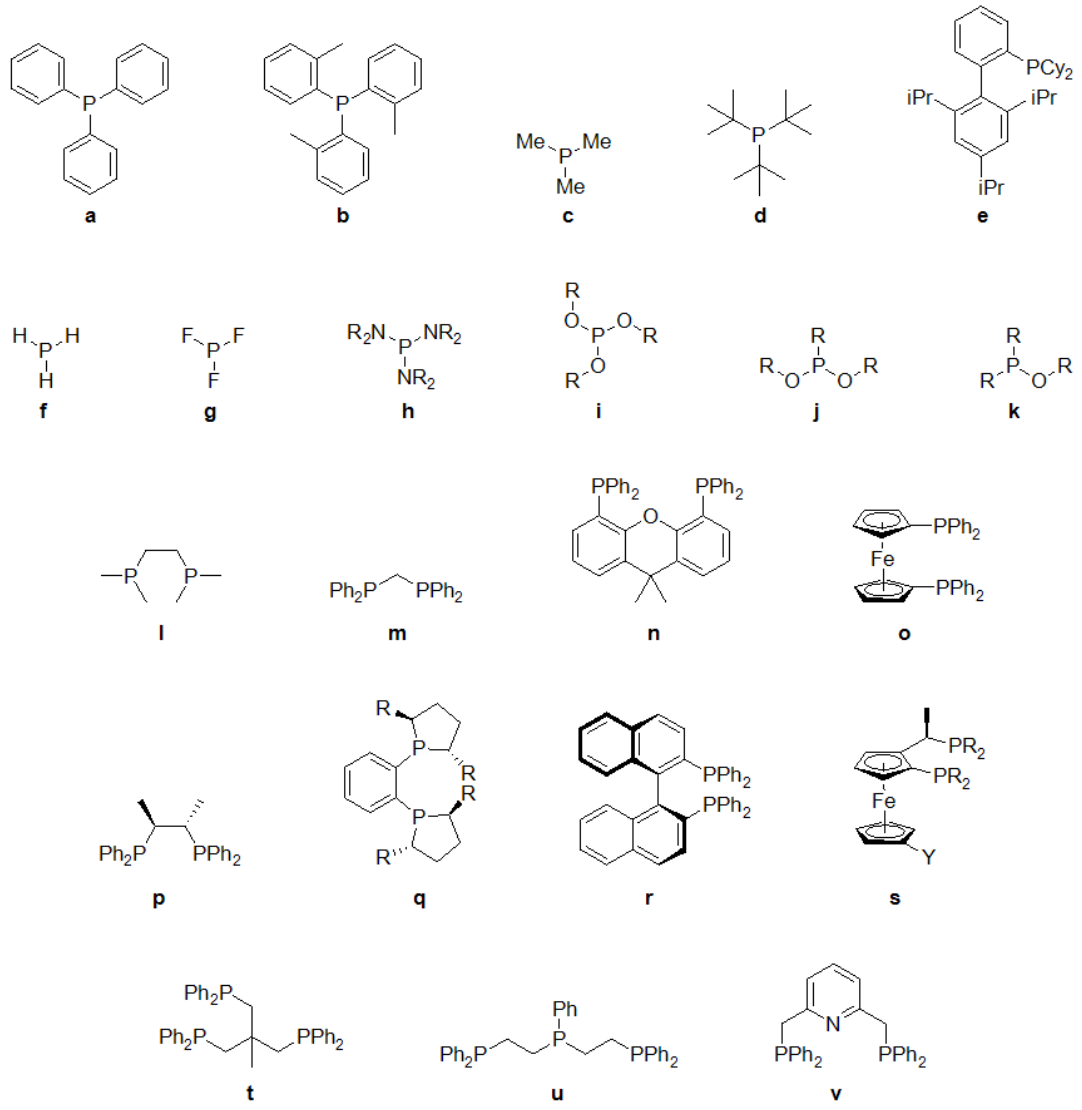

Figure 1: Selected examples of tertiary phosphines (a-e), other monodentate P(III) donors (f-k), diphosphines (l-o), chiral phosphines (p-s) and tridentate ligands (t-v)

The chemistry of phosphines was pioneered by the work of Mann and Chatt in the first half of the 20th century.[3] Since then, the design and synthesis of new P donor ligands has developed at great pace and phosphorous containing compounds remain widely sought after due to their continued used in many synthetically and commercially important catalytic systems. One particular example is given by Monsanto's synthesis of L-DOPA (a drug used in the treatment of Parkinsons syndrome), which uses a Rh complex bearing a chiral phosphine in the key asymmetric hydrogenation step (Scheme 1).[4,5] Synthetic routes to new phosphine synthons are therefore of inherent interest to organometallic and coordination chemists.

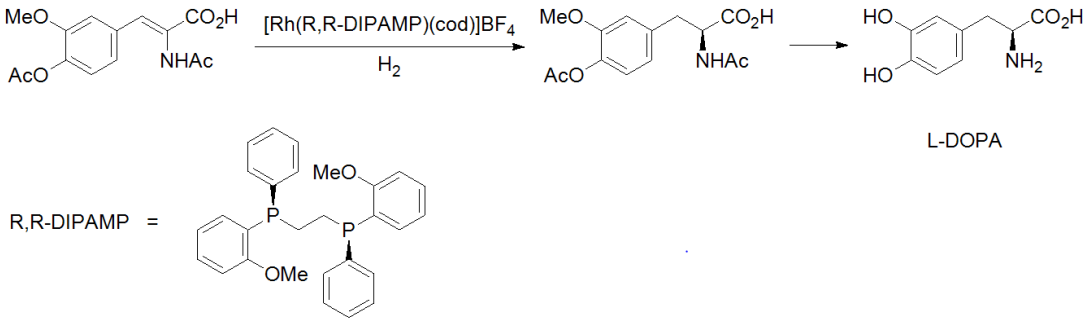

Scheme 1: The industrial synthesis of L-DOPA[4,5]

Properties of phosphines

Chemical properties

Most phosphines are colourless, often pyrophoric, distillable oils with unpleasant alliaceous odours. Furthermore, phosphorus, as with the other heavier pnictogens, differs from nitrogen in that the P(V) oxidation state is readily accessible. For this reason, phosphines are often prone to oxidation in air and must be manipulated under an inert atmosphere.[1] However, phosphoryl compounds have been proven to be effective ligands, particularly for early transition metals and other hard metal ions.[6,7,8,9,10]

Phosphines have also proven to be good Brønsted bases with pK_a values similar to those of analogous amines.[11] However, the increased size of phosphorus compared to nitrogen results in phosphines being much softer bases than amines and thus exhibit a much higher

affinity for comparatively soft metal ions.[1] As ligands they display strong bonding to most transition metals and exhibit a strong *trans*- effect which makes them ideal spectator ligands in homogeneous catalysis.

Electronic properties

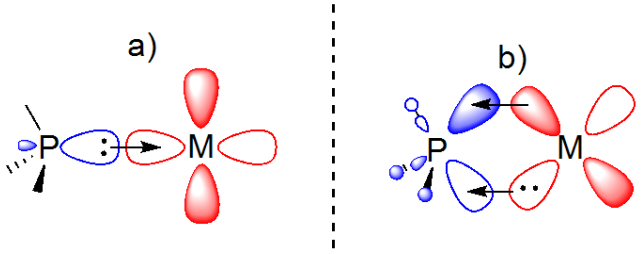

Figure 2: Orbital interactions and bonding of PR_3 donors with d-block metals. a) σ bonding, b) π backbonding

P(III) ligands are good σ-donors by virtue of the lone pair of electrons in the sp^3 hybridised orbital (Figure 2, a). The nature of the substituents has a dramatic effect on the σ- basicity of phosphines, where electron withdrawing substituents decrease the availability of the lone pair with a concomitant decrease in donor ability. Thus, an approximate basicity scale can be constructed such that PR^{alkyl}_3 > PR^{aryl}_3 > $P(OR)_3$ > PX_3; a scale which is reflected in the frequencies of the A_1 carbonyl stretching mode of phosphine containing $[Ni(CO)_3L]$ complexes (Table 1).[12] The frequency of this vibration is dependent on the degree of back-bonding from the metal, which is in turn dependent upon the electron density on the metal, hence correlating with the donor ability of the phosphorus ligand. Furthermore, PR_3 ligands can act as π-acceptor ligands by interaction of the metals d-orbitals with an appropriate orbital of the ligand (Figure 2, b). Early descriptions of this interaction invoked the σ* orbital of the PR_3 ligand in this interaction, however, it is now accepted that the orbital responsible for the π acceptor ability of phosphines results from mixing of the σ* orbital and a low lying phosphorus d-orbital. It was found that the degree of backbonding is highest for electron poor PR_3 ligands where the LUMO is relatively low in energy.[1,13–16] Electron rich trialkylphosphines are good σ donors but poor π acceptor ligands, whereas electron deficient

phosphites and halo phosphines are weak σ donors and strong π acceptors. Thus, the electronic properties of phosphorus donors are readily predictable and tuneable by systematic variation of the substituents.

Table 1: Comparison of vibrational data for a series of $Ni(CO)_3L$ complexes[12]

P ligand	ν_{CO} / cm^{-1}
P^tBu_3	2056.1
PEt_3	2061.7
PMe_3	2064.1
PPh_3	2068.9
$P(p\text{-}C_6H_4Cl)_3$	2072.8
$P(OEt)_3$	2076.3
PH_3	2083.2
$P(OPh)_3$	2085.3
PCl_3	2097.0
PF_3	2110.8

Steric properties

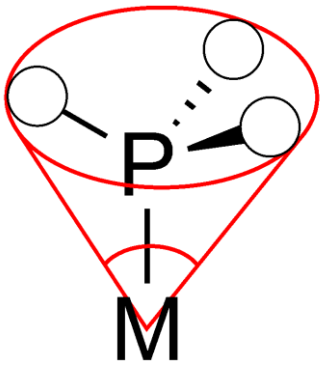

Figure 3: Pictorial representation of Tolman cone angle

The steric profile of ancillary ligands can have a critical influence on the reactivity of metal complexes and can affect factors such as coordination number, substitution kinetics and complex stability. Bulky ligands tend to promote dissociative reactions at metal centres,[2] and so catalytic cycles in which the rate determining step is the dissociation of a ligand or a reductive elimination can be expected to be promoted *via* the use of larger ancillary ligands. Conversely, reactions which are limited by the rate of substrate association are aided by the use of smaller ligands. The primary metric used to compare steric bulk in phosphine ligands

is the cone angle.[12,17,18] Tolman[17] defines a cone angle as "the apex angle of a minimum cone, centred 2.28 Å away from the centre of the P atom, which just touches the outermost extremities of a ligand folded back while maintaining C_3 symmetry". Tolman's initial studies concerned direct measurement of a physical model of tertiary phosphine Ni(0) complexes, however the concept is also useful more widely and cone angles can be more broadly defined in terms of the apex angle of a cone described by the outermost extent of a ligands substituents (Figure 3). Cone angles for phosphines can vary greatly (Table 2), as the bulkiest ligands can occupy over half of the coordination sphere whereas PH_3 is comparable to some of the least bulky ligands. The utility of this approach is demonstrated by the fact that many physical, spectroscopic and chemical parameters correlate strongly with this measure of steric bulk.

Table 2: Cone angles for some selected PR_3 ligands. For comparison, the cone angles of other common ligands are included

Ligand	**Cone Angle / °**
PH_3	87
PF_3	104
$P(OEt)_3$	109
PMe_3	118
PCl_3	124
PPh_3	145
PCy_3	170
P^tBu_3	182
$P(mes)_3$	212
H	75
CO	~95
η^5-C_5H_5	136

Care must be taken in the interpretation of these data as such measurements necessitate use of a single fixed conformation and thus for ligands whereby multiple conformations are accessible, cone angles may be more flexible than first envisioned.[19] Indeed, it is likely that a number of conformations are accessible for any given system, thus giving rise to dynamic equilibria in solution. Furthermore, the treatment of unsymmetrical and/or polydentate ligands using this method is often not straightforward and thus cone angles are best

considered as a guide in understanding trends rather than an absolute quantitative measure of steric bulk. Nonetheless, cone angles remain a useful tool for rationalising the reactivity of phosphine complexes.

Structural features of primary and secondary phosphines

Primary and secondary phosphines; RPH_2 and R_2PH respectively; exhibit a number of unique properties resulting from the presence of the P-H bond. These effects are perhaps most pronounced in the parent molecule, PH_3. The structure of PH_3 is in stark contrast to that of its lighter congener NH_3. Both compounds have a trigonal pyramidal structure with C_{3v} symmetry, NH_3 displays bond angles (107.8 °) close those of an ideal tetrahedron (109.5 °) in accordance with VSEPR theory, whereas the heavier analogue has H-P-H bond angles of 93.6°. The much reduced bond angle results from a lack of hybridisation of the phosphorus valence orbitals. As the atomic radii of the central atom increases the steric repulsion of the small H substituents diminishes and thus hybridisation of the orbitals is far less efficient giving rise to bond angles close to those expected of atomic p orbitals.[2] H atoms are thus described as binding to the 3*p* orbitals of phosphorus resulting in relatively weak and hence reactive P-H bonds. The lone pair of electrons occupies an orbital with a substantial degree of *s* character as can be observed spectroscopically by the highly shielded ^{31}P NMR chemical shift of δ = -240 ppm.

Given the unusual bonding displayed in P-H bonds, it is perhaps unsurprising that primary and secondary phosphines have been shown to be highly reactive. The reactivity of the P-H bond is such that primary and secondary phosphines are unsuitable as spectator ligands for catalysis and thus the chemistry of these species has been largely restricted to their use as synthetic intermediates in the construction of more complex phosphorus containing species (*vide infra*).[20,21]

Multidentate ligands

Multidentate ligands have long been known to form complexes which are more kinetically inert and thermodynamically stable than analogous monodentate ligands through 'the chelate effect'.[22,23] The chelate effect is demonstrated by comparison of the reactions of $[Cd(H_2O)_6]^{2+}$ with NH_3 and ethylene diamine (Figure 4).[2] During the reaction, two Cd-O bonds are broken and two similar Cd-N bonds are formed, leading to a similar enthalpic change. However, it is clear that in the case of a chelating ligand the total number of molecules increases with an associated increase in the entropy of the system. Hence, the higher thermodynamic stability is primarily an entropic effect. Additionally, it is observed that coordination of a single donor of a bidentate ligand favours chelation due to the close proximity of the pendant donor atom and hence chelate complexes are also kinetically robust.

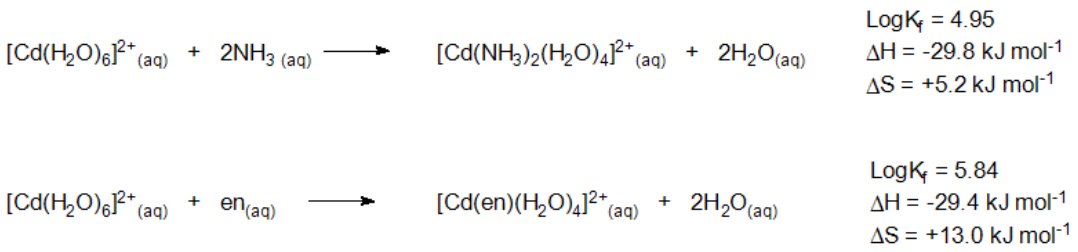

Figure 4: Formation constants and thermodynamic data for the reaction of Cd complexes. en = 1,2-ethylene diamine

Formation of a chelate complex inevitably leads to the creation of a heterocyclic ring, the length of the bridge joining the two donor atoms greatly affects the distance between the two donor groups and hence the metal coordination geometry. Indeed, it has been shown that the chelate ring size has a strong effect on complex stability. Ring sizes which minimise strain within the molecule are favoured, hence the effect is maximised for five and six membered chelate rings (especially for first row transition metals) but is diluted upon moving to larger ring sizes.

Larger bridges necessitate a wider angle between the two coordinating groups of a multidentate ligand. This 'bite angle', β (Figure 5), is a key consideration in the design of ligand architectures.

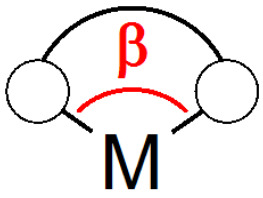

Figure 5: Bite angle of a bidentate ligand

The term, natural bite angle (β_n), is usually applied to diphosphine ligands but can also be defined more generally as the preferred chelation angle formed by the two donor atoms of a chelating ligand as determined by the ligand backbone. Furthermore, it is possible to define a flexibility range, *i.e.* the range of accessible bite angles for a given ligand.[24] It is therefore clear that the nature of the backbone in multidentate ligands has a critical effect on the properties of the complexes, the length and rigidity of the backbone can be altered to enforce particular geometries upon chelation. Multidentate ligands will tend to bind metal ions in a *cis*- geometry and thus the ideal natural bite angles for coordination to an octahedral complex would be 90°. Likewise, the equatorial sites of a trigonal bipyramid require a bite angle of 120°. Deviations from an idealised coordination geometry introduce a strain within the coordination sphere of the complex and are generally disfavoured.[25] However, this must be balanced against the strain induced in the ligand caused by deviations from the natural bite angle. Often, multiple geometries, coordination numbers and oxidation states are found at various stages throughout a catalytic cycle and thus the ability to stabilise varied coordination environments is often desirable. In these cases, some degree of geometric strain may in fact be beneficial. Selected natural bite angles for some common diphosphine ligands are shown in Table 3.

Table 3: Bite angle data for selected diphosphine ligands.[26] Ligand structures shown in Figure 6. a) average bite angle as found by X-ray diffraction; b) natural bite angle determined from molecular mechanics calculations. Values in parentheses indicate flexibility range for the given ligand.

Ligand	P-M-P angle[a] / °	β_n[b] / °	Ref.
dppe	82.55	84.4 (70-95)	[27]
dppp	91.56	82.6	[28]
DIOP	100.0	102.2 (90-120)	[29]
BISBI	119.64	122.6 (101-148)	[29]
Xantphos	104.64	111.7 (97-135)	[29,30]

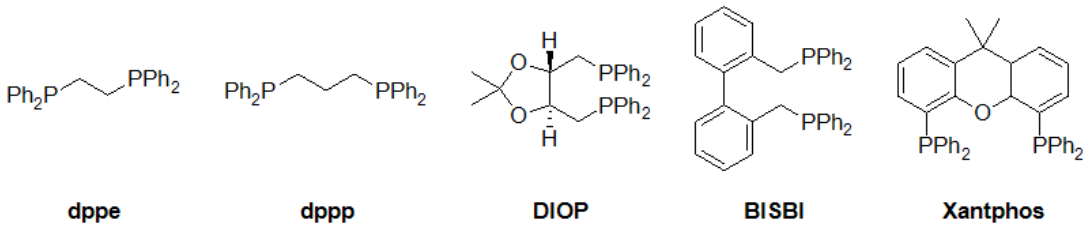

Figure 6: Structures of the ligands detailed in Table 3

Synthesis of phosphine ligands

Numerous methods have been developed for the synthesis of phosphines and other phosphorus containing species. The most common of these fall into one of two categories. The first utilises an electrophilic phosphorus centre such as PCl_3 or $P(OEt)_3$ in combination with a nucleophile such as Grignard reagents, alkyl/aryl lithium species, alcohols or amines (Scheme 7, a). The second and perhaps most straightforward procedure for the formation of P-C bonds however, is *via* the formal deprotonation of a primary or secondary phosphine to give an anionic phosphido species. Phosphides, in addition to displaying a rich coordination chemistry in their own right,[31,32] are strong nucleophiles and are thus useful reagents for organic synthesis[33] (Scheme 7, b). This methodology is particularly useful in synthesising asymmetrically substituted phosphines.[34] Neutral P(III) species are also often effective nucleophiles and can take part in nucleophilic substitution reactions.[35] However, the initial product of these reactions is either a 4 coordinate phosphonium species (Scheme 7, c) or an

oxidised P(V) species (e.g. Michaelis-Arbuzov reaction.[36–38] Scheme 7, d) which must undergo further synthetic preparation in order to be used as a ligand.

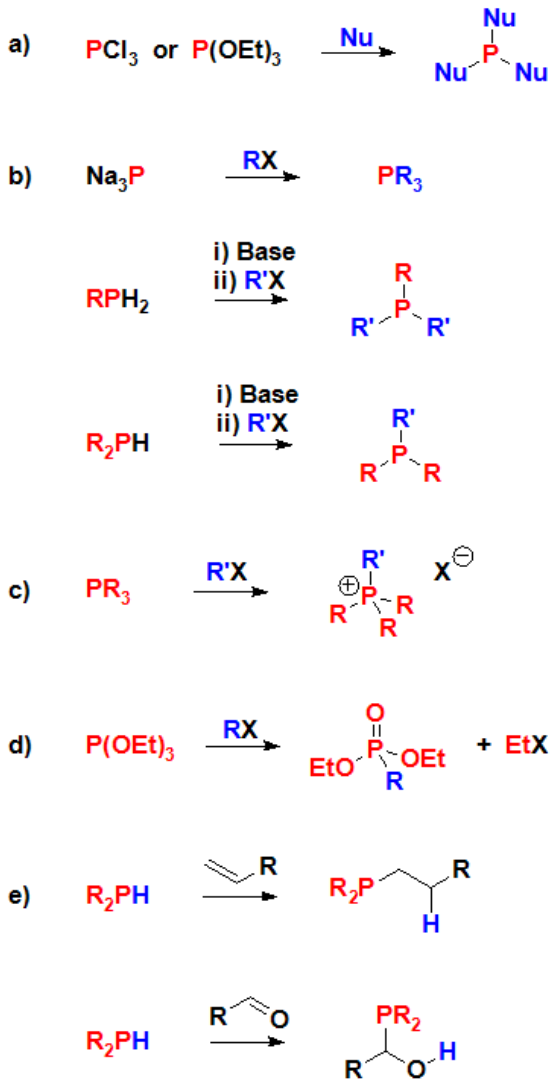

Figure 7: Some common P-C bond forming reactions

The P-H bonds of primary and secondary phosphines have been shown to add across multiple bonds in numerous unsaturated compounds, especially alkenes, alkynes and carbonyls (Scheme 7, e).[39] These reactions may occur spontaneously but are often promoted *via* the action of base, free radicals, UV light or metal catalysts. Such hydrophosphination reactions are often problematic as they have the potential to produce numerous regio- and stereo-isomers. Many primary and secondary phosphines are commercially available but are easily synthesised *via* the reduction of halo phosphines or P(OR) groups with $LiAlH_4$, $NaBH_4$ or

hydrosilanes. Similarly, trivalent species can be accessed *via* reduction of the P(V) intermediates in the presence of strong reducing agents.

Macrocyclic effect

Homogeneous catalysis is widely used in order to promote chemical transformations, these catalysts are often highly selective and can perform transformations not accessible by conventional means. Typically, this requires expensive transition metals with low natural abundance (Pt, Pd, Rh etc.) and complex ligand sets. Due to the expense of many transition metal catalysts, they must attain comparable activities and lifetimes to heterogeneous catalysts in order to become commercially viable.[40] It is for these reasons that homogeneous catalysis in industry is often limited to high-value products where alternative catalytic systems are not suitable.[41] Therefore, it is desirable to develop novel materials which exhibit high stabilities whilst retaining an advantageous reactivity profile.

Macrocycles have long been known to exhibit an exceptionally high affinity for metal ions,[42] the enhanced stability imparted upon metal complexes by the strong binding is the primary factor of interest here. Decomposition of the transition metal complex is a major issue prohibiting the large-scale exploitation of homogeneous catalysis in industrial settings and thus development of durable catalysts and catalytic processes may have significant commercial implications.[43] Furthermore, the high stability of such complexes may allow access to unconventional oxidation states, coordination numbers and geometries allowing for the development of novel reactivity. The origins of the macrocyclic effect are both thermodynamic and kinetic in nature and can be viewed as an extension of the chelate effect.

The origins of the macrocyclic effect

Thermodynamic effect

The thermodynamic macrocyclic effect can be observed as an increased binding constant (logβ) for macrocyclic ligands when compared to open chain analogues. The magnitude of this aspect can be given by the equation:

$$\Delta \log \beta = \log \beta_{macrocycle} - \log \beta_{open\ chain}$$

This effect can be demonstrated by considering the copper(II) complexes of 1, 4, 8, 11 - tetraazaundecane and (7*R*, 14*S*) – 5, 5, 7, 12, 12, 14 – hexamethyl – 1, 4, 8, 11 – tetraazacyclotetradecane (Figure 8). The open chain species has a binding constant around 10,000 times less than that of the analogous cyclic ligand. Therefore, the strength of binding in this case cannot be explained in terms of a chelate effect alone and has been interpreted as evidence for a distinct macrocyclic effect.

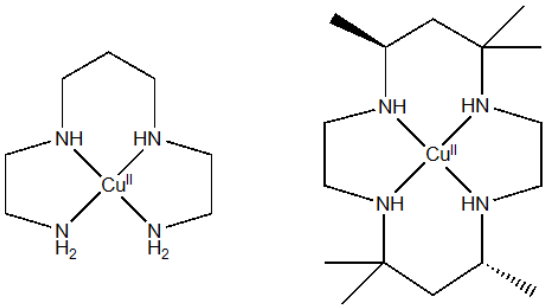

Figure 8: Binding constants of linear and macrocyclic tetraaza- ligand sets[44]

This effect in part arises as the entropic penalty paid upon binding is decreased in the case of a cyclic ligand. The free macrocycle is relatively rigid with donors 'preorganised' for binding and thus has fewer degrees of conformational flexibility available compared to the linear analogue. The ring size has an important effect in determining the extent and strength of the binding to metal ions. If the macrocycle cavity size is mismatched with respect to the metal ions diameter, then this introduces a significant strain within the molecule. Thus, the macrocyclic effect is maximised when the ring is of an appropriate size to effectively

coordinate a metal ion and the resultant metal-ligand bonds are strengthened accordingly. In some cases, factors such as pH and solvation of the macrocycle have also been shown to effect the strength of binding[45] and therefore it is often impossible to explicitly quantify the various contributions to the observed macrocyclic effect.

Kinetic effect

The kinetic contribution to the macrocycle effect results from the absence of an end which inhibits stepwise removal of each donor group thus rendering macrocyclic complexes kinetically inert with respect to dissociation of the ligands. Likewise, coordination of macrocyclic ligands is a relatively slow process, pendant donors can often be included in order to facilitate coordination of the macrocyclic moiety. Both of these effects can be observed in the tetrathioether complexes shown in Figure 9.[46] Although the rate of formation (k_f) for the macrocyclic complex is an order of magnitude slower than that of the open chain analogue, the dissociation rate (k_d) is markedly diminished.

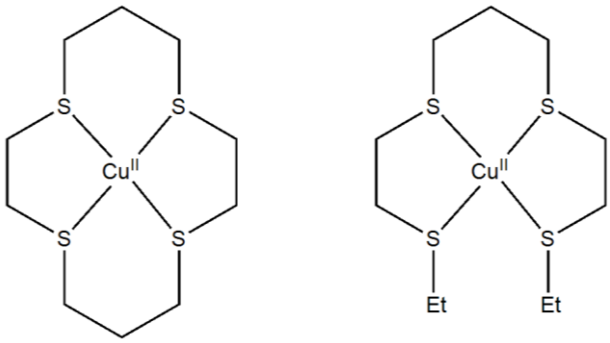

$k_f = 2.8 \times 10^4\ M^{-1}s^{-1}$
$k_d = 9\ s^{-1}$

$k_f = 4.1 \times 10^5\ M^{-1}s^{-1}$
$k_d = 3.0 \times 10^4\ s^{-1}$

Figure 9: Comparison of formation/dissociation kinetics for macrocyclic and linear thioether ligands[46]

Macrocyclic ligands

Overview

Macrocyclic ligands have found a broad range of applications such as medical imaging (TACN, cyclen, cyclam),[47,48] chelating agents (crown ethers, cryptands),[49–52] supramolecular

chemistry (calixarenes, rotaxanes),[53,54] biological systems (porphyrins)[55] and catalysis[56] (Figure 10). Due to the well-developed synthetic routes and the ability to readily introduce further functionality, the N,[57] O,[49,52,58,59] S,[60] and more recently C^{NHC} donor[61] macrocycles are most commonly studied.

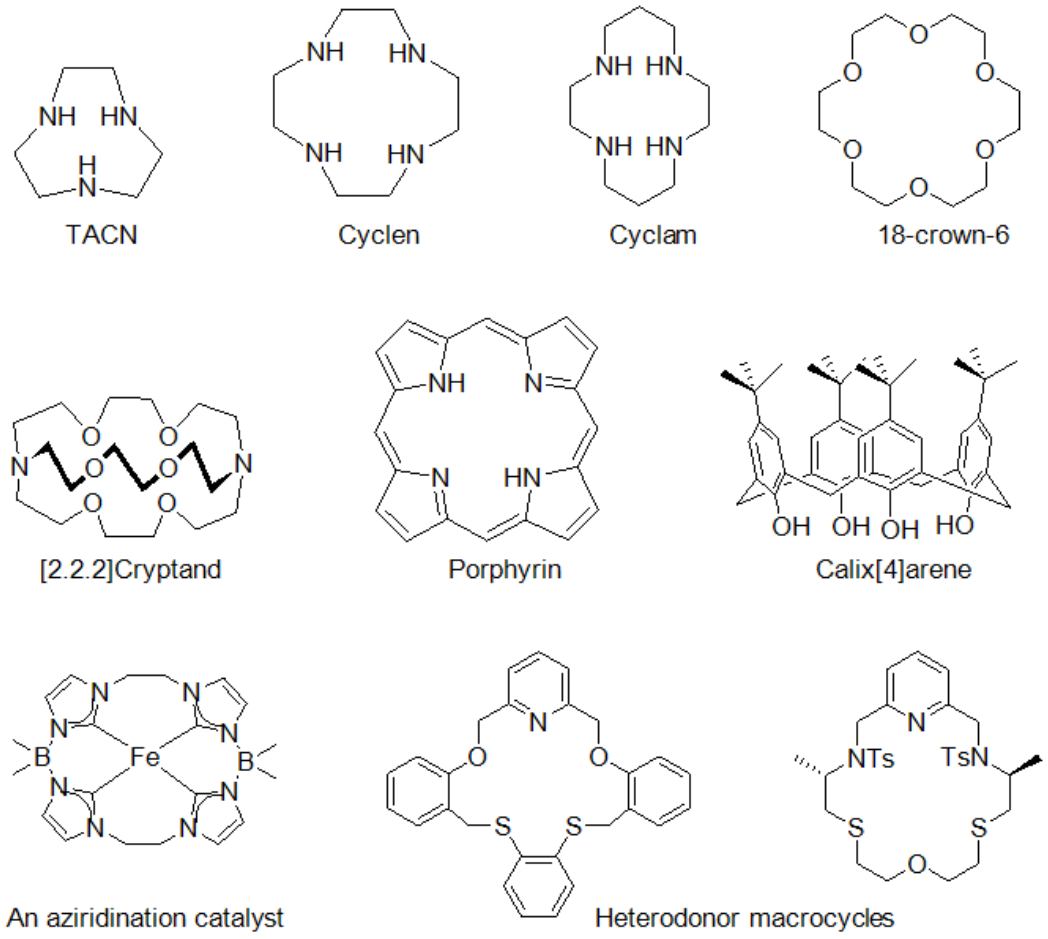

Figure 10: Selected examples of macrocyclic ligands[62,63]

Macrocyclic phosphines

Comparatively little is known about the chemistry of macrocycles containing phosphines within the carbocyclic moiety. Such species are particularly desirable as they incorporate the myriad advantages of phosphine ligands (*vide supra*) into a macrocyclic framework, thereby enhancing the strength of binding and allowing for the formation of robust complexes which may have applications in areas such as homogeneous catalysis and radionuclear imaging. The relative lack of progress in this area is largely due to synthetic difficulties.[64] A general

methodology for the synthesis of P donor macrocycles is yet to be developed and successful strategies typically entail use of highly reactive, unstable or air/moisture sensitive reagents and intermediates. Reactions typically give low to moderate yields and are only viable for small scale studies. Furthermore, the versatility of such reactions is very low and thus a bespoke synthesis must be designed for each target molecule. Despite this, numerous examples of macrocycles containing P/S, P/O, P/N and P/C^{NHC} donor sets have been reported (Figure 11).[65–70]

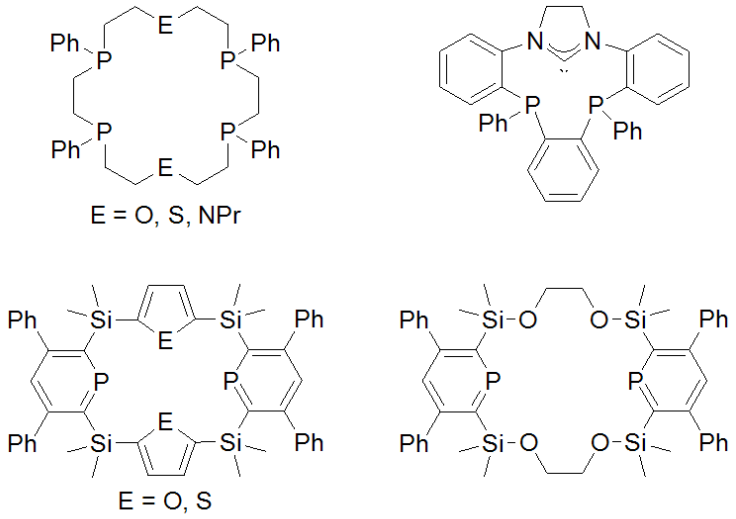

Figure 11: Selected heterodonor macrocycles containing phosphorus atoms[65–71]

Of particular interest with respect to coordination chemistry and potential applications in homogeneous catalysis are the homoleptic tridentate P donor macrocycles (Figure 12), as these are expected to display highly favourable bonding properties. The saturated macrocycles are desirable as the relatively flexible aliphatic linkers may allow these species to accommodate metal ions with a wide range of ionic radii. Comparison with analogous aza- and thia-crown chemistry indicates that the 9 membered rings are likely to display more idealised coordination geometry (*cf*. 12 membered rings) and thus cyclononane macrocycles represent the optimal ring size to encourage strong binding.[72] The small ring size restricts the ligand to a facially capping coordination geometry as they are too small to encircle a metal ion,[64] the implication of this is that a mutually *cis*– geometry is enforced upon the remaining

ligand set and are thus more prone to reactivity due to their close proximity. *Cis*-reaction sites are implicated in the key classical reaction mechanisms of small molecule transformations at transition metal centres and are thus typically required in applications such as efficient homogeneous catalytic activity amongst others. Also, σ donor/π acceptor phosphine ligands have a strong *trans* effect thereby labilising the remaining ligands which may allow for substitutions and/or introduction of a vacant site within the coordination sphere.

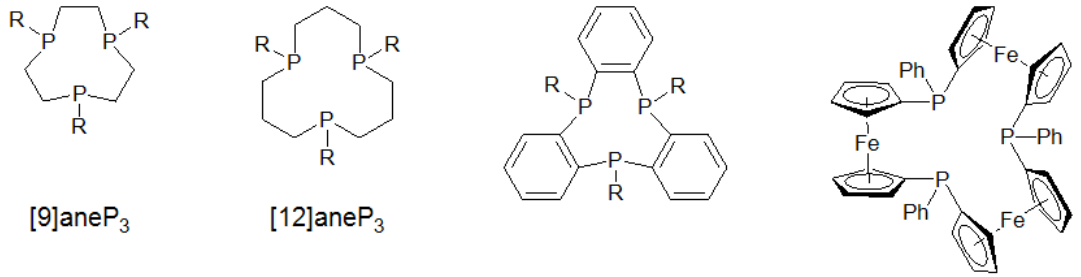

Figure 12: Selected triphosphine macrocycles.[73]

Macrocycle synthesis

General remarks

Macrocycle syntheses can be categorised as one of two methodologies.[74] The first involves the combination of one or more precursors *via* conventional organic chemistry reactions. Their synthetic simplicity make these attractive routes towards target species but polymerisation and formation of higher macrocyclic products is a common side reaction which must be minimised by careful control of reaction conditions such as concentration, stoichiometry, addition rate and reaction temperature. Furthermore, these reactions are typically carried out under high dilution conditions which can limit the practical scale at which reactions can be performed.

The second category involves the use of transition metal ions which can act as a template for macrocycle formation. These bind the reactive species and preorganise the system towards macrocycle formation; the proximity of the reactive groups discourages polymerisation as

the reaction becomes intramolecular and thus is kinetically favoured. This allows for a greater degree of control over stoichiometry and stereochemistry but care must be taken in the choice of template to allow for release of the macrocyclic product through decomplexation of the metal.

Numerous examples of P containing macrocycles have now been prepared *via* these techniques. A brief summary of the key developments in this field are given herein but for a thorough treatment of the synthesis and coordination chemistry of macrocyclic phosphine ligands readers are directed to the recent review by Swor and Tyler.[64]

Direct synthesis

Early syntheses of macrocyclic phosphines focussed on cyclocondensation reactions of acyclic precursors. The first example of such a species was prepared by Horner in 1975 and involved equimolar reaction of α, ω – *bis*(dibenzyl)phosphines with α, ω – dihaloalkanes to generate tetraphosphonium species in low yields (Scheme 2).[75,76] Reductive cleavage of the benzyl groups with $LiAlH_4$ produces the parent tetraphospha-macrocycles as a mixture of stereoisomers.

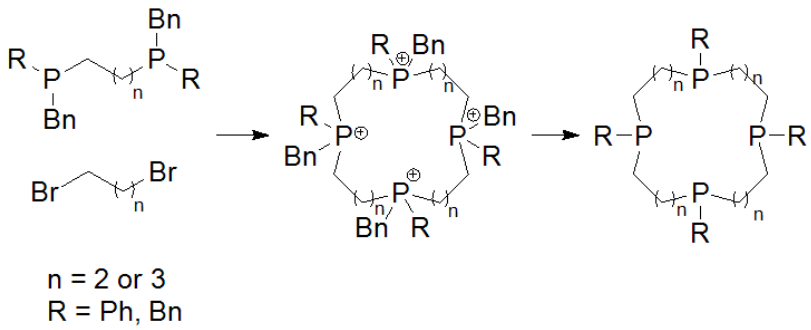

Scheme 2: Horner's synthesis of P_4 macrocycles.[75,76]

Kyba synthesised 11- and 14-membered benzanullated macrocycles under high dilution conditions (Figure 13).[77–80] The use of aromatic moieties in the ligand backbone may promote cyclisation as the rigid linkers reduce the conformational flexibility of the intermediate species. This technique was further utilised to generate macrocyclic secondary phosphines by subsequent cleavage of a 1-naphthylmethyl group with potassium naphthalenide.[81] The

presence of secondary phosphines in the macrocyclic ring is highly desirable as they provide a route to numerous P-substituted derivatives *via* nucleophilic substitution and hydrophosphination reactions. The ability to easily investigate the stereoelectronic profile whilst introducing further functionality and complexity into a ligand structure is crucial for the design of any homogeneous catalytic system.

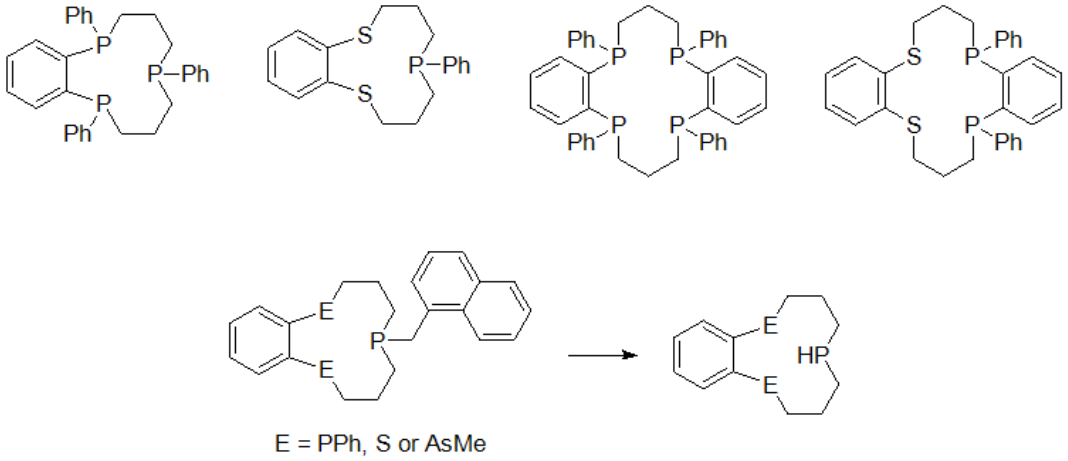

Figure 13: Kyba's benzannulated macrocycles[77–81]

A notable recent example is given by Helm's synthesis of a [9]aneP_3 species by the slow mixing of dilute solutions of a linear triphosphorus species with 1,2-dichloroethane at elevated temperatures (Scheme 3).[82] This represents the only synthesis of a [9]aneP_3 species in the absence of a transition metal template (*vide infra*). The macrocycle is reportedly formed in 85 % yield with a 3:7 ratio of the *syn/syn* and *syn/anti* stereoisomers respectively.

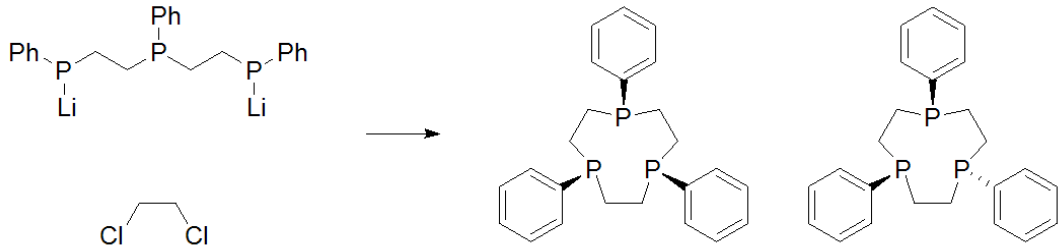

Scheme 3: Helm's synthesis of [9]aneP_3Ph_3.[82]

Cyclocondensation reactions can provide efficient routes to some macrocyclic systems although these routes do suffer from some significant drawbacks. Reactions typically give poor yields of macrocycle, suffer from slow kinetics and require large solvent volumes and

lengthy work-up procedures. The products are further complicated by the presence of multiple stereoisomers as a stereoselective route has yet to be developed, significantly only one isomer will be able to fully coordinate to a metal centre as the inversion barrier at P centres is typically high. Furthermore, uncoordinated macrocycles and many of their P(III) precursors are prone to oxidation or hydrolysis and reactions must be carried out using rigorously dried and degassed solvents, apparatus and reagents.

Template methods

In an attempt to overcome some of the problems associated with the cyclocondensation route to macrocyclic phosphines a number of researchers have turned to transition metal templates. Use of a template affords a greater degree of control over the reactive species and can lead to improved yields for the cyclisation step. The metal centre also increases the acidity of P-H bonds present in many key intermediates thereby activating the P centre with respect to alkylation. Furthermore, the ability to carry out reactions at higher concentrations and in a stereospecific manner are particularly advantageous.

A typical example of a templated synthesis is given by the works of Rosen,[83,84] Stelzer[85–88] and Mizuta[89] in their syntheses of tetradentate macrocycles around square planar Ni(II) or Pd(II) templates (Scheme 4). This methodology draws the reactive sites into close proximity thereby favouring the cyclisation reaction as can be seen in the excellent yields of tetraphosphine macrocycles observed. This methodology has proved to be remarkably versatile in the preparation of 14- to 16-membered tetraphosphine macrocycles.

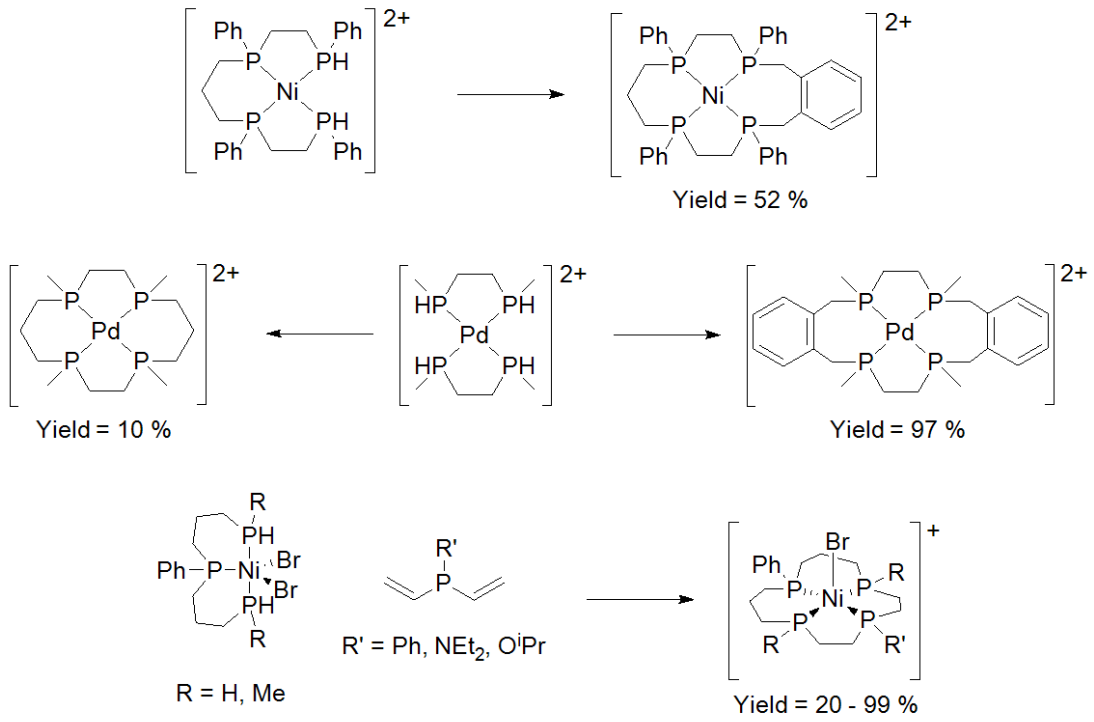

Scheme 4: P_4 Macrocycle synthesis around group 10 templates

Gladysz *et al.* provide an impressive demonstration of the power of this approach in the synthesis of a 1, 16, 31 – triphosphacyclopentatetraconta – 8, 23, 38 – triene, a 45-membered triphosphine macrocycle, on a tungsten(0) tricarbonyl template (Scheme 5).[90] Somewhat unusually, the ring closure step is carried out *via* ring closing metathesis using the 1st generation Grubbs' catalyst rather than the more conventional hydrophosphinations or nucleophilic substitution reactions. Despite the fact that such a large ring is unlikely to show any significant macrocyclic effect this example is instructive in that it demonstrates the ability of a template to facilitate cyclisation over other less desirable reactions. Indeed, cyclisation appears to be favoured to a remarkable degree as the macrocyclic product is formed in 83 % yield. Furthermore, such a species would be highly unlikely to form by other means, even if carried out at very low concentrations. Recently, this methodology has been adapted in the synthesis of a series of tricyclic dibridgehead diphosphines around an $Fe(CO)_3$ template featuring 22- to 38-membered macrocyclic rings.[91] No attempts were made to isolate the

free ligand and the complexes and their derivatives were found to exhibit molecular rotator behaviours.

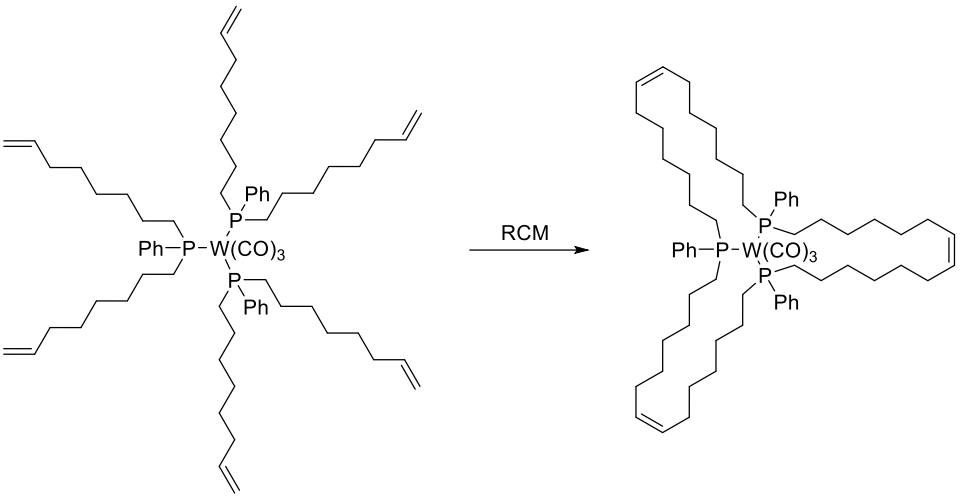

Scheme 5: Gladysz's synthesis of a 45-membered P_3 macrocycle[90]

As can be seen from the analogous aza-, oxa- and thia-macrocylic chemistry, 9- to 15 membered ring systems demonstrate the most favourable characteristics for many potential applications. Norman prepared [12]aneP_3 and [15]aneP_3 macrocycles in good yield around a $Mo(CO)_3$ template *via* the free radical catalysed hydrophosphination of allyl and butenyl phosphine respectively (Scheme 6).[92,93] A key advantage of this approach is that the resultant macrocycles contain only secondary phosphines and thus can be readily alkylated in the final step allowing for the straightforward preparation of a diverse range of derivatives containing alkyl, aryl, amino, ethereal, thioether and phosphino functional groups.[94,95] Despite this early success, a number of limitations to this procedure are apparent. Attempts to extend the scope of this methodology to 9 membered rings failed, instead leading to formation of polymeric by-products or partially cyclised products.[96] Most significantly, the strength of binding was such that the ligand could not be demetallated and isolated in an uncoordinated state. While this is a promising indication of the formidable stability of this type of complex, it severely limits the utility of this route for further studies. However, it has since been shown that although these complexes do not undergo dissociation, the phosphine can be made labile by oxidation at Mo (*vide infra*).[97,98]

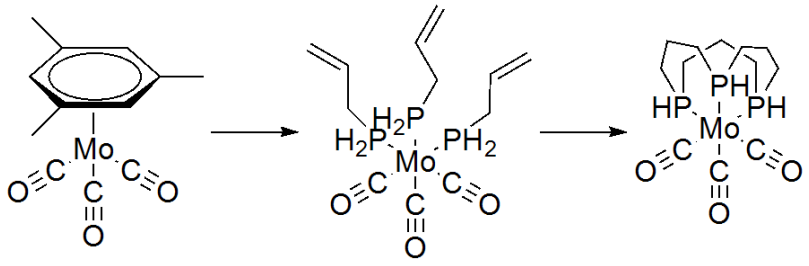

Scheme 6: Norman's seminal synthesis of [12]aneP$_3$H$_3$[92,93]

Building on the work of Norman, the Edwards group have investigated the free radical hydrophosphination of vinyl phosphines with diphosphines around an Fe(II) template (Scheme 7).[99–104] These 'piano stool' templates allow for the stereospecific synthesis of the previously inaccessible 9- to 12-membered macrocycles. The smaller ionic radius of Fe(II) compared to Mo(0) results in a contraction of the non-bonded P-P distance and hence the formation of 5-membered chelate rings becomes viable.

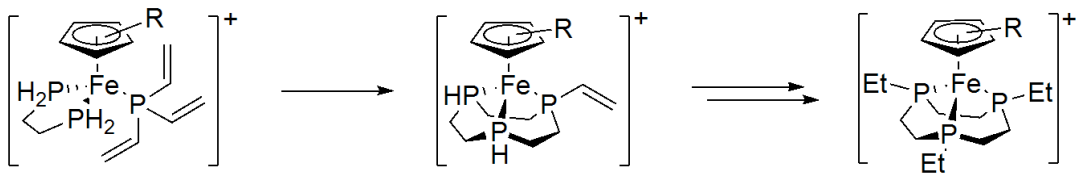

Scheme 7: Edward's synthesis of [9]aneP$_3$ species around an Fe piano stool template[99]

Demetallation

Templated syntheses for the full series of 9- to 12- membered rings have now been developed. However, these procedures do have one major drawback, the strength of binding which makes these ligands so desirable means that they are exceedingly difficult to demetallate. Access to the uncoordinated macrocyclic compounds is crucial if their potential is to be realised. Common routes to macrocycle demetallation involve displacement with other strongly binding ligands (CN^-, S^{2-}, phosphines, chelating agents) or digestion in highly acidic or basic solutions. In the case of kinetically inert metal centres it is often necessary to disrupt the coordination sphere by changing oxidation states with oxidants such as halogens, peroxides or ozone or reducing agents such as alkali metals.

Norman's molybdenum tricarbonyl templated macrocycles were observed to be particularly inert and were unreactive to displacement upon exhaustive treatment with PPh_3, PF_3, $P(OMe)_3$ or KCN, even at elevated temperatures.[93] However, it was later shown that these Mo(0) species could be oxidised to Mo(II) compounds with Cl_2 or Br_2.[97] Reaction of the initially formed cationic halo-halide species, $[Mo(CO)_3P_3X]X$, with KCN reforms the original Mo(0) species.[98] However, upon standing in CH_2Cl_2 a neutral dihalo species, $Mo(CO)_2P_3X_2$, forms with concomitant loss of one carbonyl (Scheme 8). It was found that treatment of this compound with ethanolic NaOH or KCN in DMSO resulted in liberation of the free macrocycle from the metal template.[98,105]

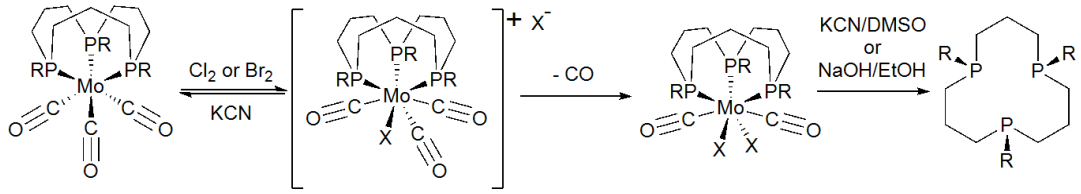

Scheme 8: Oxidation and demetallation of ([12]aneP$_3$)Mo(CO)$_3$

Digestion of Edwards' [12]aneP_3 Fe piano stool complexes with Na/NH_3 leads to demetallation of the macrocycle in good yield (Scheme 9). Analagous reactions with the 9- to 11-membered macrocycles did not result in release of the ligand reflecting the superlative binding properties of these species. It was found that [9]aneP_3 species could be oxidatively demetallated from these templates with aqueous Br_2 or H_2O_2 to give the trioxide in high yield.[99] Attempts to recover the phosphino species by reducing the trioxide with $LiAlH_4$ or $PhSiH_3$ failed due to its insolubility in compatible solvent systems.

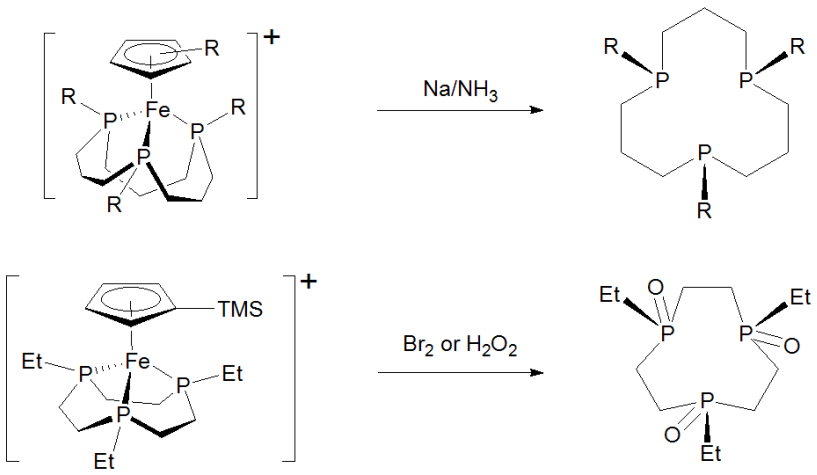

Scheme 9: Macrocycle liberation from Fe piano stool templates

Reactivity of macrocyclic phosphine complexes

The only system to receive any detailed study with respect to coordination chemistry is the [12]aneP_3 ligand isolated by Edwards (*vide supra*). M([12]aneP_3)Cl_3 (M = Ti, V, Cr) complexes are readily formed from coordination of the macrocycle to the metal chlorides or their THF adducts (Scheme 10).[106] A related species bearing a tripodal phosphine has been reported as the seven coordinate THF adduct by Girolami.[107] However, $TiCl_3P_3$ complexes (where P = PCy_3, P^iPr_3 or PBu_3) have only been isolated at low temperature.[108] Upon warming to room temperature, phosphine dissociation occurs forming $TiCl_3P_2$ species, the macrocyclic P_3 ligands stabilise the hexacoordinate Ti(III) complex as dissociation rates for macrocycles are much slower. V([12]aneP_3Et_3)Cl_3 is indefinitely stable as a solid in air in contrast to many other V^{III}(phosphine) complexes which are typically 5 coordinate and sensitive to air and moisture. The macrocyclic effect in addition to coordinative saturation appears to impart unusual stability upon this complex. However, solutions of the complex exposed to air undergo selective oxidation of the metal forming V(O)([12]aneP_3Et_3)Cl_2, the first octahedral vanadyl phosphine complex (Scheme 10).[106]

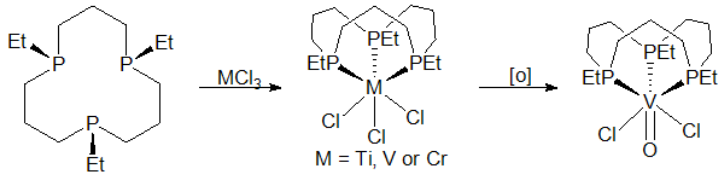

Scheme 10: Some early transition metal complexes of [12]aneP$_3$ and formation of the octahedral vanadyl complex

Addition of [12]aneP$_3$ to solutions of TiCl$_4$, ZrCl$_4$ and HfCl$_4$ resulted in coordination of the phosphine as observed by spectroscopic methods but the complexes could not be isolated for further study. Treatment of frozen solutions of NbCl$_3$(DME) or NbCl$_4$(THF)$_2$ with [12]aneP$_3$Et$_3$ produced air sensitive materials which were too unstable for reliable characterisation to be obtained, although EPR spectra indicated the presence of Nb^{III} and Nb^{IV} compounds respectively. The Nb^{IV} solution exhibited reversible thermochromism, potentially due to the dimerisation of the Nb species above room temperature.

Ti, V and Ni complexes of [12]aneP$_3$R$_3$ (where R = Et or (CH$_2$)$_3$OMe) when combined with a suitable initiator (such as MAO) have been shown to be active catalysts for ethene and propene polymerisation.[109] The activity and stability of the complexes, whilst only moderate; was considerably larger than that of related catalysts with linear phosphine ligands suggesting that the macrocyclic effect is responsible for the enhanced stability.

Reaction of the macrocycle with ReCl$_3$(PPh$_3$)$_2$(MeCN) leads to formation of Re([12]aneP$_3$^{i}Bu$_3$)Cl$_3$, which can be reduced with Na amalgam under a CO atmosphere, producing Re([12]aneP$_3$^{i}Bu$_3$)(CO)$_2$Cl in high yield.[110] An analogous Mn compound was synthesised directly by photolysis with Mn(CO)$_5$Br producing Mn([12]aneP$_3$^{i}Bu$_3$)(CO)$_2$Br. The Re(I) complex can undergo a number of further transformations; reaction with LiAlH$_4$ leads to the monohydride, whilst halide abstraction followed by coordination of terminal alkynes generates vinylidene and cumulene structures (Figure 11). Reactions of the Re and Mn halides and the related complex, ([12]-ane-P$_3$Et$_3$)RuCl$_2$(dmso),[111] with norbornene were investigated leading to the polymerisation of the alkene monomer *via* a ROMP mechanism.

The molecular weight and polydispersity of the resulting polymers was highly dependent on the steric environment surrounding the metal centre, thus it is possible to tune the reactivity by varying the pendant alkyl chain of the macrocycle. Analogous reactions with the well-known Ru alkylidene catalysts such as Grubbs' catalyst,[112] are thought to require a labile phosphine ligand in order to open a vacant site to accommodate the incoming alkene. Intriguingly, no phosphine dissociation was observed spectroscopically and an associative mechanism is unlikely in these electronically saturated species, suggesting that these complexes follow a unique mechanistic pathway.

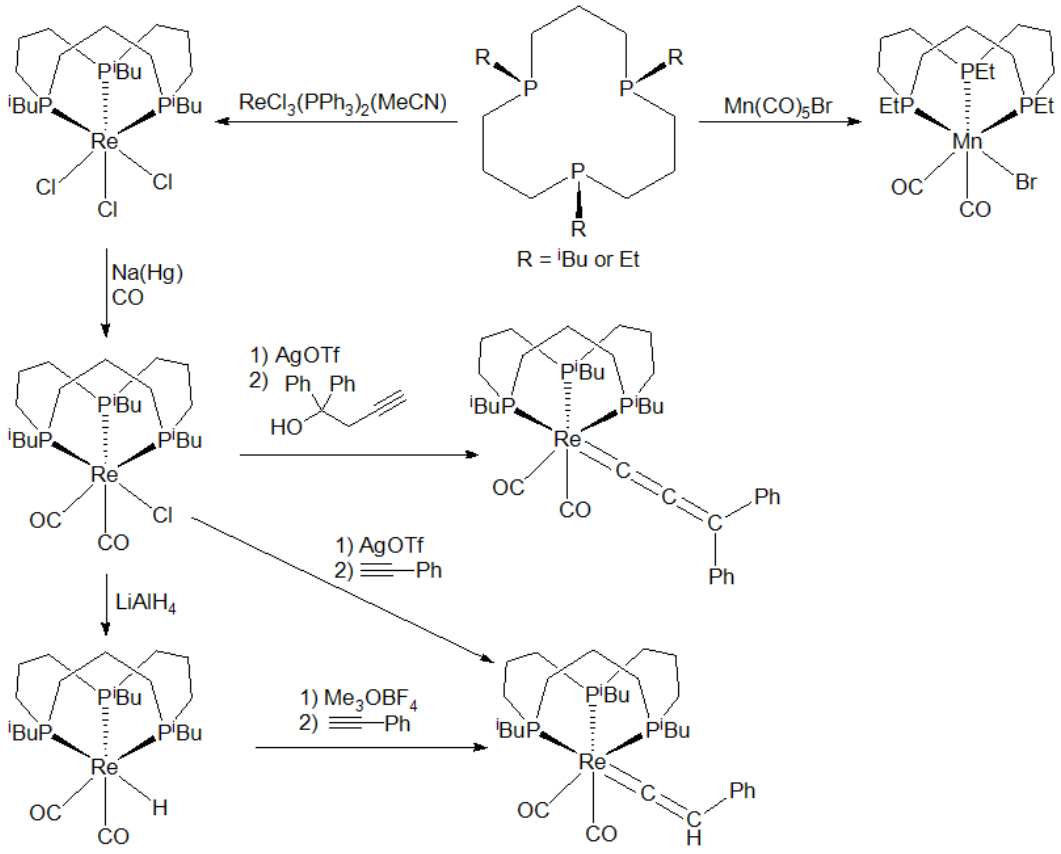

Scheme 11: Synthesis of Re and Mn complexes

Recently, it has been shown that coordination of [12]aneP_3R_3 to Cu(I) halides results in formation of a novel bimetallic complex featuring a unique mono-halide bridged Cu-Cu interaction (Figure 14). It was found that increasing the steric congestion around the metal

centre with bulkier R groups or larger halides switches off this novel coordination mode and instead favouring the typical monometallic tetrahedral geometry (Scheme 12).[113]

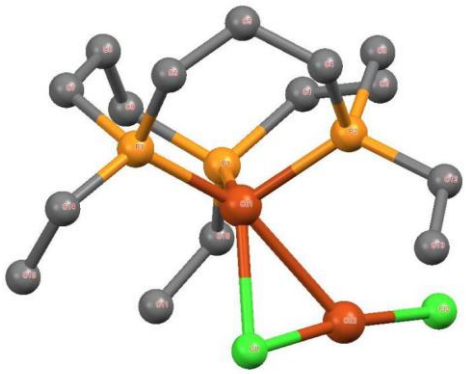

Figure 14: Molecular structure of ([12]aneP$_3$Et$_3$)Cu$_2$Cl$_2$

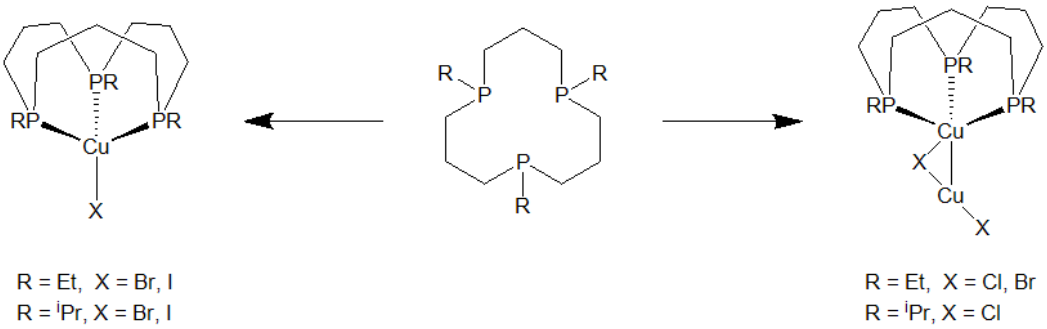

Scheme 12: Variable product formation in Cu(I) halides

Aside from the Fe piano stool template species (*vide supra*), there is a single example of [9]aneP$_3$ ligands being coordinated to a metal centre.[82] [9]aneP$_3$Ph$_3$ was synthesised as a mixture of the *syn/syn* and *syn/anti* isomers. Treatment of [9]aneP$_3$Ph$_3$ with Mo(C$_7$H$_8$)(CO)$_3$ results in formation of *fac*-([9]aneP$_3$)Mo(CO)$_3$ in moderate yield; in this case, the increased bond strength associated with the macrocyclic effect appears to be sufficient to overcome the energetic barrier to P inversion as the *syn/syn*- isomer was the sole product observed (Scheme 13). Comparison of this complex with the analogous [12]aneP$_3$ species prepared by Norman (*vide supra*) suggests a higher degree of σ- basicity in the former ligand. This is evident in the shorter Mo-P bond lengths and the increased π back-bonding to the carbonyls,

apparent in both the bond lengths and vibrational frequencies. This supports the contention that the cyclononane species displays exceptionally strong binding properties.

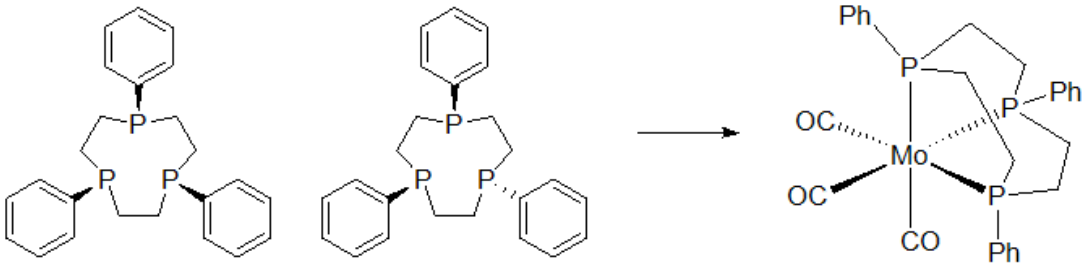

Scheme 13: Formation of ([9]aneP$_3$)Mo(CO)$_3$

Aims

Multidentate phosphines and other ligands containing P donor atoms are of continued interest due to their applications in homogeneous catalysis where ligand choice can drastically effect activity and efficiency of the system. Modern catalysts are expected to deliver ever higher performance in terms of turnover, activity and substrate scope, often under mild conditions. There is also a need to develop catalysts capable of novel transformations in order to expand the applicability of catalysis in synthetic chemistry. Furthermore, there is a desire to move away from noble metals as active species due to cost and toxicity issues.[114] The stringent demands placed upon catalysts provide a substantial challenge to the organometallic chemist and the preparation of new ligand structures is imperative to the continued progress in this area.

Therefore, there is a need to develop novel ligands to support these endeavours and presented herein are recent investigations in this field. In particular, this thesis will describe work towards a synthetic route to macrocyclic phosphines (Chapter 2), investigations of glycidyl phosphines as intermediates in the synthesis of ambidentate heterodonor ligands (Chapter 3), synthesis of chiral-at-aluminium complexes (Chapter 4) and finally a discussion of the coordination chemistry of a chiral expanded ring N-heterocyclic carbenes bearing pendant phosphine donors (Chapter 5).

References

1 J. F. Hartwig, *Organotransition Metal Chemistry: From Bonding to Catalysis*, 1st edn., 2010.

2 P. Atkins, T. Overton, J. Rourke, M. Weller and F. Armstrong, *Shriver & Atkins Inorganic Chemistry*, Oxford University Press, Oxford, 4th edn., 2006.

3 N. Winterton and G. J. Leigh, Eds., *Modern Coordination Chemistry*, Royal Society of Chemistry, Cambridge, 2002.

4 W. S. Knowles, *J. Chem. Educ.*, 1986, **63**, 222.

5 W. S. Knowles, *Acc. Chem. Res.*, 1983, **16**, 106–112.

6 V. V. Grushin, *Chem. Rev.*, 2004, **104**, 1629–1662.

7 Y. Hirai, T. Nakanishi and Y. Hasegawa, *J. Lumin.*, 2016, **170**, 801–807.

8 T. M. Shaikh, C.-M. Weng and F.-E. Hong, *Coord. Chem. Rev.*, 2012, **256**, 771–803.

9 R. K. Agarwal, H. Agarwal and K. Arora, *Rev. Inorg. Chem.*, 2000, **20**, 1–62.

10 K. Arora, R. C. Goyal, D. D. Agarwal and R. K. Agarwal, *Rev. Inorg. Chem.*, 1998, **18**, 283–315.

11 W. A. Henderson and C. A. Streuli, *J. Am. Chem. Soc.*, 1960, **82**, 5791–5794.

12 C. A. Tolman, *Chem. Rev.*, 1977, **77**, 313–348.

13 S. Xiao, W. C. Trogler, D. E. Ellis and Z. Berkovitch-Yellin, *J. Am. Chem. Soc.*, 1983, **105**, 7033–7037.

14 D. S. Marynick, *J. Am. Chem. Soc.*, 1984, **106**, 4064–4065.

15 J. A. Tossell, J. H. Moore and J. C. Giordan, *Inorg. Chem.*, 1985, **24**, 1100–1103.

16 J. C. Giordan, J. H. Moore and J. A. Tossell, *Acc. Chem. Res.*, 1986, **19**, 281–286.

17 C. A. Tolman, *J. Am. Chem. Soc.*, 1970, **92**, 2956–2965.

18 C. A. Tolman, W. C. Seidel and L. W. Gosser, *J. Am. Chem. Soc.*, 1974, **96**, 53–60.

19 T. R. Cundari, *Computational organometallic chemistry*, Marcel Dekker, 2001.

20 J. T. Fleming and L. J. Higham, *Coord. Chem. Rev.*, 2015, **297**, 127–145.

21 B. P. Nell and D. R. Tyler, *Coord. Chem. Rev.*, 2014, **279**, 23–42.

22 A. Martell, American Chemical society, 1967, vol. 62, pp. 272–294.

23 G. T. Morgan and H. D. K. Drew, *J. Chem. Soc., Trans.*, 1920, **117**, 1456–1465.

24 C. P. Casey and G. T. Whiteker, *Isr. J. Chem.*, 1990, **30**, 299–304.

25 R. D. Hancock, *J. Chem. Educ.*, 1992, **69**, 615.

26 P. Dierkes and P. W. N. M. van Leeuwen, *J. Chem. Soc. Dalt. Trans.*, 1999, **77**, 1519–1530.

27 C. P. Casey, G. T. Whiteker, M. G. Melville, L. M. Petrovich, J. A. Gavney and D. R. Powell, *J. Am. Chem. Soc.*, 1992, **114**, 5535–5543.

28 M. Kranenburg, P. C. J. Kamer and P. W. N. M. van Leeuwen, *Eur. J. Inorg. Chem.*, 1998, **1998**, 25–27.

29 M. Kranenburg, Y. E. M. van der Burgt, P. C. J. Kamer, P. W. N. M. van Leeuwen, K. Goubitz and J. Fraanje, *Organometallics*, 1995, **14**, 3081–3089.

30 M. Kranenburg, J. G. P. Delis, P. C. J. Kamer, P. W. N. M. van Leeuwen, K. Vrieze, N. Veldman, A. L. Spek, K. Goubitz and J. Fraanje, *J. Chem. Soc. Dalt. Trans.*, 1997, **77**, 1839–1850.

31 U. Segerer, R. Felsberg, S. Blaurock, G. A. Hadi and E. Hey-Hawkins, *Phosphorus. Sulfur. Silicon Relat. Elem.*, 1999, **144**, 477–480.

32 T. Li, S. Kaercher and P. W. Roesky, *Chem. Soc. Rev.*, 2014, **43**, 42–57.

33 R. Waterman, *Dalt. Trans.*, 2009, **104**, 18–26.

34 A. Grabulosa, J. Granell and G. Muller, *Coord. Chem. Rev.*, 2007, **251**, 25–90.

35 W. A. Henderson and S. A. Buckler, *J. Am. Chem. Soc.*, 1960, **82**, 5794–5800.

36 A. E. Arbuzov, *J. Russ. Phys. Chem. Soc.*, 1906, 687.

37 A. E. Arbuzov, *Chem. Zentralblatt*, 1906, 1639.

38 A. Michaelis and R. Kaehne, *Berichte der Dtsch. Chem. Gesellschaft*, 1898, **31**, 1048–1055.

39 V. Koshti, S. Gaikwad and S. H. Chikkali, *Coord. Chem. Rev.*, 2014, **265**, 52–73.

40 D. Friedman, T. Masciangioli and S. Olson, *The Role of the Chemical Sciences in Finding Alternatives to Critical Resources*, National Academies Press, Washington, D.C., 2012.

41 G. W. Parshall and R. E. Putscher, *J. Chem. Educ.*, 1986, **63**, 189.

42 D. K. Cabbiness and D. W. Margerum, *J. Am. Chem. Soc.*, 1970, **92**, 2151–2153.

43 S. S. Joshi and V. V. Ranade, *Industrial catalytic processes for fine and specialty chemicals*, Elsevier Inc., 1st edn., 2016.

44 D. K. Cabbiness and D. W. Margerum, *J. Am. Chem. Soc.*, 1969, **91**, 6540–6541.

45 * C. Allen Chang, and Bo Hong Wu and B. Y. Kuan, 2005.

46 T. E. Jones, L. L. Zimmer, L. L. Diaddario, D. B. Rorabacher and L. A. Ochrymowycz, *J. Am. Chem. Soc.*, 1975, **97**, 7163–7165.

47 D. Brasse and A. Nonat, *Dalt. Trans.*, 2015, **44**, 4845–4858.

48 E. Boros, E. M. Gale and P. Caravan, *Dalt. Trans.*, 2015, **44**, 4804–4818.

49 C. J. Pedersen, *J. Am. Chem. Soc.*, 1967, **89**, 7017–7036.

50 B. Dietrich, J. M. Lehn and J. P. Sauvage, *Tetrahedron Lett.*, 1969, **10**, 2885–2888.

51 B. Dietrich, J. M. Lehn and J. P. Sauvage, *Tetrahedron Lett.*, 1969, **10**, 2889–2892.

52 C. J. Pedersen, *J. Am. Chem. Soc.*, 1967, **89**, 2495–2496.

53 C. D. Gutsche, *Calixarenes*, Royal Society of Chemistry, Cambridge, 2nd edn., 2008.

54 I. T. Harrison and S. Harrison, *J. Am. Chem. Soc.*, 1967, **89**, 5723–5724.

55 A. Vannotti, *Porphyrins: Their Biological and Chemical Importance*, Hilger & Watts, Hilger Division, 1954.

56 K. B. Yatsimirskii, *Russ. Chem. Rev.*, 1990, **59**, 1150–1156.

57 R. M. Izatt, K. E. Krakowiak and J. S. Bradshaw, in *Chemistry of Heterocyclic Compounds*, John Wiley & Sons, Inc., 1993, vol. 51, pp. 1–29.

58 J. R. Price, M. Fainerman-Melnikova, R. R. Fenton, K. Gloe, L. F. Lindoy, T. Rambusch, B. W. Skelton, P. Turner, A. H. White and K. Wichmann, *Dalt. Trans.*, 2004, **105**, 3715–

3726.

59 G. Coudert, G. Guillaumet and M. Léonard, *Tetrahedron Lett.*, 1981, **22**, 4703–4704.

60 F. Devillanova and W.-W. du Mont, Eds., *Handbook of Chalcogen Chemistry*, Royal Society of Chemistry, Cambridge, 2013, vol. 2.

61 P. G. Edwards and F. E. Hahn, *Dalt. Trans.*, 2011, **40**, 10278.

62 P. P. Chandrachud, H. M. Bass and D. M. Jenkins, *Organometallics*, 2016, **35**, 1652–1657.

63 O. K. Rasheed, P. D. Bailey, A. Lawrence, P. Quayle and J. Raftery, *European J. Org. Chem.*, 2015, **2015**, 6988–6993.

64 C. D. Swor and D. R. Tyler, *Coord. Chem. Rev.*, 2011, **255**, 2860–2881.

65 M. Ciampolini, P. Dapporto, N. Nardi and F. Zanobini, *Inorganica Chim. Acta*, 1980, **45**, L239–L240.

66 M. Ciampolini, P. Dapporto, N. Nardi and F. Zanobini, *J. Chem. Soc. Chem. Commun.*, 1980, 177.

67 M. Ciampolini, P. Dapporto, A. Dei, N. Nardi and F. Zanobini, *Inorg. Chem.*, 1982, **21**, 489–495.

68 M. Ciampolini, N. Nardi, F. Zanobini, R. Cini and P. L. Orioli, *Inorganica Chim. Acta*, 1983, **76**, L17–L19.

69 O. Kaufhold, A. Stasch, P. G. Edwards and F. E. Hahn, *Chem. Commun.*, 2007, **35**, 1822.

70 N. Mézailles, tNicole Maigro, S. Hamon, L. Ricard, F. Mathey and P. Le Floch, *J. Org. Chem.*, 2001, **66**, 1054–1056.

71 N. Avarvari, N. Maigrot, L. Ricard, F. Mathey and P. Le Floch, *Chem. - A Eur. J.*, 1999, **5**, 2109–2118.

72 L. R. Gahan, *Coord. Chem. Rev.*, 2016, **311**, 168–223.

73 T. Mizuta, T. Aotani, Y. Imamura, K. Kubo and K. Miyoshi, *Organometallics*, 2008, **27**, 2457–2463.

74 L. F. Lindoy, *The chemistry of macrocyclic ligand complexes*, Cambridge University Press, 1990.

75 L. Horner, P. Walach and H. Kunz, *Phosphorous*, 1975, **6**, 63.

76 L. Horner, P. Walach and H. Kunz, *Phosphorous Sulfur Relat. Elem.*, 1978, **5**, 171–184.

77 E. P. Kyba, R. E. Davis, C. W. Hudson, A. M. John, S. B. Brown, M. J. McPhaul, L.-K. Liu and A. C. Glover, *J. Am. Chem. Soc.*, 1981, **103**, 3868–3875.

78 R. E. Davis, E. P. Kyba, A. M. John and J. M. Yep, *Inorg. Chem.*, 1980, **19**, 2540–2544.

79 E. P. Kyba and S. B. Brown, *Inorg. Chem.*, 1980, **19**, 2159–2162.

80 E. P. Kyba and S.-S. P. Chou, *J. Org. Chem.*, 1981, **46**, 860–863.

81 E. P. Kyba and S. T. Liu, *Inorg. Chem.*, 1985, **24**, 1613–1616.

82 D. J. Lowry and M. L. Helm, *Inorg. Chem.*, 2010, **49**, 4732–4734.

83 T. A. De Donno and W. Rosen, *Inorg. Chem.*, 1978, **17**, 3714–3716.

84 T. A. DelDonno and W. Rosen, *J. Am. Chem. Soc.*, 1977, **99**, 8051–8052.

85 D. J. Brauer, F. Dörrenbach, T. Lebbe and O. Stelzer, *Chem. Ber.*, 1992, **125**, 1785–1794.

86 D. J. Brauer, T. Lebbe and O. Stelzer, *Angew. Chemie Int. Ed. English*, 1988, **27**, 438–439.

87 D. J. Brauer, F. Gol, S. Hietkamp, H. Peters, H. Sommer, O. Stelzer and W. S. Sheldrick, *Chem. Ber.*, 1986, **119**, 349–365.

88 M. Baacke, O. Stelzer and V. Wray, *Chem. Ber.*, 1980, **113**, 1356–1369.

89 T. Mizuta, A. Okano, T. Sasaki, H. Nakazawa and K. Miyoshi, *Inorg. Chem.*, 1997, **36**, 200–203.

90 E. B. Bauer, J. Ruwwe, F. A. Hampel, S. Szafert, J. A. Gladysz, J. M. Martín-Alvarez, T. B. Peters, J. C. Bohling and T. Lis, *Chem. Commun.*, 2000, **6**, 2261–2262.

91 G. M. Lang, T. Shima, L. Wang, K. J. Cluff, K. Skopek, F. A. Hampel, J. Blumel and J. A. Gladysz, *J. Am. Chem. Soc.*, 2016, **138**, 7649–7663.

92 B. N. Diel, R. C. Haltiwanger and A. D. Norman, *J. Am. Chem. Soc.*, 1982, **104**, 4700–4701.

93 B. N. Diel, P. F. Brandt, R. C. Haltiwanger, M. L. J. Hackney and A. D. Norman, *Inorg. Chem.*, 1989, **28**, 2811–2816.

94 P. G. Edwards, J. S. Fleming and S. S. Liyanage, *J. Chem. Soc. Dalt. Trans.*, 1997, **99**, 193–198.

95 D. J. Jones, P. G. Edwards, R. P. Tooze and T. Albers, *J. Chem. Soc. Dalt. Trans.*, 1999, **35**, 1045–1046.

96 P. G. Edwards, J. S. Fleming, S. S. Liyanage, S. J. Coles and M. B. Hursthouse, *J. Chem. Soc. Dalt. Trans.*, 1996, **104**, 1801.

97 S. J. Coles, P. G. Edwards, J. S. Fleming and M. B. Hursthouse, *J. Chem. Soc. Dalt. Trans.*, 1995, **25**, 4091.

98 P. G. Edwards, J. S. Fleming and S. S. Liyanage, *Inorg. Chem.*, 1996, **35**, 4563–4568.

99 Peter G. Edwards, Robert Haigh, A. Dongmei Li and P. D. Newman, 2006.

100 P. G. Edwards and M. L. Whatton, *Dalt. Trans.*, 2006, **39**, 442–450.

101 A. R. Battle, P. G. Edwards, R. Haigh, D. E. Hibbs, D. Li, S. M. Liddiard and P. D. Newman, *Organometallics*, 2007, **26**, 377–386.

102 A. J. Price and P. G. Edwards, *Chem. Commun.*, 2000, **104**, 899–900.

103 P. G. Edwards, P. D. Newman and D. E. Hibbs, *Angew. Chemie Int. Ed.*, 2000, **39**, 2722–2724.

104 P. G. Edwards, P. D. Newman and K. M. A. Malik, *Angew. Chemie*, 2000, **39**, 2922–2924.

105 S. J. Coles, P. G. Edwards, J. S. Fleming, M. B. Hursthouse and S. S. Liyanage, *Chem. Commun.*, 1996, **99**, 293.

106 R. J. Baker, P. C. Davies, P. G. Edwards, R. D. Farley, S. S. Liyanage, D. M. Murphy and B. Yong, *Eur. J. Inorg. Chem.*, 2002, **2002**, 1975–1984.

107 T. G. Gardner and G. S. Girolami, *Organometallics*, 1987, **6**, 2551–2556.

108 N. Koide and K. Limura, *Polym. Prepr.*, 1979, **20**, 558–561.

109 R. J. Baker and P. G. Edwards, *J. Chem. Soc. Dalt. Trans.*, 2002, **34**, 2960–2965.

110 R. J. Baker, P. G. Edwards, J. Gracia-Mora, F. Ingold and K. M. Abdul Malik, *J. Chem. Soc. Dalt. Trans.*, 2002, **1**, 3985–3992.

111 P. G. Edwards, J. S. Fleming, S. J. Coles and M. B. Hursthouse, *J. Chem. Soc. Dalt. Trans.*, 1997, **99**, 3201–3206.

112 M. Scholl, S. Ding, C. W. Lee and R. H. Grubbs, *Org. Lett.*, 1999, **1**, 953–956.

113 L. Wickramatunga, Cardiff University, 2014.

114 S. Chakraborty and H. Guan, *Dalt. Trans.*, 2010, **39**, 7427.

Chapter 2

Towards the synthesis of macrocyclic phosphines

Aims of chapter 2

Ligand design and methodology

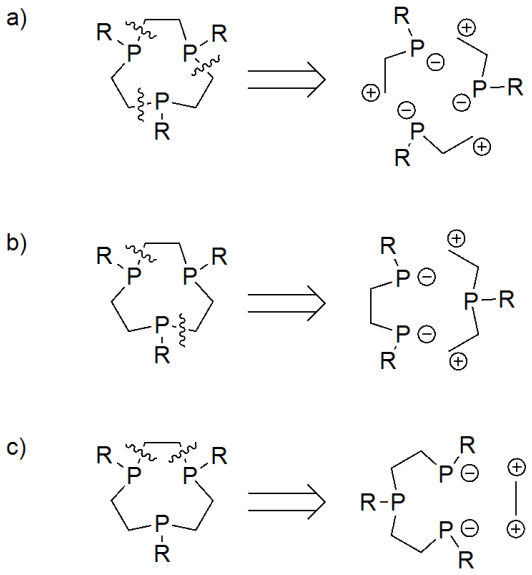

Scheme 1: Selected retrosynthetic approaches to [9]aneP_3 species

Selected strategies for the synthesis of [9]aneP_3 macrocycles are shown in Scheme 1. The success of each route critically relies on the choice of macrocycle template. Furthermore, the choice of route may influence factors such as synthetic complexity, cost and the stability of intermediates. The work of Norman provides an illustrative example of route a);[1,2] whereas route b) has been demonstrated by Edwards[3] (See Chapter 1). Both routes resulted in macrocyclic species, although they each have significant drawbacks. The latter of these routes, C, has received relatively little attention and has only been attempted under high dilution conditions.[4]

Previous work within the Edwards group investigated the reactivity of α, ω - diprimary phosphines around an Fe piano-stool template.[5] Treatment of these species with strong bases results in deprotonation to cleanly form the terminal phosphido species. However, reaction of this species with dibromopropane does not result in macrocycle formation instead forming a coordinated phosphetane species (Scheme 2). Similar observations were made following treatment with dibromoethane.

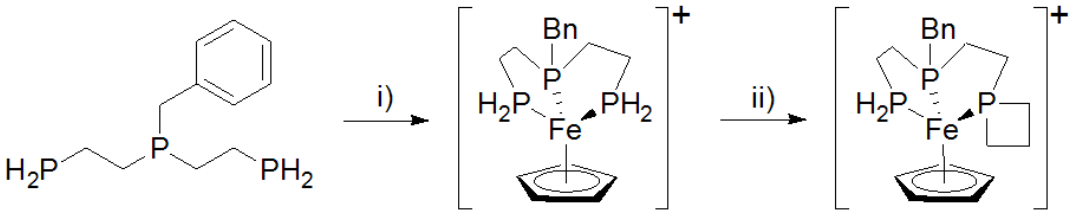

Scheme 2: Attempted synthesis of macrocycles from α,ω-diprimary phosphines. Reagents and conditions: i) $[\eta^5$-CpFe(C_6H_6)$]^+$, MeCN, hv; ii) KO^{t}Bu, 1,3-dibromopropane, THF

This chapter will assess the reactivity of α, ω – disecondary phosphines (Figure 1) towards the synthesis of 9- to 11- membered macrocycles. It is anticipated that use of secondary phosphines over primary phosphines will prevent formation of the heterocyclic by-products and support macrocyclisation. Numerous synthetic routes to linear triphosphines have been developed; indeed, some oligomeric phosphines are commercially available. Alteration and functionalisation of these ligand structures is comparatively straightforward using well known protocols. It should be noted that triphosphine species are putative intermediates in the macrocyclisations in most other macrocycle syntheses. Introduction of bulky groups at the central tertiary phosphine centre can be expected to further promote cyclisation due to the Richman-Atkins effect.[6,7]

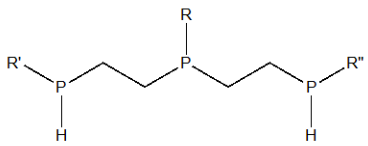

Figure 1: Generic structure of target molecule for cyclisation studies

As has been demonstrated (*vide supra*), the major limiting factor in the exploration of [9]aneP_3 chemistry is the inability to demetallate the macrocyclic ligand from the template of choice. The increased chelate effect of a tridentate ligand (*cf.* bidentate and monodentate ligands) can be envisioned to allow ligand binding with relatively 'hard' metal centres. It is anticipated that the desired [9]aneP_3 species would bind to such metals in a way which is more favourable towards demetallation than the 'softer' ions studied to date. This effect can

be accentuated *via* use of phosphido- species which, in addition to being more nucleophilic than phosphines, are more likely to bind to 'hard' ions.

Results and Discussion

Ligand synthesis

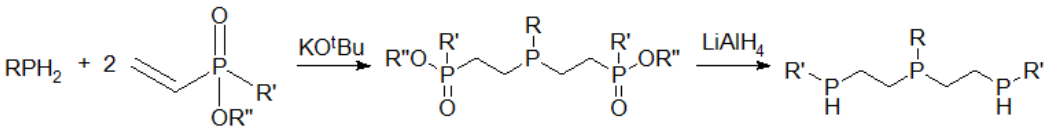

Scheme 3: Initial synthetic route to cyclisation substrate

The first route investigated was *via* Michael-type additions of a primary phosphine to vinyl phosphinates followed by reduction of the resultant diphosphinate with $LiAlH_4$ affording the desired α,ω-disecondary triphosphines (Scheme 3).[8] In principal, this allows for a wide range of triphosphine derivatives to be made. Therefore, it would be possible to methodically approach the cyclisation reaction by systematically varying the steric and electronic environments at the central and terminal phosphine. Unfortunately, it was found that preparation of such species was highly problematic. Reaction of the diphosphinate species with $LiAlH_4$ at room temperature resulted in incomplete reaction with $^{31}P\{^1H\}$ NMR spectra suggesting the presence of various phosphine oxide species. Use of more forcing conditions did not give improved results and none of the desired products could be isolated. The difficulties encountered in this route likely arise from the high P=O bond strength, making the reduction unfeasible. Due to the relative complexity and synthetic difficulty associated with this route, hydrophosphination reactions of vinyl phosphines were attempted.

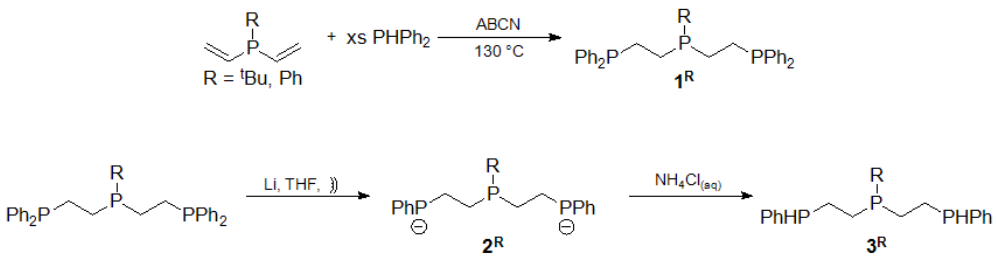

Scheme 4: Synthesis of α,ω-disecondary phosphines

The triphosphine backbone is constructed *via* a modified version of Du Bois' protocol[9] for free radical coupling of diphenyl phosphine with a divinylphosphine to produce the tri-tertiary phosphine intermediate, **1**, in good yield (Scheme 4).[10] Cleavage of two terminal phenyl groups using the procedure developed by Helm[11] furnishes the α,ω-diphosphido phosphine, **2**, which can be conveniently identified by the upfield shift of the two resonances (which appear at δ_P = –4.6 (t, $^3J_{PP}$ = 44.6 Hz) and –53.7 (d, $^3J_{PP}$ = 44.6 Hz) ppm for the ^{t}Bu derivative) in the $^{31}P\{^1H\}$ NMR spectrum for the central and terminal P nuclei respectively (c.f. δ_P = 9.5 and -12.3 ppm for the tritertiary species). **2** is readily protonated *in situ* with deoxygenated saturated NH_4Cl solution. After filtration and extensive drying *in vacuo*, the target α,ω-disecondary phosphine, **3**, is collected as a viscous oil of sufficient purity for subsequent coordination studies. This procedure produces a significant improvement upon the reported yield of diphosphide[11] and has been performed on a scale to produce around 100 g of material with no apparent detriment to yield or purity of the product. Compound **3** can also be prepared directly by the hydrophosphination of divinylphosphines with $PhPH_2$ under UV irradiation. However, a large excess of the primary phosphine is required in order to achieve selectivity for the triphosphine and the purity of **3** is inferior when produced in this manner.

Unfortunately, this procedure does not allow for control of the stereochemistry at the terminal P centres and thus the secondary phosphines are found as mixtures of stereoisomers. The $^{31}P\{^1H\}$ NMR spectra display two signals consistent with the expected overlapping AXX' spin systems; a pseudotriplet and a complex multiplet centred at δ_P = –18.6 ($^3J_{PP}$ = 61.1 Hz) and –45.9 ppm or δ_P = 4.8 ($^3J_{PP}$ = 20.7 Hz) and –46.2 ppm for $\mathbf{3^{Ph}}$ and $\mathbf{3^{tBu}}$ respectively. The latter of these resonances corresponds to the secondary phosphine groups as can be shown by the upfield resonance compared to the tertiary phosphine environment observed in **1** and the splitting by $^1J_{PH}$ = 211.0 and 208.4 Hz respectively in the ^{31}P NMR spectra, characteristic of secondary phosphine resonances.[12] The ^1H NMR spectrum shows

the R_2PH protons as doublets of triplets centred at δ_H = 4.22 ($^1J_{HP}$ = 211.0 Hz) and 4.16 ($^1J_{HP}$ = 208.4 Hz, $^3J_{HH}$ = 6.8 Hz) ppm respectively. The remaining resonances are of little diagnostic value with respect to coordination and reactivity.

The higher σ- basicity of alkyl phosphines make it desirable to substitute the phenyl rings with alkyl chains. Analogous reactions with alkylphosphines or alkyl(benzyl) phosphines gave no indication of any hydrophosphination products, it appears that the relatively electron rich phosphines do not undergo hydrophosphination under the conditions studied. Helm demonstrated that the diphosphido species may undergo nucleophilic attack to generate a terminal alkyl-aryl phosphine.[11] Treatment of these compounds with Li in an analogous procedure to that carried out in the synthesis of **3** failed to yield the desired $PH(alkyl)_2$ compounds. The P-C cleavage in this case was found to lack the requisite selectivity for the aryl substituent. Finally, attempts were made to cleave both phenyl groups under similar conditions, which would provide terminal diphosphido compounds which may subsequently be alkylated with various electrophiles. However, following prolonged exposure to Li or Na/NH_3 the desired species were not observed spectroscopically. It seems likely that coulombic repulsions of **2** with the reactive metals prevents further phenyl cleavage reactions.

Cyclisation reactions with 'hard' metal templates

Alkaline earth metals as transient templates

A prime consideration for the choice of template is the ability to dissociate the macrocyclic ligand, thus, it is important to consider the reaction kinetics. High rates of dissociation/substitution are desirable, and thus alkaline earth metals are an attractive system for consideration. Helm demonstrated that linear lithium α,ω-diphosphides (**2^{Ph}**) can be cyclised under high dilution conditions;[4] it is anticipated that metathesis of **2** with a group 2 metal halide or deprotonation of **3** with an alkaline earth metal base would result in an analogous alkaline earth metal diphosphide (equivalent to the well-known *bis*-dialkylamide

complexes).[13] This approach is conceptually similar to the Cs thiolate templated macrocycle synthesis pioneered by Kellog and Butler.[14] Use of a divalent cation will inevitably bring the reactive phosphides within close proximity and therefore reduce the possibility of competing oligomerisation by-products. Furthermore, the potential for coordination of the tertiary phosphine to the metal centre may improve the stereoselectivity *via* a 'transient template effect'. Reaction of this α, ω - diphosphide with a suitable electrophilic reagent, such as ethylene sulfate, will result in macrocycle formation and concurrent precipitation of an insoluble salt (Scheme 5).

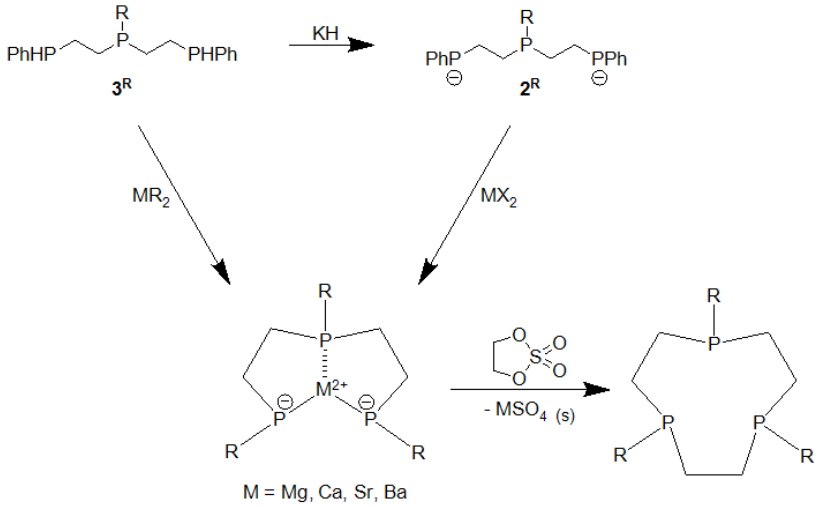

Scheme 5: 'Transient template' methodology to P_3 macrocycles

It is likely that the success of this approach will depend on balancing the two conflicting parameters of size and 'softness'. In order to improve stereoselectivity, a strongly σ-basic trialkyl phosphine must coordinate to the metal ion. There is some evidence for the existence of these species, especially with the relatively 'soft' heavier group 2 metals but due to the highly labile phosphine the complexes are very unstable.[15] Moreover, Müller has shown that trialkylphosphine complexes of Mg can be stabilised by exploiting chelating ligands,[16] it seems plausible therefore that some degree of coordination of the neutral phosphine may occur with many of the alkaline earth metals. Conversely, the only examples of group 2 metals with 'hard' phosphide ligands exist with the lighter elements in the group, although

even these are rare.[17–19] Additionally, the size/dimensions of the ions vary greatly down the group and so, the propensity for chelate formation is also variable.

Deprotonation of the secondary phosphine enhances nucleophilicity at P and produces a donor ligand more suited to coordination to a 'hard' metal centre. In some cases, deprotonation *in situ* with a strong base is sufficient; however, it is advantageous to isolate **2** prior to reaction with the appropriate metal centres. This can be readily achieved *via* the action of very strong bases such as ^{n}BuLi or Na(dimsyl). However, the stoichiometry of these reactions must be controlled with great care as any excess metal alkyls are difficult to remove and may hinder subsequent reactivity. A superior methodology is to deprotonate using an alkali metal hydride, which can be easily removed by filtration. Reaction of **3** with KH in THF at elevated temperatures quantitatively forms **2** with concurrent evolution of H_2 gas. After filtration the red/orange solution can either be used directly for subsequent reactions or dried to yield an orange microcrystalline powder.

Reaction of **2** with anhydrous MX_2 (M = Mg, Ca, Ba; X = Cl, I) in THF or DMSO gives pale yellow solutions with a fine white solid suspended therein. As discussed above the P donors are not expected to interact strongly with the group 2 cations; accordingly, there is a negligible shift in the resonances observed by $^{31}P\{^{1}H\}$ NMR spectroscopy but cation exchange is assumed on the basis of the observed colour change.

Direct formation of such species with alkaline earth metal bases was also investigated. **3** was found to be unreactive with CaH_2 even after heating to reflux, likely a result of the reduced basicity of CaH_2 compared to KH. However, treatment of **3** with an equimolar quantity of $Mg^{i}Pr_2$ gives a pale yellow solution with a beige precipitate. $^{31}P\{^{1}H\}$ NMR spectra indicate the presence of both **2** and **3** in this solution.

These materials were found to be highly unstable; further characterisation was not attainable and these solutions were used directly in cyclisation studies. Treatment of these materials with various dielectrophiles (ethylene sulfate, dichloroethane, dibromoethane,

dibromopropane and α,α'-dibromo-*o*-xylene) in either THF or DMSO gave oily residues after filtration and removal of the solvent. No macrocyclic products could be identified by either NMR spectroscopy or mass spectrometry and the resultant oily residues most likely consist of oligomeric species. Given the polar nature of the solvents it is likely that the bonding between the phosphides and the metal centres is largely ionic in nature. There is very little evidence for the formation of discrete M-P bonds and thus this methodology does not afford the desired level of chemoselectivity to necessitate further investigation.

Fe piano stool complexes

Previous work within the Edwards group has shown Fe piano stool complexes to act as excellent templates for the stereoselective formation of triphosphorus macrocycles (*vide supra*).[20] As triphosphine species were spectroscopically detected as intermediates in these reactions the analogous chemistry with **3** was investigated in order to better understand the reactivity with respect to macrocyclisation. Two-fold deprotonation of the triphosphine piano stool complex was predicted to form an anionic diphosphido complex, $[FeCp(\mathbf{2})]^-$, which upon treatment with various dielectrophiles would furnish macrocyclic products. Alternatively, reaction with vinyl and allyl halides can be envisioned to produce complexes structurally related to the intermediates identified by Edwards,[3] which could be converted to the macrocycles *via* hydrophosphination of the pendant alkenes.

Synthesis

Photolysis of an acetonitrile solution of $[Fe(Cp)(CO)_2(NCMe)]^+$ (where Cp = $C_5H_5^-$, $C_5Me_5^-$ or $C_5H_3(SiMe_3)_2^-$) in the presence of $\mathbf{3^R}$ delivers the corresponding iron piano stool template compounds, $[Fe(Cp)\mathbf{3^R}]^+$, in high yield. Examination of the $^{31}P\{^1H\}$ NMR spectra indicate a mixture of the various isomers in all cases. The tertiary phosphine environments appear in the range 117 - 153 ppm, whereas the secondary phosphines are observed between 60 – 86 ppm. The *meso*- isomers appear as an apparent triplet and a pair of double doublets as expected of an AMX spin system, while the *syn*- and *anti*- isomers display the typical AB_2

patterns. Examination of the ^{1}H and ^{13}C NMR spectra of [Fe(Cp)**3**^{R}]$^{+}$ suggests a degree of fluxionality as broad resonances are observed even at temperatures down to -80 °C, probably as a result of the relatively flexible ligand backbone.

Reactivity

Due to its favourable solubility in appropriate solvents, [Fe(C_5Me_5)**3**^{tBu}]PF_6 was used as a model system for further reactivity with respect to macrocycle formation. Surprisingly, treatment of this compound with an excess (≥4 equivalents) of ^{n}BuLi does not yield the analogous anionic diphosphido species, resulting instead in the formation of a highly air and moisture sensitive dark red material which is readily soluble in hydrocarbon solvents.

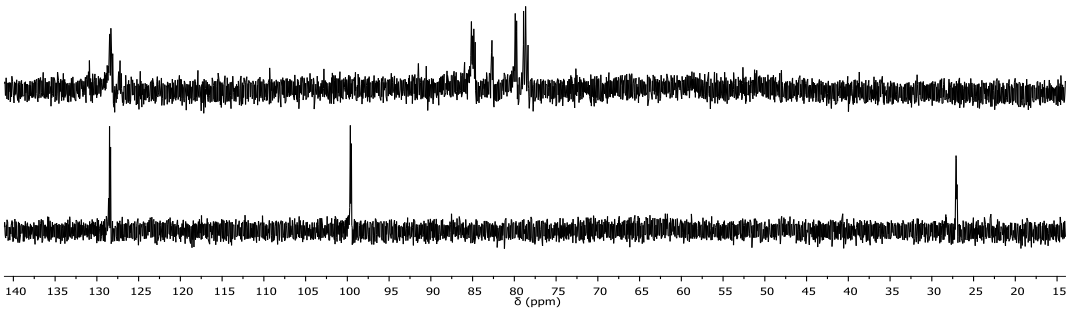

*Figure 2: $^{31}P\{^{1}H\}$ NMR spectra of [Fe(C_5Me_5)**3**^{tBu}]$^{+}$ (top) and after reaction with excess BuLi (bottom)*

The $^{31}P\{^{1}H\}$ NMR spectra (Figure 2) suggests three distinct P environments. Two downfield resonances, a doublet of doublets (δ_P = 128.3 ppm, $^{3}J_{PP}$ = 14.7, 11.9 Hz) and a doublet (δ_P = 99.4 ppm, $^{3}J_{PP}$ = 14.7 Hz), are reminiscent of the tertiary and secondary phosphines of the precursor respectively, while an upfield doublet (δ_P = 26.9 ppm, $^{3}J_{PP}$ = 11.9 Hz) is also observed. The presence of secondary phosphine environments is shown by a large splitting of the peak at δ_P = 99.4 ppm ($^{1}J_{PH}$ = 339.5 Hz) in the ^{31}P NMR spectra. The upfield peak does not appear to have any strong coupling to ^{1}H nuclei and has thus been attributed to a phosphido group. The spectroscopic evidence suggests deprotonation only occurs at one of the two chemically identical secondary phosphines to yield an unusual phosphido-phosphine complex (Scheme 6). Further characterisation (IR, mass spectrometry, elemental analyses)

was attempted but no reasonable data could be attained due to the instability of the material. The proposal of a neutral complex is further supported by its solubility in non-polar solvents (petroleum ether, toluene, diethyl ether) in contrast to the ionic precursor.

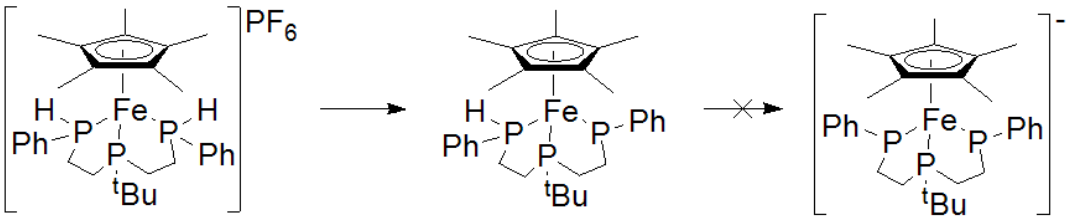

Scheme 6: Deprotonation of Fe piano stool complex

The presence of a secondary phosphine environment is surprising given the large excess of strong base used. Furthermore, DFT calculations confirm that the deprotonation of such a species with a monomeric butyl anion in a THF solvent field is thermodynamically favourable (ΔG = -272.0 KJ mol^{-1}) and therefore the lack of reactivity can be ascribed to kinetic deactivation rather than any inherent decrease in reactivity. Upon examination of the frontier molecular orbitals, it is clear that the HOMO is largely centred on the phosphido group and projects into the space between the two terminal phosphorus atoms (Figure 3); the proximity of this electron density to the remaining secondary phosphine may introduce a prohibitively high activation barrier with respect to further deprotonation by anionic bases.

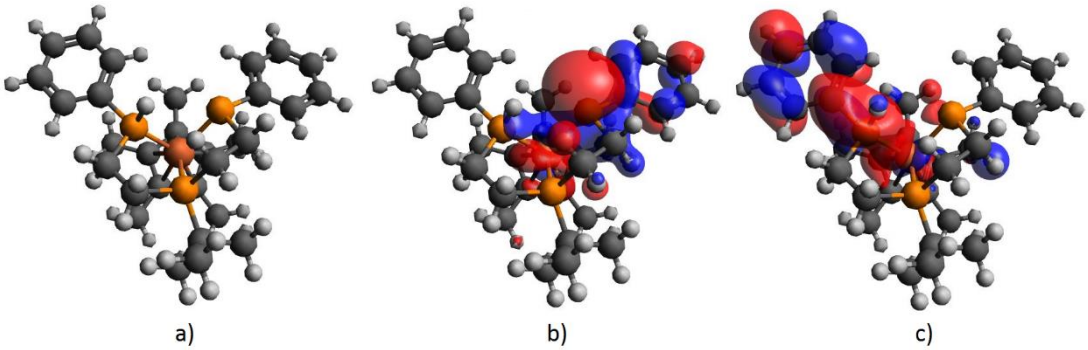

Figure 3: a) Optimised structure of Fe Piano stool cation b) HOMO c) LUMO

To further examine the reactivity of this remaining secondary phosphine moiety, the solutions were treated with various strong bases (potassium hydride, ^{t}BuLi, LDA or KO^{t}Bu) but no further reaction was witnessed in any case. Attempts to protonate the phosphido

group with deoxygenated saturated aqueous NH_4Cl solution or NH_4PF_6 thus reforming $[Fe(C_5Me_5)\mathbf{3}^{tBu}]^+$, led to decomposition to an intangible brown solid. Likewise, attempts to alkylate this material with a variety of mono and dielectrophilic reagents failed, no reasonable structure could be assigned to the resulting materials.

Coordination chemistry of *tert*butyl*bis*(2-phenylphosphinoethyl)phosphine

Due to this unfavourable reactivity coupled with the well-known problems associated with dissociating macrocyclic phosphine ligands from Fe-piano stool templates,[3] the coordination chemistry of **3** with other transition metals was assessed in an effort to identify novel templates for macrocycle formation. The *tert*butyl derivative was chosen as the basis for these studies as its larger steric bulk is likely to favour macrocycle formation due to the Richman-Atkins effect.

Template Survey

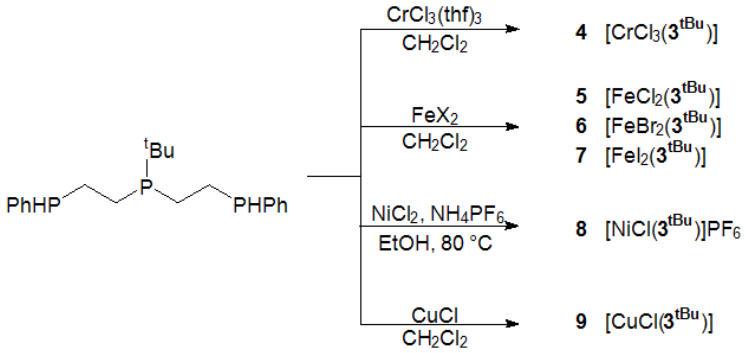

Scheme 7: Coordination chemistry of ligand ***3^{tBu}***

Initial studies of the reactivity of $\mathbf{3}^{tBu}$ with respect to selected first row transition metals have been carried out (Scheme 7) and the products characterised by spectroscopic and analytical techniques (Table 1). IR spectroscopy is an invaluable tool for the characterisation of secondary phosphine complexes as the energy of the characteristic ν_{P-H} stretching mode is increased upon coordination due to the increased s character of the P–H bond.[21,22] In all cases, coordination of the secondary phosphine function can be identified by a significant

increase in the P–H stretching frequency of between 32 – 108 cm^{-1}. In order to gain further insights into the coordination chemistry of **3** the structures of **4**-**9** were evaluated computationally. In all cases the optimised structures were found to have only a negligible energetic difference between the *syn*-, *anti*- and *meso*- isomers. Hence, it is likely that complexes **4**-**9** exist as statistical mixtures of the various diastereomers.

*Table 1: Characterisation data for **3-9***

Compound	Appearance	Elemental analysis / %				δ_P / ppm		ν_{P-H} /cm^{-1}	λ (ε)	Λ_m / Scm^2mol^{-1}
		C		H						
		Calcd.	Found	Calcd.	Found	PR_3	PHR_2			
$\mathbf{3^{tBu}}$	Colourless oil	66.3	66.4	8.1	8.2	4.8	–46.2	2278	–	–
$CrCl_3(3^{tBu})$	Blue solid	46.1	46.0	5.6	5.5	–	–	2361	616 (715)	30.7
$FeCl_2(3^{tBu})$	Red solid	49.1	48.8	6.0	6.0	126.3	88.0, 78.2	2318	–	28.5
$FeBr_2(3^{tBu})$	Red–brown solid	41.6	41.8	5.1	5.1	119.5	87.9, 80.3	2325	–	28.2
$FeI_2(3^{tBu})$	Purple solid	35.8	35.9	4.4	4.5	124.5	100.6, 93.3	2319	–	49.9
$[NiCl(3^{tBu})]^+$	Brown solid	39.9	40.1	4.9	5.0	133.6, 135.9	67.8	2337	416 (980)	80.5
$CuCl(3^{tBu})$	White solid	52.1	51.9	6.3	6.5	39.9	12.5, –43.6	2310	–	5.3

Treatment of a suspension of $Cr(thf)_3Cl_3$ in methylene chloride with $\mathbf{3^{tBu}}$ results in the formation of a dark blue paramagnetic material, **4**, which exhibits similar physical behaviour to the related *mer*-(triphos)$CrCl_3$ (where triphos = $PhP(CH_2CH_2PPh_2)_2$).[23] The 1:1 stoichiometry is confirmed by elemental analysis and a strong molecular ion ($[M–Cl+MeOH]^+$, 516.0527) with the appropriate isotopic distribution is observed in the mass spectrum. Solutions of **4** in acetone are not strongly conductive (Λ_m = 30.7 Sm^2mol^{-1}) suggesting that

the chloride ligands remain coordinated under these conditions. Interrogation of the IR spectrum of **4** reveals a weak peak (ν_{P-H}) at 2361 cm^{-1} and the magnetic moment (μ_{eff} = 3.6 μ_B) is consistent with an octahedral d^3 metal ion.

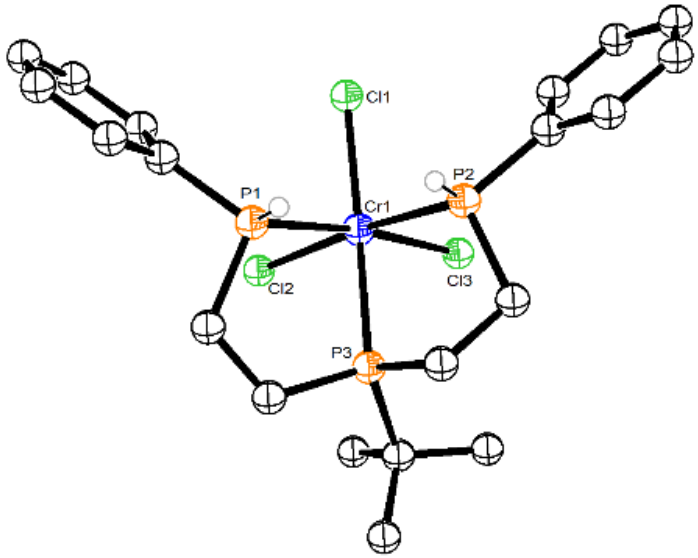

*Figure 4: ORTEP representation of the structure of **4**. Selected bond lengths (Å) and angles (°): Cr1-P1 2.4536 (16), Cr1-P2 2.4536 (15), Cr1-P3 2.4858 (14), Cr1-Cl1 2.3132 (16) Cr1-Cl2 2.3274 (15), Cr1-Cl3 2.3100 (16), P1-Cr1-P2 88.63 (5), P1-Cr1-P3 78.01 (5), P2-Cr-P3 80.53 (5), P1-Cr1-Cl3 170.34 (6), P2-Cr1-Cl2 169.55 (6), P3-Cr1-Cl1 164.50 (8)*

Crystals of **4** were grown from a methylene chloride/diethyl ether solution at –25 °C. An ORTEP diagram of the X–ray crystal structure is shown in Figure 4. The neutral complex consists of a distorted octahedral Cr centre with the *syn*–triphosphine ligand coordinated in a facial manner. The average Cr–P and Cr–Cl bond lengths (2.464 and 2.317 Å respectively) are typical and resemble those of the related compound *mer*–$CrCl_3(P(CH_2CH_2PPh_2)_3)$.[23] The Cr–P3 bond is marginally elongated with respect to the Cr–P1/2 bonds likely due to the higher steric bulk at the central position. The structure shows a distinct distortion which can be attributed to the strain incumbent in the two chelate rings. The *trans*– P–Cr–Cl bond angles range from 170.3 ° to 164.4 ° and the bite angles of the two chelate rings are 78.0 ° and 80.5 °. Analysis of the extensive literature on Cr complexes reveals that complexes of this type usually show a marked preference for either *fac*- or *mer*- geometries for any given

ligand set.[24] Facial binding of the triphosphine is advantageous as this minimises the P(H) – P(H) distance and thus provides the optimum geometry for macrocycle formation. Interestingly, Levason and co–workers obtained exclusively *mer*–Cr(triphos)X_3 (where X = F, Cl, Br) using an identical procedure.[23] To our knowledge, no other chelating triphosphine of the general form $RP(CH_2CH_2PR_2)_2$ (where R denotes various alkyl and aryl groups) has been found to bind in a *fac*– geometry. The differing steric bulk present at the terminal phosphine positions may explain the observed dissimilarities between these two ligands as relatively small secondary phosphines present in **3** allow the P centres to be placed in a *cis*– position with respect to one another without inducing a prohibitive steric repulsion between the arms of the ligand. Furthermore, Levason reported that complexes containing facially coordinated triphosphine ligands tend to exhibit greater sensitivity to moisture. Contrarily, **4** appears to be entirely air and moisture stable as no decomposition is observed even upon suspension in water for prolonged periods. This may be due to decreased steric strain incumbent within the coordination sphere. The calculated structure of the chromium complex, **4**, displays the expected octahedral geometry and there appears to be no significant thermodynamic preference for either *fac*- or *mer*- coordination of the ligand. Calculated bond lengths and angles are generally in good agreement with those measured by crystallographic means.

Addition of $\mathbf{3^{tBu}}$ to FeX_2 (X= Cl, Br, I) in methylene chloride leads to the immediate formation of diamagnetic non–conductive red (**5**, **6**) or purple (**7**) solutions. The properties of these materials appear in stark contrast to the analogous triphos complexes which are found as either colourless polymeric materials[25] or paramagnetic complexes (μ_{eff} = 4.8 μ_B)[26] for the chloro– and bromo– analogues respectively. Similarly, the phenyl(*bis*(2–(dimethylphosphonityl)ethyl)phosphine complex, $FeCl_2(PhP(CH_2CH_2P(OMe)_2)_2)$, is a paramagnetic ($\mu_{eff}$ = 5.2 μ_B) conductive brown material.[27] Elemental analyses confirm the empirical formulae as Fe($\mathbf{3^{tBu}}$)X_2 and the $[M–X]^+$ species ($[M–Cl]^+$, 453.0509; $[M–Br]^+$, 497.0015; $[M–I]^+$, 544.9883) are observed in the mass spectrum. The solids are moderately

stable in air but decompose rapidly in solution forming orange/brown precipitates. Conductivity measurements suggest that the complexes are neutral although the higher conductivity of the iodo complex likely reflects the higher lability of the iodide ligands compared to the lighter halides. Three distinct P environments are detected in the $^{31}P\{^{1}H\}$ NMR spectra, all of which are shifted downfield in comparison to the free ligand. The most downfield chemical shifts are associated with the central tertiary phosphine whilst the other two signals are attributable to secondary phosphine environments. Assuming a trigonal bipyramidal geometry, the apparent inequivalence of the secondary phosphine environments suggests that both axial and equatorial positions are occupied with the two secondary phosphines in a mutually *cis* geometry with respect to one another. ^{1}H and ^{13}C NMR spectroscopy is of little benefit to the characterisation of these complexes as only broad resonances are observed, even at low temperatures (–80 °C). The flexibility of the ligand may result in a high degree of fluxionality although the existence of solution phase equilibria with other (paramagnetic) species must also be considered a possibility as must the existence of several stereoisomers. Coordination of the ligand to Fe is further confirmed by examination of the IR spectra which show strong broad peaks at ν_{P-H} = 2318, 2325 and 2319 cm^{-1} for **5**, **6** and **7** respectively.

DFT optimised structures of the iron(II) halide complexes, **5**-**7**, suggest that these species are likely to adopt square pyramidal geometries (Figure 5). This prediction provides a potential explanation of the observed broadening in the NMR spectra as these structures may exist in equilibria with trigonal bipyramidal geometries.

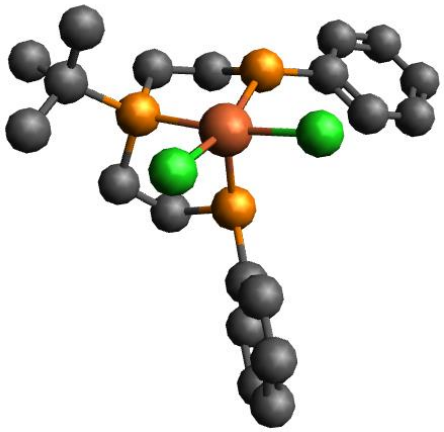

*Figure 5: Structure of Fe(**3**)Cl_2 as calculated by DFT simulations. Hydrogen atoms omitted for clarity*

Reaction of $\mathbf{3^{tBu}}$ with $NiCl_2$ in the presence of NH_4PF_6 in refluxing ethanolic solution leads to the formation of a dark brown diamagnetic material formulated as [Ni($\mathbf{3^{tBu}}$)Cl]PF_6 (**8**) on the basis of elemental analysis. Furthermore, the conductivity of a 1.06 mM solution of **8** in acetone (Λ_m = 80.5 Scm^2mol^{-1}), while relatively low, is consistent with a 1:1 electrolyte.[28] Coordination of the secondary phosphine can be confirmed by the ν_{P-H} stretch in the IR spectrum (2337 cm^{-1}), and the electronic spectrum displays a single absorption band at 416 nm (ε = 980 $M^{-1}cm^{-1}$), characteristic of square planar Ni(II) complexes, a structure which is supported by DFT optimisations of this species (Figure 6).

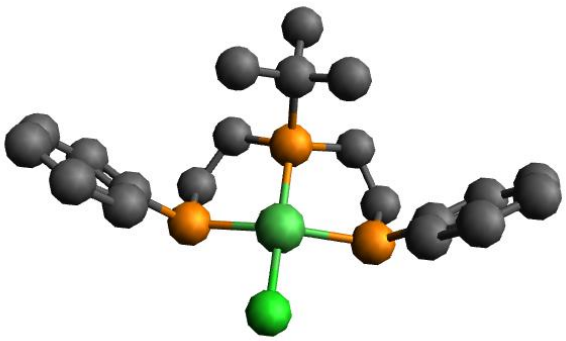

*Figure 6: Structure of [Ni(**3**)Cl]$^+$ as calculated by DFT simulation. Hydrogen atoms omitted for clarity*

At room temperature only the heptet of the PF_6 anion is visible by $^{31}P\{^1H\}$ NMR spectroscopy; however, upon cooling to -80 °C at least 15 separate phosphorus environments are observed. These appear in 2 discrete groups between δ_P = 125–150 ppm and 32–75 ppm for the tertiary and secondary phosphine environments respectively. In the former group, two major resonances are observed as triplets centred at δ_P = 133.6 ppm (*J* = 29.2 Hz) and 135.9 ppm (*J* = 28.3 Hz) with other peaks of low intensity found at δ_P = 143.4, 144.8, 146.8, 148.3 and 150.7 ppm. The major secondary phosphine resonances appear as doublets centred at δ_P = 67.8 ppm (*J* = 26.8 Hz) and 54.5 ppm (*J* = 35.7 Hz) and an apparent triplet centred at δ_P = 65.4 ppm (*J* = 26.7 Hz) while other peaks in this range are found at δ_P = 32.3, 41.1, 62.1, 63.3 and 70.8 ppm. Similar chemical shifts to these have been reported for closely related systems.[29] The ^1H and ^{13}C NMR spectra of **8** are not informative, the resonances are considerably broadened and do not sharpen upon cooling. The complexity observed by NMR spectroscopy must be attributed to solution-phase equilibria whereby rapid interconversion between several related structures; further complicated by the presence of at least 3 distinct stereoisomers; gives rise to the numerous observed resonances. Such fluxional behaviour is reflective of the high degree of flexibility of the ligand backbone.

Addition of a methylene chloride solution of $\mathbf{3^{tBu}}$ to CuCl yields **9** as a white solid. The 1:1 stoichiometry is confirmed by elemental analysis and the molecular ion ($[M–Cl]^+$, 425.0786) is observed in the mass spectrum. The IR spectrum shows an increase in the $\nu_{P–H}$ stretching mode of 32 cm^{-1} to 2310 cm^{-1}; this is the smallest change in vibration frequency upon complexation observed for any of the complexes reported here and may reflect a weaker M–P bond. NMR spectroscopy is complicated by coupling to the quadrupolar ^{63}Cu and ^{65}Cu nuclei (both S = 3/2) which is known to result in broad signals, although it has been shown that this effect can be minimised at high temperature.[30] Indeed, at 140 °C in proteo–*o*–dichlorobenzene signals in the $^{31}P\{^1H\}$ NMR spectrum appear sharper although the fine structure remains unresolved. The ligand appears to display a degree of fluxional behaviour

as numerous peaks attributed to the various κ^3-, κ^2- and κ^1- coordination modes are identified although the two peaks associated with free ligand (δ_P = 4.8, –46.2 ppm) are of very low intensity suggesting that complete dissociation only occurs at highly elevated temperature. The major peaks are recorded at δ_P = 57.4, 45.3, 39.1, 27.5 to 26.1, 16.9 to 14.2, –6.3 and –37.4 to –44.0 ppm. In particular, the broad overlapping resonances between δ_P = –37.4 and –44 ppm are of similar chemical shift to the free ligand and therefore likely arise from uncoordinated secondary phosphines in the κ^2– and κ^1– coordination modes. Likewise, the broad resonance at δ_P = –6.3 ppm is attributed to uncoordinated tertiary phosphines. The presence of uncoordinated phosphines may facilitate equilibria between higher oligomeric species further obfuscating the NMR spectra. The remaining signals are shifted significantly downfield from the free ligand and can thus be assigned as the various coordinated P centres. The peak at δ_P = 45.3 ppm appears as a triplet (J = 41.7 Hz) and can thus be assigned as a tertiary phosphine and it is likely that the other two downfield peaks (δ_P = 57.4 and 39.1 ppm) also arise from tertiary phosphine environments. The remaining two peaks are in the expected range for the coordinated secondary phosphines of the κ^3– and κ^2– coordination modes. It is likely that dissociation of the ligand is facilitated by the high temperatures necessary to attain a reasonable level of resolution in the $^{31}P\{^1H\}$ NMR spectrum although it appears that this occurs to some extent in solution even at room temperature as very broad features can be discerned in the appropriate ranges. Measurement of the $^{31}P\{^1H\}$ NMR spectrum at –80 °C did not noticeably alter the appearance and only broad features were observed. Only two examples of similar chelating triphosphine complexes of Cu(I) have been reported.[31,32] In both cases, the NMR data are broad and the structures are poorly defined. DFT calculations suggest a highly distorted tetrahedral structure for **9** (Figure 7). The P-Cu-P bite angles are calculated to be *ca*. 88 °, a significant contraction from the ideal tetrahedral bond angle. The difference in this case can likely be ascribed to the steric restraints imposed by the chelate rings. Nonetheless, this is likely to introduce a significant amount of strain

within the molecule which may account for the ligand dissociation observed in solution. This strain is further demonstrated by an elongation of the Cu-P bond lengths when compared to related tetracoordinate Cu(I) species.[33]

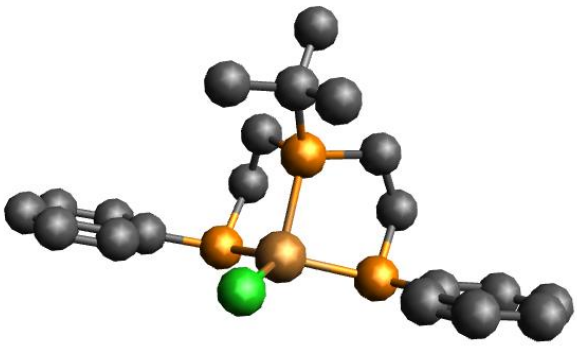

*Figure 7: Structure of Cu(**3**)Cl as calculated by DFT simulations. Hydrogen atoms omitted for clarity*

Analogous reactions of $\mathbf{3}^{\mathbf{tBu}}$ with $MnCl_2$ and $CoCl_2$ failed to yield clearly defined products. In the case of the reaction with $MnCl_2$, only starting materials were recovered which is perhaps unsurprising as to our knowledge there are no known MnP_3X_2 (where P = Phosphine, X = halide) complexes. The reaction with $CoCl_2$ yields a dark green paramagnetic solid. IR spectroscopy confirms coordination of the ligand (ν_{P-H} = 2345 cm^{-1}) but despite elemental analyses and mass spectrometry, the identity of this material remains elusive.

Reactivity with respect to macrocycle formation

Facial coordination of the triphosphine is thought to be a prerequisite for macrocycle formation, thus the Cr, Fe and Cu complexes have potential as novel templates. However, the observed dissociation of the triphosphine in the Cu complex **9** is likely to be problematic as this is likely to lead to polymeric side products.

Treatment of a THF solution of the Cr complex **4** with 2 equivalents of LDA at –78 °C results in formation of a dark green solution. Following treatment with 1,2-dichloroethane the green colour persists. Upon warming to room temperature an insoluble precipitate forms. The material appears to be highly unstable towards both air and moisture and no products could be reliably identified in the mass spectrum. It is known that the ionic radius of the template

is an important factor determining the minimum accessible ring size (*vide supra*) as the terminal P-P distance must be matched to accommodate the dielectrophilic reagent. Accordingly, the reactivity of this system with α,α'-dibromo-*o*-xylene was studied. The rigid 4 carbon bridge may be more favourable towards cyclisation, the result of which would be an 11-membered triphosphine species. Treatment of **4** in Et_2O with 2 equivalents of BuLi at –100 °C again resulted in a green solution. Addition of α,α'-dibromo-*o*-xylene gives an orange solution and a dark coloured precipitate which appears unchanged upon warming to room temperature. Again, no products were readily identified by mass spectrometry and the identity of these species cannot be assigned with any certainty. Orange-red colours are often associated with Cr(VI) compounds. Oxidation of the Cr ion may occur either by the action of adventitious oxygen or by disproportionation of two Cr(III) centres.

Treatment of **5** with 2 equivalents of KO^tBu in THF yields a brown solution which upon reaction with 1,2-dichloroethane and removal of the solvent gives a poorly defined brown solid. Interrogation of the ^{31}P and ^{1}H NMR spectra shows only very broad features. Furthermore, no macrocyclic species could be identified by mass spectrometry. Analogous reactions with **6** and **7** also failed to yield the desired macrocyclic products.

A common feature of these complexes are the halide co-ligands, formation of a macrocycle around these complexes would be beneficial as the halide ligands are relatively easily substituted for other anionic and neutral ligands allowing for the study of a broad range of reactivity. Unfortunately, it appears that this same reactivity may play a role in the apparent decomposition of the intermediary species. Deprotonation of the secondary phosphine ligand in **4** – **7** gives rise to putative anionic species. It is reasonable that the halide ligands in such complexes would dissociate resulting in coordinatively and electronically unsaturated complexes. Such species are expected to be extremely unstable and are likely to rapidly decompose under normal conditions. These complexes do not appear to display the level of stability necessary for successful macrocycle formation.

Cationic Cu complexes

Replacement of the X type halide donors with neutral L type ligands should yield materials which are less prone to competing side reactions. Specifically, Cu(I) complexes are of particular interest as templates for macrocycle formation. Cu(I) is a d^{10} ion with inherently fast reaction kinetics comparable to the main group metals. Furthermore, oxidation to Cu(II) introduces a Jahn-Teller distortion which radically increases the lability of the ligands. Coordination of a linear triphosphine to a Cu(I) centre is envisioned to produce a tetrahedral complex where the P_3 ligand occupies one face. It is anticipated that the coordination sphere will remain sufficiently flexible to accommodate a range of dielectrophiles allowing for the synthesis of a number of macrocyclic ring systems. Oxidation of the metal would induce significant distortions in the coordination sphere allowing for displacement of the poorly suited phosphine ligand by hard chelating agents such as EDTA.

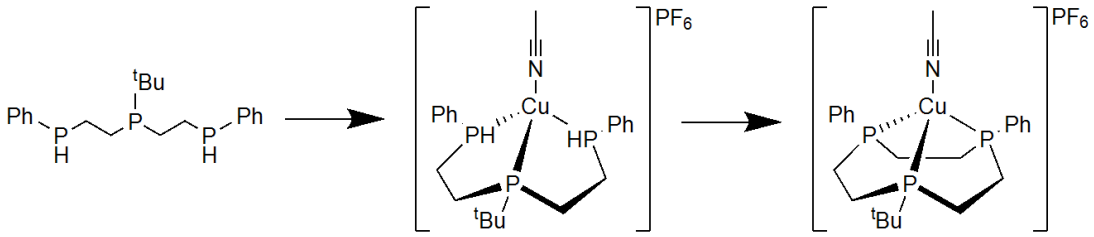

10

Scheme 8: Synthetic route to Cu-Macrocycles

Reaction of **3^{tBu}** with $[Cu(NCMe)_4]PF_6$ gives **10** as a hygroscopic white powder (Scheme 8). As with the chloro complex, **9**, NMR spectra of **10** are very broad. However, no improvement in resolution could be attained by measurement of the spectra at either high or low temperature. The ^{1}H NMR spectrum displays only broad features associated with the aromatic and aliphatic hydrogen environments. The PH environments are apparent as a broad doublet centred at δ_H = 5.41 ($^1J_{HP}$ = 316.8 Hz) ppm. The downfield shift compared to the free ligand (**3^{tBu}**, δ_H = 4.16 ($^1J_{HP}$ = 208.4 Hz) ppm) confirms coordination and deshielding

of the secondary phosphine moieties. The $^{31}P\{^{1}H\}$ NMR spectrum shows two broad features at δ_P = 34.9 and -31.6 ppm, which are consistent with Cu coordination of the tertiary and secondary phosphines respectively. This is further confirmed by examination of the IR spectrum, which displays a shift in the $\nu_{P\text{-}H}$ stretching mode to 2311 cm^{-1}. A second absorption is detected at $\nu_{P\text{-}H}$ = 2274 cm^{-1} which can be attributed to the uncoordinated secondary phosphine suggesting that the ligand may undergo dissociation. This observation is supported by the presence of some very weak signals in the $^{31}P\{^{1}H\}$ NMR spectrum reminiscent of **3^{tBu}**. Satisfactory elemental analyses could not be attained for this complex, although the parent ion is observed in the mass spectrum (**10** = 466.1044, $[M]^+$ = 466.1045). Treatment of a THF solution of **10** with KO^{t}Bu generates an orange solution, suggesting deprotonation of the secondary phosphines. Treatment of this solution with dielectrophilic reagents (Scheme 9) causes the colour to fade and a fine white precipitate to form. Filtration and removal of the solvent yielded white powders. ^{1}H spectra of this material do not appear to show PH environments and new broad features are observed in the $^{31}P\{^{1}H\}$ NMR spectra between 20 and 60 ppm consistent with tertiary phosphines bound to Cu(I). Furthermore, mass spectra of these materials show strong peaks compatible with **11** and **12** (*m/z* = 492.1197 and 568.1493 respectively). Satisfactory elemental analyses could not be attained, but taken together, this is compelling evidence for the Cu(I) templated synthesis of macrocyclic ligands.

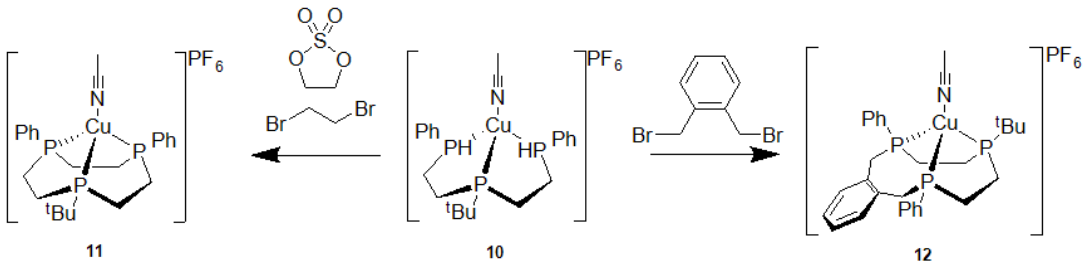

Scheme 9: Synthesis of macrocyclic phosphines

Attempts were made to demetallate the macrocycle directly by treating this compound with a concentrated aqueous NaOH solution. However, after prolonged heating for several days

the material appears unchanged and thus oxidation of the Cu ion was investigated in an effort to liberate the free ligand. **12** was mixed with 1 equivalent of ferrocenium hexafluorophosphate and the dark blue solution gradually turns yellow/green at which time an excess of EDTA was added and the solution stirred briefly. Following removal of the solvent and extraction of the residue with methylene chloride, no P containing species where detected by NMR spectroscopy. Furthermore, mass spectral analysis of the residue did not reveal the presence of any oxidised macrocycles. Aqueous solutions of **12** exposed to atmospheric oxygen exhibited the blue hue typical of Cu(II) species, however, free macrocycle or any of its oxides could not be detected by any spectroscopic technique.

Conclusion

In conclusion, the synthesis of triphosphine macrocycles *via* the ring closure of a linear triphosphine around a metal template has been investigated. An efficient synthetic route to α, ω – disecondary phosphines was developed in order to facilitate these studies. The use of alkaline earth metal ions as templates failed to provide adequate selectivity to prevent polymerisation. A series of Fe piano stool complexes were synthesised but were unable to be converted to the diphosphido species resulting instead in the production of an unusual phosphino-phosphido compound. The reactivity of this species was examined by experimental and computational techniques but no macrocyclic ligands were prepared. A survey of the coordination chemistry of these α, ω – disecondary phosphines was carried out. The ligand was found to be extremely flexible and able to accommodate a range of metal ions and geometries. In some cases, the ligand was observed to be dynamic in solution and numerous species were identified spectroscopically. Attempts to cyclise the phosphine ligand in these cases resulted in decomposition due to the highly reactive template moieties. Attention was subsequently turned to a cationic Cu(I) template which was shown to support the desired cyclisation reactions. Unfortunately, initial attempts to selectively oxidise the

metal centre and isolate the free macrocyclic ligands failed. Nonetheless, this methodology appears to be a promising basis for future studies.

Experimental

General considerations

All synthetic procedures and manipulations were performed under dry nitrogen using standard Schlenk line techniques. Solvents were freshly distilled from sodium (petroleum ether, toluene), sodium/benzophenone (tetrahydrofuran, diethyl ether) or calcium hydride (dichloromethane, ethanol, acetonitrile) under N_2 before use. ^{1}H (500 or 400 MHz) NMR spectra were obtained on Bruker 500 or 400 spectrometers whilst the ^{31}P (121.7 MHz) and ^{13}C (75.6 MHz) NMR spectra were recorded on a Jeol Eclipse 300 spectrometer. Chemical shifts were determined relative to 85% H_3PO_4 (δ_P = 0 ppm) or tetramethylsilane ($\delta_{H/C}$ = 0 ppm) and are reported in ppm. Infrared spectra were recorded either as KBr disks on a Jasco FT/IR-660 Plus spectrometer or on a Shimadzu IRAffinity-1S spectrometer equipped with an ATR attachment. Mass spectra were obtained on a Waters LCT Premier XE mass spectrometer at Cardiff University. UV–Vis absorption spectroscopy was performed on a Perkin Elmer Lambda 20 UV/Vis spectrometer or a Shimadzu UV-1800 spectrometer in methylene chloride solutions (10^{-4} M). X-ray crystallography was carried out by Dr B. Kariuki, Cardiff University. Magnetic susceptibility measurements were carried out using a Sherwood Scientific MK 1 Magnetic Susceptibility Balance at 21 °C. Conductivity was measured on a Hanna HI 8733 conductivity meter in acetone or methylene chloride solutions (10^{-4} M). Elemental analysis was carried out by the elemental analysis service at London Metropolitan University. *Tert*butyldivinylphosphine,[34] anhydrous iron(II) iodide,[35] $CrCl_3(thf)_3$,[36] $[Fe(C_5H_5)(CO)_2(NCMe)]BF_4$ and $[Fe(C_5R_5)(CO)_2(NCMe)]PF_6$[37] were prepared according to the literature procedures. Diphenylphosphine was prepared by the action of $LiAlH_4$ on Ph_2PCl.

Freshly cut Li was washed successively with petroleum ether prior to use. All other chemicals were obtained commercially and used as received.

DFT calculations

Density functional theory calculations were carried out using the Gaussian 09 package.[38] Proposed structures were initially optimised using the Universal Forcefield (UFF) molecular mechanics forcefield.[39] The resultant structures were then subjected to DFT geometry optimisations using the B3LYP hybrid functional[40–42] with the Stuttgart/Dresden basis set and pseudo core potentials for all heavy atoms (Z>20) and 6-31G(d,p) basis set on all other atoms. Vibrational frequency analysis was performed on the optimised structures to confirm that the structures were minima.

Synthesis of *tert*butyl*bis*(2–(diphenylphosphino)ethyl)phosphine, $\mathbf{1^{tBu}}$

To a mixture of *tert*butyldivinylphosphine (23.2 g, 149 mmol) and diphenylphosphine (120 mL, 690 mmol) held at 130 °C was added ABCN in small portions (ca. 5 mg) over a period of 4 hours. Excess diphenylphosphine and other volatiles were removed *in vacuo* at 150 °C to yield *tert*butyl*bis*(2-(diphenylphosphino)ethyl)phosphine as a colourless oil (68.5 g, 130 mmol, 87 %).

δ_H (400 MHz, $CDCl_3$) 0.98 (9H, d, $^3J_{PH}$ = 11.4 Hz, ^{t}Bu), 1.39–2.22 (8H, m, CH_2CH_2), 7.37–7.51 (20H, m, Ph); δ_C (75.6 MHz, $CDCl_3$) 19.5 (dd, $^1J_{CP}$ = 20.3 Hz, $^2J_{CP}$ = 15.3 Hz), 25.8 (dd, $^1J_{CP}$ = 20.3 Hz, $^2J_{CP}$ = 13.7 Hz), 27.0 (d, $^2J_{CP}$ = 13.1 Hz), 28.0 (d, $^2J_{CP}$ = 12.8 Hz), 128.2, 132.4, 133.6, 138.1; δ_P (121.7 MHz, $CDCl_3$) –12.3 (d, $^3J_{PP}$ = 33.5 Hz, PPh_2), 9.5 (t, $^3J_{PP}$ = 33.5 Hz P^{t}Bu)

Synthesis of *tert*butyl*bis*(2–(phenylphosphino)ethyl)phosphine, $\mathbf{3^{tBu}}$

A solution of $\mathbf{1^{tBu}}$ (10.0 g, 18.9 mmol) in THF (75 mL) was transferred onto Li pieces (5 g, 720 mmol) and briefly stirred. The reaction flask was irradiated in an ultrasonic bath held at 0 °C for up to 4 hours. The reaction was followed by ^{31}P NMR spectroscopy. Once all of $\mathbf{1^{tBu}}$ was consumed the resultant red solution was filtered from the Li before treatment with minimal

deoxygenated, saturated aqueous NH_4Cl. The mixture was filtered, and the solvents removed *in vacuo*. The residues were redissolved in DCM and dried over $MgSO_4$. Removal of solvent and other volatiles *in vacuo* at 150 °C yielded *tert*butyl*bis*(2-(phenylphosphino)ethyl)phosphine as a viscous colourless oil (4.45 g, 65 %). Found: C, 66.4; H, 8.2. $C_{20}H_{29}P_3$ requires C, 66.3; H, 8.1; ν_{max}/cm^{-1} 3067 (CH), 3050 (CH), 2933 (CH), 2278 (PH); δ_H (300 MHz; $CDCl_3$) 0.88 (9H, d, $^3J_{HP}$ = 11.4, ^{t}Bu), 1.33-1.52 (4H, m, CH_2PH), 1.83 (4H, m, ^{t}BuPCH_2), 3.81-4.50 (2H, dt, $^1J_{HP}$ = 208.1, $^3J_{HH}$ = 6.8 ppm, PH), 7.2 –7.4 (10H, m, Ph); δ_C (75.6 MHz, $CDCl_3$) 15.43, 22.81, 27.59, 28.58, 128.60, 133.18, 133.91, 135.21; δ_P (121.7 MHz, $CDCl_3$) – 46.2 (dm, $^1J_{PH}$ = 208.1, PH), 4.8 (t, $^3J_{PP}$ = 20.7, ^{t}BuP); *m/z* (ES+) 363.1558 ($[M+H]^+$, $C_{20}H_{30}P_3$ = 363.1560)

Synthesis of phenylbis(2–(phenylphosphino)ethyl)phosphine, 3^{Ph}

This compound was prepared similarly to **3^{tBu}** from phenyl*bis*(2-diphenylphosphinoethyl) phosphine (73 %).

Found: C, 69.2; H, 6.7. $C_{22}H_{25}P_3$ requires C, 69.1; H, 6.6; ν_{max}/cm^{-1} 3051 (CH), 2903 (CH), 2280 (PH); δ_H (300 MHz; $CDCl_3$) 1.63-2.02 (8H, m, CH_2), 4.22 (2H, d, $^1J_{HP}$ = 211.0 Hz, PH), 7.28–7.55 (15H, m, Ph); δ_C (75.6 MHz, $CDCl_3$) 19.1, 25.9, 128.3, 128.7, 132.0, 132.2, 133.5, 134.6; δ_P (121.7 MHz, $CDCl_3$) –45.9 (dm, $^1J_{PH}$ = 211.0, PH), -18.6 (tt, $^3J_{PP}$ = 61.1 Hz, *J* = 18.0 Hz, PhR_2P)

General synthesis of Fe piano stool complexes

A solution of $[Fe(C_5H_5)(CO)_2(NCMe)]BF_4$ (84 mg , 0.28 mmol) and **3** (0.28 mmol) in acetonitrile (5 mL) was stirred at room temperature under UV irradiation for 24 hours. The resultant red solution was filtered through celite and the solvent removed *in vacuo* to yield the product as a dark brown solid

Cyclopentadienyl *tert*butyl*bis*(2–(phenylphosphino)ethyl)phosphine iron(II) tetrafluoroborate

This material was prepared similarly using $[Fe(C_5H_5)(CO)_2(NCMe)]BF_4$ (84 mg, 0.28 mmol) and **3^{tBu}** (0.1 g, 0.28 mmol) (153 mg, 97 %).

Found: C, 52.6; H, 6.0. $C_{25}H_{34}BF_4FeP_3$ requires C, 52.7; H, 6.0; ν_{max}/cm^{-1} 3054 (CH), 2922 (CH), 2869 (CH), 2298 (PH) ; δ_P (121.7 MHz, acetone–d_6) 68.2 (d, J_{PP} = 29.8 Hz, *syn/anti*-PHR_2), 70.3 (dd, J_{PP} = 53.6 Hz, J_{PP} = 29.8 Hz, *meso*-PHR_2), 79.6 (dd, J_{PP} = 50.6 Hz, J_{PP} = 26.8 Hz, *meso*-PHR_2), 86.5 (d, J_{PP} = 26.8 Hz, *syn/anti*-PHR_2), 143.8 (t, J_{PP} = 29.8 Hz, *syn/anti*-PR_3), 149.2 (app. t, J_{PP} = 29.8 Hz, *meso*-PR_3), 152.5 (t, J_{PP} = 26.8 Hz, *syn/anti*-PR_3); *m/z* (ES+) 483.1212 ($[M–BF_4]^+$, $C_{25}H_{34}FeP_3$ = 483.1223)

Cyclopentadienyl phenyl*bis*(2–(phenylphosphino)ethyl)phosphine iron(II) hexafluorophosphate

This material was prepared similarly using $[Fe(C_5H_5)(CO)_2(NCMe)]PF_6$ (500 mg, 1.31 mmol) and **3^{Ph}** (0.5 g, 1.31 mmol) (830 mg, 98 %).

Found: C, 50.25; H, 4.60. $C_{27}H_{30}F_6FeP_4$ requires C, 50.0; H, 4.7; ν_{max}/cm^{-1} 3057 (CH), 2922 (CH), 2359 (PH), 2323 (PH); δ_P (121.7 MHz, acetone–d_6) 63.7 (d, J_{PP} = 33.9 Hz, syn/anti-PHR_2), 63.8 (dd, J_{PP} = 53.1 Hz, J_{PP} = 31.8 Hz, *meso*-PHR_2), 65.4 (dd, J_{PP} = 53.1 Hz, J_{PP} = 31.8 Hz, *meso*-PHR_2), 82.6 (d, J_{PP} = 27.1 Hz, *syn/anti*-PHR_2), 123.6 (t, J_{PP} = 33.9 Hz, *syn/anti*-PR_3), 128.0 (app. t, J_{PP} = 31.8 Hz, *meso*-PR_3), 132.0 (t, J_{PP} = 27.1 Hz, *syn/anti*-PR_3); m/z (AP+) 503.0906 ($[M–PF_6]^+$, $C_{27}H_{30}FeP_3$ = 503.0910)

Pentamethylcyclopentadienyl *tert*butyl*bis*(2–(phenylphosphino)ethyl)phosphine iron(II) hexafluorophosphate

This material was prepared similarly using $[Fe(C_5Me_5)(CO)_2(NCMe)]PF_6$ (598 mg, 1.38 mmol) and **3^{tBu}** (0.5 g, 1.38 mmol) (952 mg, 99 %).

Found: C, 51.5; H, 6.3. $C_{30}H_{44}F_6FeP_4$ requires C, 51.6; H, 6.35; ν_{max}/cm^{-1} 3057 (CH), 2961 (CH), 2917 (CH), 2369 (PH); δ_C (75.6 MHz, acetone–d_6) 9.4, 10.8, 10.9, 19.7, 28.1, 89.6, 129.8, 131.6, 133.0, 133.8; δ_P (121.7 MHz, acetone–d_6) -140.1 (sept, PF_6), 78.7 (dd, J_{PP} = 35.7 Hz, J_{PP} = 26.8 Hz, *meso*-PHR_2), 79.8 (d, J_{PP} = 17.8 Hz, *syn/anti*-PHR_2), 82.6 (d, J_{PP} = 11.9 Hz, *syn/anti*-PHR_2), 84.9 (dd, J_{PP} = 35.7 Hz, J_{PP} = 17.8 Hz, *meso*-PHR_2), 127.1 (t, J_{PP} = 17.8 Hz, *syn/anti*-PR_3),

128.3 (app. t, J_{PP} = 22.3 Hz, *meso*-PR_3), 130.9 (t, J_{PP} = 11.9 Hz, *syn/anti*-PR_3); *m/z* (ES+) 553.1981 ($[M\text{-}PF_6]^+$, $C_{30}H_{44}FeP_3$ = 553.2005)

Pentamethylcyclopentadienyl phenyl*bis*(2–(phenylphosphino)ethyl)phosphine iron(II) hexafluorophosphate

This material was prepared similarly using $[Fe(C_5Me_5)(CO)_2(NCMe)]PF_6$ (567 mg, 1.38 mmol) and **3^{Ph}** (0.5 g, 1.31 mmol) (904 mg, 96 %).

Found: C, 53.6; H, 5.7. $C_{32}H_{40}F_6FeP_4$ requires C, 53.5; H, 5.6; ν_{max}/cm^{-1} 3057 (CH), 2906 (CH), 2312 (PH); δ_C (75.6 MHz, acetonitrile–d_3) 9.9, 24.7, 31.1, 89.8, 129.5, 130.0, 131.4, 131.5, 131.9, 132.7, 133.1, 133.6; δ_P (121.7 MHz, acetonitrile–d_3) -143.3 (sept, PF_6), 74.2 (br s, *meso*-PHR_2), 74.4 (br s, *meso*-PHR_2), 77.5 (d, J_{PP} = 20.8 Hz, *syn/anti*-PHR_2), 114.7 (t, J_{PP} = 17.8 Hz, *syn/anti* -PR_3), 116.6 (app. t, J_{PP} = 19.7 Hz, *meso* -PR_3); *m/z* (ES+) 573.1706 ($[M\text{-}PF_6]^+$, $C_{32}H_{40}FeP_3$ = 573.1692)

1,2-*bis*(trimethylsilyl)cyclopentadienyl *tert*butyl*bis*(2–(phenylphosphino)ethyl)phosphine iron(II) hexafluorophosphate

This material was prepared similarly using $[Fe(C_5H_3(SiMe_3)_2)(CO)_2(NCMe)]PF_6$ (598 mg , 1.38 mmol) and **3^{tBu}** (0.5 g, 1.38 mmol) (1.048 g, 98 %).

ν_{max}/cm^{-1} 2953 (CH), 2872 (CH); δ_P (121.7 MHz, acetonitrile–d_3) -139.9 (sept, PF_6), 66.4 (br s, *syn/anti*-PHR_2), 71.4 (dd, J_{PP} = 52.3 Hz, J_{PP} = 32.1 Hz, *meso*-PHR_2), 83.6 (dd, J_{PP} = 52.3 Hz, J_{PP} = 32.1 Hz, *meso*-PHR_2), 140.4 (br s, *syn/anti*-PR_3), 145.9 (app. t, J_{PP} = 32.1 Hz, *meso*-PR_3); *m/z* (ES+) 627.2032 ($[M\text{-}PF_6]^+$, $C_{31}H_{50}FeP_3Si_2$ = 627.2013)

1,2-*bis*(trimethylsilyl)cyclopentadienyl phenyl*bis*(2–(phenylphosphino)ethyl)phosphine iron(II) hexafluorophosphate

This material was prepared similarly using $[Fe(C_5H_3(SiMe_3)_2)(CO)_2(NCMe)]PF_6$ (133 mg, 0.26 mmol) and **3^{Ph}** (0.1 g, 0.26 mmol) (195 mg, 94 %).

ν_{max}/cm^{-1} 3059 (CH), 2953 (CH), 2902 (CH), 2322 (PH); δ_C (75.6 MHz, acetone–d_6) -0.9, 128.1, 128.7, 129.0, 129.9, 130.4, 131.0, 131.3, 132.1; δ_P (121.7 MHz, acetone–d_6) -140.3 (sept, PF_6),

60.7 (d, J_{PP} = 28.3 Hz, *syn/anti*-PHR_2), 61.3 (d, J_{PP} = 30.9 Hz, *syn/anti*-PHR_2), 67.6 (dd, J_{PP} = 47.4 Hz, J_{PP} = 31.0 Hz, *meso*-PHR_2), 80.1 (dd, J_{PP} = 47.4 Hz, J_{PP} = 35.7 Hz, *meso*-PHR_2), 117.0 (t, J_{PP} = 30.9, *syn/anti*-PR_3), 121.6 (dd, J_{PP} = 35.7, 31.0 Hz, *meso*-PR_3), 125.4 (t, J_{PP} = 28.3, *syn/anti*-PR_3); *m/z* (ES+) 647.1714 ($[M\text{-}PF_6]^+$, $C_{33}H_{46}Si_2FeP_3$ = 647.1700)

Synthesis of trichloro *tert*butyl*bis*(2–(phenylphosphino)ethyl)phosphine chromium(III), 4

To a suspension of $CrCl_3(thf)_3$ (114 mg, 0.30 mmol) in methylene chloride (1 mL) was added a solution of **3^{tBu}** (110 mg, 0.30 mmol) in methylene chloride (1.1 mL). The purple solid rapidly dissolves to form a deep blue solution. After stirring at room temperature for 5 minutes the crude product was filtered through celite to remove an insoluble blue by–product. The product was isolated by removal of solvent to give a blue solid material (91 mg, 0.17 mmol, 58 %).

Found: C, 46.0; H, 5.5. $C_{20}H_{29}Cl_3CrP_3$ requires C, 46.1; H, 5.6; λ_{max}/nm 482, 616 (ε/$dm^3\,mol^{-1}\,cm^{-1}$ 227, 715); ν_{max}/cm^{-1} 3054 (CH), 2956 (CH), 2918 (CH), 2361 (PH); *m/z* (ES+) 516.0527 ($[M–Cl+CH_3OH]^+$, $C_{21}H_{33}Cl_2CrOP_3$ = 516.0526); Λ_m/Scm^2mol^{-1} 30.7.

Synthesis of dichloro *tert*butyl*bis*(2–(phenylphosphino)ethyl)phosphine iron(II), 5

To a suspension of anhydrous iron chloride (70 mg, 0.55 mmol) in methylene chloride (2 mL) was added a solution of **3^{tBu}** (0.20 g, 0.55 mmol) in methylene chloride (2 mL). After 5 minutes the red solution was filtered through celite and the solvent removed from the filtrate *in vacuo* yielding the product as dark red solid (146 mg, 54%).

Found: C, 48.8; H, 6.0. $C_{20}H_{29}Cl_2FeP_3$ requires C, 49.1; H, 6.0; ν_{max}/cm^{-1} 3050 (CH), 2919 (CH), 2864 (CH), 2318 (PH); δ_P (121.7 MHz, CD_2Cl_2, –80 °C) 78.2 (br s, PH), 88.0 (br s, PH), 126.3 (br S, P^{t}Bu); *m/z* (ES+) 453.0509 ($[M–Cl]^+$, $C_{20}H_{29}ClFeP_3$ = 453.0520); Λ_m/Scm^2mol^{-1} 28.5.

Synthesis of dibromo *tert*butyl*bis*(2–(phenylphosphino)ethyl)phosphine iron(II), 6

This material was prepared similarly to **5** from $FeBr_2$ (60 mg, 0.28 mmol) and **3^{tBu}** (0.1 g, 0.28 mmol) yielding the product as a red solid (99 mg, 62 %).

Found, C, 41.8; H, 5.1. $C_{20}H_{29}Br_2FeP_3$ requires C, 41.6; H, 5.1; ν_{max}/cm^{-1} 3051 (CH), 2918 (CH), 2325 (PH); δ_P (121.7 MHz, CH_2Cl_2) 80.3 (br s, PH), 87.9 (br s, PH), 119.5 (br s, P^{t}Bu); *m/z* (ES+) 497.0015 ([M–Br]$^+$, $C_{20}H_{29}BrFeP_3$ = 497.0015); Λ_m/Scm^2mol^{-1} 28.2.

Synthesis of diiodo *tert*butyl*bis*(2–(phenylphosphino)ethyl)phosphine iron(II), 7

This material was prepared similarly to **5** from FeI_2 (85 mg, 0.28 mmol) and **3^{tBu}** (0.1 g, 0.28 mmol) yielding the product as a purple solid (91 mg, 49 %).

Found, C, 35.9; H, 4.5. $C_{20}H_{29}I_2FeP_3$ requires C, 35.8; H, 4.4; ν_{max}/cm^{-1} 3049 (CH), 2918 (CH), 2865 (CH), 2319 (PH); δ_P (121.7 MHz, CH_2Cl_2) 93.3 (br s, PH), 100.6 (br s, PH), 124.5 (br s, P^{t}Bu); *m/z* (ES+) 544.9883 ([M–I]$^+$, $C_{20}H_{29}IFeP_3$ = 544.9876); Λ_m/Scm^2mol^{-1} 49.9.

Synthesis of chloro *tert*butyl*bis*(2–(phenylphosphino)ethyl)phosphine nickel(II) hexafluorophosphate, 8

A solution of $NiCl_2{\cdot}6H_2O$ (0.39 g, 1.6 mmol) in ethanol (15 mL) was slowly added to a refluxing mixture of **3^{tBu}** (0.60 g, 1.7 mmol) and NH_4PF_6 (0.27 g, 1.7 mmol) in ethanol (30 mL) immediately forming a red–brown solution. After 3 hours, the mixture was filtered hot, the filtrate cooled and solvent removed *in vacuo*. The residue was washed with petroleum ether (3 × 10 mL), taken up in methylene chloride (20 mL) and filtered through celite. Removal of the solvent *in vacuo* yielded the product as a brown powder (0.83 g, 1.4 mmol, 84 %).

Found: C, 40.1; H, 5.0. $C_{20}H_{29}ClF_6NiP_4$ requires C, 39.9; H, 4.9; λ_{max}/nm 416 ($\varepsilon/dm^3\ mol^{-1}\ cm^{-1}$ 980); ν_{max}/cm^{-1} 2962 (CH), 2337 (PH); δ_P (121.7 MHz, acetone–d_6, –80 °C) –141.7 (heptet, $^1J_{PF}$ = 711.6 Hz, PF_6), 32.3 (br s, PH), 41.1 (br s, PH), 54.5 (d, *J* = 35.7 Hz, PH), 62.1 (s, PH), 63.3 (br s, PH), 65.4 (app t, *J* = 26.7 Hz, PH), 67.8 (d, *J* = 26.8 Hz, PH), 70.8 (d, *J* = 29.7 Hz), 133.6 (t, *J* = 29.2 Hz, P^{t}Bu), 135.9 (t, *J* = 28.3 Hz, P^{t}Bu), 143.4 (m, P^{t}Bu), 144.8 (m, P^{t}Bu), 146.8 (s, P^{t}Bu), 148.3 (d, *J* = 41.7 Hz, P^{t}Bu), 150.7 (d, *J* = 38.7 Hz, P^{t}Bu); Λ_m/Scm^2mol^{-1} 80.5.

Synthesis of chloro *tert*butyl*bis*(2–(phenylphosphino)ethyl)phosphine copper(I), 9

To a suspension of CuCl (27 mg, 0.27 mmol) in methylene chloride (1 mL) was added **3^{tBu}** (100 mg, 0.28 mmol) in methylene chloride (1 mL). The resultant pale yellow solution was stirred at room temperature for 5 minutes before filtration through celite. The filtrate was concentrated and the product precipitated by addition of petroleum ether (2 mL). The white solid was isolated by filtration (117 mg, 0.25 mmol, 93 %).

Found: C, 51.9; H, 6.5. $C_{20}H_{29}ClCuP_3$ requires C, 52.1; H, 6.3; ν_{max}/cm^{-1} 3047 (CH), 2935 (CH), 2898 (CH), 2864 (CH) 2310 (PH); δ_P (121.7 MHz, *o*–dichlorobenze, 140 °C) –44.0 – –37.4 (m, PH), –6.3 (br s, P^{t}Bu), 14.2 – 16.9 (m, PH), 26.1 – 27.5 (m, PH), 39.1 (m, P^{t}Bu), 45.3 (t, *J* = 41.7 Hz, P^{t}Bu), 57.4 (br s, P^{t}Bu); *m/z* (ES+) 425.0786 ([M–Cl]$^+$, $C_{20}H_{29}CuP_3$ = 425.0778); Λ_m/Scm^2mol^{-1} 5.3.

Synthesis of acetonitrile (bis(2-(phenylphosphino)ethyl)tert-butylphosphino) copper(I) hexafluorophosphate, 10

A solution of bis(2-(phenylphosphino)ethyl) *tert*-butylphosphine (0.50 g, 1.4 mmol) in THF (5 mL) was added to $[Cu(NCMe)_4]PF_6$ (0.60 g, 1.6 mmol) suspended in methylene chloride (50 mL). The mixture is stirred at room temperature for 30 mins before being filtered and concentrated *in vacuo*. The product is precipitated by addition of petroleum ether to yield a fine white powder in good yield (0.74 g, 88 %).

δ_H (400 MHz, d^6–acetone) 1.02 (9 H, br s, ^{t}Bu), 1.5–2.5 (8 H, br m, CH_2), 4.9–5.6 (2 H, br d, PH), 7.0-7.6 (10 H, br s, Ph); δ_P (121.7 MHz, $CDCl_3$) –143.5 (1 P, sept, PF_6), – 31.6 (2 P, br s, PH), 34.9 (1 P, br s, ^{t}BuP); *m/z* (AP+) 466.1045 (M^+, $C_{22}H_{32}NP_3Cu$ = 466.1044)

General procedure for cyclisation reactions

To a suspension of **10** (100 mg, 0.16 mmol) in THF (40 mL) was added KO^{t}Bu (72 mg, 0.64 mmol). The resulting yellow solution was stirred at room temperature for 1 hour before addition of a suitable dielectrophilic reagent (1.00 equivalents). The mixture is filtered and

the filtrate concentrated *in vacuo*. The product is isolated as a white powder following precipitation with petroleum ether.

Acetonitrile 1-*tert*butyl-4,7-diphenyl-1,4,7-triphosphacyclononane copper hexafluorophosphate, 11

δ_P (121.7 MHz, $CDCl_3$) -144.1 (1 P, sept, PF_6), 27.6 (2 P, br s, PPh), 57.8 (1 P, br s, ^{t}BuP); *m/z* (AP+) 492.12 (M+, $C_{24}H_{34}CuNP_3$ = 568.1513)

Acetonitrile 5-(tert-butyl)-2,8-diphenyl-2,3,4,5,6,7,8,9-octahydro-1H-benzo[i][1,4,7]triphosphacycloundecine copper hexafluorophosphate, 12

δ_P (121.7 MHz, $CDCl_3$) -144.1 (1 P, sept, PF_6), 25.9 (2 P, br s, PPh), 57.2 (1 P, br s, ^{t}BuP); *m/z* (AP+) 568.1493 (M+, $C_{30}H_{38}CuNP_3$ = 568.1513)

References

1 B. N. Diel, R. C. Haltiwanger and A. D. Norman, *J. Am. Chem. Soc.*, 1982, **104**, 4700–4701.

2 B. N. Diel, R. C. Haltiwanger and A. D. Norman, *J. Am. Chem. Soc.*, 1982, **104**, 4700–4701.

3 Peter G. Edwards, Robert Haigh, A. Dongmei Li and P. D. Newman, 2006.

4 D. J. Lowry and M. L. Helm, *Inorg. Chem.*, 2010, **49**, 4732–4734.

5 M. L. Whatton, Cardiff University, 2001.

6 J. E. Richman and T. J. Atkins, *J. Am. Chem. Soc.*, 1974, **96**, 2268–2270.

7 T. J. Atkins, J. E. Richman and W. F. Oettle, *Org. Synth.*, 1978, **58**, 86.

8 D. Moiseev, B. R. James, B. O. Patrick and T. Q. Hu, *Inorg. Chem.*, 2006, **45**, 2917–2924.

9 D. L. DuBois, A. Miedaner and R. C. Haltiwanger, *J. Am. Chem. Soc.*, 1991, **113**, 8753–8764.

10 J. A. Feducia, A. N. Campbell, J. W. Anthis and M. R. Gagné, *Organometallics*, 2006, **25**, 3114–3117.

11 L. J. Mason, A. J. Moore, A. Carr and M. L. Helm, *Heteroat. Chem.*, 2007, **18**, 675–678.

12 L. D. Quin, *A guide to organophosphorus chemistry*, Wiley, 2000.

13 M. Westerhausen, *Inorg. Chem.*, 1991, **30**, 96–101.

14 J. Buter and R. M. Kellogg, *J. Org. Chem.*, 1981, **46**, 4481–4485.

15 C. J. Burns and R. A. Andersen, *J. Organomet. Chem.*, 1987, **325**, 31–37.

16 A. Pape, M. Lutz and G. Müller, *Angew. Chemie Int. Ed. English*, 1994, **33**, 2281–2284.

17 J. L. Atwood, S. G. Bott, R. A. Jones and S. U. Koschmieder, *J. Chem. Soc., Chem. Commun.*, 1990, **196**, 692–693.

18 E. Hey, L. M. Engelhardt, C. L. Raston and A. H. White, *Angew. Chemie Int. Ed. English*, 1987, **26**, 81–82.

19 H. H. Karsch and M. Reisky, *Eur. J. Inorg. Chem.*, 1998, **1998**, 905–911.

20 P. G. Edwards, P. D. Newman and K. M. A. Malik, *Angew. Chemie*, 2000, **39**, 2922–2924.

21 A. B. Burg, *Inorg. Chem.*, 1964, **3**, 1325–1327.

22 I. H. Sabherwal and A. B. Burg, *J. Chem. Soc. D Chem. Commun.*, 1969, 853.

23 L. R. Gray, A. L. Hale, W. Levason, F. P. McCullough and M. Webster, *J. Chem. Soc. Dalt. Trans.*, 1984, 47.

24 C. S. Garner and D. H. House, *Transition Metal Chemistry*, New York, 1970.

25 S. G. Davies, S. J. Simpson, H. Felkin, F. Tadj and O. Watts, *J. Chem. Soc., Dalt. Trans.*, 1983, 981–985.

26 T. K. Mukhopadhyay, R. K. Feller, F. N. Rein, N. J. Henson, N. C. Smythe, R. J. Trovitch and J. C. Gordon, *Chem. Commun.*, 2012, **48**, 8670.

27 R. B. King and J. W. Bibber, *Inorganica Chim. Acta*, 1982, **59**, 197–201.

28 W. J. Geary, *Coord. Chem. Rev.*, 1971, **7**, 81–122.

29 C. Tedesco, M. Lamberti and M. Mazzeo, *Acta Crystallogr. Sect. E*, 2012, **68**, m1459–m1459.

30 B. Mohr, E. E. Brooks, N. Rath and E. Deutsch, *Inorg. Chem.*, 1991, **30**, 4541–4545.

31 M. I. García-Seijo, P. Sevillano, R. O. Gould, D. Fernández-Anca and M. E. García-Fernández, *Inorganica Chim. Acta*, 2003, **353**, 206–216.

32 WO2012144530 (A1), *PCT Int. Appl.*, 2012.

33 S. J. Lippard and G. J. Palenik, *Inorg. Chem.*, 1971, **10**, 1322–1324.

34 K. Naka, T. Umeyama, A. Nakahashi and Y. Chujo, *Macromolecules*, 2007, **40**, 4854–4858.

35 G. Winter, D. W. Thompson and J. R. Loehe, in *Inorganic Syntheses*, eds. A. Wold and J. K. Ruff, John Wiley & Sons, Inc., 1973, vol. 14, pp. 99–104.

36 R. J. Kern, *J. Inorg. Nucl. Chem.*, 1962, **24**, 1105–1109.

37 W. E. Williams and F. J. Lalor, *J. Chem. Soc., Dalt. Trans.*, 1973, 1329–1332.

38 M. J. Frisch, G. W. Trucks, H. B. Schlegel, G. E. Scuseria, M. A. Robb, J. R. Cheeseman, G. Scalmani, V. Barone, B. Mennucci, G. A. Petersson, H. Nakatsuji, M. Caricato, X. Li, H. P. Hratchian, A. F. Izmaylov, J. Bloino, G. Zheng, J. L. Sonnenberg, M. Hada, M. Ehara, K. Toyota, R. Fukuda, J. Hasegawa, M. Ishida, T. Nakajima, Y. Honda, O. Kitao, H. Nakai, T. Vreven, J. Montgomery, J. A., J. E. Peralta, F. Ogliaro, M. Bearpark, J. J. Heyd, E. Brothers, K. N. Kudin, V. N. Staroverov, R. Kobayashi, J. Normand, K. Raghavachari, A. Rendell, J. C. Burant, S. S. Iyengar, J. Tomasi, M. Cossi, N. Rega, J. M. Millam, M. Klene, J. E. Knox, J. B. Cross, V. Bakken, C. Adamo, J. Jaramillo, R. Gomperts, R. E. Stratmann, O. Yazyev, A. J. Austin, R. Cammi, C. Pomelli, J. W. Ochterski, R. L. Martin, K. Morokuma, V. G. Zakrzewski, G. A. Voth, P. Salvador, J. J. Dannenberg, S. Dapprich, A. D. Daniels, Ö. Farkas, J. B. Foresman, J. V. Ortiz, J. Cioslowski and D. J. Fox, *Gaussian 09, Revis. C.01*, 2009.

39 A. K. Rappe, C. J. Casewit, K. S. Colwell, W. A. Goddard and W. M. Skiff, *J. Am. Chem. Soc.*, 1992, **114**, 10024–10035.

40 A. D. Becke, *J. Chem. Phys.*, 1993, **98**, 5648.

41 C. Lee, W. Yang and R. G. Parr, *Phys. Rev. B*, 1988, **37**, 785–789.

42 B. Miehlich, A. Savin, H. Stoll and H. Preuss, *Chem. Phys. Lett.*, 1989, **157**, 200–206.

Chapter 3

Synthesis and reactivity of novel ligands derived from glycidyl phosphine

Introduction

The high ring strain inherent in epoxides make them highly reactive electrophiles (Scheme 1) and has given rise to their widespread use in organic synthesis.[1] They are useful motifs for introducing further functionality into a molecule of interest. Furthermore, stereochemical information is retained during the course of these reactions and thus chiral epoxides are often used in the asymmetric synthesis of natural products, pharmaceuticals and ligands for homogeneous catalysis.

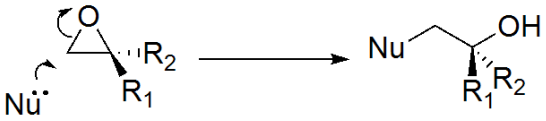

Scheme 1: S_N2 reaction of an epoxide with a nucleophile

A wide range of nucleophiles have been shown to react with epoxides, most commonly, amines, alcohols, water and thiols. The analogous reactivity with phosphorus based nucleophiles is relatively unexplored and may represent a valuable methodology for the synthesis of chiral phosphine ligands. Despite recent progress in the design and synthesis of phosphine ligands (See Chapter 1), novel routes to these structures remain of interest due to the demand for ever more effective asymmetric catalysts for organic transformations.

Numerous groups have utilised this reactivity to synthesise phosphino-alcohol structures,[2–7] however, these examples are mostly trivial variations and derivatives lacking any further functionality which may allow for construction of more complex multidentate ligands and/or systematic variation of their steric and electronic properties. Ciardi *et al.* have synthesised a series of enantiomerically enriched β – hydroxyl - γ – amino phosphines derived from amino acids (Scheme 2).[8] The naturally occurring amino acids were first converted to epoxides which were subsequently ring-opened with lithium diphenylphosphido borane. Following deprotection, these phosphines were used as ligands in complexes of Rh(II), Ir(II) and Ru(II)

where they act as monodentate P donor ligands despite their potential to chelate *via* the other heteroatoms.

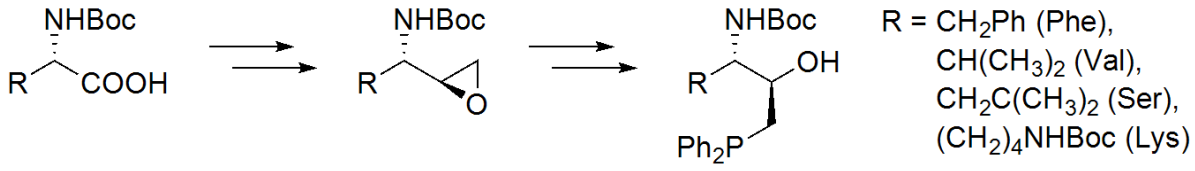

Scheme 2: Synthesis of chiral β – hydroxyl - γ – amino phosphines[8]

Müller and Feustel investigated a symmetrical ambidentate tripodal ligand derived from the exhaustive substitution of 1,1 – bis(chloromethyl)oxirane with $LiPMe_2$ (Scheme 3).[9] This methodology is of particular interest in the development of novel ligand structures as initial attack of the phosphide at the epoxide results in formation of a halohydrin, which under the reaction conditions collapses again to reform an epoxide. The symmetrical tripod ligand is built up through successive substitution and ring closure reactions. The proposed intermediary species in this scheme are themselves attractive synthetic targets. If such species could be isolated, it may allow for the selective formation of asymmetrically substituted ligands.

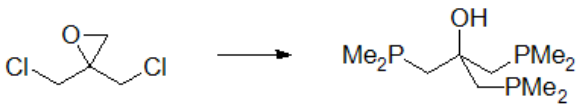

Scheme 3: Müller and Feustel's synthesis of a tripodal ligand[9]

A similar methodology has been applied in the synthesis of carbohydrate based 1,3 – bisphosphines (Scheme 4).[10] Furthermore, in this case the intermediary epoxy phosphine species could be isolated facilitating the controlled synthesis of an asymmetrically substituted species bearing both P and S donors. The Rh and Ru complexes of these were found to be active catalysts for the asymmetric hydrogenation of olefins and ketones, although ee's were found to be poor. Nonetheless, this illustrates the potential utility of the glycidylphosphine motif in the synthesis of chiral multidentate ligands.

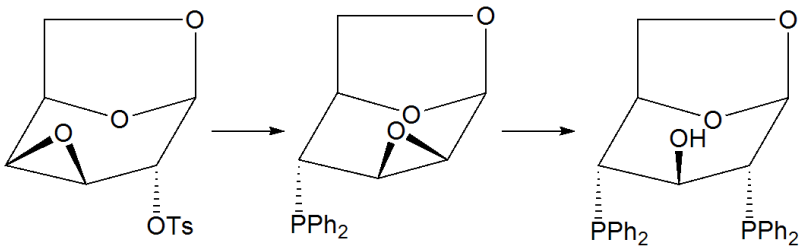

Scheme 4: Stepwise synthesis of chiral carbohydrate based diphosphines[10]

An early report from Issleib and Rockstroh demonstrates the reaction of potassium diphenylphosphide with epichlorohydrin in order to generate the archetypal glycidyl phosphine species in 61 % yield.[11] More recently, the same procedure was used by the group of Huttner to synthesise a series of chiral diphosphine ligands (Figure 1, a).[12] The phosphide was found to attack epichlorohydrin selectively at the terminal position of the epoxide rather than at the halide position and thus racemisation of the chiral centre was not observed. The scope of this reaction was also successfully extended to encompass amine and thiol nucleophiles (Figure 1, b). The Rh complexes of these ligands were active catalysts in the hydrogenation of (*Z*)-2-acetamidocinnamic acid although reported ee's were low. These ligands were further developed to convert the alcohols to various phosphite donor groups (Scheme 5).[13,14] Reaction of these ligands with $[Rh(COD)Cl]_2$ in the presence of KPF_6 furnishes $[(tripod)Rh(COD)]PF_6$ in good yield.

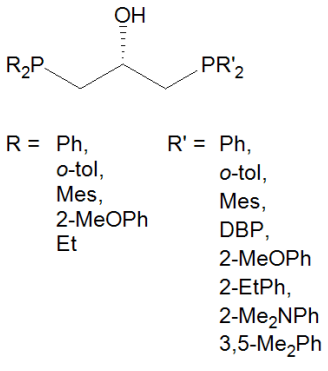

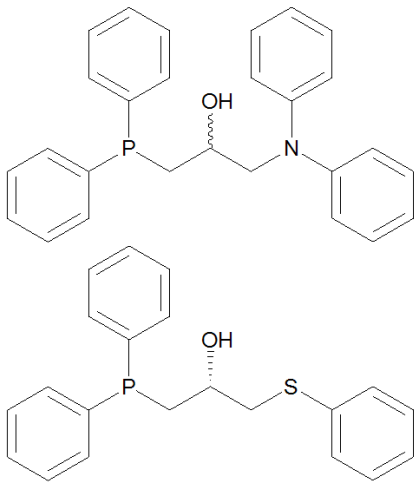

a) b)

Figure 1: a) chiral diphosphines; b) examples of amino- and thio- phosphine ligands[12]

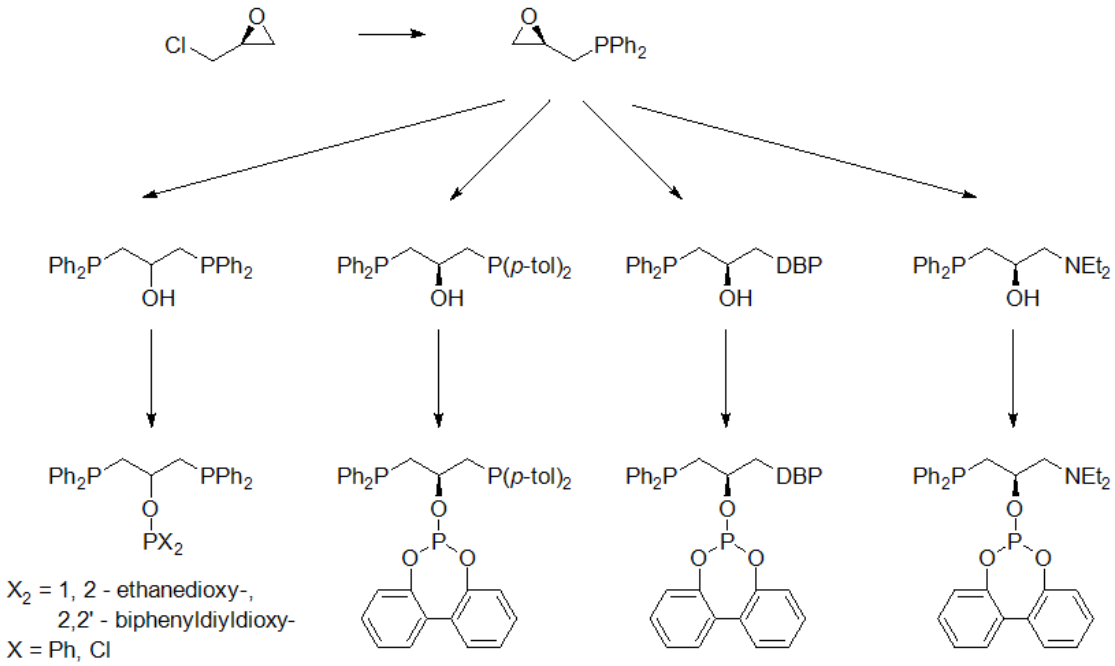

Scheme 5: Synthetic route to chiral tripodal phosphines[13]

The glycidylphosphine motif is attractive as a potential synthon for the construction of novel ligand structures but has remained relatively unexplored. To date, diphosphine ligands have received most attention; complexes of these ligands and their derivatives have been used in Negishi couplings,[15] catalytic hydrogenation,[10,12,14,16,17] solid supported catalysis[18–22] and myocardial imaging.[23] The ligands typically chelate *via* the two P donors, however alkoxide binding has been observed in Li and Na aggregates[9,24] and Ti and Ta alkylidene complexes.[25]

Aims of chapter 3

This chapter will assess the scope and utility of the glycidyl phosphine motif in the synthesis of a number of chiral heterodonor ligands. Epichlorohydrin is a cheap and readily available precursor and *via* well-known hydrolytic kinetic resolution techniques can be readily enantiomerically enriched to a high degree.[26] The reaction of epichlorohydrin with lithium diphenylphosphide occurs cleanly in a stereospecific and regioselective manner (*vide supra*) allowing rapid access to glycidyldiphenylphosphine. The subsequent reaction of this key intermediary species with various nucleophiles will result in ring opening to produce a series

of heterodonor ligands (Scheme 6). The presence of a pendant alcohol in such structures may result in these species acting as hemilabile ligands which have proven useful in the stabilisation of many interesting structures.[27] Incorporation of a chiral alcohol is also of interest synthetically as it may allow for functionalisation of the ligand backbones *via* formation of various ether/ester derivatives. Derivatives such as these will allow for rational catalyst development by tuning properties such as steric bulk or solubility.

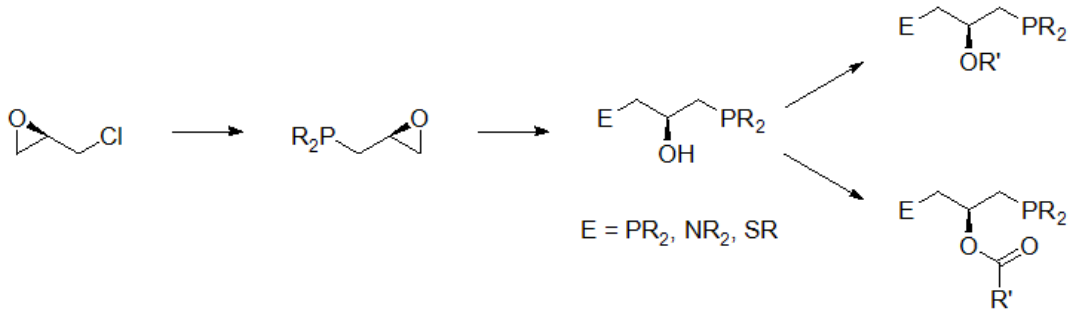

Scheme 6: Design of chiral heterodonor ligands

Synthesis and stability of glycidyl phosphines

Glycidyldiphenylphosphine, **1**, is unstable and cannot be stored for prolonged periods. The initial colourless oil becomes a viscous orange resin-like substance within hours. Similar observations have previously been made with the analogous glycidyl amines.[28] These observations suggest that the mechanism of decomposition is not a simple matter of oxidation at phosphorus and is likely due to a polymerisation reaction. This may potentially occur *via* two pathways (Scheme 7), either through nucleophilic attack of the phosphine lone pair at the epoxide ring generating phosphonium alkoxides or *via* ring opening of the epoxide to give a polyether bearing pendant phosphines. Additionally, it is likely that some degree of oxidation to P(v) species does indeed occur and in principle a combination of all three degradation routes is possible.

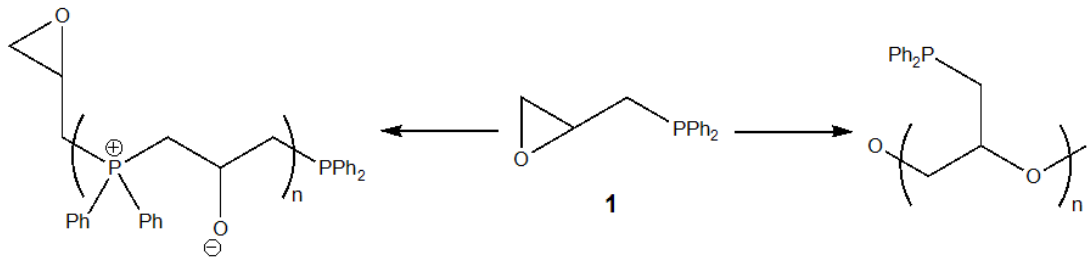

*Scheme 7: Potential polymerisation products of **1***

The pendant phosphine material may possess some utility in applications such as immobilised heterogeneous catalysis or heavy metal scavenging materials, thus it is of interest to further explore the nature of this material. The MALDI mass spectrum shows peaks attributable to di-, tri- and tetrameric species suggesting that although oligomerisation is occurring large polymeric chains are not formed under these conditions. The $^{31}P\{^{1}H\}$ NMR spectrum (Figure 2) of this material displays a number of peaks between δ_P = –25 and –12 ppm while a second grouping of resonances are observed between δ_P = 10 and 40 ppm. **1** appears at δ_P = -24.8 ppm,[13] thus the primary grouping are likely those of similar tertiary phosphine environments. The downfield grouping correlates with resonances of phosphine oxide and/or phosphonium species.

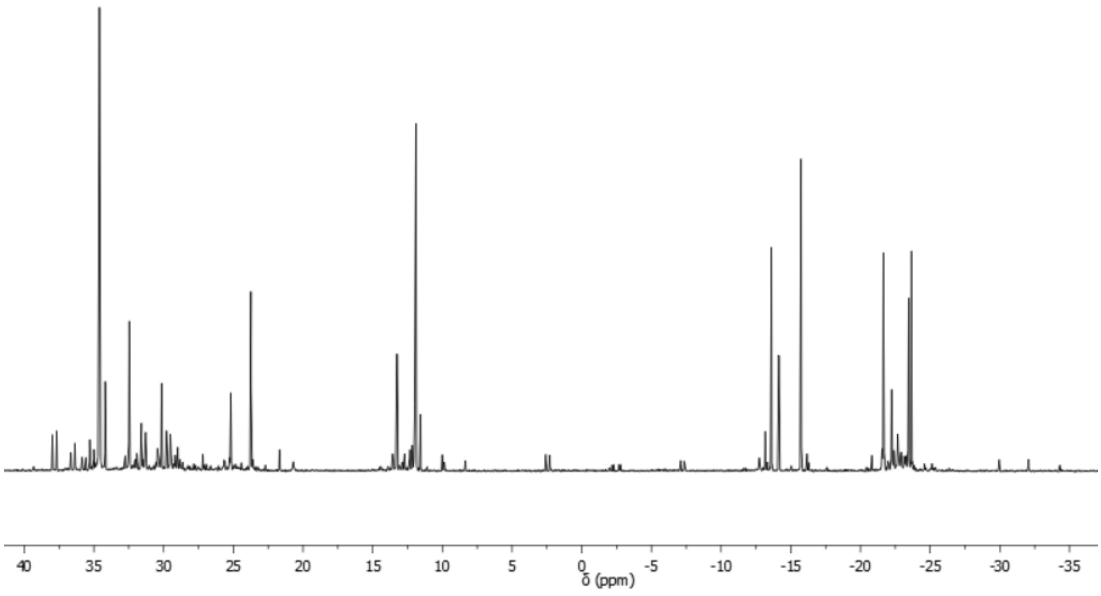

Figure 2: $^{31}P\{^{1}H\}$ NMR spectrum of glycidylphosphine after degradation

The spectroscopic evidence suggests that the decomposition route proceeds largely *via* nucleophilic attack at the epoxide yielding phosphonium alkoxide species. It has been shown that phosphonium salts are unstable in the presence of alkoxides and tend to degrade to phosphine oxides and ethers.[29,30] The presence of the internal alkoxide moiety may further promote this pathway. Many of the potential intermediary species in this process have the potential for further side reactions thus providing a source for the observed complexity in the $^{31}P\{^{1}H\}$ NMR spectrum.

In order to fully investigate the reactivity of these species an alternative system was sought which would provide air stability and prevent nucleophilic substitution reactions. It was envisaged that donation of the phosphine lone pair to a suitable Lewis acid would achieve both of these goals and thus the borane adduct, **2** (Scheme 8), was prepared and characterised by ^{1}H, ^{13}C and ^{31}P NMR spectroscopy. Due to the complexity of its ^{1}H NMR spectrum, **2** can be conveniently identified by its resonance (δ = 22.2 ppm) in the ^{31}P NMR spectrum.

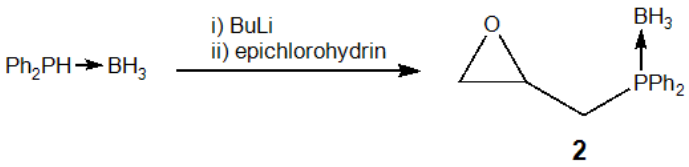

*Scheme 8: Preparation of borane adduct **2***

Initial stability tests of **2** proved favourable as no obvious degradation occurred of the white solid when exposed to air. However, after 2 hours it was apparent that **2** was hygroscopic as the friable solid gradually became oily. The ^{31}P NMR spectrum of the oil shows a small quantity of **1** present in this sample. The presence of water appears to slowly displace the borane, liberating the free phosphine which is then free to undergo various degradation processes (*vide supra*). Dissolution of the oil in chloroform gives a white solid, presumably borane hydrolysis products, suspended in a pale yellow solution. Subsequently, for synthetic

ease and integrity of the products, **1** was not routinely isolated, but formed immediately prior to reaction with various nucleophilic substrates.

Reactions with phosphides

Given the prevalence of diphosphino ligands in the literature (*vide supra*), the reaction of **1** with dialkylphosphines was studied. Thus, reaction of **(*S*)-1** with lithium di*iso*propylphosphide at -78 °C affords (*S*)-1-(di*iso*propylphosphanyl)-3-(diphenylphosphanyl)propan-2-ol, **3**, in good yield (Scheme 9).

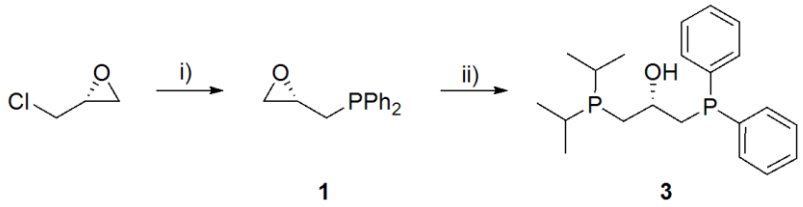

Scheme 9: Synthesis of chiral diphosphine. Reagents and conditions; i) Ph_2PH, BuLi, THF, -78 °C; ii)$^{i}Pr_2PH$, , BuLi, THF, -78 °C

Diphosphine **3** was isolated as a colourless oil and displayed two peaks in the ^{31}P NMR spectrum typical of diarylalkyl and trialkyl phosphines. Preliminary studies of the coordination chemistry of **3** were carried out. Hence, a solution of **3** in toluene was added to a suspension of $CoCl_2 \cdot 6H_2O$ in toluene, whereupon the pink solid dissolved to give a green/blue solution. Following workup, the paramagnetic product was identified as the bis-diphosphine complex, **4**, on the basis of mass spectrometry and elemental analysis. Likewise, following treatment of **3** with excess $NiCl_2 \cdot 6H_2O$ a dark red crystalline material, **5**, was collected. Upon coordination the two ^{31}P NMR peaks are significantly broadened and shifted downfield. The material has been formulated as the neutral bisphosphino complex (Scheme 10) on the basis of X-ray diffraction data (*vide infra*). Contrarily, the mass spectrum of this material shows no evidence for the 1:1 adduct, instead displaying a strong signal associated with the cationic 2:1 complex. This unexpected observation can be rationalised as a result of fragmentation under the conditions within the spectrometer. All evidence suggests a

chelating κ^2-P,P' coordination mode of the diphosphine rather than any of the potential alternative bridging, mono- or tridentate coordination modes.

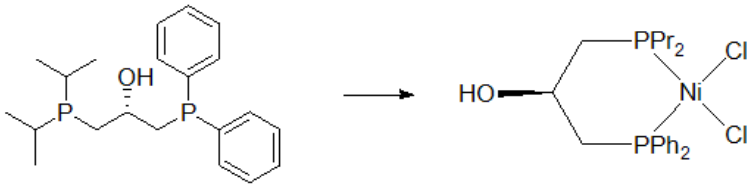

3 **5**

Scheme 10: Formation of Ni diphosphine complex

The Ni complex, **5**, crystallises readily from saturated MeOH solution giving crystals suitable for X-ray diffraction. There are 4 independent molecules in the unit cell, one of which is shown below (Figure 3). The complex adopts a square planar geometry around Ni as might be expected of such a complex. The average bond lengths (P1-Ni = 2.156 Å, P2-Ni = 2.176 Å, Cl1-Ni = 2.195 Å, Cl2-Ni = 2.195 Å) are typical of such complexes and are in accord with other known structures. The slight increase in bond length of the P2-Ni bond compared to that of P1-Ni bond is reflective of the increased steric bulk provided by the isopropyl substituents. The average P1-Ni-P2 bite angle of 95.4 ° is slightly in excess of the ideal bond angle for a square planar geometry due to the need to accommodate a six membered chelate ring at Ni.

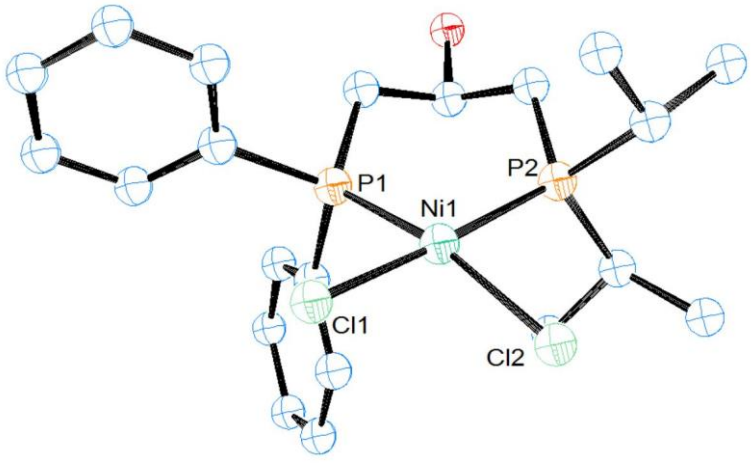

*Figure 3: ORTEP representation of the structure of **5**. H atoms omitted for clarity. Asymmetric unit contains 4 independent molecules. Selected bond lengths (Å) and angles (°): P1-Ni1 = 2.164(2), P2-Ni1 = 2.177(2), Cl1-Ni = 2.196(2), Cl2-Ni = 2.211(2), P1-Ni-P2 = 94.04(9), P1-Ni-Cl2 = 165.96(11), P2-Ni-Cl1 = 173.97(11)*

Reactions with amines

Ligand synthesis

Reaction of **1** with dialkylamines allows ready access to a series of chiral γ-amino-β-hydroxyphosphines (Scheme 11). The dimethyl-, diethyl- and morpholinyl- substituted species, **6**, **7** and **8**, respectively, were formed as air stable colourless oils in moderate to good yield. The stereochemistry of the hydroxyl group can be controlled by use of chirally resolved epichlorohydrin in the preparation of **1**. It was anticipated that these species would exhibit rich coordination chemistry due to the varied properties and characteristics of the three potential donor sites.

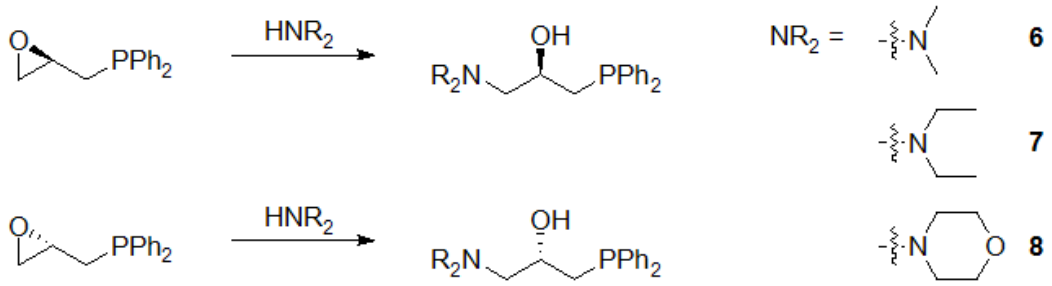

Scheme 11: Synthesis of chiral aminophosphines

Ru complexes

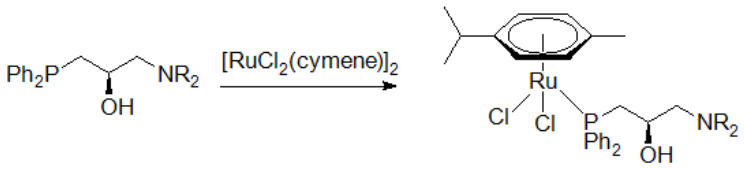

(*R*)-6
(*R*)-7
(*R*)-8

(*R*)-9
(*R*)-10
(*R*)-11

Scheme 12: Synthesis of $RuCl_2$(cymene)(phosphine) complexes. Identical procedure used for the synthesis of (S)- enantiomers.

Reaction of the chiral phosphino amines with $[RuCl_2(cymene)]_2$ in methylene chloride gives the κ^1-*P* Ru piano stool complexes, **9-11** (Scheme 12). Coordination to Ru is accompanied by a shift in the ^{31}P NMR signature from around δ = -20 ppm to around δ = 20 ppm. ^1H NMR

spectra resemble those of the free ligands with additional resonances associated with the cymene moiety. A large number of Ru(η^6-arene) complexes are now known and such complexes have found extensive use as catalysts for various organic transformations,[31,32] including oxidation,[33] epoxidation,[34] hydroformylation,[35] olefin metathesis,[36] hydrogenation[37,38] and hydrogen transfer.[39] It is of interest therefore to assess the catalytic competency of Ru complexes **9-11**. The pendant chiral hydroxyl can be anticipated to impart only a small steric influence but may affect the stereochemistry of the product through hydrogen bonding interactions with polar substrates.[40] The systems developed by Noyori *et al.* affect the catalytic reduction of benzoin and benzils to the 1,2-diol species in high yield and enantiomeric excess under relatively mild conditions (Scheme 13).[41] The catalyst structure in this reaction has proven to be remarkably variable; a number of chiral co-ligands are able to be incorporated in order to tune the properties of catalyst.[42]

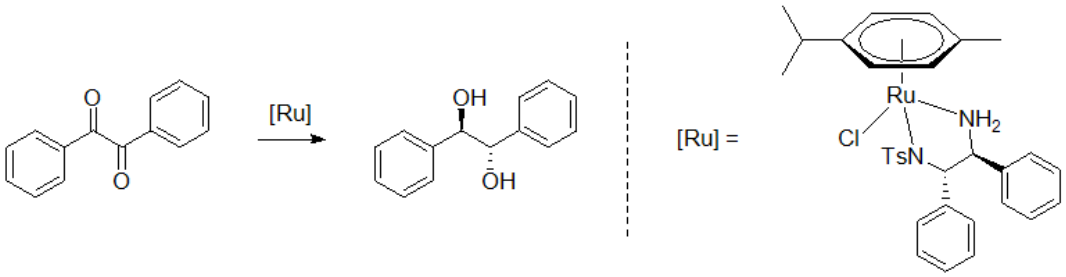

Scheme 13: Noyori's asymmetric reduction of benzil[41]

Under identical conditions to those used by Noyori[41] using **9-11** in place of RuCl[(R,R)-Tsdpen](cymene) no conversion was seen and benzil was recovered quantitatively. The presence of the anionic sulfonamide is critical for operation of Noyori's catalyst by facilitating efficient hydrogen transfer to the substrate.[43] Given the absence of this functionality in the present systems it is unsurprising that similar reactivity is not observed. Beyond this, the most striking dissimilarity between the two catalyst structures is the differing coordination modes of supporting chiral ligands, **8-10** possess monodentate phosphine ligands whereas most other systems incorporate a bidentate chelating ligand at

the Ru centre.[42] This will have a marked influence on the electronic properties of the Ru centre in addition to influencing the stability and longevity of the complex under the reaction conditions. Furthermore, a more rigidly bound ligand can be expected to more precisely define the chiral space around the metal centre resulting in a greater degree of chiral discrimination. The amine and/or alcohol functional groups present in ligands **6-8** may potentially facilitate such a chelating geometry. Halide abstraction is envisioned to open up a vacant site around the metal centre and allow for coordination of the pendant donor atoms.

Described below is the reactivity and spectroscopic data associated with complex **(*S*)-9**, closely similar results were observed in the case of **(*R*)-9**, **(*S*)-10**, **(*R*)-10, (*S*)-11** and **(*R*)-11**. Following addition of 1 equivalent of $AgPF_6$ to a solution of **(*S*)-9** in methylene chloride, the solution turned a paler shade of orange and a cloudy, off white precipitate was formed. After filtration and removal of the solvent the product was collected as a red solid. High resolution mass spectra indicated the presence of mono-chloro cations, [Ru(*p*-cymene)(**(*S*)-9**)Cl]$^+$, in the sample. ^{31}P NMR spectrum (Figure 4) shows a number of species with resonances at δ_P = 19.9, 20.4 and 49.9 ppm alongside three small signals appearing at δ_P = 51.1, 53.6 and 56.8 ppm. The peak at δ = 20.4 ppm corresponds to **(*S*)-9** and thus the peak at δ_P = 19.9 ppm can be assumed to be a similarly monodentate ligated complex, potentially a dimeric structure formed from the putative coordinatively unsaturated species. A downfield shift of the ^{31}P NMR signal is often associated with chelate ring formation.[44,45] Furthermore, the similar complexes [(η^6-C_6Me_6)Ru(P^O)Cl]BPh_4 and [(η^6-*p*-cymene)Ru(P^N)Cl]BF_4 (where P^O = $PPh_2(CH_2CH_2OMe)$,[46] and P^N = [η^6-(*R,R*)-*o*-{$(NMe_2)CHMe$}$C_6H_4PPh_2$]$Cr(CO)_3$)[47] display ^{31}P NMR chemical shifts in this region (δ_P = 51.2 and 42.7 ppm respectively); thus the peaks between 49.9 and 56.8 ppm can be reasonably assigned as chelating structures.

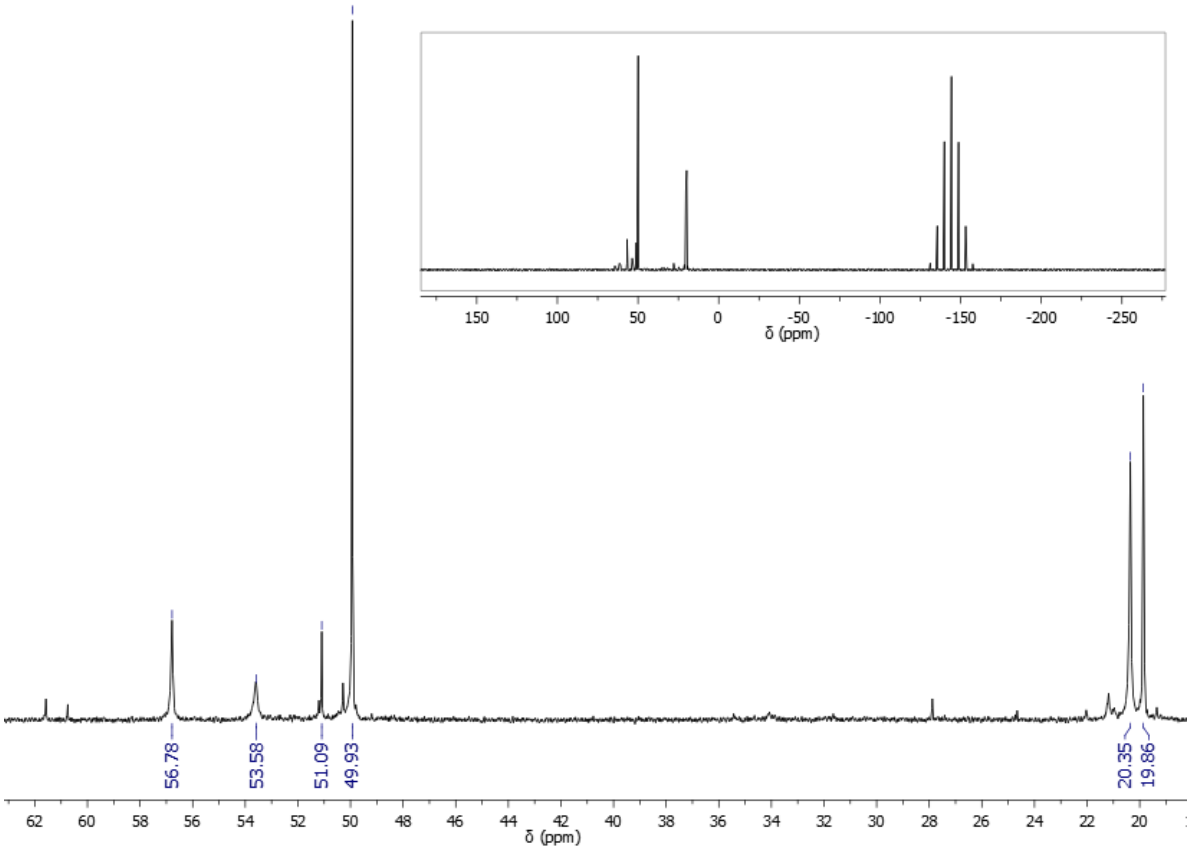

*Figure 4: Expanded ^{31}P NMR spectrum of **(S)-9** following treatment with 1 equivalent of $AgPF_6$. Inset: Full spectrum*

It is hypothesised that abstraction of a chloride from **(*S*)-9** generates a transient 16 e^- intermediate, which is highly reactive towards incoming ligands. One potential route by which this species may alleviate the electronic unsaturation is *via* dimerization giving a bis(chloro-bridged) diruthenium complex. In subsequent reactions MeCN was used as the solvent as its donor ability may mitigate the tendency towards decomposition of the coordinatively unsaturated species. Indeed, following addition of further $AgPF_6$ in MeCN the resonance at δ_P = 19.9 ppm was no longer observed. Otherwise the ^{31}P NMR spectrum remains unaffected. The major resonances in this case were those of **(*S*)-9** and the peak at δ_P = 49.9 ppm presumably that of the P^N chelate species. Attempts to purify these materials further to allow for catalytic studies and structural determination failed.

Reactions with thiols

Ligand Synthesis

Reaction of **1** with *p*-thiocresol in the presence of catalytic triethylamine gives 1-(diphenylphosphanyl)-3-(*p*-tolylthio)propan-2-ol (Figure 14), **12**, as an air stable pale yellow oil. Similarly, reaction of 1,2-ethanedithiol with **(*S*)-1** gives the multidentate ligand (2R,2'R)-3,3'-(ethane-1,2-diylbis(sulfanediyl))bis(1-(diphenylphosphanyl)propan-2-ol), **13**. In contrast to compound **12**, this compound is sensitive to oxidation in air. The ^{31}P NMR spectrum of **13** shows a single resonance at δ = -22.9 ppm, whereas the oxide appears at δ = 35.1 ppm. The ^{1}H NMR spectrum of **13** confirms the proposed structure; in particular, the resonance associated with the ethylene bridge appears as a singlet (δ = 2.59 ppm) reflecting the symmetry of the ligand and confirming twofold substitution of the dithiol.

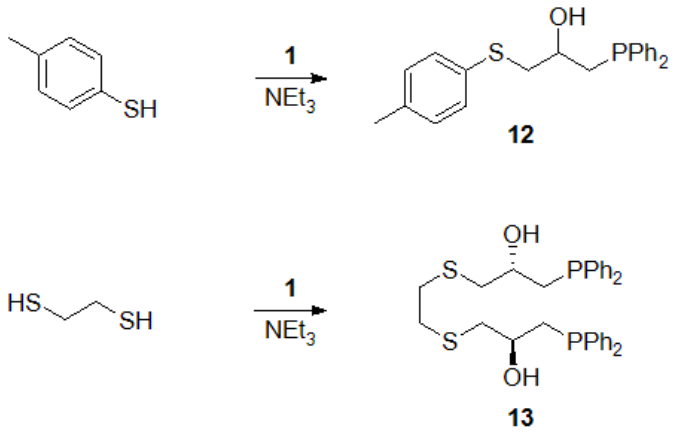

Scheme 14: Synthesis of P,O,S donors

To date only very few reports have been made of compounds containing this P,O,S motif,[10,12,48] and the coordination chemistry of these ligands is relatively unexplored. The soft nature of thioether donors give them similar utility to phosphines as supporting moieties in homogeneous catalysis. Furthermore, S donors tend to be more labile than phosphines and are used in homogeneous catalysis to temporarily introduce vacant coordination sites during catalytic cycles.[49]

Coordination chemistry with transition metals

Complexes of the general form [M(**13**)]Cl_2; where M = Ni (**14**), Pd (**15**) or Pt (**16**); were formed by refluxing the ligand in EtOH or EtOH/H_2O mixtures with $NiCl_2 \cdot 6H_2O$, $Na_2[PdCl_4]$ or $K_2[PtCl_4]$ respectively. All complexes were characterised by NMR, MS, IR and elemental analyses. Crystals suitable for X-ray diffraction of the Pd complex, **15**, were grown from a saturated solution in MeOH. The structure of **15** is shown in Figure 5. Complex **15** has C_2 symmetry with the ligand bound in a P,S,S,P tetradentate manner around a distorted square planar metal centre. The two alcohol groups are *trans* to one another and have a hydrogen bond to the chloride anions. Bond lengths and angles are in good agreement with similar complexes from the literature.[50] The five membered S-Pt-S chelate ring adopts a puckered conformation, while the two six membered P-Pd-S chelate rings adopt distorted chair conformations. The stereochemical information of the ligand backbone appears to have been transferred to the S donors, which are both of *(S)*- stereochemistry, upon coordination. The hydroxyls are observed in both axial and equatorial arrangements with only a slight preference for the equatorial conformation (53% equatorial).

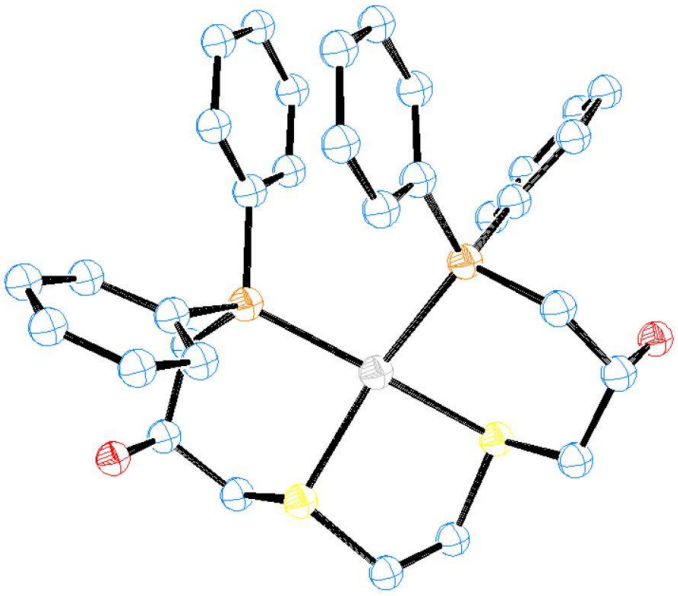

*Figure 5: ORTEP Representation of complex **15**. Hydrogen atoms, chloride counter ions and disordered -OH groups (47:53%) omitted for clarity. Selected bond lengths (Å) and angles (°): Pd-S 2.3227(12), Pd-P 2.2867(10), S-Pd-S′ 90.65(6), P-Pd-S 87.34(4), P-Pd-P' 99.88(5)*

The structure of the Ni complex, **14**, appears to be far more complex than that of the heavier congeners. The ^{31}P NMR spectrum shows the presence of at least three distinct P environments with resonances visible at δ = 21.7, 31.4 and 34.0 ppm. Further qualitative evidence of this diversity is given by the fact that in chloroform solution **14** has a distinctive violet colour rather than the red/orange colour usually associated with square planar Ni(II) complexes. Furthermore, upon standing for a prolonged period small green crystals were precipitated from the violet solution. The colour observed for complexes of this type typically arises from electronic transitions between d orbitals of the metal and thus the observed colour is indicative of the ligands and coordination geometry of the inner coordination sphere. Machan *et al.* have observed a similar complexity in the coordination chemistry of a very closely related complex, $[Ni(\kappa^2\text{-}P,S\text{-}Ph_2PCH_2CH_2SMe)_2Cl_2]$.[51] The structure of this green complex was unambiguously identified as an octahedral coordination with the two bidentate ligands in the equatorial plane and two chlorides occupying apical positions. Given the qualitative similarities between the properties of this complex with **14** it is plausible to assign a similar octahedral structure to observed the green precipitate. The nature of the species in solution is less clear, it is likely that the ligands are similarly labile but dissociation of the internal thioethers is unlikely in this case. Ciampolini *et al.* have reported a number of violet Ni complexes bearing a tetraphosphino-dithia-macrocyclic ligand which display pseudo-octahedral geometries with elongated Ni-S bonds.[52] It is highly likely that in solution the halide ligands dissociate to some extent resulting in a square planar species. This is corroborated by conductivity measurements of **14** in MeOH (Λ_m = 120.5 S cm^{-1} mol^{-1}) which are consistent with a structure intermediate between a 1:1 and a 1:2 electrolyte. As previously mentioned, square planar Ni(II) complexes usually display an orange/red colouration although it is possible that a weak octahedral interaction may affect the square planar NiS_2P_2 chromophore in a similar manner to that observed in Ciampolini's complex.

Such an interaction could occur with the halide ions, the pendant alcohol moieties or solvent molecules. ^{1}H and ^{13}C NMR spectra are very broad and offer no relevant structural data but mass spectra of **14** show the presence of both $[M\text{-}H]^-$ and $[M\text{-}HCl_2]^+$ species in solution, providing further support to the proposed structures in solution (Scheme 15).

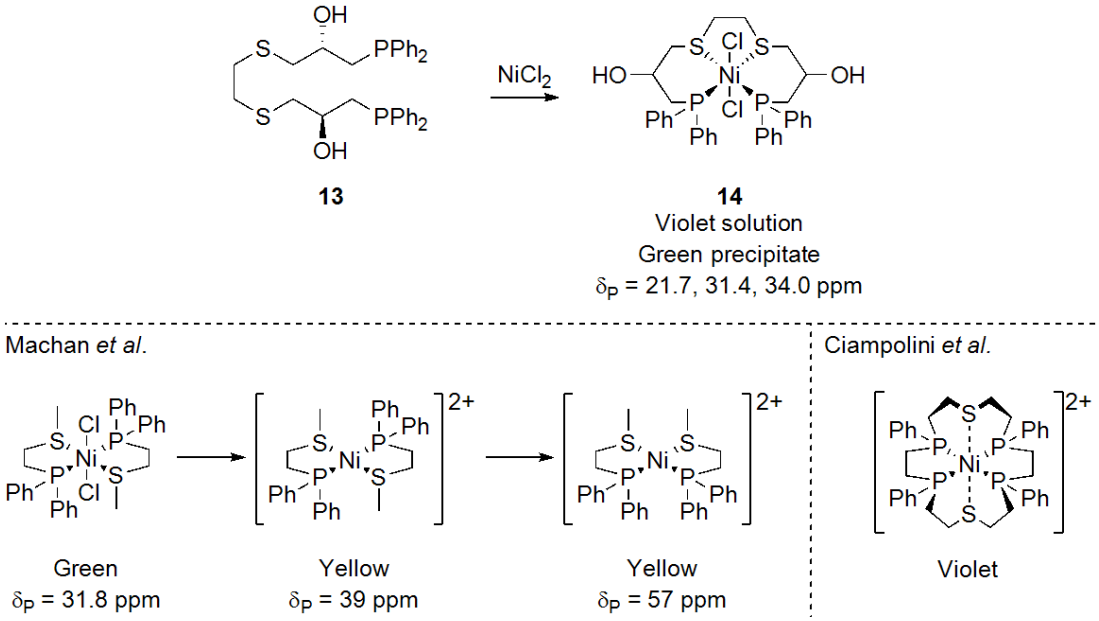

*Scheme 15: Synthesis of Ni complex **16** and comparison with related species from the literature*[51,52]

Conclusion

In, conclusion this chapter has investigated the synthesis of a number of phosphine ligands incorporating P, N or S donors and a chiral alcohol within the ligand backbone. Preliminary investigations into the coordination chemistry of these ligands have been carried out and a number of transition metal complexes have been synthesised. Many of the complexes investigated herein have potential applications in homogeneous catalysis, although further studies are required to investigate this promising area. Nonetheless, it is clear that the use of glycidyl phosphine intermediates, as discussed here, is a highly effective method of rapidly introducing heteroatoms, chirality and complexity into multidentate ligand structures.

Experimental

General considerations

All synthetic procedures and manipulations were performed under dry nitrogen using standard Schlenk line techniques. Dry solvents were freshly distilled from sodium/benzophenone (tetrahydrofuran, diethyl ether) or calcium hydride (dichloromethane, ethanol) under N_2 before use. All other solvents (chloroform, hexane, water) were sparged with N_2 immediately prior to use. NaOH (2 M) and HCl (1 M) solutions were prepared from NaOH pellets and 37% HCl respectively, and thoroughly sparged with N_2 immediately prior to use. ^{1}H (500 or 400 MHz), ^{31}P (121.7 MHz) and ^{13}C (75.6 MHz) NMR spectra were obtained on Bruker 500 or 400 spectrometers. Chemical shifts were determined relative to 85% H_3PO_4 (δ_P = 0 ppm) or tetramethylsilane ($\delta_{H/C}$ = 0 ppm) and are given in ppm. Infrared spectra were recorded on a Shimadzu IRAffinity-1S spectrometer equipped with an ATR attachment. Mass spectra were obtained by the mass spectrometry service at Cardiff University. Conductivity was measured on a Hanna HI 8733 conductivity meter in methanol solutions (10^{-3} M). Elemental analyses were carried out by the elemental analysis service at London Metropolitan University. (*R*/*S*)-epichlorohydrin was resolved from the racemate using the procedure of Jacobsen.[26] Diphenylphosphine was prepared by the action of $LiAlH_4$ on Ph_2PCl. All other chemicals were obtained commercially and used as received.

(oxiran-2-ylmethyl)diphenylphosphinoborane, 2

To a solution of diphenylphosphine (5 mL, 28.7 mmol) in THF (10 mL) was added borane-tetrahydrofuran solution (30 mL, 30 mmol) and stirred for 3 hours at room temperature. The solution was cooled to -78 °C and BuLi in hexanes (18 mL, 28.8 mmol) was added. The orange solution was allowed to warm to room temperature before the addition of *rac*-epichlorohydrin (2.5 mL, 31.8 mmol). The volatiles were removed *in vacuo* and the

residue dissolved in chloroform. Filtration through celite and removal of the solvent yields the product as a white solid (5.6 g, 77 %).

δ_H (400 MHz, $CDCl_3$) 0.77 – 0.94 (3H, m, BH_3), 1.19 – 1.37 (2H, m, CH_2P), 1.46 – 1.54 (1H, m, CH_2), 3.44 – 3.71 (^{1}H, m, CH), 3.73 – 3.82 (1H, m, CH_2), 7.35 – 7.79 (10H, m, aromatics); δ_c (100.6 MHz, $CDCl_3$) 14.0, 19.2, 33.9, 129.1 (d, *J* = 13.9 Hz), 130.9 (d, *J* = 12.7 Hz), 132.2, 132.7; δ_P (121.7 MHz, $CDCl_3$) 22.2

(*S*)-1-(diisopropylphosphanyl)-3-(diphenylphosphanyl)propan-2-ol, 3

To a solution of diphenylphosphine (4.5 mL, 25.8 mmol) in THF (30 mL) at -78 °C was added ^{n}BuLi in hexanes (16 mL, 25.8 mmol). The resulting orange solution was warmed to room temperature for 10 minutes before cooling back to -78 °C. The above solution was then transferred onto a solution of *R*-epichorohydrin (2 mL, 25.5 mmol) in THF (20 mL) also held at -78 °C. The solution was warmed to room temperature and stirred until the orange colour faded. To a separate flask containing di*iso*propylphosphine (3.8 mL, 25.8 mmol) in THF (30 mL) was added ^{n}BuLi in hexanes (16 mL, 25.8 mmol). This solution was stirred for 30 mins at room temperature before addition of the former solution at -78 °C. The solution was heated to reflux for 30 mins and then allowed to stir at room temperature for 2 hrs. The reaction was treated with deoxygenated saturated aqueous NH_4Cl solution (5 mL) and filtered through celite. The filtrate was dried with Na_2SO_4 filtered and the solvent removed *in vacuo*. Passage of the residual oil through a short plug of alumina (eluent: diethyl ether) gave the product as a colourless oil (8.046 g, 81%).

Found: C, 69.9; H, 8.5; $C_{21}H_{30}OP_2$ requires C, 70.0; H, 8.4; ν_{max}/cm^{-1} 3467, 2975, 2914, 1463, 1382; δ_H (400 MHz, $CDCl_3$) 1.02 (12H, m, CH_3), 1.52 – 1.91 (4H, m, CH_2), 2.46 (2H, ddd, *J* = 21.0, 13.7, 6.5 Hz, $CH(Me)_2$), 2.64 (1H, br s, OH), 3.79 (1H, m, C*H*(OH)), 7.31 – 7.48 (10H, m, Ph); δ_c (100.6 MHz, $CDCl_3$) 18.6 (dd, *J* = 11.5, 8.7 Hz, Me), 19.9 (dd, *J* = 15.4, 5.4 Hz, Me), 23.0 (d, *J* = 10.0 Hz, $C(Me)_2$), 23.4, (d, *J* = 10.3 Hz, $C(Me)_2$), 32.0 (dd, *J* = 16.9, 7.4 Hz, $CP(iPr)_2$), 38.35 (dd, *J* = 12.7, 7.3 Hz, $CPPh_2$), 68.7 (dd, *J* =18.7, 16.9 Hz, COH), 128.5 (dd, *J* = 6.9, 2.3 Hz, *m*-Ph),

128.7 (d, *J* = 11.7 Hz, *p*-Ph), 132.9 (dd, *J* = 22.2, 19.0 Hz, *o*-Ph), 138.4 (dd, *J* = 26.7, 11.8 Hz, *i*-Ph); δ_P (121.7 MHz, $CDCl_3$) -20.9 (s, PPh_2), -3.84 (s, P^iPr_2); *m/z* (ES-) 395.1473 ($[M+Cl]^-$, $C_{21}H_{30}OP_2Cl$ = 395.1460)

Dichloro *bis*((*S*)-1-(diisopropylphosphanyl)-3-(diphenylphosphanyl)propan-2-ol) Cobalt, 4

To a suspension of $CoCl_2 \cdot 6H_2O$ (45.1 mg, 0.19 mmol) in toluene (10 mL) was added (*S*)-1-(diisopropylphosphanyl)-3-(diphenylphosphanyl)propan-2-ol (0.138 g, 0.38 mmol) whereupon the pink solid dissolved giving a green/blue solution. Following filtration the solvent was removed *in vacuo* to give the product as a paramagnetic solid. (161 mg, 99 %)

Found: C, 59.2; H, 7.1; $C_{42}H_{60}Cl_2CoO_2P_4$ requires C, 59.3 H, 7.1; *m/z* (ES-) 845.26 ($[M\text{-}HCl+MeOH]^+$, $C_{43}H_{63}ClCoO_3P_4$ = 845.27)

Dichloro (*S*)-1-(diisopropylphosphanyl)-3-(diphenylphosphanyl)propan-2-ol Nickel, 5

To a solution of (*S*)-1-(diisopropylphosphanyl)-3-(diphenylphosphanyl)propan-2-ol (0.58 g, 1.6 mmol) in toluene (5 mL) was added an excess of $NiCl_2 \cdot 6H_2O$ (0.75 g, 3.2 mmol) in methanol (50 mL). An immediadte colour change is observed to dark red. After stirring for 15 minutes the solvent was removed *in vacuo*. The residue was taken up in chloroform, dried over $MgSO_4$ and filtered. The solvent was removed to give the product as a red solid (405 mg, 52 %). Crystals suitable for x-ray diffraction were grown from a saturated solution in MeOH.

ν_{max}/cm^{-1} 2876, 2056, 1485, 1382, 833; δ_H (400 MHz, $CDCl_3$) 1.24 (6H, br s, CH_3), 1.54 (3H, br s, CH_3), 1.75 (3H, br s, CH_3), 1.94 (2H, br s, CH_2), 2.17 (2H, br m, CH_2), 2.74 (2H, br s, C*H*Me_2), 3.04 (^{1}H, br s, *H*COH), 3.73 (1H, br s, OH), 7.23-8.29 (10H, m, Ph); δ_c (100.6 MHz, $CDCl_3$) 18.1, 19.1, 25.0, 35.4, 64.8, 128.4, 128.95, 130.6, 131.6, 133.2; δ_P (121.7 MHz, $CDCl_3$) 14.1 (br s, PPh_2), 37.0 (br s, P^iPr_2); *m/z* (ES+) 777.2809 ($[M+L\text{-}2Cl\text{-}H]^+$, $C_{42}H_{59}NiO_2P_4$ = 777.2819)

(*S*)-1-(dimethylamino)-3-(diphenylphosphanyl)propan-2-ol, (*S*)-6

This material was prepared according to a variation on a previously reported procedure.[13] To a solution of diphenylphosphine (4.5 mL, 25.8 mmol) in THF (30 mL) at -78 °C was added ^{n}BuLi in hexanes (16 mL, 25.8 mmol). The resulting orange solution was warmed to room temperature for 10 minutes before cooling back to -78 °C. The above solution was then transferred onto a solution of (*R*)-epichorohydrin (2 mL, 25.5 mmol) in THF (20 mL) also held at -78 °C. The solution was warmed to room temperature and stirred until the orange colour was faded at which time the volatiles where removed *in vacuo*. The colourless oily residue was immediately redissolved in ethanol (25 mL) and deoxygenated water (10 mL). A solution of dimethylamine in ethanol (10 mL, 56 mmol) was added and the emulsion stirred at room temperature for 16 hrs. The volatiles were removed *in vacuo* followed by addition of deoxygenated water (10 mL). The pH of the mixture was lowered with deoxygenated HCl solution (pH 2) before extraction with diethyl ether. The aqueous phase was then treated with deoxygenated NaOH solution (pH 10) and extracted with dichloromethane. The organic washings were combined and dried over Na_2SO_4. The solvent was removed and the residue passed through a short plug of silica (eluent: petroleum ether/THF/NEt_3, 79:20:1) yielding the product as a pale yellow oil (5.57 g, 75%).

Found: C, 71.25; H, 7.9; N, 5.0; $C_{17}H_{22}NOP$ requires C, 71.1; H, 7.7; N, 4.9; ν_{max}/cm^{-1} 3840, 3406, 2868, 1477, 1385, 839; δ_H (400 MHz, $CDCl_3$) 2.13-2.18 (2H, m, C*H*$_2$PPh$_2$), 2.21 (6H, s, NMe_2), 2.33-2.39 (2H, m, CH_2NMe_2), 3.66 (1H, br s, OH), 3.70-3.78 (1H, m, C*H*OH), 7.31-7.47 (10H, m, PPh_2); δ_c (100.6 MHz, $CDCl_3$) 34.5(d, $^1J_{CP}$ = 13.7 Hz), 45.5, 65.3 (d, $^2J_{CP}$ = 16.8 Hz), 66.2 (d, $^3J_{CP}$ = 9.2 Hz), 128.5, 128.6, 132.8, 138.7; δ_P (121.7 MHz, $CDCl_3$) -22.9; *m/z* (EI+) 287.1436 ($[M]^+$, $C_{17}H_{22}NOP$ = 287.1439)

(*R*)-1-(dimethylamino)-3-(diphenylphosphanyl)propan-2-ol, (*R*)-6

This material was prepared similarly to **(*S*)-6** using diphenylphosphine (25.8 mmol), (*S*)-epichlorohydrin (25.5 mmol) and dimethylamine (56 mmol) (6.63 g, 91%). Spectroscopic data

for this compound were identical to that of (*S*)-1-(dimethylamino)-3-(diphenylphosphanyl)propan-2-ol.

(*S*)-1-(diethylamino)-3-(diphenylphosphanyl)propan-2-ol, (*S*)-7

This material was prepared similarly to **(*S*)-6** using diphenylphosphine (25.8 mmol), (*R*)-epichlorohydrin (25.5 mmol) and diethylamine (97 mmol) (4.66 g, 58%).

Found: C, 72.15; H, 8.1; N, 4.3; $C_{19}H_{26}NOP$ requires C, 72.4; H, 8.3; N, 4.4; ν_{max}/cm^{-1} 2945, 2870, 2769, 2135, 1477, 1387, 1007; δ_H (400 MHz, $CDCl_3$) 0.97 (6H, t, $^3J_{HH}$ = 7.1 Hz, $N(CH_2CH_3)_2$, 2.11-2.68 (8H, m, CH_2), 3.68 (1H, m, C*H*OH), 3.93 (1H, br s, OH), 7.28-7.50 (10 H, m, PPh_2) ; δ_c (100.6 MHz, $CDCl_3$) 12.0, 34.5 (d, $^1J_{CP}$ = 13.5 Hz), 47.0, 60.4 (d, $^2J_{CP}$ = 16.8 Hz), 65.1 (d, $^3J_{CP}$ = 9.5 Hz), 128.4, 128.6, 132.8, 138.9; δ_P (121.7 MHz, $CDCl_3$) -23.2; *m/z* (ES+) 316.1835 ($[M+H]^+$, $C_{19}H_{27}NOP$ = 316.1830)

(*R*)-1-(diethylamino)-3-(diphenylphosphanyl)propan-2-ol, (*R*)-7

This material was prepared similarly to **(*S*)-6** using diphenylphosphine (25.8 mmol), (*S*)-epichlorohydrin (25.5 mmol) and diethylamine (97 mmol) (4.99 g, 62%). Spectroscopic data for this compound were identical to that of (*S*)-1-(diethylamino)-3-(diphenylphosphanyl)propan-2-ol.

(*S*)-1-(diphenylphosphanyl)-3-morpholinopropan-2-ol, (*S*)-8

This material was prepared similarly to **(*S*)-6** using diphenylphosphine (25.8 mmol), (*R*)-epichlorohydrin (25.5 mmol) and morpholine (70 mmol) (7.21 g, 86%).

Found: C, 69.15; H, 74.4; N, 4.3; $C_{19}H_{24}NO_2P$ requires C, 69.3; H, 7.3; N, 4.25; ν_{max}/cm^{-1} 2864, 2227, 2011, 1824, 1477, 1386, 858; δ_H (400 MHz, $CDCl_3$) 2.16 (1H, dd, $^2J_{HH}$ = 13.8 Hz, $^3J_{HH}$ = 6.3 Hz, CH_2N), 2.32-2.41 (4H, m, morpholine), 2.45-2.62 (3H, m, CH_2N + CH_2P), 3.51 (1H, s, OH), 3.61-3.72 (4H, m, morpholine), 3.80 (1H, m, C*H*OH), 7.29-7.52 (10H, m, PPh_2) ; δ_c (100.6 MHz, $CDCl_3$) 34.4 (d, $^1J_{CP}$ = 14.0 Hz), 53.7, 64.6 (d, $^2J_{CP}$ = 16.5 Hz), 65.4 (d, $^3J_{CP}$ = 9.6 Hz), 67.1,

128.6, 128.8, 132.9, 138.6; δ_P (121.7 MHz, $CDCl_3$) -22.9; *m/z* (ES+) 330.1624 ($[M+H]^+$, $C_{19}H_{25}NO_2P$ =330.1623)

(*R*)-1-(diphenylphosphanyl)-3-morpholinopropan-2-ol (*R*)-8

This material was prepared similarly to **(*S*)-6** using diphenylphosphine (25.8 mmol), (*S*)-epichlorohydrin (25.5 mmol) and morpholine (70 mmol) (6.627 g, 91%). Spectroscopic data for this compound were identical to that of (*S*)-1-(diphenylphosphanyl)-3-morpholinopropan-2-ol.

General procedure for the synthesis of Ru complexes (*R*/*S*) - 9-11

To a solution of ligand **(*R*/*S*) – 6-8** (ca. 100mg) in methylene chloride (25 mL) was added $[RuCl_2(cymene)]_2$ (0.5 eq.). The solution was stirred at room temperature for 24 hours at which point it was filtered through celite and the solvent removed *in vacuo*. Products were collected as red/orange solids.

(*S*)-1-(dimethylamino)-3-(diphenylphosphanyl)propan-2-ol *p*-cymene ruthenium dichloride, (*S*)-9

ν_{max}/cm^{-1} 2939, 2868, 1389, 815; δ_H (400 MHz, $CDCl_3$) 0.87 (d, 3H, $^3J_{HH}$ = 6.9 Hz, cymene-CH(C*H*$_3$)$_2$), 1.05 (d, 3H, $^3J_{HH}$ = 6.9 Hz, cymene-CH(C*H*$_3$)$_2$), 1.21-1.34 (m, 6H, N(C*H*$_3$)$_2$), 1.42 (br m, 1H, C*H*Me$_2$), 1.86 (s, 3H, cymene-C*H*$_3$), 2.51 (septet, 1H, $^3J_{HH}$ = 6.9 Hz, cymene-C*H*(CH$_3$)$_2$), 2.5-2.92 (m, 8H, C*H*$_2$), 3.95 (br s, 1H, OH), 4.90 – 5.32 (m, 4H, cymene-C$_6$*H*$_4$), 7.41-7.95 (m, 10H, Ph); δ_c (100.6 MHz, $CDCl_3$) 17.6, 21.4, 22.3, 30.1, 44.6, 53.6, 62.9, 85.0, 87.0, 88.5, 91.4, 95.4, 109.3, 128.5, 130.7, 132.7, 134.2; δ_P (121.7 MHz, $CDCl_3$) 20.35; *m/z* (ES+) 586.0934 ($[M-H]^+$, $C_{27}H_{35}NOPRuCl2$ = 586.0909)

(*R*)-1-(dimethylamino)-3-(diphenylphosphanyl)propan-2-ol *p*-cymene ruthenium dichloride, (*R*)-9

All spectroscopic and analytical data are concurrent with that of the opposite enantiomer.

(*S*)-1-(diethylamino)-3-(diphenylphosphanyl)propan-2-ol *p*-cymene ruthenium dichloride, (*S*)-10

ν_{max}/cm^{-1} 2947, 2868, 1489, 1389, 829; δ_H (400 MHz, $CDCl_3$) 0.79 (d, 3H, $^3J_{HH}$ = 6.9 Hz, cymene-CH(CH_3)$_2$), 1.01 (d, 3H, $^3J_{HH}$ = 6.9 Hz, cymene-CH(CH_3)$_2$), 1.16 (br s, 6H, N(CH_2CH_3)$_2$), 1.42 (br m, 1H, C*H*Me_2), 1.81 (s, 3H, cymene-CH_3), 2.44 (septet, 1H, $^3J_{HH}$ = 6.9 Hz, cymene-C*H*(CH_3)$_2$), 2.54-3.49 (m, 8H, CH_2), 4.18 (br s, 1H, OH), 4.81 – 5.31 (m, 4H, cymene-C_6H_4), 7.36-7.89 (m, 10H, Ph); δ_c (100.6 MHz, $CDCl_3$) 9.4, 17.5, 21.1, 22.3, 24.1, 30.1, 34.2, 48.1, 124.5, 126.3, 128.6, 129.0, 130.7, 131.4, 132.2, 134.3; δ_P (121.7 MHz, $CDCl_3$) 20.5; *m/z* (ES+) 614.1227 ([M-H]$^+$, $C_{29}H_{39}NOPRuCl_2$ = 614.1222)

(*R*)-1-(diethylamino)-3-(diphenylphosphanyl)propan-2-ol *p*-cymene ruthenium dichloride, (*R*)-10

All spectroscopic and analytical data are concurrent with that of the opposite enantiomer.

(*S*)-1-(diphenylphosphanyl)-3-morpholinopropan-2-ol *p*-cymene ruthenium dichloride, (*S*)-11

ν_{max}/cm^{-1} 3404, 2966, 1393, 837; δ_H (400 MHz, $CDCl_3$) 0.86 (d, 3H, $^3J_{HH}$ = 6.9, cymene-CH(CH_3)$_2$), 1.01 (d, 3H, $^3J_{HH}$ = 6.9 Hz, cymene-CH(CH_3)$_2$), 1.86 (s, 3H, cymene-CH_3), 2.03-2.31 (m, 6H, CH_2N), 2.53 (septet, 1H, $^3J_{HH}$ = 6.9 Hz, cymene-C*H*(CH_3)$_2$), 2.70-2.75 (m, 2H, CH_2P), 3.36 (br s, 1H, C*H*OH), 3.52 (br s, 4H, CH_2O), 3.68 (br s, 1H, OH), 4.94-5.29 (m, 4H, cymene-C_6H_4), 7.46-7.97 (m, 10H, Ph); δ_c (100.6 MHz, $CDCl_3$) 17.6, 21.4, 22.2, 30.1, 53.6, 62.5, 67.1, 85.0, 86.8, 89.0, 95.0, 109.1, 128.4, 130.7, 133.1, 133.9; δ_P (121.7 MHz, $CDCl_3$) 19.7; *m/z* (ES+) 630.1183 ([M+H]$^+$, $C_{29}H_{39}NO_2PRuCl_2$ =630.1171)

(*R*)-1-(diphenylphosphanyl)-3-morpholinopropan-2-ol *p*-cymene ruthenium dichloride, (*R*)-11

All spectroscopic and analytical data are concurrent with that of the opposite enantiomer.

1-(diphenylphosphanyl)-3-(p-tolylthio)propan-2-ol, 12

To a solution of diphenylphosphine (4.5 mL, 25.8 mmol) in THF (30 mL) at -78 °C was added ^{n}BuLi in hexanes (16 mL, 25.8 mmol). The resulting orange solution was warmed to room temperature for 10 minutes before cooling back to -78 °C. The above solution was then transferred onto a solution of *rac*-epichorohydrin (2 mL, 25.5 mmol) in THF (20 mL) also held at -78 °C. The solution was warmed to room temperature and stirred until the orange colour was faded at which time the volatiles where removed *in vacuo*. The colourless oily residue was immediately redissolved in ethanol (25 mL) and *p*-thiocresol (5.97 g, 48.1 mmol) was added. The solution was treated with a catalytic amount of triethylamine and stirred at room temperature for 16 hrs. The volatiles were removed *in vacuo* and the residual material was taken up into chloroform (20 mL) and filtered through celite. Removal of solvent and chromatographic purification of the residue (eluting with hexane, CH_2Cl_2 and finally MeOH) yields the product as a yellow oil (5.75 g, 61%).

Found: C, 72.3; H, 6.4; $C_{22}H_{23}OPS$ requires C, 72.1; H, 6.3; ν_{max}/cm^{-1} 3477, 2981, 2864, 1604, 1475, 1386, 810; δ_H (400 MHz, $CDCl_3$) 2.32 (3H, s, CH_3), 2.38 (2H, dd, $^2J_{HP}$ = 6.6 Hz, $^3J_{HH}$ = 2.5 Hz, C*H*$_2$PPh$_2$), 2.61 (1H, br s, OH), 2.94 (1H, dd, $^2J_{HH}$ = 13.8Hz, $^3J_{HH}$ = 8.2 Hz, CH_2S), 3.23 (1H, dd, $^2J_{HH}$ = 13.8 z, $^3J_{HH}$ = 3.9 Hz, CH_2S), 3.67 (1H, m, CHOH), 7.06 (2H, d, $^3J_{HH}$ = 7.9Hz, SC$_6$*H*$_4$CH$_3$), 7.22 (2H, d, $^3J_{HH}$ = 7.9Hz, SC$_6$*H*$_4$CH$_3$), 7.28-7.43 (10H, m, PPh_2); δ_c (100.6 MHz, $CDCl_3$) 21.1, 35.9 (d, $^1J_{CP}$ = 13.8), 43.4 (d, $^3J_{CP}$ = 9.0 Hz), 67.7 (d, $^2J_{CP}$ = 16.9 Hz), 128.6, 128.8, 129.9, 130.9, 131.3, 132.9, 136.9, 138.1; δ_P (121.7 MHz, $CDCl_3$) -22.6; *m/z* (EI+) 366.1204 ([M]$^+$, $C_{22}H_{23}OPS$ = 366.1207)

(2*R*, 2'*R*)-3,3'-(ethane-1,2-diylbis(sulfanediyl))bis(1-(diphenylphosphanyl)propan-2-ol), 13

To a solution of diphenylphosphine (2.2 mL, 12.6 mmol) in THF (30 mL) held at -78 °C was added ^{n}BuLi in hexanes (5.1 mL, 12.6 mmol). The resulting orange solution was warmed to room temperature for 10 minutes before cooling back to -78 °C. The above solution was then transferred onto a solution of (*S*)-epichorohydrin (1 mL, 12.8 mmol) in THF (20 mL) also held

at -78 °C. The solution was warmed to room temperature and stirred until the orange colour was faded at which time the volatiles where removed *in vacuo*. The colourless oily residue was immediately redissolved in ethanol (25 mL) and 1,2-ethanedithiol (0.5 mL, 6.0 mmol) was added. The solution was treated with a catalytic amount of triethylamine and stirred at room temperature for 16 hrs. The volatiles were removed *in vacuo* and the residue taken up in methylene chloride (10 mL). Filtration and removal of the solvent gave the product as a colourless oil (3.47 g, 100 %)

ν_{max}/cm^{-1} 3478, 2981, 2864, 1475, 1386; δ_H (400 MHz, methanol-d_4) 2.38 (4H, ddd, $^2J_{HH}$ = 70.1 Hz, $^2J_{HP}$ = 13.8 Hz, $^3J_{HH}$ = 6.9 Hz, CH_2P), 2.59 (4H, s, $(CH_2SR)_2$), 2.63 – 2.78 (4H, m, C*H*$_2$CH(OH)), 3.61 (2H, q, *J* = 6.9 Hz, C*H*OH), 3.70 (2H, br s, OH), 7.28 – 7.48 (20 H, m, Ph); δ_c (100.6 MHz, methanol-d_4) 33.7, 37.9 (d, *J* = 12.7 Hz), 40.9 (d, *J* = 7.2 Hz), 70.0 (d, *J* = 16.4 Hz), 129.6 (t, *J* = 5.0 Hz), 129.8 (d, *J* =25.6 Hz), 133.9 (dd, *J* = 43.9, 18.8 Hz), 139.9 (dd, *J* = 40.9, 12.1 Hz); δ_P (121.7 MHz, methanol-d_4) -22.9; *m/z* (ES+) 579.1726 ($[M+H]^+$, $C_{32}H_{37}O_2P_2S_2$ = 579.1710)

Dichloro (2*R*, 2'*R*)-3,3'-(ethane-1,2-diylbis(sulfanediyl))bis(1-(diphenylphosphanyl)propan-2-ol) Nickel, 14

To a solution of $NiCl_2{\cdot}6H_2O$ (200 mg, 0.84 mmol) in EtOH (50 mL) was added **13** (0.534 g, 0.92 mmol) in toluene (6 mL). The mixture was stirred at room temperature for 4 hours over which time the solution changed colour from green to violet. The solvent was removed *in vacuo* and the residual oily solid was triturated with diethyl ether (10 mL). The product was isolated as a violet solid. (544mg, 92%)

ν_{max}/cm^{-1} 3292, 2870, 2194, 2075, 1475, 1454, 1377, 831; δ_P (121.7 MHz, $CDCl_3$) 21.6, 31.4, 33.9; *m/z* (ES+) 635.0902 ($[M\text{-}HCl_2]^+$, $C_{32}H_{35}NiO_2P_2S_2$ = 635.0907); (ES-) 705.0317 ($[M\text{-}H]^-$, $C_{32}H_{35}Cl_2NiO_2P_2S_2$ = 705.0284); Λ_m/Scm^2mol^{-1} 120.5

(2*R*, 2'*R*)-3,3'-(ethane-1,2-diylbis(sulfanediyl))bis(1-(diphenylphosphanyl)propan-2-ol) Palladium dichloride, 15

To a solution of **13** (290 mg, 0.5 mmol) in ethanol (50 mL) and water (2 mL) was added $Na_2[PdCl_4]$ (147 mg, 0.5 mmol). The mixture was heated to reflux for 1 hour before being allowed to cool. The solvent was removed *in vacuo* and the pale yellow residue was redissolved in chloroform. The solution was filtered and the filtrate dried over Na_2SO_4. Following removal of the solvent the product was collected as a yellow solid. Crystals suitable for X-ray diffraction were grown from saturated solutions in methanol. (265 mg, 70 %)

ν_{max}/cm^{-1} 2870, 2198, 2096, 1492; δ_H (400 MHz, methanol-d_4, -50 °C) 1.0 – 4.5 (m, 14H, aliphatics), 6.5-8.5 (m, 20H, aromatics); δ_P (121.7 MHz, $CDCl_3$) 24.8; *m/z* (ES+) 681.0602 ([M-HCl_2]$^+$, $C_{32}H_{35}PdO_2P_2S_2$ = 681.0594)

(2*R*, 2'*R*)-3,3'-(ethane-1,2-diylbis(sulfanediyl))bis(1-(diphenylphosphanyl)propan-2-ol) Platinum dichloride, 16

To a solution of **13** (247 mg, 0.43 mmol) in ethanol (50 mL) and water (10 mL) was added $K_2[PtCl_4]$ (177 mg, 0.43 mmol). The mixture was heated to reflux for 24 hours before being allowed to cool. The volatiles were removed *in vacuo* and the remainder was extracted with $CHCl_3$ (3 × 10 mL). The organic solution was dried over Na_2SO_4 and the solvent was removed *in vacuo* yielding the product as a pale yellow solid. (81 mg, 22 %)

ν_{max}/cm^{-1} 3406, 2875; δ_H (400 MHz, methanol-d_4, -50 °C) 0.5 – 4.0 (m, 16H, aliphatics), 7.0-8.5 (m, 20H, aromatics); δ_P (121.7 MHz, $CDCl_3$) 34.7; *m/z* (ES+) 789.1291 ([M-HCl_2+H_2O]$^+$, $C_{32}H_{37}PtO_3P_2S_2$ = 789.1286)

References

1 J. Clayden, N. Greeves, S. Warren and P. Wothers, *Organic Chemistry*, Oxford University Press, 8th edn., 2008.

2 E. N. Tsvetkov, N. A. Bondarenko, I. G. Malakhova and M. I. Kabachnik, *Synthesis (Stuttg).*, 1986, **1986**, 198–208.

3 S. M. Baxter and P. T. Wolczanski, *Organometallics*, 1990, **9**, 2498–2509.

4 I. Arribas, S. Vargas, M. Rubio, A. Suárez, C. Domene, E. Álvarez and A. Pizzano, *Organometallics*, 2010, **29**, 5791–5804.

5 D. L. Fox, A. A. Robinson, J. B. Frank and R. N. Salvatore, *Tetrahedron Lett.*, 2003, **44**, 7579–7582.

6 K. Huang, T. J. Emge and X. Zhang, *Heteroat. Chem.*, 2014, **25**, 131–134.

7 K. Issleib and H.-R. Roloff, *Chem. Ber.*, 1965, **98**, 2091–2098.

8 C. Ciardi, A. Romerosa, M. Serrano-Ruiz, L. Gonsalvi, M. Peruzzini and G. Reginato, *J. Org. Chem.*, 2007, **72**, 7787–7789.

9 G. Müller and A. Feustel, *Organometallics*, 2003, **22**, 3049–3058.

10 C. Li, B. Bernet, A. Vasella, E. A. Broger and A. Meili, *Carbohydr. Res.*, 1992, **216**, 149–169.

11 K. Issleib and K. Rockstroh, *Chem. Ber.*, 1963, **96**, 407–410.

12 J. Karas, G. Huttner, K. Heinze, P. Rutsch and L. Zsolnai, *Eur. J. Inorg. Chem.*, 1999, **1999**, 405–420.

13 J. Scherer, G. Huttner and M. Büchner, *Chem. Ber.*, 1996, **129**, 697–713.

14 J. Scherer, G. Huttner, M. Büchner and J. Bakos, *J. Organomet. Chem.*, 1996, **520**, 45–58.

15 S. Ejiri, S. Odo, H. Takahashi, Y. Nishimura, K. Gotoh, Y. Nishihara and K. Takagi, *Org. Lett.*, 2010, **12**, 1692–1695.

16 I. M. Angulo, E. Bouwman, R. van Gorkum, S. M. Lok, M. Lutz and A. L. Spek, *J. Mol.*

Catal. A Chem., 2003, **202**, 97–106.

17 H. Brunner and A. Sicheneder, *Angew. Chemie Int. Ed. English*, 1988, **27**, 718–719.

18 M. Bartholin, J. Conan and A. Guyot, *J. Mol. Catal.*, 1977, **2**, 307–320.

19 S. Reinhard, P. Šoba, F. Rominger and J. Blümel, *Adv. Synth. Catal.*, 2003, **345**, 589–602.

20 C. Merckle, S. Haubrich and J. Blümel, *J. Organomet. Chem.*, 2001, **627**, 44–54.

21 G. Tsiavaliaris, S. Haubrich, C. Merckle and J. Blumel, *Synlett*, 2001, **2001**, 0391–0393.

22 F. Benvenuti, C. Carlini, A. M. Raspolli Galletti, G. Sbrana, M. Marchionna and R. Patrini, *J. Mol. Catal. A Chem.*, 1999, **137**, 49–63.

23 J. R. Dilworth, C. M. Archer, I. A. Latham, J. D. Kelly, D. V. Griffiths, D. C. York, P. M. Mahoney and B. Higley, *Int. J. Radiat. Appl. Instrumentation. Part B. Nucl. Med. Biol.*, 1991, **18**, 547–550.

24 A. Feustel and G. Müller, *Chem. Commun.*, 2001, **18**, 1024–1025.

25 J. A. van Doorn, H. van der Heijden and A. G. Orpen, *Organometallics*, 1994, **13**, 4271–4277.

26 S. E. Schaus, B. D. Brandes, J. Larrow, M. Tokunaga, K. Hansen, A. E. Gould, M. E. Furrow and E. N. Jacobsen, *J. Am. Chem. Soc.*, 2002, **124**, 1307–1315.

27 G. A. Lawrance, in *Encyclopedia of Inorganic Chemistry*, ed. R. B. King, John Wiley & Sons, Ltd, Chichester, UK, 2006.

28 D. M. Burness and H. O. Bayer, *J. Org. Chem.*, 1963, **28**, 2283–2288.

29 L. Hey and C. K. Ingold, *J. Chem. Soc.*, 1933, 531.

30 M. Grayson and P. T. Keough, *J. Am. Chem. Soc.*, 1960, **82**, 3919–3924.

31 C. Bruneau and P. H. Dixneuf, Eds., *Ruthenium Catalysts and Fine Chemistry*, Springer Berlin Heidelberg, Berlin, Heidelberg, 2004, vol. 11.

32 T. Naota, H. Takaya and S.-I. Murahashi, *Chem. Rev.*, 1998, **98**, 2599–2660.

33 M. Bressan, N. d'Alessandro, L. Liberatore and A. Morvillo, *Coord. Chem. Rev.*, 1999,

185, 385–402.

34 G. A. Barf and R. A. Sheldon, *J. Mol. Catal. A Chem.*, 1995, **102**, 23–39.

35 P. Kalck, Y. Peres and J. Jenck, *Adv. Organomet. Chem.*, 1991, **32**, 121–146.

36 A. Noels, A. Demonceau and L. Delaude, *Curr. Org. Chem.*, 2006, **10**, 203–215.

37 V. Ratovelomanana-Vidal and J.-P. Genêt, *J. Organomet. Chem.*, 1998, **567**, 163–171.

38 U. Matteoli, P. Frediani, M. Bianchi, C. Botteghi and S. Gladiali, *J. Mol. Catal.*, 1981, **12**, 265–319.

39 R. Noyori and S. Hashiguchi, *Acc. Chem. Res.*, 1997, **30**, 97.

40 I. Yamada, M. Ohkouchi, M. Yamaguchi and T. Yamagishi, *J. Chem. Soc. Perkin Trans. 1*, 1997, **99**, 1869–1874.

41 T. Ikariya, S. Hashiguchi, K. Murata and R. Noyori, *Org. Synth.*, 2005, **82**, 10.

42 J. Václavík, P. Šot, B. Vilhanová, J. Pecháček, M. Kuzma and P. Kačer, *Molecules*, 2013, **18**, 6804–6828.

43 J. Václavík, P. Šot, J. Pecháček, B. Vilhanová, O. Matuška, M. Kuzma and P. Kačer, *Molecules*, 2014, **19**, 6987–7007.

44 E. Lindner, R. Fawzi, H. A. Mayer, K. Eichele and W. Hiller, *Organometallics*, 1992, **11**, 1033–1043.

45 P. E. Garrou, *Chem. Rev.*, 1981, **81**, 229–266.

46 E. Lindner, S. Pautz, R. Fawzi and M. Steimann, *J. Organomet. Chem.*, 1998, **555**, 247–253.

47 D. Totev, A. Salzer, D. Carmona, L. A. Oro, F. J. Lahoz and I. T. Dobrinovitch, *Inorganica Chim. Acta*, 2004, **357**, 2889–2898.

48 M. Coll, O. Pàmies and M. Diéguez, *Adv. Synth. Catal.*, 2013, **355**, 143–160.

49 D. K. Dutta and B. Deb, *Coord. Chem. Rev.*, 2011, **255**, 1686–1712.

50 C. J. Smith, V. S. Reddy, S. R. Karra, K. V. Katti and B. Leonard J., *Inorg. Chem.*, 1997, **36**, 1786–1791.

51 C. W. Machan, A. M. Spokoyny, M. R. Jones, A. A. Sarjeant, C. L. Stern and C. A. Mirkin, *J. Am. Chem. Soc.*, 2011, **133**, 3023–3033.

52 M. Ciampolini, N. Nardi, P. Dapporto, P. Innocenti and F. Zanobini, *J. Chem. Soc., Dalt. Trans.*, 1984, 575–579.

Chapter 4

Synthesis of chiral at metal aluminium complexes

Introduction

Chiral-at-metal complexes

Asymmetric synthesis relies on the ability to selectively favour formation of one enantiomer over another. One method by which this is commonly achieved is by use of a chiral catalyst; In general, for metal based catalysis, the chiral environment around the metal centre controls the approach of the substrate such that the pathway leading to a particular enantiomer is favoured over the other. If one considers the conversion of a prochiral substrate such as an alkene or ketone into a chiral product it is clear that attack on one face will lead to formation of the (*R*)-enantiomer whereas attack on the opposite face will lead to an (*S*)-stereocentre in the product. The catalyst binds to the substrate in order to facilitate the transformation and if the catalyst is achiral then the resulting product will be a racemate. Contrarily, if the catalyst is chiral and enantiomerically pure then the transition state leading to the product will inevitably be diastereotopic. If one of these diasteromeric transition states is of higher energy than the other, it will disfavour formation of the product *via* that pathway and hence the product will become enriched in one enantiomer over the other. Thus, the ability to induce asymmetry in a catalytic transformation relies on the presence of chirality around a metal centre

The most common way to introduce chiral space around a metal centre is by use of chiral ligands, i.e. ligands which posess at least one stereocentre and/or axial chirality within the ligand scaffold. However, in recent years a number of systems have emerged which contain stereogenic centres at the metal ion.[1,2] The simplest case is given by tetrahedral complexes which are directly comparable to chiral carbon centres. In cases where at least 4 differing donor groups coordinate the metal centre the resultant complexes contain a chiral centre at the metal ion (Figure 1, a).[2]

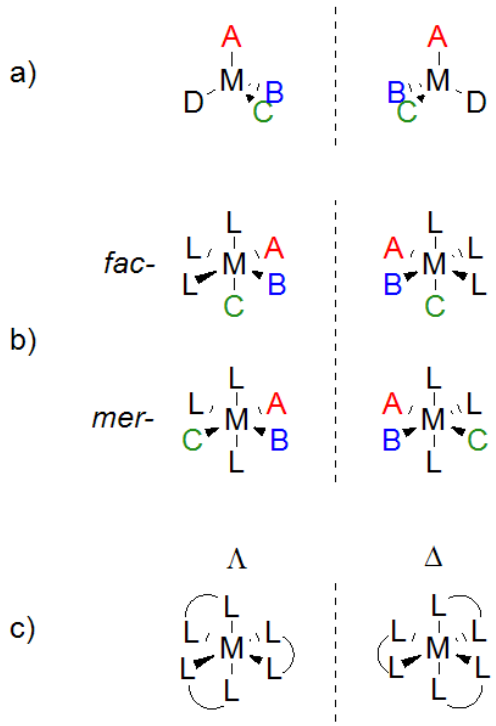

Figure 1: Selected generic structures of chiral-at-metal complexes. a) tetrahedral complexes; b) fac- complexes are chiral whereas mer- complexes are not; c) helical chirality

The complexity of the chiral-at-metal systems rises with increasing coordination number as, in principal, any metal ion bound to four or more dissimilar donors may be chiral. Variations in the configuration of the ligands and geometry of the metal centre can further complicate the picture (Figure 1, b). A special case is given by octahedral metal ions bound to at least two bidentate ligands, e.g. $[Ru(bpy)_3]^{2+}$. Such complexes exhibit helical chirality and are found in both Λ and Δ forms (Figure 1, c).

In practice, compounds containing stereogenic metal centres are usually found as a mixture of isomers as the potential number of isomers is very large. Several strategies have been employed in an effort to reduce the number of potential isomers; rigid facially bound ligands, such as Cp^- or η^6-arenes, and/or induction by a chiral ligand or counterion can be used in the preparation of enantiomerically enriched coordination compounds. A further strategy is the chiral resolution of a racemate through chromatography or selective crystallisation. A number of compounds containing stereogenic metal centres have now been prepared by these methods (Figure 2). A further complication is encountered when one considers

reactions at metal centres. Labile metals, e.g. Al(III), will not form stable stereocentres as rapid redistribution of the ligands leads to complex mixtures. Hence, it is necessary to incorporate multidentate ligands to control the chirality.

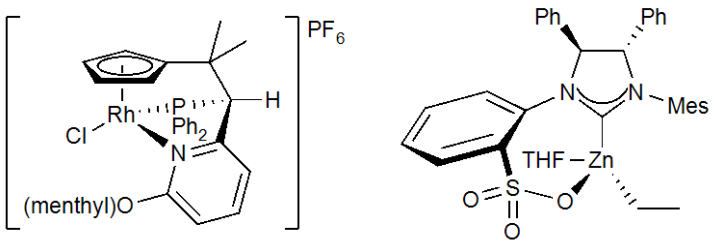

Figure 2: Selected examples of chiral-at-metal complexes[3,4]

Organoaluminium chemistry

Organoaluminium compounds have long been of interest as initiators and/or catalysts for ethylene polymerisation.[5,6] The propensity for Al alkyls to undergo insertion, β-hydride elimination and alkane elimination reactions (under protic conditions) in addition to the high Lewis acidity of Al make these attractive systems for the development of novel C-C bond forming agents. Al complexes typically contain hard X-type ligands (e.g. alcoholato-, alkyl-, amido-, halo-) but the inherent Lewis acidity of aluminium species means that neutral L-type donors (e.g. amino-,[7] ethereal,[8] phosphoryl-[9]) can also be incorporated under appropriate conditions. Al complexes typically show relatively low coordination numbers of 4-6 where at least 3 of the ligands are anionic to achieve charge neutrality and the remaining sites are filled by various other donors depending on the precise steric requirements of the ligands in question.

Aims of chapter 4

Use of chiral tridentate ligands invariably induces chirality at the metal ion and thus the tridentate donors investigated here may provide a framework for the construction of chiral Al complexes which may be active for stereoselective C-C bond formation. This chapter will investigate the synthesis of chiral-at-aluminium compounds *via* the complexation of

aluminium with an enantiopure, tridentate ligand containing three disparate donors. The phosphine donors explored elsewhere in this thesis are poor ligands for aluminium. However, phosphine oxides have been shown to bind very well to hard metals such as Al and thus oxidation of γ-amino-β-hydroxyphosphines (see Chapter 3) will furnish a novel tridentate ligand ideally suited to form chiral-at-aluminium complexes.

Results and discussion

Ligand synthesis and reactivity

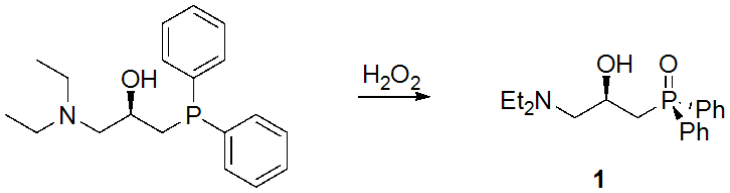

1

*Scheme 1: Synthesis of phosphine oxide ligand **1***

Treatment of (*R*)-1-(diethylamino)-3-(diphenylphosphanyl)propan-2-ol (synthesised as reported in Chapter 3) with hydrogen peroxide gives the phosphine oxide species, **1**, as a colourless oil (Scheme 1). ^{1}H and ^{13}C NMR spectra of **1** are very similar to those of the phosphine precursor and so the phosphine oxide can be readily identified by its ^{31}P NMR signal which shifts downfield to δ=32.1 ppm upon oxidation.

Initial reactivity studies of **1** with an excess of $AlEt_3$ (5 equivalents) in toluene showed strong evidence for complexation. ^{1}H NMR spectra were shifted downfield with respect to the free ligand but were considerably broadened and fine structure was not observable. The ^{31}P NMR spectrum displayed a number of signals with major peaks observed at δ = 32.1, 36.1 and 49.4 ppm in addition to numerous other low intensity signals. The former corresponds to the free ligand but the downfield shift of the remaining signals is suggestive of coordination of the P=O moiety to Al. Reaction of an equimolar quantity of $AlEt_3$ with **1** displayed the same three major peaks but with little or no evidence of further side products. It is apparent that

several species are formed in solution in potential equilibria through the operation of dynamic solution processes.

In order to better understand the solution speciation, some NMR titrations were performed. To a solution of **1** in toluene was added sequentially 0.25 equivalent aliquots of $AlEt_3$ at room temperature. After each addition the mixture was stirred for 30 minutes before interrogation of the ^{31}P NMR spectra to gain insight into the processes in solution (Figure 3). At low concentrations of $AlEt_3$ the free ligand predominates but as the concentration increases a broad peak at δ = 36.1 ppm grows in intensity with a concurrent decrease in the intensity of the ligand signal. This reaches a maximum at *ca*. 0.5 equivalents at which point addition of further $AlEt_3$ results in the appearance of the sharp peak at δ = 49.4 ppm. The second peak reaches a maximum at a 1:1 stoichiometry (Figures 3 & 4) and addition of further $AlEt_3$ does not significantly alter the appearance of the spectrum.

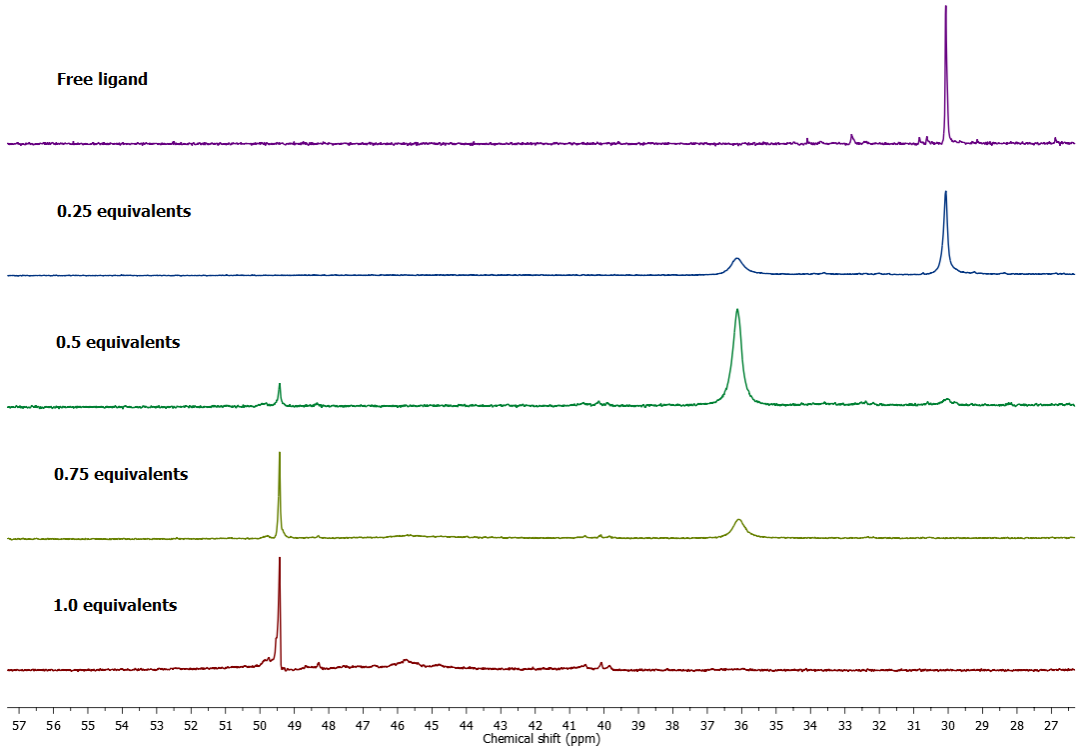

*Figure 3: Stacked plot showing the observed changes to the ^{31}P NMR spectra of **1** as it is titrated with $AlEt_3$*

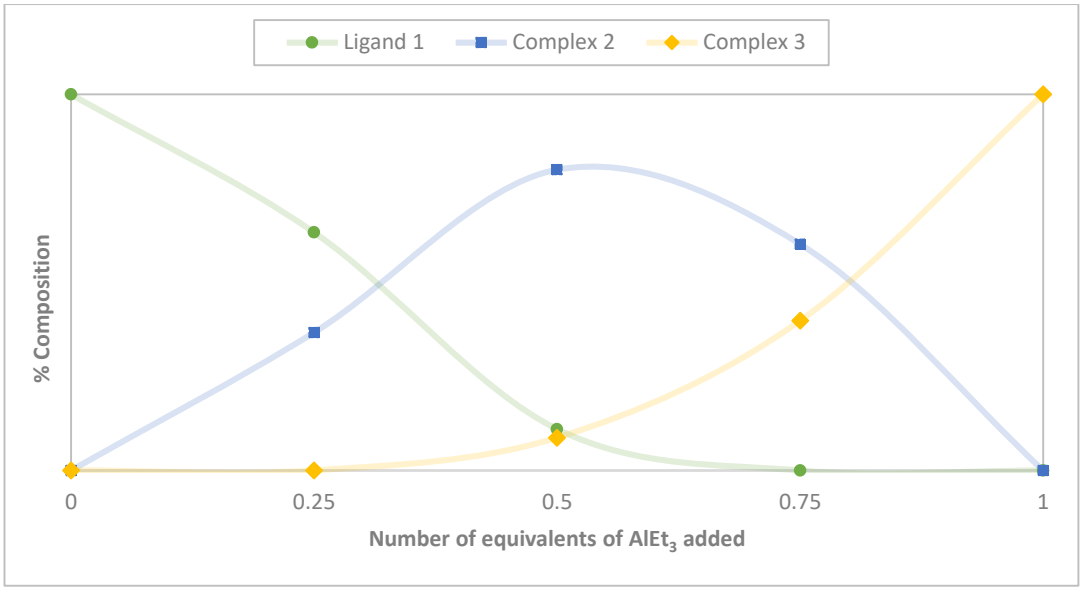

Figure 4: Change in composition of the reaction mixture as a function of stoichiometry. Values measured from integration of the ^{31}P NMR spectra shown in Figure 3

These data can be rationalised as the result of an equilibrium in solution between 3 distinct species; the free ligand, **1**, and two discreet complexes, **2** and **3.** Given the stoichiometries at which these signals were observed a tentative composition for complex **2** and complex **3** can be suggested as Al(**1**)$_2$Et and Al(**1**)Et$_2$ respectively (Scheme 2). Signals attributable to both **2** and **3** are observed in the mass spectra of these solutions as the [M-Et]$^+$ ions. No evidence was observed of a threefold substituted species, likely as a result of steric congestion around the metal centre. Compound **2** is represented here (Scheme 2) as a trigonal bipyramidal structure with *trans*- P=O groups. This is one of a number of potential isomers including square pyramidal and tridentate species; The observation of but a single signal in the ^{31}P NMR spectrum suggests either one thermodynamically preferred species or rapid interconversion between the various isomeric structures (*vide infra*).

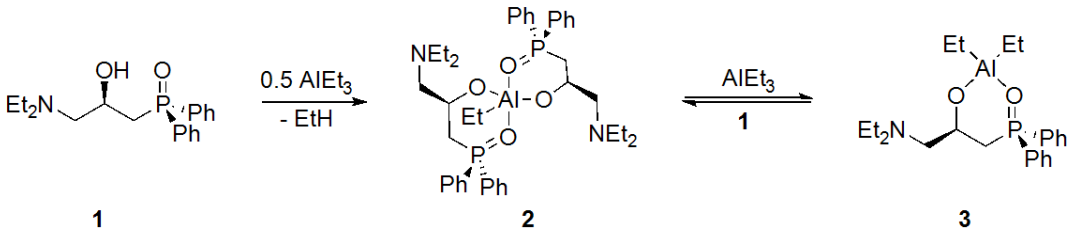

1 **2** **3**

*Scheme 2: Proposed equilibrium of aluminium complexes **2** and **3**. Coordination geometries at Al are arbitrary*

With the knowledge gained from the NMR titrations to hand, larger scale preparations were performed. Hence, reactions of $AlEt_3$ with ligand **1** in the appropriate stoichiometries allowed for the preparation of solutions of complexes **2** and **3**. The composition of these solutions was confirmed by ^{31}P NMR spectroscopy before removal of the solvent to isolate the complexes as white solids. As before, complex **2** gives a broad signal in the ^{31}P NMR spectrum and a signal is observed at the appropriate mass for the $[M\text{-}Et]^+$ species in the mass spectrum. The ^{1}H NMR spectrum closely resembles that of the free ligand **1** with the addition of signals associated with the Al-Et group. Integration of the signals indicates the presence of one ethyl group for every two ligands, confirming the composition of this complex. As for the ^{31}P NMR spectra, the signals associated with ligand **1** in the ^{1}H NMR spectra are considerably broadened and shifted downfield, indicating both coordination of the ligand to the Al centre and the likely presence of fluxional behaviour.

Similarly, complex **3** was isolated from the reaction of **1** with 1 equivalent of $AlEt_3$. The ^{31}P NMR spectrum consists of a single sharp peak at $\delta = 49.4$ ppm and the mass spectrum shows the peak associated with an $[M\text{-}Et]^+$ ion. The ^{1}H NMR spectrum again resembles that of ligand **1** with a downfield shift and some broadening, however in this case fine structure is observed with many of the peaks and thus it is possible to ascertain some structural information about the complex. In particular, the peaks associated with the $AlEt_2$ moeity appear as complex multiplets, similar observations have previously been made with related complexes where the complexity was ascribed to inequivalence of the alkyls resulting from proximity to a chiral centre.[10]

Al has a maximum coordination number of 6, therefore assuming that each of the X type donors are bound then there is potential to accomodate up to three more ligands in the coordination sphere. The ^{31}P NMR spectra give strong evidence for interaction of the phosphine oxides as the P centres are deshielded by the Lewis acidic Al drawing electron density away through the Al-O=P bonds. Furthermore, the ^{31}P NMR chemical shift of complex

2 is less deshielded than that of complex **3**, which could be rationalised as a result of decreased interaction between a hemilabile ligand and the Al centre. The remaining coordination site may be left vacant or occupied by one or other of the two amine donors. Each of these amines is identical and so there is no preference for binding either one. DFT optimisation calculations carried out at the B3LYP level of theory with a 6-31G(d,p) basis set indicate that the systems in which ligand **1** is bound in a tridentate manner do not represent a stationary point on the potential energy surface. Complexes of lower coordination number with non-coordinated amines had the lowest energy for both **2** and **3**. It appears that the phosphine oxides are prefered over the tertiary amines despite the fact that the amines would form a five membered chelate ring rather than the six membered ring formed with the κ^2-*O,O'* coordination mode.

The lowest energy structure of complex **2** is a five coordinate trigonal bipyramid with both ligands in chelating κ^2-*O,O'* coordination modes whereby the phosphine oxides are positioned trans to each other in the axial sites (Figure 2, a). A second geometry was found whereby the metal adopts a tetrahedral geometry with both bidentate κ^2-*O,O'* and monodentate κ-*O* coordination modes (Figure 2, b). The former structure whereby both ligands chelate *via* the alcohol and phosphoryl groups was found to be 10.6 kJ mol^{-1} lower in energy than the tetrahedral structure. Similarly, complex **3** was calculated to display a tetrahedral geometry with ligand **1** bound in a κ^2-*O,O'* coordination mode (Figure 2, c).

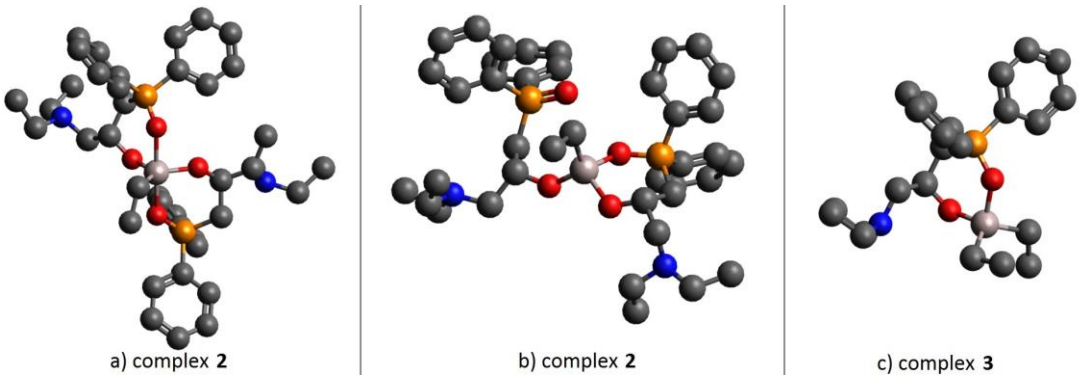

*Figure 5: DFT optimised structures of complexes **2** and **3***

The tridentate coordination mode of the ligand is likely disfavoured as it would require formation of 5 and 6 membered chelate rings fused along two sides. Given the small size of Al^{3+} ions it is likely that such a coordination mode would introduce high levels of strain within the chelate rings and steric repulsion between ligands both of which would favour lower coordination numbers. The interchange of the two phosphoryl donors provides a plausible explanation for the observed broadening in the NMR spectra of complex **2** as the hemilabile nature of similar ligands is well documented.[11–13] There is only minimal energetic difference between the four and five coordinate species of 10.6 kJ mol^{-1}. The magnitude of this energy change is well within the experimental error associated with the DFT calculations and thus the thermodynamic barriers to this process are negligible under standard conditions and hence such a fluxional process is feasible at room temperature. However, in the absence of low temperature NMR experiments or crystallographic characterisation this assertion currently remains speculative.

Conclusion

In conclusion, the synthesis of a chiral alkoxy phosphoryl ligand has been achieved. Reaction of this novel ligand with $AlEt_3$ resulted in the formation of two distinct complexes, which were observed to interconvert in solution depending on the stoichiometry of the mixture. Crystals suitable for X-ray diffraction were not available and thus a detailed crystallographic investigation was not possible. However, both species were isolated and characterised by multinuclear NMR spectroscopy and mass spectrometry. Furthermore, the equilibrium between the mono- and bis- ligated species was investigated by spectroscopic and computational means.

Experimental

General considerations

All synthetic procedures and manipulations were performed under dry nitrogen using standard Schlenk line techniques. Dry solvents were freshly distilled from sodium/benzophenone (tetrahydrofuran, diethyl ether) or calcium hydride (dichloromethane, ethanol) under N_2 before use. All other solvents (chloroform, hexane, water) were sparged with N_2 immediately prior to use. NaOH (2 M) and HCl (1 M) solutions were prepared from NaOH pellets and 37% HCl respectively, and thoroughly sparged with N_2 immediately prior to use. ^{1}H (500 or 400 MHz), ^{31}P (121.7 MHz) and ^{13}C (75.6 MHz) NMR spectra were obtained on Bruker 500 or 400 spectrometers. Chemical shifts were determined relative to 85% H_3PO_4 (δ_P = 0 ppm) or tetramethylsilane ($\delta_{H/C}$ = 0 ppm) and are given in ppm. Mass spectra were obtained by the mass spectrometry service at Cardiff University. (*R*)-1-(diethylamino)-3-(diphenylphosphanyl)propan-2-ol was prepared as reported in Chapter 3. All other chemicals were obtained commercially and used as received.

DFT Calculations

Density functional theory calculations were carried out using the Gaussian 09 package.[14] Proposed structures were initially optimised using the Universal Forcefield (UFF) molecular mechanics forcefield.[15] The resultant structures were then subjected to DFT geometry optimisations using the B3LYP[16–18] hybrid functional with the 6-31G(d,p) basis set on all atoms. Vibrational frequency analysis was performed on the optimised structures to confirm that the structures were minima.

(*R*)-(3-(diethylamino)-2-hydroxypropyl)diphenylphosphine oxide, 1

To a vigorously stirred solution of (*R*)-1-(diethylamino)-3-(diphenylphosphanyl)propan-2-ol (3.9 g, mmol) in methylene chloride (30 mL) was added H_2O_2 solution (30 wt % in H_2O, 7mL). The biphasic mixture was stirred for 12 hours before separation of the organic layer. The

aqueous phase was extracted with methylene chloride (3 × 15 mL) and the combined organic phase was dried over Na_2SO_4. Removal of the solvent *in vacuo* yielded the product as a yellow oil. (2.65 g, 63 %)

δ_H (300 MHz, $CDCl_3$) 0.89 (t, $^3J_{HH}$ = 7.1 Hz, 6H, NCH_2CH_3), 2.40-2.71 (m, 8H, CH_2), 4.05 (m, ^{1}H, C*H*OH), 7.55-7.71 (m, 10H, Ph); δ_c (100.6 MHz, $CDCl_3$) 11.9, 35.4, 47.3, 60.1, 63.6, 128.8, 130.8, 133.6; δ_P (121.7 MHz, $CDCl_3$) 32.1; *m/z* (AP+) 332.2 ($[M+H]^+$, $C_{19}H_{27}NO_2P$ =332.18)

bis(((*R*)-1-(diethylamino)-3-(diphenylphosphoryl)propan-2-yl)oxy)(ethyl)aluminum, 2

To a solution of **1** in toluene (0.79 mL, 0.151 mmol) was added $AlEt_3$ in toluene (0.87 mL, 0.075 mmol). The mixture was stirred at room temperature for 30 minutes before removal of the solvent *in vacuo*. The resultant oil was triturated with petroleum ether (5 mL) yielding a white solid which was isolated by filtration. (73 mg, 67%)

δ_H (400 MHz, C_6D_6) 0.30, (s, 2H, $AlCH_2$), 0.77 (t, 12H, *J* = 7.0 Hz, NCH_2CH_3), 0.82 – 1.46 (m, 8H, CH_2), 2.01-2.70 (m, 8H, CH_2), 2.25 (m, 3H, $AlCH_2CH_3$), 4.26 (br s, 1H, CH), 4.88 (br s, 1H, CH), 7.03-7.79 (m, 20H, Ph); δ_P (121.7 MHz, C_6D_6) 36.1; *m/z* (EI+) 687.33 ($[M-Et]^+$, $C_{38}H_{50}AlN_2O_4P_2$ = 366.1207)

(*R*)-((1-(diethylamino)-3-(diphenylphosphoryl)propan-2-yl)oxy)diethylaluminum, 3

To a solution of **1** in toluene (0.79 mL, 0.151 mmol) was added $AlEt_3$ in toluene (1.37 mL, 0.151 mmol). The mixture was stirred at room temperature for 30 minutes before removal of the solvent *in vacuo*. The resultant oil was triturated with petroleum ether (5 mL) yielding a pale yellow solid which was isolated by filtration. (148 mg, 78%)

δ_H (400 MHz, d_8-tol) 0.57 (app dq, 4H, *J* = 22.0, 8.1 Hz, $AlCH_2$), 1.01 (t, 6H, $^3J_{HH}$ = 7.1 Hz, NCH_2CH_3), 1.50 (m, 2H, CH_2P), 1.73 (app dt, 6H, *J* = 22.0, 8.1 Hz, $AlCH_2CH_3$), 2.24-2.26 (m, 2H) 2.40-2.62 (m, 4H, NCH_2), 4.75 (m, ^{1}H, C*H*OH), 7.05 – 7.24 (m, 10H, Ph); δ_c (100.6 MHz, d_8-tol) 1.4, 10.3, 10.5, 12.6, 21.4, 30.3, 35.4, 64.0, 66.4, 130.5-133.2 δ_P (121.7 MHz, d_8-tol) 49.4; *m/z* (AP+) 386.18 ($[M-H]^+$)

References

1 A. von Zelewsky and O. Mamula, *J. Chem. Soc. Dalt. Trans.*, 2000, **27**, 219–231.

2 M. Fontecave, O. Hamelin and S. Ménage, in *Chiral Diazaligands for Asymmetric Synthesis*, Springer-Verlag, Berlin/Heidelberg, pp. 271–288.

3 H. Brunner, A. Köllnberger, A. Mehmood, T. Tsuno and M. Zabel, *Organometallics*, 2004, **23**, 4006–4008.

4 Y. Lee, B. Li and A. H. Hoveyda, *J. Am. Chem. Soc.*, 2009, **131**, 11625–11633.

5 G. Wilke, *Angew. Chemie Int. Ed.*, 2003, **42**, 5000–5008.

6 K. Ziegler, E. Holzkamp, H. Breil and H. Martin, *Angew. Chemie*, 1955, **67**, 426–426.

7 Y. Hua, Z. Guo, H. Suo and X. Wei, *J. Organomet. Chem.*, 2015, **794**, 59–64.

8 R. Benn, A. Rufińska, H. Lehmkuhl, E. Janssen and C. Krüger, *Angew. Chemie Int. Ed. English*, 1983, **22**, 779–780.

9 L.-C. Liang, F.-Y. Chen, M.-H. Huang, L.-C. Cheng, C.-W. Li and H. M. Lee, *Dalt. Trans.*, 2010, **39**, 9941.

10 R. Kumar, M. L. Sierra and J. P. Oliver, *Organometallics*, 1994, **13**, 4285–4293.

11 J. A. Francis, S. G. Bott and A. R. Barron, *J. Chem. Soc. Dalt. Trans.*, 1998, **15**, 3305–3310.

12 C. N. McMahon, J. A. Francis, S. G. Bott and A. R. Barron, *J. Chem. Soc. Dalt. Trans.*, 1999, **15**, 67–72.

13 J. Lewiński, P. Horeglad, K. Wójcik and I. Justyniak, *Organometallics*, 2005, **24**, 4588–4593.

14 M. J. Frisch, G. W. Trucks, H. B. Schlegel, G. E. Scuseria, M. A. Robb, J. R. Cheeseman, G. Scalmani, V. Barone, B. Mennucci, G. A. Petersson, H. Nakatsuji, M. Caricato, X. Li, H. P. Hratchian, A. F. Izmaylov, J. Bloino, G. Zheng, J. L. Sonnenberg, M. Hada, M. Ehara, K. Toyota, R. Fukuda, J. Hasegawa, M. Ishida, T. Nakajima, Y. Honda, O. Kitao, H. Nakai, T. Vreven, J. Montgomery, J. A., J. E. Peralta, F. Ogliaro, M. Bearpark, J. J.

Heyd, E. Brothers, K. N. Kudin, V. N. Staroverov, R. Kobayashi, J. Normand, K. Raghavachari, A. Rendell, J. C. Burant, S. S. Iyengar, J. Tomasi, M. Cossi, N. Rega, J. M. Millam, M. Klene, J. E. Knox, J. B. Cross, V. Bakken, C. Adamo, J. Jaramillo, R. Gomperts, R. E. Stratmann, O. Yazyev, A. J. Austin, R. Cammi, C. Pomelli, J. W. Ochterski, R. L. Martin, K. Morokuma, V. G. Zakrzewski, G. A. Voth, P. Salvador, J. J. Dannenberg, S. Dapprich, A. D. Daniels, Ö. Farkas, J. B. Foresman, J. V. Ortiz, J. Cioslowski and D. J. Fox, *Gaussian 09, Revis. C.01*, 2009.

15 A. K. Rappe, C. J. Casewit, K. S. Colwell, W. A. Goddard and W. M. Skiff, *J. Am. Chem. Soc.*, 1992, **114**, 10024–10035.

16 A. D. Becke, *J. Chem. Phys.*, 1993, **98**, 5648.

17 B. Miehlich, A. Savin, H. Stoll and H. Preuss, *Chem. Phys. Lett.*, 1989, **157**, 200–206.

18 C. Lee, W. Yang and R. G. Parr, *Phys. Rev. B*, 1988, **37**, 785–789.

Chapter 5

Coordination chemistry of chiral expanded ring N-heterocyclic carbenes

Introduction

Carbenes are neutral divalent species in which the C atom possesses only six valence electrons, two of which are non-bonding. As a consequence, carbenes are inherently reactive and are usually very short lived.[1] Recently, a number of carbenes derived from deprotonation of azolium salts have been prepared and the resultant N-heterocyclic carbenes, NHCs (*vide infra*), have attained great popularity as supporting ligands in organometallic chemistry.[2]

The electronic configuration of carbenes can be described as either singlet or triplet states. Triplet carbenes have a linear structure with an sp hydbridised C atom, the two remaining *p* orbitals each contain a single electron. Whereas singlet carbenes display a bent structure with a pair of electrons located in the sp^2 orbital and an empty orthogonal *p* orbital (Figure 1)

Figure 1: Structure of carbenes. Left: a triplet carbene, Right: a singlet carbene

N-Heterocyclic carbenes

N-Heterocyclic carbenes contain a carbene centre which is stabilised by one or more adjacent N atoms. The singlet electron configuration is enforced by the cyclic structure and the non-bonding electron pair are stabilised by an inductive effect from the electron withdrawing N atoms. Furthermore, orbital overlap between the lone pairs centred on the N atoms with the empty *p* orbitals provide further stability through mesomeric effects (Figure 2)

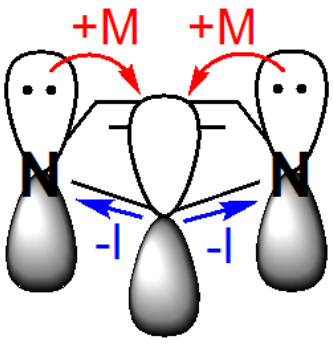

Figure 2: Stabilisation of NHCs via inductive (-I) and mesomeric (+M) effects

NHCs are strong σ-donor ligands are capable of stabilising both high and low valent complexes of metals from across the periodic table. Their similarity in binding and exceptional utility in organometallic chemistry has led them to be widely compared with phosphines. However, it is increasingly apparent that rather than surpassing phosphine ligands, NHCs offer a range of complimentary properties which add to the growing number of supporting ligands available to the organometallic chemist. NHCs tend to form very robust bonds to metals by virtue of their higher bond strength compared to phosphine ligands. Furthermore, the electronic properties are highly tuneable by variation of the backbone and sidearm structures and NHCs are readily synthesised from azolium (typically imidazolium) species. One noteworthy dissimilarity to phosphines is in the steric profile of the ligands. Whereas substituents on phosphines point away from the metal centre in three dimensions, NHCs are typically planar and project their substituents towards the metal (Figure 3). In cases where large substituents (adamantyl, dipp etc.) are incorporated, this can impart kinetic stability on the metal complex.

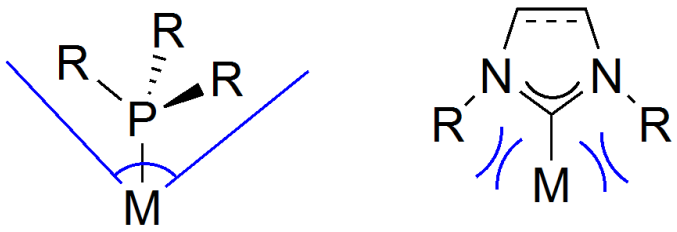

Figure 3: Differing steric profile of NHCs compared to phosphines

NHC complexes have found many applications in homogeneous catalysis; perhaps the most well-known example is the Grubbs 2nd generation catalyst, which employs the *bis* (mesityl)imidazolidinylidene ligand in place of a tricyclohexylphosphine ligand (Figure 4). The greater coordinating ability of NHCs results in higher activity and greater air stability.

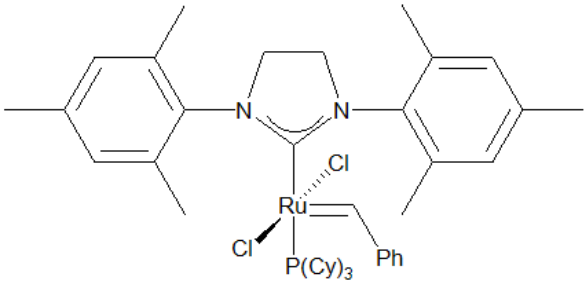

Figure 4: 2nd generation Grubbs catalyst

Expanded ring N-heterocyclic carbenes

NHCs typically contain 5-membered heterocycles, however there is growing interest in six-[3,4] seven-[5–7] and eight-membered[8] carbenes (Figure 5).[9] The greater ring size inherent to these species induces a significantly wider NCN bond angle (often >120 °). Expanded ring carbenes (ER-NHCs) are stronger σ donors than conventional NHCs due to the resulting changes in hybridisation at the carbene centre. Furthermore, the expansion of the NCN angle projects the substituents towards the metal centre even more conferring greater steric shielding over the resultant complexes (Figure 5).

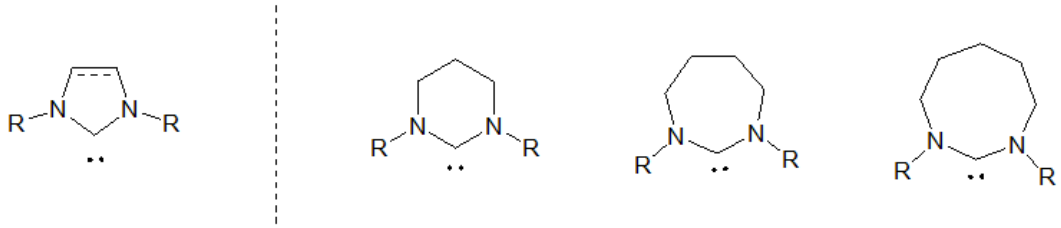

Figure 5: Comparison of 5-membered NHC with expanded ring NHC structures

Chiral carbenes

Given the growing prevalence of NHCs in organometallic chemistry it is perhaps unsurprising that many chiral derivatives of these species have now been developed. Two methods are typically used to introduce chiral space around the metal centre. The first involves use of a chiral backbone. However, in this instance the stereochemistry is fairly remote from the metal centre and very bulky groups must be included to achieve any significant stereoselectivity from catalysts based on these structures. The second common

methodology uses chiral N-substituents to introduce stereochemical information close to the reactive metal centre although reported ee's typically remain low. Indeed, there are numerous reviews detailing the design, synthesis and applications of chiral NHCs.[10–15]

Investigations of chiral expanded ring NHCs are far less well developed and only a few examples of this class of ligand have emerged. Trapp *et al.* developed a series of 6 membered NHCs bearing (*d*)-camphor N-substituents (Figure 6, a).[16] The Pd complexes of these ligands gave good yields in the asymmetric α-arylation of amides, although the stereoselectivity was low. McQuade synthesised a rigid imidazoquinazolinium based species which acted as a precursor to a chiral 6 membered carbene (Figure 6, b).[17] The Cu complex has proven to be an effective catalyst for the borylation[18–20] or silylation[21–23] of many unsaturated substrates. Finally, Stahl *et al.* have synthesised a number of 7 membered carbenes based around a biaryl scaffold (Figure 6, c).[5,24–27] The biaryl backbone in these molecules induces a significant torsional twist into the N-heterocycle and hence these compounds display axial chirality along the M-C^{NHC} bond.

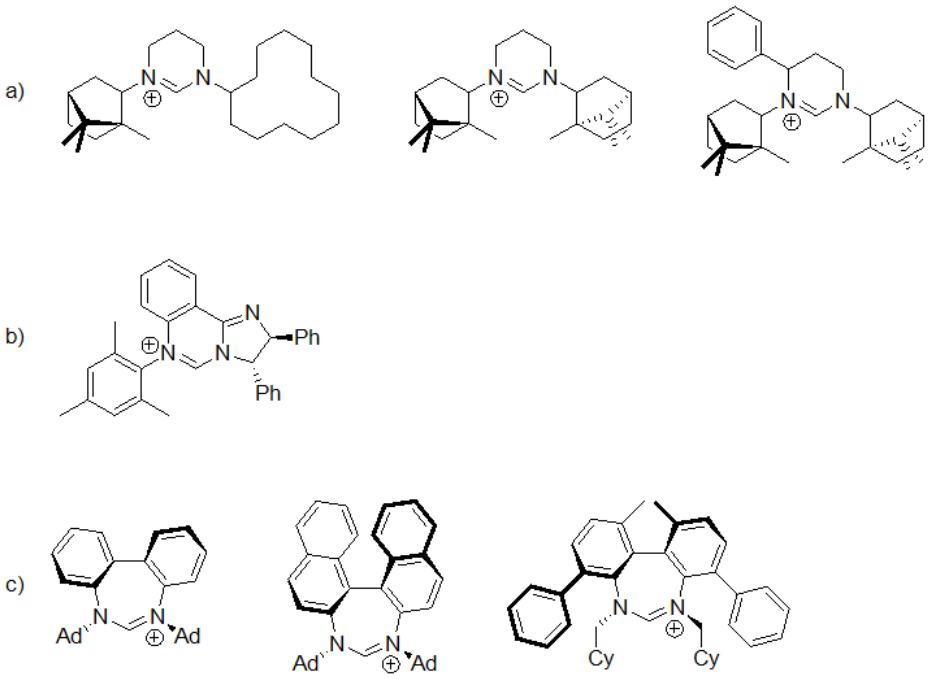

Figure 6: Chiral expanded ring NHCs. a) Trapp's camphor substituted NHCs,[16] b) McQuade's chiral imidazoquinazolium,[17] c) Stahl's biaryl carbenes[5,24–27]

Further to these, a number of species based upon a rigid bicyclic skeleton derived from (1*R*,3*S*)-(+)-camphoric acid have been investigated, such species embed the carbene within fused six- and seven- membered rings providing a novel framework for carbene formation. Camphoric acid is first converted to the diamine *via* a Schmidt reaction, the amines may then be alkylated with either a reductive amination or by nucleophilic substitution of an alkyl halide. Finally, the bicyclic structure is constructed *via* ring closure with triethylorthoformate (Scheme 1).

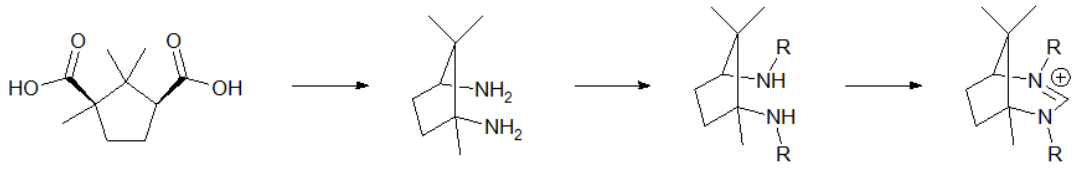

Scheme 1: Synthetic route to camphor base bicyclic carbenes

Initial reports from Wilhelm *et al.* describe a series of variously substituted benzyl derivatives.[28] Furthermore, it was found that the differing steric bulk surrounding the two amine moieties facilitated selective alkylation and hence construction of asymmetrically substituted carbenes. Newman has further incorporated pendant pyridyl and phosphino moieties within the N-substituents, thereby creating a series of tridentate pincer-type ligands.[29–34] Notably, despite the superficial similarity of the pendant donors, they are inequivalent due to the chirality of the carbene backbone and thus the complexes resulting from such ABA' ligands can contain a stereogenic metal centre. Catalysts incorporating these ligands are of interest for applications in homogeneous catalysis, although, preliminary studies have failed to deliver any significant enantioselectivity. It has been shown that the coordination chemistry of the diphosphino-NHC is far more variable and complex than originally envisaged. Reactions with Pd(0), Pd(II), Pt(II), Ag(I), Rh(0) and Rh(I) precursors demonstrated a rich wealth of chemistry with μ-P,P', κ^2-P,P' and κ^3-P,C^{NHC},P' coordination modes identified (Figure 7).[32]

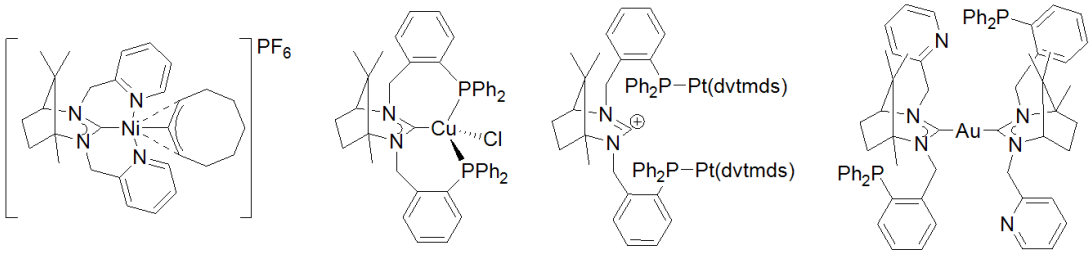

Figure 7: Selected complexes of Newman's tridentate pincer ligands[29,31,32,34]

Recently, Günay prepared a series of PEPPSI-type Pd-NHC complexes using this camphor derived bicyclic carbene bearing substituted benzyl groups.[35] The conformation of the resultant complexes was found to be highly dependent on the nature of the N-substituents.

Aims

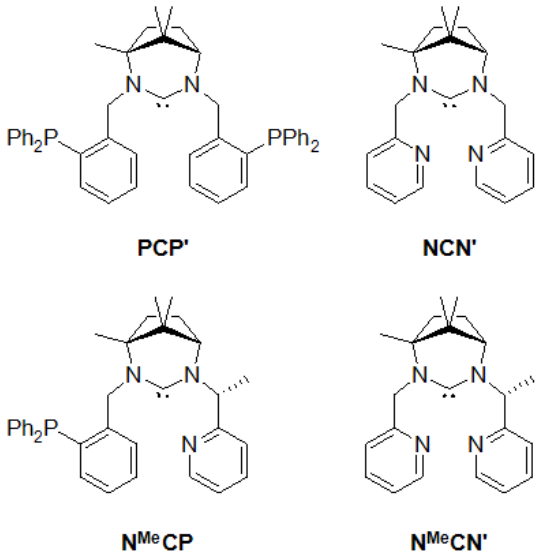

Figure 8: Newman's multidentate heterodonor ER-NHCs

This chapter will further develop the coordination chemistry of Newman's camphor-based expanded ring NHC ligands (Figure 8). By virtue of the chiral centre in the carbene backbone the two phosphine donors are non-equivalent and thus complexes featuring tridentate coordination of the ligand can possess a stereocentre at the metal ion, most notably when the metal adopts a tetrahedral structure.[30–33] Furthermore, the PCP' and related NCN' and $N^{Me}CP$ ligands (Figure 8) have previously been shown to bridge multiple metal centres.[32,34] The factors which effect the preference for one configuration over another are not entirely

clear and thus further investigations are of importance to the fundamental understanding of this unusual ligand system. It is envisaged that through thorough examination of such factors, a degree of control can be exerted upon the structural conformation and hence properties of the complexes.

Results and Discussion

Amidinium proligand synthesis

Each of Newman's tridentate amidinium proligands are derived from 1*R*,3*S*-diamino-1,2,2-trimethylcyclopentane *via* reductive amination and subsequent ring closure with triethylorthoformate.[29,32] It has been shown that the differing steric profiles of the amines can be exploited to selectively substitute at the 3-amino position prior to functionalisation of the 1-amino group, enabling construction of unsymmetrically substituted carbenes.[33,34] To date, this methodology has only been utilised in the synthesis of tridentate heterodonor ligands; analogous bidentate species have not been investigated. NHCs bearing only a single pendant donor species can reasonably be expected to display less complexity and variability in their coordination chemistry and may therefore be of interest in the effort to provide a rational grounding for the observed chemistry of these species.

Buchwald-Hartwig amination of 1*R*,3*S*-diamino-1,2,2-trimethylcyclopentane with mesitylbromide selectively substituted the less sterically encumbered amine to give the mono-mesityl species.[36] Reductive amination of the remaining primary amine with 2-pyridine carboxaldehyde gave the disecondary intermediate **1** which is converted to the amidinium proligand **[2]BF$_4$** *via* treatment with triethyl orthoformate (Scheme 2).

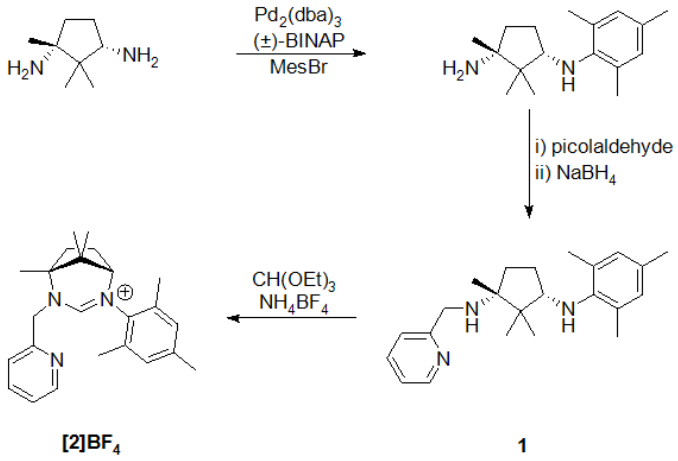

Scheme 2: Synthesis of bidentate amidinium proligand

The ^{1}H NMR spectrum of **[2]BF$_4$** is in agreement with the proposed structure and similar to the previously reported complexes. A notable feature is the inequivalence of the ortho-methyls (δ = 2.25, 2.37 ppm) and meta-hydrogens (δ = 6.95, 6.98 ppm) of the mesityl group. The observed dissimilarity of these peaks strongly suggests that the rotation of the aryl ring about the C-N bond is restricted. The amidinium proton is observed to have a chemical shift of δ = 7.97 ppm, slightly upfield of the relevant signal in the spectrum of [NCN']BF$_4$ (δ = 8.16 ppm). The ^{1}H NMR chemical shift associated with this proton has been used as a proxy for the basicity of the conjugate base, i.e. the free carbene.[29] As may be anticipated, this N-aryl species is less acidic than the previously studied tridentate ligands.

Reactions with zerovalent metals

Both carbenes and phosphines are particularly adept at stabilising soft low oxidation state metal centres. Complexes of PCP' with Cu(I),[31] Ag(I), Pd(II), Pt(II) and Pt(0)[32] metal centres have been reported. To date, little has been reported of the zerovalent metal complexes. Pd(0) and Pt(0) complexes have a d^{10} electronic configuration and hence show a preference for four coordinate tetrahedral geometries. Coordination of the enantiopure chiral PCP' ligand previously synthesised by Newman as tridentate donors should therefore facilitate construction of chiral-at-metal complexes.

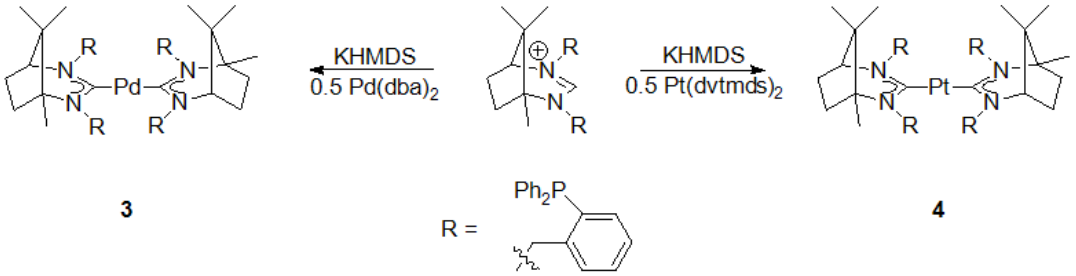

Scheme 3: Synthesis of bis-NHC complexes

Treatment of the amidinium diphosphine proligand with KHMDS (potassium hexamethyldisilazide) in THF followed by addition of 0.5 equivalents of either $Pd(dba)_2$ or $Pt(dvtmds)_2$ (dba = dibenzylideneacetone; dvtmds = 1,3-divinyltetramethyldisiloxane) gave the bis-NHC complexes, **3** and **4** respectively (Scheme 3). Both complexes have been characterised by mass spectrometry, elemental analysis and NMR spectroscopy. Given the similarity between the ^{31}P NMR chemical shifts to the proligand (Table 1), it is likely that the ligand adopts a κ^1-*C*-coordination mode and the pendant phosphines remain uncoordinated in these complexes.

Table 1: ^{31}P chemical shift for PCP' proligand and M(0) complexes

Compound	**δ_P / ppm**
[PCP']PF_6	-16.6, -17.5
3, Pd(PCP')$_2$	-15.25, -15.3
4, Pt(PCP')$_2$	-15.0, -15.3

Such two coordinate species, although less numerous than analogous tetracoordinate M(II) species, are known in the literature and analogous bis-carbene complexes of palladium[37–41] and platinum[42] have been constructed, although to date, no examples have been reported containing chiral ligands or expanded ring carbenes.

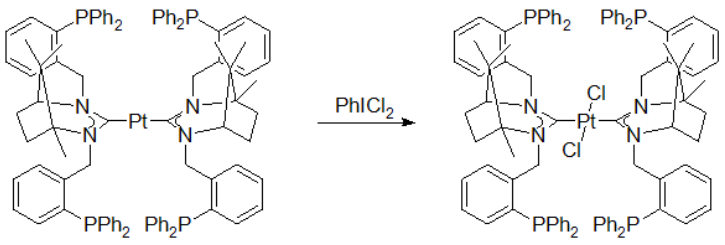

4 **5**

Scheme 4: Oxidation of Pt(0) complex

The reaction of the Pt complex with $PhICl_2$ oxidised the metal to give the tetracoordinate Pt(II) complex, Pt(PCP')Cl_2 **5** (Scheme 4). Two signals were observed in the ^{31}P NMR spectrum at δ = -17.3 and -15.5 ppm suggesting that the carbenes remain in a κ^1-*C*-coordination mode upon oxidation. Satisfactory elemental analysis was not obtained but the identity of the material was confirmed by NMR spectroscopy and mass spectrometry where a peak at *m/z* = 1663 ($[M\text{-}Cl+MeOH]^+$) was observed. The proposed structure of **5** is distinct form the κ^2-*P,P* and κ^3-*P,C,P* complexes previously formed with the PCP' ligand (Scheme 5).[32] This variation is likely observed as a result of the differing synthetic strategies and suggests that the preferred coordination mode may be dependent on the order in which the ligands coordinate.

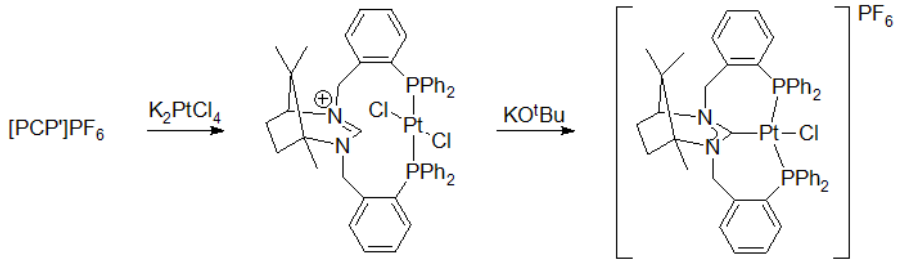

Scheme 5: Newman's synthesis of Pt(II) complexes[32]

A further explanation to the observed differences in coordination mode of the ligand may lie in the stoichiometry of the reactions. Accordingly, 1:1 reactions of PCP' with $Pd(dba)_2$ and $Pt(dvtmds)_2$ were examined. Pd(PCP')(dba), **6**, was isolated from the former reaction as confirmed by a peak in the mass spectrum corresponding to the mono-oxide species ($[M+O+H]^+$ = 1055.3284, $C_{64}H_{61}N_2O_2P_2Pd$ = 1055.3249). No analogous Pt species was found.

The ^{31}P NMR spectrum of **6** indicated the presence of two distinct phosphine environments, the first (δ_P = -14.3, -17.5 ppm) correlates well with the uncoordinated phosphine (*vide supra*) whilst the second environment (δ_P = 9.4, 11.3 ppm) likely corresponds to phosphine coordinated to Pd. The PCP' ligand appears to adopt a κ^2-*C,P*-coordination mode (Figure 9) although given that two signals are observed in each environment it would appear that there is little, if any, preference for coordination of one phosphine over the other. **6** is extremely prone to oxidation, which prohibited attempts to further characterise the complex. Satisfactory elemental analysis could not be obtained and the ^1H NMR spectrum displayed only broad features associated with the PCP' framework. The proposed structure of **6** is tentatively suggested based on the available data and by comparisons with similar compounds in the literature.[43–45]

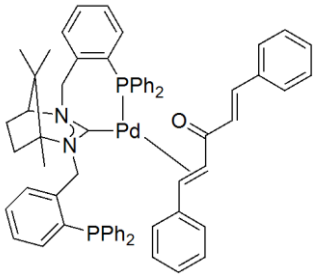

6

*Figure 9: Proposed structure of Pd complex **6***

Given the presence of pendant donors in complexes **4**-**6** it seemed prudent to investigate the reaction of PCP' with higher quantities of metal. Thus, to a solution of PCP' was added 2 equivalents of $Pd(dba)_2$ or $Pt(dvtmds)_2$. The reaction with Pd did not yield any identifiable product, whereas the bimetallic Pt complex, **7**, was obtained from the latter reaction (Figure 10).

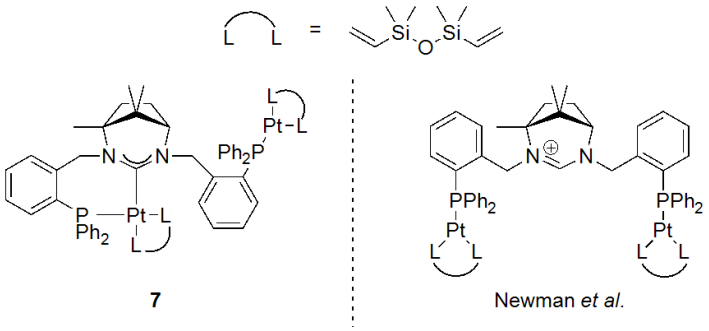

*Figure 10: Proposed structure of complex **7** (left) and comparison to previously reported structure (right)*

A peak associated with the parent ion ($[M+H]^+$ = 1461.4243, $C_{63}H_{83}N_2O_2Si_4P_2Pt$ = 1461.4261) was observed in the high resolution mass spectrum of compound **7**. Furthermore, the complex has been characterised by ^1H and ^{31}P NMR spectroscopy. The ^{31}P NMR spectrum displayed two signals at δ_P = 18.6 and 20.7 ppm which correspond to coordinated phosphine environments; coordination of the phosphine environments is further confirmed by the presence of satellites in the ^{31}P NMR spectrum ($^1J_{P\text{-}Pt}$ = 3505, 3521 Hz). The chemical shift and coupling constants are comparable to those reported for a closely related complex previously reported by Newman *et al.* (Figure 10)[32] as well as similar complexes reported elsewhere in the literature.[46] Newman's previously reported bimetallic complex differs from **7** only in that the amidinium of the latter is deprotonated facilitating chelation with a Pt centre. The PCP' ligand adopts a bridging coordination mode whereby one Pt atom is chelated by both carbene and a phosphine while the remaining phosphine coordinates to the second Pt atom. Attempts to grow crystals of complexes **3-7** suitable for X-ray crystallography were frustrated by their instability in solution and propensity for oxidation of the metal and pendant phosphines. In the absence of crystallographic characterisation, it is difficult to draw any quantitative conclusions, but nonetheless, a number of general features can be elucidated. Firstly, as may be expected considering the greater kinetic stability of carbenes (*cf.* phosphines), in all experiments, both those reported here and previously by Newman *et al.*,[29–34] wherever the amidinium is deprotonated, the resulting carbene will coordinate to the metal in preference to the phosphine donors.

For the reactions reported here, chelating coordination modes appear to be disfavoured. Upon reaction with Pd(0) and Pt(0), the PCP' ligand adopts κ^1-*C* or κ^2-*C,P* coordination modes, in no cases were κ^3 coordination modes observed. This is in stark contrast to the previously observed prevalence of κ^3-*LCL'*-coordination (where LCL' is any of the variously substituted carbenes reported by Newman (Figure 8)) wherever the amidinium is deprotonated.[29–34] It would appear that the order in which the donor groups coordinate is critical in determining the coordination mode. If the metal source is added to a preformed carbene in solution, then monodentate coordination appears to be favoured (**3-5**) with the phosphines only coordinating in instances where the metal is sterically unencumbered (**6-7**). However, as noted above, in situations whereby bonds to the pendant donors (either N or P based) are preformed, deprotonation of the carbene proligand invariably results in tridentate coordination. Care must be taken in the interpretation of this data and in the comparison to previous works as there are numerous factors which may account for this differing reactivity. Further work is required to confirm these assertions and examine whether this hypothesis holds for the other carbene ligands and with other metal centres.

Synthesis of Gold(I) complexes

Recently, there has been growing interest in the chemistry of gold(I) and its complexes with NHC's; Gold(NHC) complexes have found particular use within catalysis and medicine.[47–50] Au(I) is a d^{10} ion and thus its coordination chemistry is characterised by a preponderance of linear two-coordinate species. This inclination towards linear structures limits the denticity of the ligands to κ^1-coordination and thus the pendant donors of Newman's carbenes will remain available for coordination to other metal centres. To date, only the reactivity of the unsymmetrical $N^{Me}CP$ ligand with Au(I) has been reported.[34] The potential to form multimetallic species is intriguing as similar complexes have proven to display novel photophysical properties.[51–54]

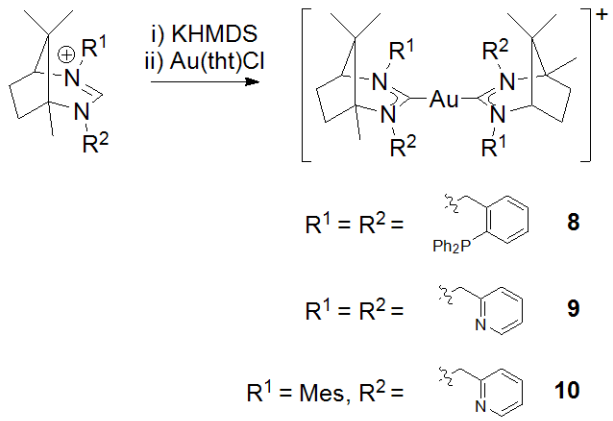

Scheme 6: Synthetic scheme for bis(ER-NHC)Au complexes

Treatment of [PCP']PF_6, [NCN']BF_4 and **[2]BF_4** with KHMDS followed by the addition of 0.5 equivalents of Au(tht)Cl yielded the bis-NHC complexes, **8-10** respectively (Scheme 6). The complexes were characterised by mass spectrometry, ^{1}H and ^{13}C NMR spectroscopy which all confirm the proposed structures. The ^{31}P NMR spectrum of **8** contains a single broad resonance at δ_P = -17.8 ppm arising from the uncoordinated phosphine environments. The broadening likely arises from rotation about the Au-C^{NHC} axis. ^{1}H NMR are comparable to those of the respective ligands and no duplication of the peaks is apparent suggesting that the complex is symmetrical on the NMR timescale. Furthermore, crystallographic characterisation of complexes **8** and **9** was obtained, their molecular structures are displayed in Figures 11 and 12.

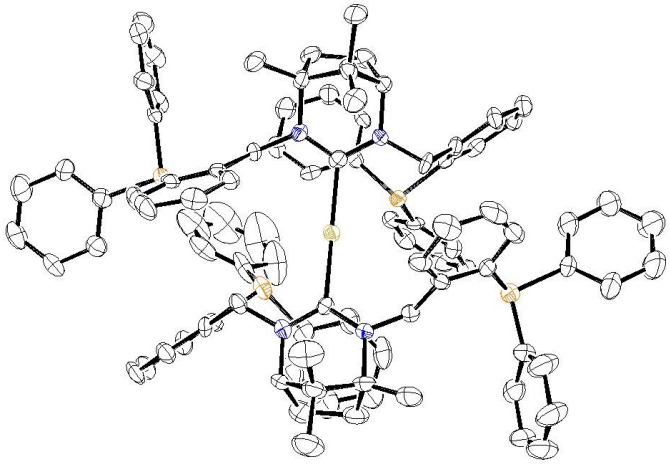

*Figure 11: ORTEP representation of the molecular structure of **8**. Hydrogen atoms and PF_6 counter ion omitted for clarity*

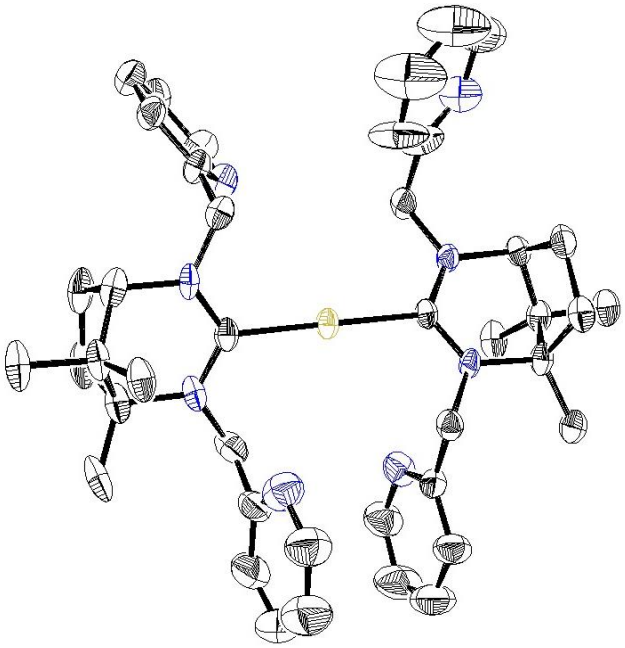

*Figure 12: ORTEP representation of the molecular structure of **9**. Hydrogen atoms and BF_4 counter ion omitted for clarity*

Both complexes display a linear two coordinate geometry around the Au centre and the average C-Au-C bond angles are 168.2° and 175° for complexes **8** and **9** respectively. Au-C bond lengths range from 2.043 – 2.065 Å for compound **8** and between 2.009 – 2.065 Å for the pyridyl complex and are closely similar to bis(ER-NHC) Au complexes reported in the literature.[55] Furthermore, the structures of (ER-NHC)AuCl complexes of N-alkyl camphor based bicyclic carbenes have been reported.[56] The Au-C bonds of **8** and **9** are slightly elongated compared to the chloro- complexes but all other structural metrics are in close agreement with those observed here.

Conclusion

In conclusion, a novel bidentate ER-NHC proligand has been synthesised and the coordination chemistry of this and other carbenes bearing the camphor based backbone have been investigated. The reactivity of the PCP' ligand with Pd(0) and Pt(0) metal centres has been investigated and found to display diverging chemistry from that previously displayed. This study has allowed for the proposal of a rational description of the coordination chemistry which is consistent with the observations presented here and with

those reported elsewhere in the literature. Further work is necessary to confirm and expand upon these hypotheses.

Experimental

General Considerations

All synthetic procedures and manipulations were performed under dry nitrogen using standard Schlenk line techniques. Solvents were freshly distilled from sodium (petroleum ether, toluene), sodium/benzophenone (tetrahydrofuran, diethyl ether) or calcium hydride (dichloromethane, ethanol, acetonitrile) under N_2 before use. ^{1}H (500 or 400 MHz), ^{31}P (121.7 MHz) and ^{13}C (75.6 MHz) NMR spectra were obtained on Bruker 500 or 400 spectrometers. Chemical shifts were determined relative to 85% H_3PO_4 (δ_P = 0 ppm) or tetramethylsilane ($\delta_{H/C}$ = 0 ppm) and are given in ppm. X-ray crystallography was carried out by Dr B. Kariuki, Cardiff University. Mass spectra were obtained by the mass spectrometry service at Cardiff University. PCP',[32] NCN'[29] and (1*R*,3*S*)-N^1-mesityl-2,2,3-trimethylcyclopentane-1,3-diamine[36] were synthesised according to published procedures. All other chemicals were obtained commercially and used as received.

(1*S*,5*R*)-2-mesityl-5,8,8-trimethyl-4-(pyridin-2-ylmethyl)-2,4-diazabicyclo[3.2.1]oct-2-en-2-ium tetrafluoroborate, [2]BF_4

A solution containing (1*R*,3*S*)-N^1-mesityl-2,2,3-trimethylcyclopentane-1,3-diamine (0.660 g, 2.54 mmol) and picolaldehyde (0.041 mL, 2.54 mmol) in ethanol was heated to reflux for one hour. The mixture was cooled to room temperature before the addition of $NaBH_4$ (0.14 g, 3.80 mmol). After 4 hours the excess reductant was quenched by the slow addition of HCl (1 mL) and the solvent was removed *in vacuo*. The resultant brown oil was dissolved in H_2O and basified with NaOH solution (2 M, pH 9). The solution was extracted with methylene chloride (3 × 20 mL) and the combined organic layers were dried over $MgSO_4$. The solution was filtered and the solvent removed *in vacuo* to leave the diamine intermediate, **1**, as a brown

oil. To a solution of **1** (0.742 g, 2.1 mmol) in triethylorthoformate (15 mL) was added ammonium tetrafluoroborate (92 mg, 2.8 mmol) and the resulting solution was heated to reflux for two hours. After cooling the excess triethylorthoformate was decanted and the residue was triturated with Et_2O to give the azolium salt **[2]BF_4** as a green solid. (0.596 g, 52%)

δ_H (400 MHz; $CDCl_3$) 1.19 (s, 3H, CH_3), 1.46 (s, 6H), 1.92 - 2.06 (m, 4H), 2.25 (s, 3H), 2.37 (s, 3H), 2.51 (s, 3H), 2.74 - 2.81 (m, 1H), 4.86 (d, $^2J_{HH}$ = 16 Hz, 1H), 5.13 (d, $^2J_{HH}$ = 20 Hz, 1H), 6.95 (s, 1H), 6.98 (s, 1H), 7.01 (s, 1H), 7.49 (d, $^3J_{HH}$ = 16 Hz, 1H), 7.76 (t, $^3J_{HH}$ = 8 Hz, 1H), 7.97 (s, 1H), 8.58 (d, $^3J_{HH}$ = 4 Hz, 1H); δ_C (75.6 MHz, $CDCl_3$) 17.9, 18.2, 19.1, 20.8, 22.0, 31.5, 39.3, 42.4, 55.0, 70.8, 122.8, 123.6, 130.5, 131.0, 134.6, 137.6, 139.6, 149.5, 154.1, 156.7; *m/z* (ES+) 362.27 ($[M]^+$, $C_{24}H_{32}N_3$ = 362.26)

***bis*((1*R*,5*S*)-2,4-bis(2-(diphenylphosphanyl)benzyl)-1,8,8-trimethyl-2,4-diazabicyclo[3.2.1]octan-3-ylidene))palladium(0), 3**

To a solution of [PCP']PF_6 (101 mg, 0.12 mmol) in THF (3 mL) held at -78 °C was added KHMDS (30 mg, 0.15 mmol). The mixture was stirred for 10 minutes and transferred *via canula* onto a solution of $Pd(dba)_2$ (34 mg, 0.06 mmol) in THF (2 mL) at -78 °C. The mixture was allowed to warm to room temperature at which point the solvent was removed *in vacuo*. The residue was washed with petroleum ether (5 mL) and then taken up in toluene (10 mL). The solution was filtered through celite and the solvent removed *in vacuo* to give the product. (63 mg, 70%)

Found: C, 74.7; H, 6.1; N, 3.6. $C_{94}H_{92}N_4P_4Pd$ requires C, 74.9; H, 6.15; N, 3.7; δ_P (121.7 MHz; C_6D_6) -15.3, -15.25; *m/z* (ES+) 1557.50 ($[M+MeOH+NH_4]^+$, $C_{95}H_{100}N_5OP_4Pd$ = 1557.59

***bis*((1*R*,5*S*)-2,4-bis(2-(diphenylphosphanyl)benzyl)-1,8,8-trimethyl-2,4-diazabicyclo[3.2.1]octan-3-ylidene))platinum(0), 4**

To a solution of [PCP']PF_6 (403 mg, 0.48 mmol) in THF (5 mL) held at -78 °C was added KHMDS (0.1043 g, 0.52 mmol). The mixture was stirred for 10 minutes and transferred *via canula*

onto a solution of $Pt(dvtmds)_2$ (0.216 g, 21.2 wt % Pt, 0.24 mmol) in THF (2 mL) at -78 °C. The mixture was allowed to warm to room temperature at which point the solvent was removed *in vacuo*. The residue was washed with petroleum ether (5 mL) and then taken up in toluene (4 mL). The solution was filtered through celite and the solvent removed *in vacuo* to give the product. (196 mg, 51%)

Found: C, 70.8; H, 5.8; N, 3.6. $C_{94}H_{92}N_4P_4Pt$ requires C, 70.7; H, 5.8; N, 3.5; δ_H (400 MHz; C_6D_6) 0.47 (s, 6H), 0.80 (s, 6H), 0.92 (s, 3H), 1.04-1.67 (m, 8H), 2.45 (dd, 2H *J* = 17.7, 8.8 Hz), 3.86 – 3.94 (m, 2H), 4.06 (ddd, 2H *J* = 13.0, 5.7, 2.1 Hz), 4.97 (dd, 2H, *J* = 16.5, 4.0), 5.29 (d, 2H, *J* = 6.3 Hz), 7.11-7.23 (m, 28H); δ_C (75.6 MHz, C_6D_6) 17.9, 21.5, 22.5, 27.7, 33.9, 44.6 (d, $^3J_{CP}$ = 36 Hz), 48.6, 51.6 (d, $^3J_{CP}$ = 22.6 Hz) 65.4, 68.5, 118.6-152.7 (m, aromatics), 163.2; δ_P (121.7 MHz; C_6D_6) -15.3, -15.0; *m/z* (ES+) 895.2870 ($[M\text{-}L+H]^+$, $C_{47}H_{47}N_2P_2Pt$ = 895.2841

bis((1*R*,5*S*)-2,4-bis(2-(diphenylphosphanyl)benzyl)-1,8,8-trimethyl-2,4-diazabicyclo[3.2.1]octan-3-ylidene))platinum(II) dichloride, 5

To a solution of **4** (123 mg, 0.08 mmol) in toluene (2 mL) was added $PhICl_2$ (21.1 mg, 0.08 mmol). The solution was stirred at room temperature for 48 hours during which time a yellow precipitate was formed. After filtration the residue was taken up in THF (3 mL) filtered through celite and evaporated to give the product as a yellow solid. (57 mg, 43%)

δ_H (400 MHz; $CDCl_3$) 0.89 (s, 6H), 1.01 (s, 6H), 1.08 (s, 6H), 1.64-1.88 (m, 8H), 2.10 (s, 2H),2.91 (dd, 2H, *J* = 18.3, 9.2 Hz), 3.65 (s, 2H), 4.28 (d, 2H, *J* =13.7 Hz), 5.08 (s, 2H), 7.0-7.5 (m, 28H); δ_C (75.6 MHz; $CDCl_3$) 18.6, 21.1, 21.6, 24.7, 25.7, 33.0, 48.0, 63.9, 68.1, 68.2, 125.3-134.2 (m, aromatics), 163.5; δ_P (121.7 MHz; $CDCl_3$) -17.3, -15.5 *m/z* (ES+) 1663.56 ($[M\text{-}Cl+MeOH]^+$, $C_{95}H_{96}ClN_4OP_4Pt$ = 1663.59)

(1*R*,5*S*)-2,4-bis(2-(diphenylphosphanyl)benzyl)-1,8,8-trimethyl-2,4-diazabicyclo[3.2.1]octan-3-ylidene)(dibenzylideneacetone)palladium(0), 6

To a solution of $[PCP']PF_6$ (100 mg, 0.12 mmol) in THF (3 mL) held at -78 °C was added KHMDS (28 mg, 0.14 mmol). The mixture was stirred for 10 minutes and transferred *via canula* onto

a solution of $Pd(dba)_2$ (68 mg, 0.12 mmol) in THF (4 mL) at -78 °C. The mixture was allowed to warm to room temperature at which point the solvent was removed *in vacuo*. The residue was washed with petroleum ether (5 mL) and then taken up in toluene (10 mL). The solution was filtered through celite and the solvent removed *in vacuo* to give the product. (95 mg, 76%)

Found: C, 74.7; H, 6.1; N, 3.6. $C_{64}H_{60}N_2OP_2Pd$ requires C, 73.8; H, 5.8; N, 2.7; δ_P (121.7 MHz; Toluene-d_8) -17.5, -14.3, 9.4, 11.3; *m/z* (ES+) 1055.3284 ($[M+H]^+$, $C_{64}H_{61}N_2O_2P_2Pd$ = 1055.3249)

((1*R*,5*S*)-2,4-bis(2-(diphenylphosphanyl)benzyl)-1,8,8-trimethyl-2,4-diazabicyclo[3.2.1]octan-3-ylidene)) *bis*(1,3-divinyl-1,1,3,3-tetramethyldisiloxane) diplatinum(0), 7

To a solution of $[PCP']PF_6$ (147 mg, 0.17 mmol) in THF (5 mL) held at -78 °C was added KHMDS (0.36 mg, 0.18 mmol). The mixture was stirred for 10 minutes and transferred *via canula* onto a solution of $Pt(dvtmds)_2$ (0.319 g, 21.2 wt % Pt, 0.34 mmol) in THF (2 mL) at -78 °C. The mixture was allowed to warm to room temperature at which point the solvent was removed *in vacuo*. The residue was washed with petroleum ether (5 mL) and then taken up in toluene (4 mL). The solution was filtered through celite and the solvent removed *in vacuo* to give the product. (196 mg, 51%)

δ_H (400 MHz; $CDCl_3$) -0.5 - -0.15 (m, 24H), 0.47 (s, 3H), 0.67 (s, 3H), 0.85 (s, 3H) 1.37-1.77 (m, 4H), 3.71 (d, 1H, *J* = 15 Hz), 4.43 (d, 1H, *J* = 16.7 Hz), 4.53 (d, 1H, *J* = 15.1 Hz), 4.71 (d, 1H, *J* = 14.6 Hz), 4.85 (d, 1H, *J* = 18.4 Hz), 5.54-6.19 (m, 12H), 6.87-7.51 (m, 28H); δ_P (121.7 MHz; $CDCl_3$) 18.6 ($^1J_{P\text{-}Pt}$ = 3521 Hz), 20.7 ($^1J_{P\text{-}Pt}$ = 3505 Hz); *m/z* (ES+) 1461.4243 ($[M+H]^+$, $C_{63}H_{83}N_2O_2P_2Si_4Pt$ = 1461.4261)

bis((1_R_,5_S_)-2,4-bis(2-(diphenylphosphanyl)benzyl)-1,8,8-trimethyl-2,4-diazabicyclo[3.2.1]octan-3-ylidene)) gold(I) hexafluorophosphate, 8

A solution of [PCP']PF_6 (0.245 g, 0.29 mmol) and Au(tht)Cl (43 mg, 0.15 mmol) in THF was stirred for 4 hours. The mixture was cooled to – 40 °C and KHMDS (70 mg, 0.35 mmol) was added. The solution was stirred at room temperature overnight after which the solvent was removed *in vacuo*. The residual solid was dissolved in $CHCl_3$ and filtered. Removal of the solvent and crystallisation by vapour diffusion of Et_2O into acetone solution gave the product as an orange solid. (0.058 g, 23%)

δ_H ($CDCl_3$, 400 MHz) 0.83 (s, 6H) 0.87 (s, 6H), 1.22 (s, 6H), 1.76-1.89 (m, 8H), 3.10 (s, 2H), 4.40 (d, $^2J_{HH}$ = 16 Hz, 2H), 4.47 (s, $^2J_{HH}$ = 20 Hz, 2H), 4.70 (d, $^2J_{HH}$ = 8 Hz, 4H), 6.85-7.53 (m, 70H); δ_C ($CDCl_3$, 400 MHz) 13.2, 14.7, 17.9, 20.8, 29.4, 37.9, 41.2, 65.3, 71.65, 71.7, 125.8, 125.9, 126.3, 126.4, 126.5, 126.8, 126.9, 127.4, 127.8, 128.8, 128.8, 128.9, 129.1, 129.5, 129.6, 130.1, 130.2, 132.4, 133.5, 133.7, 133.9, 134.8; δ_P ($CDCl_3$, 400 MHz) -17.8, -144.29 (sept, $^1J_{PF}$ 714.42 Hz); *m/z* (ES+) 1598.62 ($[M+H]^+$, $C_{94}H_{93}N_4P_4Au$ = 1598.60)

bis((1_R_,5_S_)-2,4-bis(pyridine-2-ylmethyl)-1,8,8-trimethyl-2,4-diazabicyclo[3.2.1]octan-3-ylidene)) gold(I) tetrafluoroborate, 9

A solution of [NCN']BF_4 (0.253 g, 0.60 mmol) and Au(tht)Cl (87 mg, 0.30 mmol) in THF was stirred for 4 hours. The mixture was cooled to – 40 °C and KHMDS (130 mg, 0.65 mmol) was added. The solution was stirred at room temperature overnight after which the solvent was removed *in vacuo*. The residual solid was dissolved in $CHCl_3$ and filtered. Removal of the solvent and crystallisation by vapour diffusion of Et_2O into acetone solution gave the product as an orange solid. (0.251 g, 44%)

δ_H (DMSO-d_6, 400MHz) 0.60 (s, 6H), 0.66 (s, 6H), 0.80 (s, 6H), 1.62-1.64 (m, 4H), 1.95-2.00 (m, 4H), 3.00 (d, $^3J_{HH}$ = 2 Hz, 2H), 4.67 (d, $^2J_{HH}$ = 12 Hz, 2H), 4.86 (d, $^2J_{HH}$ = 20 Hz, 2H), 4.90 (d, $^2J_{HH}$ = 16 Hz, 2H), 5.01 (d, $^2J_{HH}$ = 16 Hz, 2H), 7.01-7.15 (m, 8H), 7.47 (dt, $^3J_{HH}$ = 36 Hz, $^3J_{HH}$ = 8 Hz, 4H) 8.25 (d, $^3J_{HH}$ = 20 Hz, 4H); δ_H ($CDCl_3$, 400MHz) 0.76 (s, 6H), 0.78 (s, 6H), 0.95 (s, 6H), 1.86

(m, 4H), 2.12 (m, 4H), 3.03 (d, $^3J_{HH}$ = 2 Hz, 2H), 4.73-5.16 (m, 8H), 7.01 (q, $^3J_{HH}$ = 8 Hz, 2H), 7.11 (q, $^3J_{HH}$ = 8 Hz, 2H), 7.24 (d, $^3J_{HH}$ = 4 Hz, 2H), 7.28 (d, $^3J_{HH}$ = 4 Hz, 2H), 7.45 (t, $^3J_{HH}$ = 8 Hz, 2H), 7.54 (t, $^3J_{HH}$ = 8 Hz, 2H), 8.27 (d, $^3J_{HH}$ = 2 Hz, 2H), 8.34 (d, $^3J_{HH}$ = 2 Hz, 2H); δ_C (acetone-d_6, 400 MHz) 15.6, 16.6, 18.4, 22.0, 31.7, 39.7, 41.2, 59.0, 62.9, 68.7, 71.4, 122.2, 123.5, 123.8, 124.0, 137.4, 134.5, 150.0, 156.7, 158.9, 203.5; *m/z* (ES+) 865.39 ($[M]^+$, $C_{42}H_{52}N_8Au$ = 865.4)

***bis*(((1*R*,5*S*)-4-mesityl-1,8,8-trimethyl-2-(pyridin-2-ylmethyl)-2,4-diazabicyclo[3.2.1]octan-3-ylidene))gold(I) tetrafluoroborate, 10**

A solution of **[2]BF_4** (0.237 g, 0.67 mmol) and Au(tht)Cl (96 mg, 0.33 mmol) in THF was stirred for 4 hours. The mixture was cooled to – 40 °C and KHMDS (143 mg, 0.72 mmol) was added. The solution was stirred at room temperature overnight after which the solvent was removed *in vacuo*. The residual solid was dissolved in $CHCl_3$ and filtered. Removal of the solvent and crystallisation by vapour diffusion of Et_2O into acetone solution gave the product as an orange solid. (0.251 g, 40%)

δ_H (400 MHz; $CDCl_3$) 0.83 (s, 6H), 1.04 (s, 12H), 1.55-1.78 (m, 8H), 1.91 (s, 6H), 2.04 (s, 6H), 2.21 (s, 6H), 2.95 (d, $^2J_{HH}$ = 4 Hz, 2H), 4.04 (d, $^2J_{HH}$ = 16 Hz, 2H), 4.30 (d, $^2J_{HH}$ = 16 Hz, 2H), 7.14 (s, 2H), 7.16 (s, 2H), 7.24-7.29 (m, 4H), 7.72 (t, $^3J_{HH}$ = 8 Hz, 2H), 8.50 (d, $^3J_{HH}$ = 4 Hz, 2H); δ_C (400 MHz; $CDCl_3$) 16.7, 16.9, 17.0, 17.1, 18.5, 27.8, 28.0, 39.3, 55.8, 67.2, 67.4, 68.4, 74.8, 119.4, 120.6, 127.3, 131.6, 134.2, 135.5, 146.7; *m/z* (ES+) 919.48 ($[M]^+$, $C_{48}H_{62}N_6Au$ = 919.47)

References

1 P. Atkins, T. Overton, J. Rourke, M. Weller and F. Armstrong, *Shriver & Atkins Inorganic Chemistry*, Oxford University Press, Oxford, 4th edn., 2006.

2 J. F. Hartwig, *Organotransition Metal Chemistry: From Bonding to Catalysis*, 1st edn., 2010.

3 P. Bazinet, G. P. A. Yap and R. Darrin S., *J. Am. Chem. Soc.*, 2003, **125**, 13314–13315.

4 M. Mayr, K. Wurst, K.-H. Ongania and M. R. Buchmeiser, *Chem. - A Eur. J.*, 2004, **10**, 1256–1266.

5 C. C. Scarborough, I. A. Guzei and S. S. Stahl, *Dalt. Trans.*, 2009, **47**, 2284.

6 M. Iglesias, D. J. Beetstra, J. C. Knight, L.-L. Ooi, A. Stasch, S. Coles, L. Male, M. B. Hursthouse, K. J. Cavell, A. Dervisi and I. A. Fallis, *Organometallics*, 2008, **27**, 3279–3289.

7 M. Iglesias, D. J. Beetstra, A. Stasch, P. N. Horton, M. B. Hursthouse, S. J. Coles, K. J. Cavell, A. Dervisi and I. A. Fallis, *Organometallics*, 2007, **26**, 4800–4809.

8 W. Y. Lu, K. J. Cavell, J. S. Wixey and B. Kariuki, *Organometallics*, 2011, **30**, 5649–5655.

9 D. G. Gusev, *Organometallics*, 2009, **28**, 6458–6461.

10 M. C. Perry and K. Burgess, *Tetrahedron: Asymmetry*, 2003, **14**, 951–961.

11 V. César, S. Bellemin-Laponnaz and L. H. Gade, *Chem. Soc. Rev.*, 2004, **33**, 619–636.

12 S. Roland and P. Mangeney, in *Chiral Diazaligands for Asymmetric Synthesis*, Springer-Verlag, Berlin/Heidelberg, pp. 191–229.

13 R. E. Douthwaite, *Coord. Chem. Rev.*, 2007, **251**, 702–717.

14 L. H. Gade and S. Bellemin-Laponnaz, in *N-Heterocyclic Carbenes in Transition Metal Catalysis*, Springer Berlin Heidelberg, 2006, pp. 117–157.

15 L. Wu, A. Salvador and R. Dorta, in *N-Heterocyclic Carbenes*, Wiley-VCH Verlag GmbH & Co. KGaA, Weinheim, Germany, 2014, pp. 39–84.

16 M. J. Spallek, D. Riedel, F. Rominger, A. S. K. Hashmi and O. Trapp, *Organometallics*,

2012, **31**, 1127–1132.

17 J. K. Park, H. H. Lackey, M. D. Rexford, K. Kovnir, M. Shatruk and D. T. McQuade, *Org. Lett.*, 2010, **12**, 5008–5011.

18 J. K. Park, H. H. Lackey, B. A. Ondrusek and D. T. McQuade, *J. Am. Chem. Soc.*, 2011, **133**, 2410–2413.

19 J. K. Park and D. T. McQuade, *Angew. Chemie Int. Ed.*, 2012, **51**, 2717–2721.

20 J. K. Park, B. A. Ondrusek and D. T. McQuade, *Org. Lett.*, 2012, **14**, 4790–4793.

21 L. B. Delvos, D. J. Vyas and M. Oestreich, *Angew. Chemie Int. Ed.*, 2013, **52**, 4650–4653.

22 A. Hensel, K. Nagura, L. B. Delvos and M. Oestreich, *Angew. Chemie Int. Ed.*, 2014, **53**, 4964–4967.

23 A. Hensel and M. Oestreich, *Chem. - A Eur. J.*, 2015, **21**, 9062–9065.

24 C. C. Scarborough, M. J. W. Grady, I. A. Guzei, B. A. Gandhi, E. E. Bunel and S. S. Stahl, *Angew. Chemie Int. Ed.*, 2005, **44**, 5269–5272.

25 C. C. Scarborough, B. V. Popp, I. A. Guzei and S. S. Stahl, *J. Organomet. Chem.*, 2005, **690**, 6143–6155.

26 W. A. Herrmann, D. Baskakov and K. Ruhland, *J. Heterocycl. Chem.*, 2007, **44**, 237–239.

27 C. C. Scarborough, A. Bergant, G. T. Sazama, I. A. Guzei, L. C. Spencer and S. S. Stahl, *Tetrahedron*, 2009, **65**, 5084–5092.

28 P. V. G. Reddy, S. Tabassum, A. Blanrue and R. Wilhelm, *Chem. Commun.*, 2009, **41**, 5910.

29 P. D. Newman, K. J. Cavell and B. M. Kariuki, *Organometallics*, 2010, **29**, 2724–2734.

30 P. D. Newman, K. J. Cavell, A. J. Hallett and B. M. Kariuki, *Dalt. Trans.*, 2011, **40**, 8807.

31 P. D. Newman, K. J. Cavell and B. M. Kariuki, *Chem. Commun.*, 2012, **48**, 6511.

32 P. D. Newman, K. J. Cavell and B. M. Kariuki, *Dalt. Trans.*, 2012, **41**, 12395.

33 B. M. Kariuki, J. A. Platts and P. D. Newman, *Dalt. Trans.*, 2014, **43**, 2971–2978.

34 M. Bouché, M. Mordan, B. M. Kariuki, S. J. Coles, J. Christensen and P. D. Newman, *Dalt. Trans.*, 2016, **45**, 13347–13360.

35 R. Gümüşada, M. E. Günay, N. Özdemir and B. Çetinkaya, *J. Coord. Chem.*, 2016, **69**, 1463–1472.

36 M. Uzarewicz-Baig, M. Koppenwallner, S. Tabassum and R. Wilhelm, *Appl. Organomet. Chem.*, 2014, **28**, n/a-n/a.

37 T. Lemek, M. Mąkosza, D. S. Stephenson and H. Mayr, *Angew. Chemie Int. Ed.*, 2003, **42**, 2793–2795.

38 M. Yamashita, K. Goto and T. Kawashima, *J. Am. Chem. Soc.*, 2005, **127**, 7294–7295.

39 Michael M. Konnick, I. A. Guzei and S. S. Stahl, *J. Am. Chem. Soc.*, 2004, **126**, 10212–10213.

40 E. Lee and D. V. Yandulov, *J. Organomet. Chem.*, 2011, **696**, 4095–4103.

41 D. P. Hruszkewycz, J. Wu, N. Hazari and C. D. Incarvito, *J. Am. Chem. Soc.*, 2011, **133**, 3280–3283.

42 J. Bauer, H. Braunschweig, P. Brenner, K. Kraft, K. Radacki and K. Schwab, *Chem. - A Eur. J.*, 2010, **16**, 11985–11992.

43 P. Ai, C. Gourlaouen, A. A. Danopoulos and P. Braunstein, *Inorg. Chem.*, 2016, **55**, 1219–1229.

44 A. J. Kendall, L. N. Zakharov and D. R. Tyler, *Inorg. Chem.*, 2016, **55**, 3079–3090.

45 A. D. Burrows, N. Choi, M. McPartlin, D. M. P. Mingos, S. V Tarlton and R. Vilar, *J. Organomet. Chem.*, 1999, **573**, 313–322.

46 P. B. Hitchcock, M. F. Lappert, C. MacBeath, F. P. E. Scott and N. J. W. Warhurst, *J. Organomet. Chem.*, 1997, **534**, 139–152.

47 I. J. Lin and C. S. Vasam, *Can. J. Chem.*, 2005, **83**, 812–825.

48 D. Zuccaccia, L. Belpassi, A. Macchioni and F. Tarantelli, *Eur. J. Inorg. Chem.*, 2013,

2013, 4121–4135.

49 Y. Wang, M. E. Muratore and A. M. Echavarren, *Chem. - A Eur. J.*, 2015, **21**, 7332–7339.

50 H. G. Raubenheimer and S. Cronje, *Chem. Soc. Rev.*, 2008, **37**, 1998.

51 C. E. Strasser and V. J. Catalano, *J. Am. Chem. Soc.*, 2010, **132**, 10009–10011.

52 K. Chen, M. M. Nenzel, T. M. Brown and V. J. Catalano, *Inorg. Chem.*, 2015, **54**, 6900–6909.

53 K. Chen, C. E. Strasser, J. C. Schmitt, J. Shearer and V. J. Catalano, *Inorg. Chem.*, 2012, **51**, 1207–1209.

54 C. E. Strasser and V. J. Catalano, *Inorg. Chem.*, 2011, **50**, 11228–11234.

55 M. J. López-Gómez, D. Martin and G. Bertrand, *Chem. Commun.*, 2013, **49**, 4483.

56 K. Sampford, Cardiff University, 2013.

Appendix A

Crystallographic data

Trichloro *tert*butyl*bis*(2–(phenylphosphino)ethyl)phosphine chromium(III)

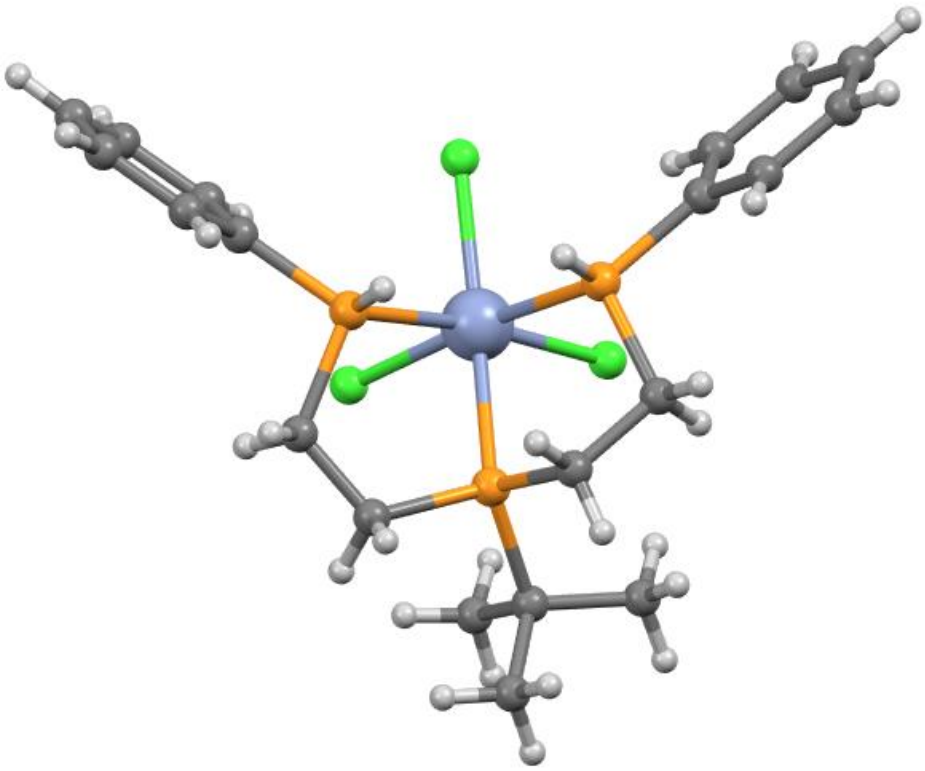

Figure 13: Molecular structure of Cr(triphosphine)Cl_3

Table 2: Crystal data and structure refinement details

Empirical formula	**$C_{20}H_{29}Cl_3CrP_3$**	
Formula weight	520.69	
Temperature	293 (2)	
Wavelength	1.54184	
Crystal system	Monoclinic	
Space group	P 21/C	
Unit cell dimensions	a = 13.1018 (6) Å	a = 90°
	b = 14.1626 (4) Å	b = 113.795 (5)°
	c = 13.8160 (6) Å	g = 90°
Volume	2345.71 (18) $Å^3$	
Z	4	
Density (calculated)	1.474 Mg / m^3	
Absorption coefficient	9.119 mm-1	
F(000)	1076	
Crystal size	0.192 × 0.055 × 0.027 mm^3	
Θ range for data collection	3.687 – 74.006°	
Index ranges	-16 ≤ h ≤ 15, -17 ≤ k ≤ 17, -17 ≤ l ≤ 17	
Reflections collected	4685	
Independent reflections	3371	
Absorption correction	Semi-empirical from equivalents	
Refinement method	Full-matrix least-squares on F^2	
Goodness-of-fit on F^2	1.049	
Final R indices [$F^2 > 2\sigma(F^2)$]	*R1* = 0.0725, *wR2* = 0.1942	
R indices (all data)	*R1* = 0.0982, *wR2* = 0.2205	
Extinction coefficient	n/a	

Table 3: Bond lengths [Å] and angles [°]

C1-C2	**1.377(9)**
C1-C6	1.418(9)
C1-P1	1.808(6)
C2-C3	1.396(9)
C2-H2	0.93
C3-C4	1.337(12)
C3-H3	0.93
C4-H5	1.394(12)
C4-H4	0.93
C5-C6	1.395(9)
C5-H5	0.93
C6-H6	0.93
C7-C8	1.499(9)
C7-P1	1.823(6)
C7-H7A	0.97
C7-H7B	0.97
C8-P_3	1.845(6)
C8-H8A	0.97
C8-H8B	0.97
C9-C10	1.549(7)
C9-P_3	1.838(5)
C9-H9A	0.97
C9-H9B	0.97
C10-P2	1.809(5)
C10-H10A	0.97
C10-H10B	0.97
C11-C12	1.393(9)
C11-C16	1.393(9)
C11-P2	1.812(5)
C12-C13	1.410(9)
C12-H12	0.93
C13-C14	1.369(11)
C13-H13	0.93
C14-C15	1.370(10)
C14-H14	0.93
C15-C16	1.399(8)
C15-H15	0.93
C16-H16	0.93
C17-C18	1.507(10)
C17-C19	1.527(9)
C17-C20	1.540(9)
C17-P3	1.859(6)
C18-H18A	0.96
C18-H18B	0.96

C18-H18C	0.96
C19-H19A	0.96
C19-H19B	0.96
C19-H19C	0.96
C20-H20A	0.96
C20-H20B	0.96
C20-H20C	0.96
P1-Cr1	2.4536(16)
P1-H1	0.98
P2-Cr1	2.4536(15)
P2-H2A	0.98
Cr1-Cl3	2.3100(16)
Cr1-Cl1	2.3132(16)
Cr1-Cl2	2.3274(15)
Cr1-P3	2.4858(14)
C2C1C6	120.0(6)
C2C1P1	122.7(5)
C6C1P1	117.3(5)
C1C2C3	119.5(7)
C1C2H2	120.3
C3C2H2	120.3
C4C3C2	120.6(8)
C4C3H3	119.7
C2C3H3	119.7
C3C4C5	122.1(7)
C3C4H4	118.9
C5C4H4	118.9
C4C5C6	118.4(7)
C4C5H5	120.8
C6C5H5	120.8
C5C6C1	119.4(7)
C5C6H6	120.3
C1C6H6	120.3
C8C7P1	115.7(4)
C8C7H7A	108.4
P1C7H7A	108.4
C8C7H7B	108.4
P1C7H7B	108.4
H7AC7H7B	107.4
C7C8P3	115.5(4)
C7C8H8A	108
P3C8H8A	108.4
C7C8H8B	108.4
P3C8H8B	108.4
H8AC8H8B	107.5
C10C9P3	110.5(4)
C10C9H9A	109.5
P3C9H9A	109.5
C10C9H9B	109.5
P3C9H9B	109.5
H9AC9H9B	108.1
C9C10P2	107.3(4)
C9C10H10A	110.2
P2C10H10A	110.2
C9C10H10B	110.2
P2C10H10B	110.2
H10AC10H10B	108.5
C12C11C16	120.6(5)
C12C11P2	118.8(5)
C16C11P2	120.6(4)
C11C12C13	118.8(7)
C11C12H12	120.6
C13C12H12	120.6
C14C13C12	119.7(7)
C14C13H13	120.1
C12C13H13	120.1
C13C14C15	121.9(6)
C13C14H14	119
C15C14H14	119
C14C15C16	119.4(6)
C14C15H15	120.3
C16C15H15	120.3
C11C16C15	119.6(6)
C11C16H16	120.2
C18C17C19	120.2
C18C17C20	110.3(6)
C19C17C20	110.1(6)
C18C17P3	107.8(5)
C19C17P3	108.8(4)
C20C17P3	111.5(5)
C17C18H18A	108.3(4)
C17C18H18B	109.5
H18AC18H18B	109.5
C17C18H18C	109.5
H18AC18H18C	109.5
H18BC18H18C	109.5
C17C19H19A	109.5
C17C19H19B	109.5
H19AC19H19B	109.5
C17C19H19C	109.5
H19AC19H19C	109.5
H19BC19H19C	109.5
C17C20H20A	109.5
C17C20H20B	109.5
H20AC20H20B	109.5
C17C20H20C	109.5
H20AC20H20B	109.5
H20BC20H20C	109.5
C1P1C7	109.5
C1P1Cr1	103.5(3)
C7P1Cr1	123.7(2)

C1P1H1	108.6(2)
C7P1H1	106.6
Cr1P1H1	106.6
C10P2C11	106.6
C10P2Cr1	105.6(2)
C10P2H2A	107.08(18)
C11P2H2A	124.6(2)
Cr1P2H2A	106.1
Cl3Cr1Cl1	106.1
Cl3Cr1Cl2	106.1
Cl1Cr1Cl2	98.52(6)
Cl3Cr1P1	98.48(6)
Cl1Cr1P1	98.37(6)
Cl2Cr1P1	170.34(6)
Cl3Cr1P2	90.22(6)
Cl1Cr1P2	84.20(5)
Cl2Cr1P2	87.41(6)
P1Cr1P2	89.22(6)
Cl3Cr1P3	169.55(6)
Cl1Cr1P3	88.63(5)
Cl2Cr1P3	92.64(5)
P1Cr1P3	164.50(8)
P2Cr1P3	90.54(5)
C9P3C8	78.01(5)
C9P3C17	80.53(5)
C8P3C17	102.6(3)
C9P3Cr1	106.4(3)
C8P3Cr1	104.6(3)
C17P3Cr1	107.07(18)

(2*R*, 2'*R*)-3,3'-(ethane-1,2-diylbis(sulfanediyl))bis(1-(diphenylphosphanyl)propan-2-ol)

Palladium dichloride

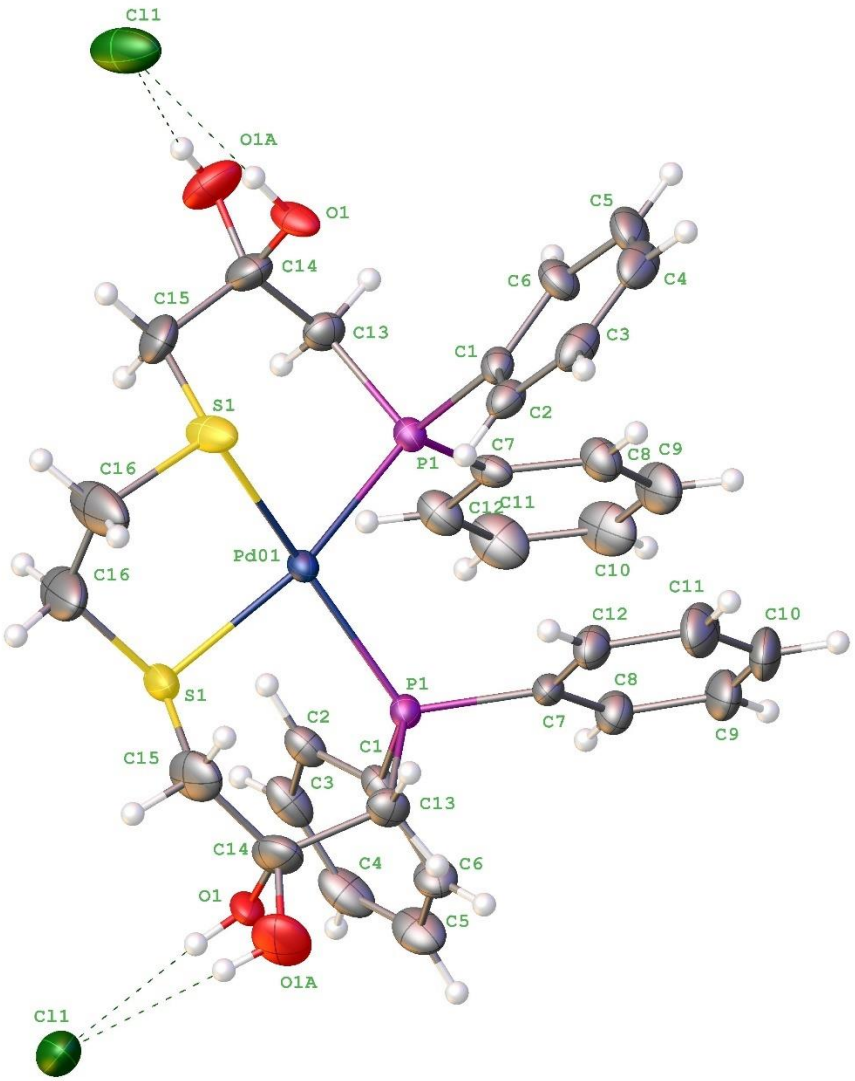

Figure 1: Molecular structure of 2016ncs0202 (MD326) – grown fragment. Atomic displacement ellipsoids – 50% probability.

Table 1: Crystal data and structure refinement details.

Identification code	**2016ncs0202 (MD326)**	
Empirical formula	$C_{32}H_{34}Cl_2O_2P_2PdS_2$	
Formula weight	753.95	
Temperature	100(2) K	
Wavelength	0.71075 Å	
Crystal system	Orthorhombic	
Space group	*Pbcn*	
Unit cell dimensions	*a* = 13.2585(4) Å	$\alpha = 90°$
	b = 19.1735(7) Å	$\beta = 90°$
	c = 13.9583(6) Å	$\gamma = 90°$
Volume	3548.3(2) Å^3	
Z	4	
Density (calculated)	1.411 Mg / m^3	
Absorption coefficient	0.908 mm^{-1}	
F(000)	1536	
Crystal	block; yellow	
Crystal size	0.1 × 0.04 × 0.02 mm^3	
Θ Range for data collection	1.867 – 29.970°	
Index ranges	$-17 \le \eta \le 17, -26 \le \kappa \le 25, -13 \le \lambda \le 18$	
Reflections collected	25906	
Independent reflections	4738 [R_{int} = 0.0575]	
Completeness to θ = 26.000°	100.00%	
Absorption correction	Semi–empirical from equivalents	
Max. and min. transmission	1.00000 and 0.59201	
Refinement method	Full-matrix least-squares on F^2	
Data / restraints / parameters	4738 / 0 / 198	
Goodness-of-fit on F^2	1.058	
Final *R* indices [$F^2 > 2\sigma(F^2)$]	*R1* = 0.0612, *wR2* = 0.1387	
***R* indices (all data)**	*R1* = 0.0775, *wR2* = 0.1454	
Extinction coefficient	n/a	
Largest diff. peak and hole	2.580 and –1.533 e Å^{-3}	

Diffractometer: Rigaku AFC12 goniometer equipped with an enhanced sensitivity (HG) Saturn724+ detector mounted at the window of an FR-E+ SuperBright molybdenum rotating anode generator with HF Varimax optics (100m focus). **Cell determination and data collection:** CrystalClear-SM Expe. rt 3.1 b27 (Rigaku, 2012). **Data reduction, cell refinement and absorption correction** CrystalClear-SM Expert 3.1 b27 (Rigaku, 2013) **Structure solution:** SHELXT (Sheldrick, G.M. (2015). J. Appl. Cryst. 40, 786-790). **Structure refinement:** SHELXL-2014 (Sheldrick, G.M. (2015). *Acta Crystallogr. Sect. A Found. Adv.* **2015**, *71*, 3–8.). **Special details**: In the crystal structure –OH group O1-H1 is disordered and modelled over two sites with approx. 53/47 ratio.

Table 2: Atomic coordinates [× 10^4], equivalent isotropic displacement parameters [$Å^2$ × 10^3] and site occupancy factors. U_{eq} is defined as one third of the trace of the orthogonalized U^{ij} tensor

Atom	x	y	z	U_{eq}	S.o.f.
Pd01	5000	4005(1)	7500	20(1)	1
S1	4743(1)	4857(1)	6342(1)	42(1)	1
P1	4235(1)	3238(1)	6478(1)	20(1)	1
C1	4873(3)	3013(2)	5376(3)	24(1)	1
C2	5845(3)	3252(2)	5203(3)	28(1)	1
C3	6341(4)	3049(3)	4365(3)	36(1)	1
C4	5871(4)	2618(3)	3721(3)	41(1)	1
C5	4909(5)	2384(3)	3878(4)	42(1)	1
C6	4400(4)	2582(2)	4701(3)	32(1)	1
C7	3837(3)	2416(2)	7007(3)	25(1)	1
C8	4142(4)	1773(2)	6656(3)	33(1)	1
C9	3801(5)	1164(3)	7090(4)	45(1)	1
C10	3177(5)	1198(3)	7867(4)	49(2)	1
C11	2885(5)	1832(3)	8222(4)	47(1)	1
C12	3204(4)	2444(2)	7805(3)	33(1)	1
C13	3020(3)	3617(2)	6118(3)	28(1)	1
C14	3037(4)	4296(3)	5550(4)	43(1)	1
C15	3384(5)	4926(3)	6118(4)	49(1)	1
C16	5085(8)	5624(3)	7008(5)	76(3)	1
O1	3438(6)	4237(4)	4763(4)	32(2)	0.470(9)
O1A	2161(6)	4416(4)	5138(6)	55(3)	0.530(9)
Cl1	2701(2)	5550(1)	3533(1)	67(1)	1

Table 3: Bond lengths [Å] and angles [°].

Pd01–S1^i	2.3228(12)
Pd01–S1	2.3227(12)
Pd01–P1^i	2.2867(10)
Pd01–P1	2.2867(10)
S1–C15	1.834(6)
S1–C16	1.798(6)
P1–C1	1.808(4)
P1–C7	1.818(4)
P1–C13	1.837(4)
C1–C2	1.389(6)
C1–C6	1.401(6)
C2–H2	0.93
C2–C3	1.398(6)
C3–H3	0.93
C3–C4	1.371(8)
C4–H4	0.93
C4–C5	1.371(8)
C5–H5	0.93
C5–C6	1.386(6)
C6–H6	0.93
C7–C8	1.386(6)
C7–C12	1.396(6)
C8–H8	0.93
C8–C9	1.392(7)
C9–H9	0.93
C9–C10	1.367(8)
C10–H10	0.93
C10–C11	1.370(8)
C11–H11	0.93
C11–C12	1.376(7)
C12–H12	0.93
C13–H13A	0.97
C13–H13B	0.97
C13–C14	1.525(7)
C14–C15	1.516(8)
C14–O1	1.225(9)
C14–O1A	1.316(8)
C15–H15A	0.97

C15–H15B	0.97
C16–C16^{i}	1.392(14)
C16–H16A	0.97
C16–H16B	0.97
O1–H1	0.82
O1A–H1A	0.82

S1–Pd01–S1^{i}	90.65(6)
P1^{i}–Pd01–S1^{i}	87.34(4)
P1–Pd01–S1	87.34(4)
P1–Pd01–S1^{i}	162.08(5)
P1^{i}–Pd01–S1	162.08(5)
P1–Pd01–P1^{i}	99.88(5)
C15–S1–Pd01	108.25(19)
C16–S1–Pd01	100.3(2)
C16–S1–C15	106.1(4)
C1–P1–Pd01	118.45(14)
C1–P1–C7	105.96(19)
C1–P1–C13	105.8(2)
C7–P1–Pd01	115.67(13)
C7–P1–C13	101.5(2)
C13–P1–Pd01	107.73(15)
C2–C1–P1	120.2(3)
C2–C1–C6	119.6(4)
C6–C1–P1	120.2(3)
C1–C2–H2	120.3
C1–C2–C3	119.3(4)
C3–C2–H2	120.3
C2–C3–H3	119.9
C4–C3–C2	120.2(5)
C4–C3–H3	119.9
C3–C4–H4	119.5
C5–C4–C3	121.1(4)
C5–C4–H4	119.5
C4–C5–H5	120.1
C4–C5–C6	119.8(5)
C6–C5–H5	120.1
C1–C6–H6	120
C5–C6–C1	120.0(5)
C5–C6–H6	120
C8–C7–P1	122.8(3)
C8–C7–C12	119.4(4)
C12–C7–P1	117.7(3)
C7–C8–H8	120.1
C7–C8–C9	119.9(5)
C9–C8–H8	120.1
C8–C9–H9	119.9
C10–C9–C8	120.2(5)
C10–C9–H9	119.9
C9–C10–H10	120
C9–C10–C11	120.1(5)
C11–C10–H10	120
C10–C11–H11	119.4
C10–C11–C12	121.1(5)
C12–C11–H11	119.4
C7–C12–H12	120.3
C11–C12–C7	119.4(5)
C11–C12–H12	120.3
P1–C13–H13A	107.8
P1–C13–H13B	107.8
H13A–C13–H13B	107.2
C14–C13–P1	117.9(3)
C14–C13–H13A	107.8
C14–C13–H13B	107.8
C15–C14–C13	114.3(4)
O1–C14–C13	113.2(5)
O1–C14–C15	114.2(6)
O1A–C14–C13	111.3(6)
O1A–C14–C15	111.0(6)
S1–C15–H15A	109.8
S1–C15–H15B	109.8
C14–C15–S1	109.3(4)
C14–C15–H15A	109.8
C14–C15–H15B	109.8
H15A–C15–H15B	108.3
S1–C16–H16A	107.8
S1–C16–H16B	107.8
C16^{i}–C16–S1	118.0(5)
C16^{i}–C16–H16A	107.8
C16^{i}–C16–H16B	107.8
H16A–C16–H16B	107.1
C14–O1–H1	109.5
C14–O1A–H1A	109.5

Symmetry transformations used to generate equivalent atoms:

(i) –x+1,y,–z+3

Dichloro (*S*)-1-(diisopropylphosphanyl)-3-(diphenylphosphanyl)propan-2-ol Nickel

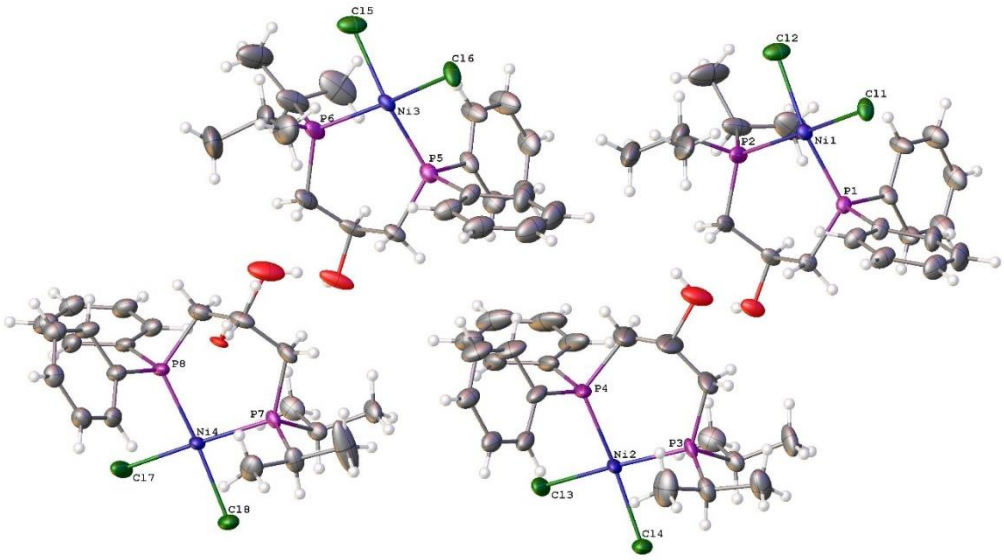

Figure 2: Molecular structure of 2016ncs0536 (MD344) – Four independent molecules present in the asymmetric part of the unit cell are shown (Z'=4). Atomic displacement ellipsoids – 50% probability

Table 4: Crystal data and structure refinement details

Identification code	**2016ncs0536 (MD344)**	
Empirical formula	$C_{84}H_{119}Cl_8Ni_4O_4P_8$	
Formula weight	1958.98	
Temperature	100(2) K	
Wavelength	0.71075 Å	
Crystal system	Monoclinic	
Space group	P1211	
Unit cell dimensions	a = 15.1710(3) Å	a = 90°
	b = 14.5398(3) Å	b = 107.698(2)°
	c = 21.5317(5) Å	g = 90°
Volume	4524.75(18) Å3	
Z	2	
Density (calculated)	1.438 Mg / m3	
Absorption coefficient	1.244 mm-1	
F(000)	2046	
Crystal	Block; orange	
Crystal size	0.16 × 0.07 × 0.05 mm^3	
q range for data collection	1.717 - 27.484°	
Index ranges	-19 ≤ h ≤ 19, -18 ≤ k ≤ 16, -27 ≤ l £ 27	
Reflections collected	57162	
Independent reflections	18812 [R_{int} = 0.0489]	
Completeness to q = 26.000°	98.40%	
Absorption correction	Semi-empirical from equivalents	
Max. and min. transmission	1.00000 and 0.88239	
Refinement method	Full-matrix least-squares on F^2	
Data / restraints / parameters	18812 / 1809 / 1005	
Goodness-of-fit on F^2	1.069	
Final R indices [$F^2 > 2\sigma(F^2)$]	*R1* = 0.0844, *wR2* = 0.2271	
R indices (all data)	*R1* = 0.0881, *wR2* = 0.2334	
Absolute structure parameter	0.07(2)	
Extinction coefficient	n/a	
Largest diff. peak and hole	2.038 and –1.165 e $Å^{-3}$	

Diffractometer: *Rigaku AFC12* goniometer equipped with an enhanced sensitivity (HG) *Saturn724+* detector mounted at the window of an *FR-E+ SuperBright* molybdenum rotating anode generator with HF *Varimax* optics (100µm focus). **Cell determination and data collection**: *CrystalClear-SM Expert 3.0 r27* (Rigaku, 2012). **Data reduction, cell refinement and absorption correction**: *CrystalClear-SM Expert 2.0 r13* (Rigaku, 2011). **Structure solution**: *ShelXT (Sheldrick, 2015)*. Acta Cryst. A64, 112-122). **Structure refinement**: *SHELXL-2014* (Sheldrick, G.M. (2008). Acta Cryst. A64, 112-122).**Special details**: In the crystal structure, O4 is disordered and modelled over two sites O4a/O4b with 75/25 ratio.

Table 5: Atomic coordinates [× 10^4], equivalent isotropic displacement parameters [$Å^2$ × 10^3] and site occupancy factors. U_{eq} is defined as one third of the trace of the orthogonalized U^{ij} tensor.

ATOM	X	Y	Z	U_{EQ}	S.O.F.
NI1	5133(1)	3513(1)	4489(1)	19(1)	1
NI2	-319(1)	6465(1)	5372(1)	26(1)	1
NI4	-275(1)	6504(1)	10443(1)	21(1)	1
NI3	5264(1)	3468(1)	9588(1)	20(1)	1
P7	-33(1)	5790(2)	9620(1)	21(1)	1
CL06	-1537(2)	7082(2)	9739(1)	35(1)	1
P3	-198(2)	5731(2)	4522(1)	25(1)	1
P1	4001(1)	4096(1)	3719(1)	19(1)	1
CL09	-1599(2)	7076(2)	4706(1)	35(1)	1
CL0A	5156(2)	2368(2)	3829(1)	31(1)	1
CL0B	5446(2)	2414(2)	8909(1)	37(1)	1
P5	4197(2)	4083(2)	8798(1)	24(1)	1
P8	871(1)	5901(2)	11179(1)	26(1)	1
P2	5056(2)	4545(2)	5203(1)	30(1)	1
CL0F	6498(2)	3115(2)	5160(1)	38(1)	1
CL0G	-535(2)	7281(2)	11246(1)	44(1)	1
CL0H	-437(2)	7319(2)	6181(1)	41(1)	1
P6	5015(2)	4319(2)	10348(1)	32(1)	1
CL0J	6575(2)	3066(2)	10331(1)	42(1)	1
P4	827(2)	5787(2)	6063(1)	40(1)	1
O1	2763(4)	6147(5)	4404(3)	30(1)	1
O3	2848(4)	6051(5)	9478(5)	44(2)	1
C81	441(7)	6323(8)	8482(5)	36(2)	1
O2	2074(5)	4083(6)	5069(5)	52(2)	1
C73	-231(7)	3813(7)	12377(5)	33(2)	1
C67	2868(7)	7951(8)	12562(5)	39(2)	1
C39	266(9)	6262(8)	3388(5)	48(3)	1
C72	705(7)	3998(7)	12559(5)	34(2)	1
C31	-242(7)	3834(7)	7347(5)	38(2)	1
C30	691(8)	3879(9)	7446(6)	50(3)	1
C69	1671(6)	6814(7)	12378(4)	32(2)	1
C64	1653(5)	6726(7)	11732(4)	29(2)	1
C61	4860(8)	3443(9)	10970(5)	47(2)	1
C32	-842(7)	4371(7)	6889(5)	37(2)	1
C9	4499(8)	6083(8)	2499(6)	42(2)	1
C45	4749(8)	6102(7)	7621(5)	39(2)	1
C68	2266(7)	7394(8)	12785(5)	41(2)	1
C27	1666(6)	6664(8)	7255(5)	39(2)	1
C1	3239(6)	3294(6)	3163(4)	27(2)	1
C13	3148(5)	4825(6)	3912(4)	22(1)	1
C6	3105(7)	3329(7)	2490(4)	35(2)	1
C79	152(6)	6676(6)	9069(4)	28(2)	1

C74	-828(7)	4289(8)	11873(5)	35(2)	1
C75	-517(6)	4921(7)	11519(4)	31(2)	1
C71	1035(6)	4631(7)	12197(5)	33(2)	1
C33	-547(7)	4962(8)	6508(4)	36(2)	1
C28	402(7)	5026(7)	6572(4)	36(2)	1
C70	428(6)	5112(7)	11671(4)	28(2)	1
C37	-40(6)	6622(7)	3962(4)	31(2)	1
C55	3288(6)	4781(6)	8957(4)	26(2)	1
C78	958(7)	5035(7)	9726(5)	33(2)	1
C14	3542(5)	5597(6)	4397(4)	22(2)	1
C25	2931(8)	7748(11)	7454(8)	68(3)	1
C7	4538(6)	4816(6)	3246(4)	25(2)	1
C43	4764(7)	4852(6)	8378(4)	28(2)	1
C22	1646(6)	6550(9)	6608(5)	42(2)	1
C49	3500(7)	3315(7)	8194(4)	32(2)	1
C54	3496(9)	3332(9)	7541(5)	51(3)	1
C65	2245(6)	7266(7)	11505(4)	33(2)	1
C44	4288(7)	5515(7)	7927(5)	37(2)	1
C8	4062(7)	5517(7)	2837(5)	33(2)	1
C17	4530(9)	3109(11)	5838(5)	58(3)	1
C3	2159(7)	2045(7)	2977(5)	36(2)	1
C16	5142(8)	3933(10)	5965(5)	53(2)	1
C66	2844(6)	7872(8)	11920(5)	39(2)	1
C47	6196(9)	5413(9)	8227(7)	59(3)	1
C77	1363(6)	4574(7)	10395(5)	34(2)	1
C56	3628(5)	5485(6)	9501(5)	31(2)	1
C10	5415(8)	5940(7)	2556(5)	41(2)	1
C80	868(7)	7396(7)	9480(5)	37(2)	1
C15	3984(6)	5215(7)	5074(4)	28(2)	1
C26	2293(7)	7245(9)	7661(6)	50(2)	1
C12	5462(6)	4684(7)	3301(5)	36(2)	1
C11	5883(7)	5230(8)	2946(6)	42(2)	1
C51	2367(8)	2100(9)	7921(6)	51(3)	1
C4	2044(8)	2083(8)	2314(5)	42(2)	1
C2	2757(6)	2646(6)	3403(4)	30(2)	1
C46	5711(8)	6057(8)	7781(5)	44(2)	1
C48	5735(7)	4831(8)	8537(6)	43(2)	1
C57	3949(6)	5006(7)	10164(5)	37(2)	1
C38	668(8)	7354(8)	4349(6)	44(2)	1
C76	1738(6)	5225(7)	10941(5)	36(2)	1
C29	1019(8)	4485(9)	7064(6)	50(3)	1
C42	-1313(9)	4598(10)	3503(6)	54(3)	1
C52	2382(9)	2120(10)	7288(7)	62(3)	1
C82	-1072(7)	5136(7)	9178(5)	33(2)	1
C62	4309(10)	2676(10)	10651(6)	62(3)	1
C58	5905(7)	5168(8)	10755(7)	55(3)	1
C60	6606(9)	4845(11)	11393(8)	75(4)	1
C40	-1258(7)	5094(8)	4135(5)	37(2)	1

C18	4961(11)	4558(13)	6486(5)	79(4)	1
C5	2523(8)	2703(8)	2076(5)	46(2)	1
C50	2919(7)	2674(7)	8378(6)	40(2)	1
C36	761(9)	4951(9)	4584(5)	51(3)	1
C35	1337(10)	4610(12)	5200(7)	72(4)	1
C84	-1006(13)	4566(13)	8613(8)	100(7)	1
C19	5978(6)	5460(8)	5364(6)	46(2)	1
C59	6362(10)	5522(9)	10286(8)	73(4)	1
C53	2937(10)	2736(9)	7101(6)	59(3)	1
C23	2297(7)	7072(11)	6405(7)	64(3)	1
C24	2917(8)	7664(12)	6820(8)	72(3)	1
C83	-1484(8)	4636(9)	9640(5)	42(2)	1
C20	6166(8)	5743(10)	4737(7)	62(3)	1
C34	1634(10)	5089(13)	5772(6)	77(4)	1
C21	6849(9)	5183(11)	5916(8)	81(4)	1
C41	-1516(12)	4489(11)	4618(7)	67(4)	1
C63	4525(12)	3963(16)	11498(7)	99(6)	1
O3A	2100(8)	4015(8)	10306(7)	59(3)	0.750(15)
O4B	679(13)	4027(16)	10560(11)	21(4)	0.250(15)

Table 6: Bond lengths [Å] and angles [°]

Ni1-P1	**2.164(2)**
Ni1-Cl0A	2.196(2)
Ni1-P2	2.177(2)
Ni1-Cl0F	2.211(2)
Ni2-P3	2.172(2)
Ni2-Cl09	2.219(2)
Ni2-Cl0H	2.191(2)
Ni2-P4	2.153(2)
Ni4-P7	2.179(2)
Ni4-Cl06	2.215(2)
Ni4-P8	2.152(2)
Ni4-Cl0G	2.200(2)
Ni3-Cl0B	2.194(2)
Ni3-P5	2.154(2)
Ni3-P6	2.175(2)
Ni3-Cl0J	2.219(3)
P7-C79	1.829(9)
P7-C78	1.818(9)
P7-C82	1.839(9)
P3-C37	1.835(9)
P3-C40	1.823(11)
P3-C36	1.819(10)
P1-C1	1.814(9)
P1-C13	1.816(8)
P1-C7	1.817(9)
P5-C55	1.827(8)
P5-C43	1.810(9)
P5-C49	1.794(9)
P8-C64	1.845(10)
P8-C70	1.824(10)
P8-C76	1.834(9)
P2-C16	1.836(12)
P2-C15	1.842(9)
P2-C19	1.885(11)
P6-C61	1.915(12)
P6-C57	1.839(10)
P6-C58	1.842(11)
P4-C28	1.809(12)
P4-C22	1.808(13)
P4-C34	1.840(12)
O1-H1	0.82
O1-C14	1.431(9)
O3-H3B	0.82
O3-C56	1.429(10)
C81-H81A	0.96
C81-H81B	0.96
C81-H81C	0.96
C81-C79	1.547(12)
O2-H2A	0.82
O2-C35	1.452(12)
C73-H73	0.93
C73-C72	1.380(14)

C73-C74	1.371(14)	**C71-C70**	1.409(12)
C67-H67	0.93	**C33-H33**	0.93
C67-C68	1.410(15)	**C33-C28**	1.407(15)
C67-C66	1.376(15)	**C28-C29**	1.420(13)
C39-H39A	0.96	**C37-H37**	0.98
C39-H39B	0.96	**C37-C38**	1.561(15)
C39-H39C	0.96	**C55-H55A**	0.97
C39-C37	1.537(12)	**C55-H55B**	0.97
C72-H72	0.93	**C55-C56**	1.523(12)
C72-C71	1.393(14)	**C78-H78A**	0.97
C31-H31	0.93	**C78-H78B**	0.97
C31-C30	1.368(16)	**C78-C77**	1.537(13)
C31-C32	1.367(14)	**C14-H14**	0.98
C30-H30	0.93	**C14-C15**	1.513(12)
C30-C29	1.394(18)	**C25-H25**	0.93
C69-H69	0.93	**C25-C26**	1.391(17)
C69-C64	1.389(12)	**C25-C24**	1.36(2)
C69-C68	1.347(15)	**C7-C8**	1.397(12)
C64-C65	1.389(13)	**C7-C12**	1.384(12)
C61-H61	0.98	**C43-C44**	1.402(13)
C61-C62	1.437(19)	**C43-C48**	1.409(13)
C61-C63	1.571(17)	**C22-C23**	1.416(15)
C32-H32	0.93	**C49-C54**	1.406(13)
C32-C33	1.354(16)	**C49-C50**	1.419(14)
C9-H9	0.93	**C54-H54**	0.93
C9-C8	1.394(13)	**C54-C53**	1.371(16)
C9-C10	1.372(15)	**C65-H65**	0.93
C45-H45	0.93	**C65-C66**	1.380(15)
C45-C44	1.390(14)	**C44-H44**	0.93
C45-C46	1.396(16)	**C8-H8**	0.93
C68-H68	0.93	**C17-H17A**	0.96
C27-H27	0.93	**C17-H17B**	0.96
C27-C22	1.393(13)	**C17-H17C**	0.96
C27-C26	1.371(17)	**C17-C16**	1.49(2)
C1-C6	1.403(11)	**C3-H3**	0.93
C1-C2	1.385(13)	**C3-C4**	1.386(14)
C13-H13A	0.97	**C3-C2**	1.387(13)
C13-H13B	0.97	**C16-H16**	0.98
C13-C14	1.525(10)	**C16-C18**	1.531(16)
C6-H6	0.93	**C66-H66**	0.93
C6-C5	1.386(14)	**C47-H47**	0.93
C79-H79	0.98	**C47-C46**	1.382(15)
C79-C80	1.573(14)	**C47-C48**	1.390(14)
C74-H74	0.93	**C77-H77**	0.98
C74-C75	1.367(15)	**C77-H77A**	0.98
C75-H75	0.93	**C77-C76**	1.483(15)
C75-C70	1.398(12)	**C77-O3A**	1.442(13)
C71-H71	0.93	**C77-O4B**	1.44(2)

C56-H56	0.98	**C40-C41**	1.503(15)
C56-C57	1.528(15)	**C18-H18A**	0.96
C10-H10	0.93	**C18-H18B**	0.96
C10-C11	1.383(15)	**C18-H18C**	0.96
C80-H80A	0.96	**C5-H5**	0.93
C80-H80B	0.96	**C50-H50**	0.93
C80-H80C	0.96	**C36-H36A**	0.97
C15-H15A	0.97	**C36-H36B**	0.97
C15-H15B	0.97	**C36-C35**	1.436(17)
C26-H26	0.93	**C35-C34**	1.367(19)
C12-H12	0.93	**C84-H84A**	0.96
C12-C11	1.385(13)	**C84-H84B**	0.96
C11-H11	0.93	**C84-H84C**	0.96
C51-H51	0.93	**C19-H19**	0.98
C51-C52	1.372(19)	**C19-C20**	1.519(19)
C51-C50	1.365(15)	**C19-C21**	1.539(16)
C4-H4	0.93	**C59-H59A**	0.96
C4-C5	1.352(17)	**C59-H59B**	0.96
C2-H2	0.93	**C59-H59C**	0.96
C46-H46	0.93	**C53-H53**	0.93
C48-H48	0.93	**C23-H23**	0.93
C57-H57A	0.97	**C23-C24**	1.38(2)
C57-H57B	0.97	**C24-H24**	0.93
C38-H38A	0.96	**C83-H83A**	0.96
C38-H38B	0.96	**C83-H83B**	0.96
C38-H38C	0.96	**C83-H83C**	0.96
C76-H76A	0.97	**C20-H20A**	0.96
C76-H76B	0.97	**C20-H20B**	0.96
C29-H29	0.93	**C20-H20C**	0.96
C42-H42A	0.96	**C34-H34A**	0.97
C42-H42B	0.96	**C34-H34B**	0.97
C42-H42C	0.96	**C21-H21A**	0.96
C42-C40	1.521(14)	**C21-H21B**	0.96
C52-H52	0.93	**C21-H21C**	0.96
C52-C53	1.37(2)	**C41-H41A**	0.96
C82-H82	0.98	**C41-H41B**	0.96
C82-C84	1.499(15)	**C41-H41C**	0.96
C82-C83	1.513(13)	**C63-H63A**	0.96
C62-H62A	0.96	**C63-H63B**	0.96
C62-H62B	0.96	**C63-H63C**	0.96
C62-H62C	0.96	**O3A-H3A**	0.82
C58-H58	0.98	**O4B-H4B**	0.82
C58-C60	1.533(19)		
C58-C59	1.48(2)	**P1-Ni1-Cl0A**	88.07(9)
C60-H60A	0.96	**P1-Ni1-P2**	94.04(9)
C60-H60B	0.96	**P1-Ni1-Cl0F**	165.96(11)
C60-H60C	0.96	**Cl0A-Ni1-Cl0F**	91.63(9)
C40-H40	0.98	**P2-Ni1-Cl0A**	173.97(11)

P2-Ni1-Cl0F	87.69(9)	**C76-P8-C64**	98.8(4)
P3-Ni2-Cl09	86.22(9)	**C16-P2-Ni1**	107.0(4)
P3-Ni2-Cl0H	174.87(12)	**C16-P2-C15**	102.2(5)
Cl0H-Ni2-Cl09	91.12(9)	**C16-P2-C19**	109.3(6)
P4-Ni2-P3	95.75(10)	**C15-P2-Ni1**	119.5(3)
P4-Ni2-Cl09	173.79(12)	**C15-P2-C19**	103.1(4)
P4-Ni2-Cl0H	87.35(10)	**C19-P2-Ni1**	114.8(3)
P7-Ni4-Cl06	87.05(9)	**C61-P6-Ni3**	103.6(4)
P7-Ni4-Cl0G	177.41(12)	**C57-P6-Ni3**	119.3(3)
P8-Ni4-P7	96.11(9)	**C57-P6-C61**	103.0(5)
P8-Ni4-Cl06	174.71(10)	**C57-P6-C58**	102.1(5)
P8-Ni4-Cl0G	85.91(9)	**C58-P6-Ni3**	118.0(4)
Cl0G-Ni4-Cl06	91.06(9)	**C58-P6-C61**	110.0(6)
Cl0B-Ni3-Cl0J	91.70(10)	**C28-P4-Ni2**	109.7(3)
P5-Ni3-Cl0B	88.86(9)	**C28-P4-C34**	105.4(7)
P5-Ni3-P6	95.63(10)	**C22-P4-Ni2**	114.8(4)
P5-Ni3-Cl0J	166.56(11)	**C22-P4-C28**	106.4(4)
P6-Ni3-Cl0B	170.25(11)	**C22-P4-C34**	99.4(7)
P6-Ni3-Cl0J	85.95(10)	**C34-P4-Ni2**	119.9(4)
C79-P7-Ni4	106.7(3)	**C14-O1-H1**	109.5
C79-P7-C82	107.7(4)	**C56-O3-H3B**	109.5
C78-P7-Ni4	121.5(3)	**H81A-C81-H81B**	109.5
C78-P7-C79	102.9(4)	**H81A-C81-H81C**	109.5
C78-P7-C82	107.4(5)	**H81B-C81-H81C**	109.5
C82-P7-Ni4	109.8(3)	**C79-C81-H81A**	109.5
C37-P3-Ni2	105.6(3)	**C79-C81-H81B**	109.5
C40-P3-Ni2	110.3(3)	**C79-C81-H81C**	109.5
C40-P3-C37	109.3(5)	**C35-O2-H2A**	109.5
C36-P3-Ni2	121.0(4)	**C72-C73-H73**	119.9
C36-P3-C37	103.1(5)	**C74-C73-H73**	119.9
C36-P3-C40	106.9(6)	**C74-C73-C72**	120.1(10)
C1-P1-Ni1	116.9(3)	**C68-C67-H67**	120.9
C1-P1-C13	99.8(4)	**C66-C67-H67**	120.9
C1-P1-C7	107.7(4)	**C66-C67-C68**	118.2(10)
C13-P1-Ni1	120.5(3)	**H39A-C39-H39B**	109.5
C13-P1-C7	105.3(4)	**H39A-C39-H39C**	109.5
C7-P1-Ni1	105.6(3)	**H39B-C39-H39C**	109.5
C55-P5-Ni3	120.7(3)	**C37-C39-H39A**	109.5
C43-P5-Ni3	107.1(3)	**C37-C39-H39B**	109.5
C43-P5-C55	104.5(4)	**C37-C39-H39C**	109.5
C49-P5-Ni3	116.7(3)	**C73-C72-H72**	120.6
C49-P5-C55	99.7(4)	**C73-C72-C71**	118.9(9)
C49-P5-C43	106.8(4)	**C71-C72-H72**	120.6
C64-P8-Ni4	115.3(3)	**C30-C31-H31**	119.5
C70-P8-Ni4	109.0(3)	**C32-C31-H31**	119.5
C70-P8-C64	108.2(4)	**C32-C31-C30**	121.0(11)
C70-P8-C76	104.4(5)	**C31-C30-H30**	120.8
C76-P8-Ni4	120.0(3)	**C31-C30-C29**	118.5(10)

C29-C30-H30	120.8	**C75-C74-H74**	119.2
C64-C69-H69	119.5	**C74-C75-H75**	119.8
C68-C69-H69	119.5	**C74-C75-C70**	120.4(9)
C68-C69-C64	121.0(9)	**C70-C75-H75**	119.8
C69-C64-P8	121.3(7)	**C72-C71-H71**	119.4
C65-C64-P8	119.9(7)	**C72-C71-C70**	121.3(9)
C65-C64-C69	118.8(9)	**C70-C71-H71**	119.4
P6-C61-H61	106.6	**C32-C33-H33**	120
C62-C61-P6	111.0(7)	**C32-C33-C28**	120.0(9)
C62-C61-H61	106.6	**C28-C33-H33**	120
C62-C61-C63	116.8(12)	**C33-C28-P4**	121.6(7)
C63-C61-P6	108.7(11)	**C33-C28-C29**	117.3(10)
C63-C61-H61	106.6	**C29-C28-P4**	121.1(9)
C31-C32-H32	119	**C75-C70-P8**	121.4(7)
C33-C32-C31	122.0(11)	**C75-C70-C71**	117.6(9)
C33-C32-H32	119	**C71-C70-P8**	120.9(7)
C8-C9-H9	120.2	**P3-C37-H37**	107.5
C10-C9-H9	120.2	**C39-C37-P3**	114.8(7)
C10-C9-C8	119.5(9)	**C39-C37-H37**	107.5
C44-C45-H45	120.2	**C39-C37-C38**	109.6(9)
C44-C45-C46	119.5(9)	**C38-C37-P3**	109.6(7)
C46-C45-H45	120.2	**C38-C37-H37**	107.5
C67-C68-H68	119.6	**P5-C55-H55A**	108.6
C69-C68-C67	120.9(10)	**P5-C55-H55B**	108.6
C69-C68-H68	119.6	**H55A-C55-H55B**	107.5
C22-C27-H27	119.6	**C56-C55-P5**	114.8(6)
C26-C27-H27	119.6	**C56-C55-H55A**	108.6
C26-C27-C22	120.8(10)	**C56-C55-H55B**	108.6
C6-C1-P1	121.5(7)	**P7-C78-H78A**	107.9
C2-C1-P1	119.6(6)	**P7-C78-H78B**	107.9
C2-C1-C6	118.9(8)	**H78A-C78-H78B**	107.2
P1-C13-H13A	108.4	**C77-C78-P7**	117.5(6)
P1-C13-H13B	108.4	**C77-C78-H78A**	107.9
H13A-C13-H13B	107.5	**C77-C78-H78B**	107.9
C14-C13-P1	115.3(5)	**O1-C14-C13**	105.4(6)
C14-C13-H13A	108.4	**O1-C14-H14**	110.6
C14-C13-H13B	108.4	**O1-C14-C15**	108.7(7)
C1-C6-H6	119.9	**C13-C14-H14**	110.6
C5-C6-C1	120.2(10)	**C15-C14-C13**	110.8(7)
C5-C6-H6	119.9	**C15-C14-H14**	110.6
P7-C79-H79	107	**C26-C25-H25**	120.8
C81-C79-P7	115.7(7)	**C24-C25-H25**	120.8
C81-C79-H79	107	**C24-C25-C26**	118.3(14)
C81-C79-C80	111.1(8)	**C8-C7-P1**	122.7(7)
C80-C79-P7	108.7(6)	**C12-C7-P1**	119.2(7)
C80-C79-H79	107	**C12-C7-C8**	118.1(8)
C73-C74-H74	119.2	**C44-C43-P5**	123.2(7)
C75-C74-C73	121.6(9)	**C44-C43-C48**	117.6(8)

C48-C43-P5	119.1(7)	**O4B-C77-C78**	111.1(11)
C27-C22-P4	121.6(8)	**O4B-C77-H77A**	108.1
C27-C22-C23	116.1(12)	**O4B-C77-C76**	106.8(12)
C23-C22-P4	122.3(9)	**O3-C56-C55**	106.0(7)
C54-C49-P5	122.4(8)	**O3-C56-H56**	110.5
C54-C49-C50	118.5(10)	**O3-C56-C57**	108.8(8)
C50-C49-P5	119.1(7)	**C55-C56-H56**	110.5
C49-C54-H54	120.2	**C55-C56-C57**	110.4(8)
C53-C54-C49	119.6(13)	**C57-C56-H56**	110.5
C53-C54-H54	120.2	**C9-C10-H10**	120.4
C64-C65-H65	119.9	**C9-C10-C11**	119.2(9)
C66-C65-C64	120.2(9)	**C11-C10-H10**	120.4
C66-C65-H65	119.9	**C79-C80-H80A**	109.5
C45-C44-C43	121.6(10)	**C79-C80-H80B**	109.5
C45-C44-H44	119.2	**C79-C80-H80C**	109.5
C43-C44-H44	119.2	**H80A-C80-H80B**	109.5
C9-C8-C7	121.6(9)	**H80A-C80-H80C**	109.5
C9-C8-H8	119.2	**H80B-C80-H80C**	109.5
C7-C8-H8	119.2	**P2-C15-H15A**	108.1
H17A-C17-H17B	109.5	**P2-C15-H15B**	108.1
H17A-C17-H17C	109.5	**C14-C15-P2**	116.9(6)
H17B-C17-H17C	109.5	**C14-C15-H15A**	108.1
C16-C17-H17A	109.5	**C14-C15-H15B**	108.1
C16-C17-H17B	109.5	**H15A-C15-H15B**	107.3
C16-C17-H17C	109.5	**C27-C26-C25**	122.3(13)
C4-C3-H3	119.7	**C27-C26-H26**	118.9
C4-C3-C2	120.6(10)	**C25-C26-H26**	118.9
C2-C3-H3	119.7	**C7-C12-H12**	120.1
P2-C16-H16	107	**C7-C12-C11**	119.9(9)
C17-C16-P2	110.8(7)	**C11-C12-H12**	120.1
C17-C16-H16	107	**C10-C11-C12**	121.6(9)
C17-C16-C18	111.8(12)	**C10-C11-H11**	119.2
C18-C16-P2	112.8(10)	**C12-C11-H11**	119.2
C18-C16-H16	107	**C52-C51-H51**	119.6
C67-C66-C65	121.0(10)	**C50-C51-H51**	119.6
C67-C66-H66	119.5	**C50-C51-C52**	120.7(13)
C65-C66-H66	119.5	**C3-C4-H4**	119.9
C46-C47-H47	119.8	**C5-C4-C3**	120.1(9)
C46-C47-C48	120.5(11)	**C5-C4-H4**	119.9
C48-C47-H47	119.8	**C1-C2-C3**	119.6(9)
C78-C77-H77	109.8	**C1-C2-H2**	120.2
C78-C77-H77A	108.1	**C3-C2-H2**	120.2
C76-C77-C78	114.3(9)	**C45-C46-H46**	120
C76-C77-H77	109.8	**C47-C46-C45**	119.9(10)
C76-C77-H77A	108.1	**C47-C46-H46**	120
O3A-C77-C78	103.1(9)	**C43-C48-H48**	119.6
O3A-C77-H77	109.8	**C47-C48-C43**	120.7(9)
O3A-C77-C76	109.8(9)	**C47-C48-H48**	119.6

P6-C57-H57A	108	**C58-C60-H60A**	109.5
P6-C57-H57B	108	**C58-C60-H60B**	109.5
C56-C57-P6	117.3(6)	**C58-C60-H60C**	109.5
C56-C57-H57A	108	**H60A-C60-H60B**	109.5
C56-C57-H57B	108	**H60A-C60-H60C**	109.5
H57A-C57-H57B	107.2	**H60B-C60-H60C**	109.5
C37-C38-H38A	109.5	**P3-C40-H40**	105
C37-C38-H38B	109.5	**C42-C40-P3**	116.8(7)
C37-C38-H38C	109.5	**C42-C40-H40**	105
H38A-C38-H38B	109.5	**C41-C40-P3**	111.1(9)
H38A-C38-H38C	109.5	**C41-C40-C42**	112.8(11)
H38B-C38-H38C	109.5	**C41-C40-H40**	105
P8-C76-H76A	108.4	**C16-C18-H18A**	109.5
P8-C76-H76B	108.4	**C16-C18-H18B**	109.5
C77-C76-P8	115.4(6)	**C16-C18-H18C**	109.5
C77-C76-H76A	108.4	**H18A-C18-H18B**	109.5
C77-C76-H76B	108.4	**H18A-C18-H18C**	109.5
H76A-C76-H76B	107.5	**H18B-C18-H18C**	109.5
C30-C29-C28	121.2(11)	**C6-C5-H5**	119.8
C30-C29-H29	119.4	**C4-C5-C6**	120.4(9)
C28-C29-H29	119.4	**C4-C5-H5**	119.8
H42A-C42-H42B	109.5	**C49-C50-H50**	120.1
H42A-C42-H42C	109.5	**C51-C50-C49**	119.9(11)
H42B-C42-H42C	109.5	**C51-C50-H50**	120.1
C40-C42-H42A	109.5	**P3-C36-H36A**	106.8
C40-C42-H42B	109.5	**P3-C36-H36B**	106.8
C40-C42-H42C	109.5	**H36A-C36-H36B**	106.7
C51-C52-H52	119.9	**C35-C36-P3**	122.1(8)
C53-C52-C51	120.2(12)	**C35-C36-H36A**	106.8
C53-C52-H52	119.9	**C35-C36-H36B**	106.8
P7-C82-H82	104.2	**C36-C35-O2**	106.9(10)
C84-C82-P7	116.6(8)	**C34-C35-O2**	112.5(11)
C84-C82-H82	104.2	**C34-C35-C36**	126.7(13)
C84-C82-C83	114.3(10)	**C82-C84-H84A**	109.5
C83-C82-P7	111.6(7)	**C82-C84-H84B**	109.5
C83-C82-H82	104.2	**C82-C84-H84C**	109.5
C61-C62-H62A	109.5	**H84A-C84-H84B**	109.5
C61-C62-H62B	109.5	**H84A-C84-H84C**	109.5
C61-C62-H62C	109.5	**H84B-C84-H84C**	109.5
H62A-C62-H62B	109.5	**P2-C19-H19**	106.4
H62A-C62-H62C	109.5	**C20-C19-P2**	111.0(7)
H62B-C62-H62C	109.5	**C20-C19-H19**	106.4
P6-C58-H58	106.3	**C20-C19-C21**	114.2(11)
C60-C58-P6	115.4(10)	**C21-C19-P2**	111.9(10)
C60-C58-H58	106.3	**C21-C19-H19**	106.4
C59-C58-P6	109.6(9)	**C58-C59-H59A**	109.5
C59-C58-H58	106.3	**C58-C59-H59B**	109.5
C59-C58-C60	112.2(11)	**C58-C59-H59C**	109.5

H59A-C59-H59B	109.5
H59A-C59-H59C	109.5
H59B-C59-H59C	109.5
C54-C53-H53	119.4
C52-C53-C54	121.1(12)
C52-C53-H53	119.4
C22-C23-H23	118.9
C24-C23-C22	122.3(13)
C24-C23-H23	118.9
C25-C24-C23	120.2(12)
C25-C24-H24	119.9
C23-C24-H24	119.9
C82-C83-H83A	109.5
C82-C83-H83B	109.5
C82-C83-H83C	109.5
H83A-C83-H83B	109.5
H83A-C83-H83C	109.5
H83B-C83-H83C	109.5
C19-C20-H20A	109.5
C19-C20-H20B	109.5
C19-C20-H20C	109.5
H20A-C20-H20B	109.5
H20A-C20-H20C	109.5
H20B-C20-H20C	109.5
P4-C34-H34A	107
P4-C34-H34B	107
C35-C34-P4	121.1(10)
C35-C34-H34A	107
C35-C34-H34B	107
H34A-C34-H34B	106.8
C19-C21-H21A	109.5
C19-C21-H21B	109.5
C19-C21-H21C	109.5
H21A-C21-H21B	109.5
H21A-C21-H21C	109.5
H21B-C21-H21C	109.5
C40-C41-H41A	109.5
C40-C41-H41B	109.5
C40-C41-H41C	109.5
H41A-C41-H41B	109.5
H41A-C41-H41C	109.5
H41B-C41-H41C	109.5
C61-C63-H63A	109.5
C61-C63-H63B	109.5
C61-C63-H63C	109.5
H63A-C63-H63B	109.5
H63A-C63-H63C	109.5
H63B-C63-H63C	109.5
C77-O3A-H3A	109.5
C77-O4B-H4B	109.5

***Bis*((1*R*,5*S*)-2,4-bis(2-(diphenylphosphanyl)benzyl)-1,8,8-trimethyl-2,4-diazabicyclo[3.2.1]octan-3-ylidene)) gold(I) hexafluorophosphate**

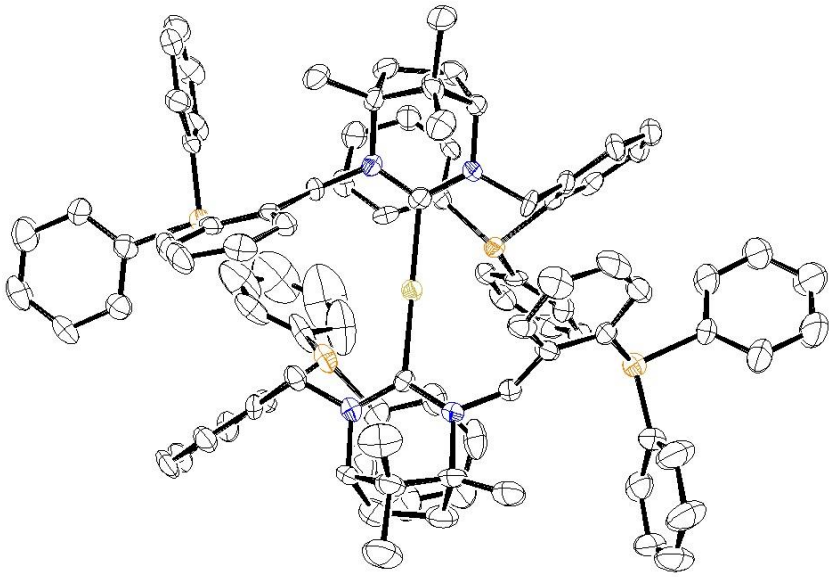

Figure 3: Molecular structure of bis(diphosphino carbene) gold complex, pdn1506d. H atoms, anion and solvent molecules omitted for clarity.

Table 7: Crystal data and structure refinement details

Identification code	**pdn1506d**	
Empirical formula	$C_{94}H_{92}AuF_6N_4P_5$	
Formula weight	1743.53	
Temperature	298(2) K	
Wavelength	0.71073 Å	
Crystal system	triclinic	
Space group	P1	
Unit cell dimensions	*a* = 13.3125(4) Å	$\alpha = 73.630(3)$ °
	b = 14.2180(5) Å	$\beta = 88.218(3)$ °
	c = 23.9651(8) Å	$\gamma = 89.839(3)$ °
Volume	4350.0(3) Å^3	
Z	2	
Density (calculated)	1.311 Mg / m^3	
Absorption coefficient	1.843 mm^{-1}	
F(000)	1784	
Crystal size	$0.229 \times 0.098 \times 0.046$ mm^3	
Θ Range for data collection	$3.363 - 29.729°$	
Index ranges	$-17 \leq \eta \leq 17, -19 \leq \kappa \leq 19, -30 \leq \lambda \leq 30$	
Reflections collected	40800	
Independent reflections	31177 [R_{int} = 0.0611]	
Absorption correction	Semi–empirical from equivalents	
Max. and min. transmission	0920 and 0.678	
Refinement method	Full-matrix least-squares on F^2	
Data / restraints / parameters	40800 / 3 / 1993	
Goodness-of-fit on F^2	1.038	
Final *R* indices [$F^2 > 2\sigma(F^2)$]	*R1* = 0.0605, *wR2* = 0.1204	
***R* indices (all data)**	*R1* = 0.0923, *wR2* = 0.1392	
Extinction coefficient	n/a	

Table 8: Bond lengths [Å]

Atom1	Atom2	Length
C1	N1	1.33(1)
C1	N2	1.33(2)
C1	Au1	2.07(1)
C2	C3	1.54(2)
C2	C6	1.54(1)
C2	C7	1.53(1)
C2	N1	1.50(1)
C3	H3A	0.97
C3	H3B	0.97
C3	C4	1.55(2)
C4	H4A	0.97
C4	H4B	0.97
C4	C5	1.53(1)
C5	H5	0.98
C5	C6	1.52(1)
C5	N2	1.49(1)
C6	C8	1.55(2)
C6	C9	1.54(2)
C7	H7A	0.96
C7	H7B	0.96
C7	H7C	0.96
C8	H8A	0.96
C8	H8B	0.96
C8	H8C	0.96
C9	H9A	0.96
C9	H9B	0.96
C9	H9C	0.96
C10	H10A	0.97
C10	H10B	0.97
C10	C11	1.51(2)
C10	N1	1.47(2)
C11	C12	1.42(2)
C11	C16	1.39(1)

C12	C13	1.37(2)
C12	P1	1.85(1)
C13	H13	0.93
C13	C14	1.38(2)
C14	H14	0.93
C14	C15	1.39(2)
C15	H15	0.93
C15	C16	1.38(2)
C16	H16	0.93
C17	C18	1.38(2)
C17	C22	1.39(1)
C17	P1	1.83(1)
C18	H18	0.93
C18	C19	1.40(2)
C19	H19	0.93
C19	C20	1.35(2)
C20	H20	0.93
C20	C21	1.37(2)
C21	H21	0.93
C21	C22	1.38(2)
C22	H22	0.93
C23	C24	1.38(2)
C23	C28	1.37(2)
C23	P1	1.83(1)
C24	H24	0.93
C24	C25	1.39(2)
C25	H25	0.93
C25	C26	1.39(2)
C26	H26	0.93
C26	C27	1.37(2)
C27	H27	0.93
C27	C28	1.40(2)
C28	H28	0.93
C29	C30	1.39(1)
C29	C34	1.41(2)
C29	C042	1.53(2)
C30	C31	1.39(2)
C30	P4	1.84(1)
C31	H31	0.93
C31	C32	1.38(2)
C32	H32	0.93
C32	C33	1.37(1)
C33	H33	0.93
C33	C34	1.40(2)
C34	H34	0.93
C35	C36	1.40(2)
C35	C40	1.40(2)
C35	P4	1.82(1)
C36	H36	0.93
C36	C37	1.38(2)
C37	H37	0.93
C37	C38	1.39(2)
C38	H38	0.93
C38	C39	1.40(2)
C39	H39	0.93
C39	C40	1.39(2)
C40	H40	0.93
C41	C42	1.41(2)
C41	C46	1.38(2)
C41	P4	1.83(1)
C042	H04A	0.97
C042	H04B	0.97
C042	N2	1.48(1)
C42	H42	0.93
C42	C43	1.38(2)
C43	H43	0.93
C43	C44	1.37(2)
C44	H44	0.93
C44	C45	1.39(2)
C45	H45	0.93
C45	C46	1.36(2)
C46	H46	0.93
C47	N3	1.33(1)
C47	N4	1.35(2)
C47	Au1	2.06(1)
C48	C49	1.52(2)
C48	C52	1.58(2)
C48	C53	1.52(2)
C48	N3	1.53(1)
C49	H49A	0.97
C49	H49B	0.97
C49	C50	1.55(2)
C50	H50A	0.97
C50	H50B	0.97
C50	C51	1.52(2)
C51	H51	0.98
C51	C52	1.53(2)
C51	N4	1.49(2)
C52	C54	1.49(2)
C52	C55	1.56(2)
C53	H53A	0.96
C53	H53B	0.96
C53	H53C	0.96
C54	H54A	0.96
C54	H54B	0.96
C54	H54C	0.96

C55	H55A	0.96
C55	H55B	0.96
C55	H55C	0.96
C56	H56A	0.97
C56	H56B	0.971
C56	C57	1.52(2)
C56	N3	1.44(2)
C57	C58	1.40(2)
C57	C62	1.39(1)
C58	C59	1.44(2)
C58	P3	1.81(1)
C59	H59	0.93
C59	C60	1.35(2)
C60	H60	0.93
C60	C61	1.36(2)
C61	H61	0.93
C61	C62	1.41(2)
C62	H62	0.93
C63	C64	1.42(2)
C63	C68	1.37(3)
C63	P3	1.82(2)
C64	H64	0.93
C64	C65	1.37(3)
C65	H65	0.93
C65	C66	1.38(3)
C66	H66	0.93
C66	C67	1.38(4)
C67	H67	0.93
C67	C68	1.41(4)
C68	H68	0.93
C69	C70	1.44(2)
C69	C74	1.38(2)
C69	P3	1.80(1)
C70	H70	0.93
C70	C71	1.38(2)
C71	H71	0.93
C71	C72	1.44(2)
C72	H72	0.93
C72	C73	1.32(3)
C73	H73	0.93
C73	C74	1.39(2)
C74	H74	0.93
C75	H75A	0.97
C75	H75B	0.97
C75	C76	1.51(2)
C75	N4	1.44(2)
C76	C77	1.42(2)
C76	C81	1.38(2)
C77	C78	1.37(2)
C77	P2	1.83(1)
C78	H78	0.93
C78	C79	1.39(2)
C79	H79	0.93
C79	C80	1.41(2)
C80	H80	0.93
C80	C81	1.36(2)
C81	H81	0.93
C82	C83	1.43(2)
C82	C87	1.35(2)
C82	P2	1.83(1)
C83	H83	0.93
C83	C84	1.40(2)
C84	H84	0.93
C84	C85	1.36(2)
C85	H85	0.93
C85	C86	1.40(3)
C86	H86	0.93
C86	C87	1.41(2)
C87	H87	0.93
C88	C89	1.45(3)
C88	C93	1.38(2)
C88	P2	1.78(1)
C89	H89	0.93
C89	C90	1.37(3)
C90	H90	0.93
C90	C91	1.38(5)
C91	H91	0.93
C91	C92	1.36(4)
C92	H92	0.93
C92	C93	1.43(2)
C93	H93	0.93
C030	H030	0.93
C030	C182	1.38(2)
C030	C186	1.40(2)
C94	N5	1.35(1)
C94	N6	1.33(2)
C94	Au2	2.05(1)
C95	C96	1.59(2)
C95	C99	1.55(2)
C95	C100	1.53(2)
C95	N5	1.50(2)
C96	H96A	0.97
C96	H96B	0.97
C96	C97	1.55(2)
C97	H97A	0.97
C97	H97B	0.97

C97	C98	1.49(2)
C98	H98	0.98
C98	C99	1.53(2)
C98	N6	1.49(1)
C99	C101	1.53(2)
C99	C102	1.56(2)
C100	H10C	0.96
C100	H10D	0.96
C100	H10E	0.96
C101	H10F	0.96
C101	H10G	0.96
C101	H10H	0.96
C102	H10I	0.96
C102	H10J	0.96
C102	H10K	0.96
C103	H10L	0.97
C103	H10M	0.97
C103	C104	1.52(2)
C103	N5	1.45(2)
C104	C105	1.40(2)
C104	C109	1.41(2)
C105	C106	1.37(2)
C105	P5	1.85(1)
C106	H106	0.93
C106	C107	1.38(2)
C107	H107	0.93
C107	C108	1.38(2)
C108	H108	0.93
C108	C109	1.38(2)
C109	H109	0.93
C110	C111	1.40(2)
C110	C115	1.36(2)
C110	P5	1.81(2)
C111	H111	0.93
C111	C112	1.37(3)
C112	H112	0.93
C112	C113	1.37(2)
C113	H113	0.93
C113	C114	1.33(2)
C114	H114	0.93
C114	C115	1.42(2)
C115	H115	0.93
C116	C117	1.39(2)
C116	C121	1.39(2)
C116	P5	1.82(1)
C117	H117	0.93
C117	C118	1.41(2)
C118	H118	0.93
C118	C119	1.37(2)
C119	H119	0.93
C119	C120	1.36(3)
C120	H120	0.93
C120	C121	1.41(2)
C121	H121	0.93
C122	H12A	0.97
C122	H12B	0.97
C122	C123	1.52(2)
C122	N6	1.45(2)
C123	C124	1.40(1)
C123	C128	1.41(2)
C124	C125	1.38(2)
C124	P6	1.86(1)
C125	H125	0.93
C125	C126	1.36(2)
C126	H126	0.93
C126	C127	1.42(2)
C127	H127	0.93
C127	C128	1.34(2)
C128	H128	0.93
C129	C130	1.39(2)
C129	C134	1.41(2)
C129	P6	1.83(1)
C130	H130	0.93
C130	C131	1.39(2)
C131	H131	0.93
C131	C132	1.40(2)
C132	H132	0.93
C132	C133	1.39(2)
C133	H133	0.93
C133	C134	1.39(2)
C134	H134	0.93
C135	C136	1.42(2)
C135	C140	1.35(2)
C135	P6	1.81(1)
C136	H136	0.93
C136	C137	1.34(2)
C137	H137	0.93
C137	C138	1.37(2)
C138	H138	0.93
C138	C139	1.37(2)
C139	H139	0.93
C139	C140	1.39(2)
C140	H140	0.93
C141	N7	1.33(1)
C141	N8	1.34(2)
C141	Au2	2.04(1)

C142	C143	1.58(2)
C142	C146	1.53(2)
C142	C147	1.53(2)
C142	N7	1.53(1)
C143	H14A	0.97
C143	H14B	0.97
C143	C144	1.59(2)
C144	H14C	0.97
C144	H14D	0.97
C144	C145	1.48(2)
C145	H145	0.98
C145	C146	1.53(2)
C145	N8	1.49(2)
C146	C148	1.56(2)
C146	C149	1.51(2)
C147	H14E	0.96
C147	H14F	0.96
C147	H14G	0.96
C148	H14H	0.96
C148	H14I	0.96
C148	H14J	0.96
C149	H14K	0.96
C149	H14L	0.96
C149	H14M	0.96
C150	H15A	0.97
C150	H15B	0.97
C150	C151	1.53(2)
C150	N7	1.48(2)
C151	C152	1.41(2)
C151	C156	1.38(1)
C152	C153	1.38(2)
C152	P7	1.86(1)
C153	H153	0.93
C153	C154	1.34(1)
C154	H154	0.93
C154	C155	1.39(2)
C155	H155	0.93
C155	C156	1.39(2)
C156	H156	0.93
C157	C158	1.36(2)
C157	C162	1.39(2)
C157	P7	1.82(1)
C158	H158	0.93
C158	C159	1.38(2)
C159	H159	0.93
C159	C160	1.39(2)
C160	H160	0.93
C160	C161	1.32(2)
C161	H161	0.93
C161	C162	1.38(2)
C162	H162	0.93
C163	C164	1.38(2)
C163	C168	1.39(2)
C163	P7	1.84(1)
C164	H164	0.93
C164	C165	1.42(3)
C165	H165	0.93
C165	C166	1.33(3)
C166	H166	0.93
C166	C167	1.37(2)
C167	H167	0.93
C167	C168	1.38(2)
C168	H168	0.93
C169	H16A	0.97
C169	H16B	0.97
C169	C170	1.52(2)
C169	N8	1.46(2)
C170	C171	1.37(1)
C170	C175	1.40(2)
C171	C172	1.41(2)
C171	P8	1.85(1)
C172	H172	0.93
C172	C173	1.40(2)
C173	H173	0.93
C173	C174	1.37(1)
C174	H174	0.93
C174	C175	1.39(2)
C175	H175	0.93
C176	C177	1.38(2)
C176	C181	1.41(2)
C176	P8	1.82(1)
C177	H177	0.93
C177	C178	1.37(2)
C178	H178	0.93
C178	C179	1.40(2)
C179	H179	0.93
C179	C180	1.37(2)
C180	H180	0.93
C180	C181	1.36(2)
C181	H181	0.93
C182	C183	1.38(2)
C182	P8	1.83(1)
C183	H183	0.93
C183	C184	1.39(2)
C184	H184	0.93
C184	C185	1.35(2)

C185	H185	0.93
C185	C186	1.37(2)
C186	H186	0.93
F1	P9	1.55(1)
F2	P9	1.54(1)
F3	P9	1.50(2)
F4	P9	1.53(1)
F5	P9	1.62(1)
F6	P9	1.52(1)
F7	P10	1.589(9)
F8	P10	1.593(9)
F9	P10	1.60(1)
F10	P10	1.595(8)
F11	P10	1.59(1)
F12	P10	1.56(1)

Table 9: Bond angles (°)

C(282)-Au(404)-C(189)	166.304
C(96)-Au(403)-C(1)	169.965
F(392)-P(402)-F(391)	178.809
F(392)-P(402)-F(390)	89.153
F(392)-P(402)-F(389)	92.027
F(392)-P(402)-F(388)	91.198
F(392)-P(402)-F(387)	90.497
F(391)-P(402)-F(390)	89.679
F(391)-P(402)-F(389)	87.72
F(391)-P(402)-F(388)	89.966
F(391)-P(402)-F(387)	89.745
F(390)-P(402)-F(389)	89.286
F(390)-P(402)-F(388)	179.238
F(390)-P(402)-F(387)	90.195
F(389)-P(402)-F(388)	90.026
F(389)-P(402)-F(387)	177.415
F(388)-P(402)-F(387)	90.478
F(386)-P(401)-F(385)	175.017
F(386)-P(401)-F(384)	91.351
F(386)-P(401)-F(383)	89.128
F(386)-P(401)-F(382)	92.112
F(386)-P(401)-F(381)	103.737
F(385)-P(401)-F(384)	88.187
F(385)-P(401)-F(383)	85.9
F(385)-P(401)-F(382)	87.987
F(385)-P(401)-F(381)	81.23
F(384)-P(401)-F(383)	88.345
F(384)-P(401)-F(382)	174.451
F(384)-P(401)-F(381)	90.493
F(383)-P(401)-F(382)	87.373
F(383)-P(401)-F(381)	167.108
F(382)-P(401)-F(381)	92.895
C(364)-P(400)-C(353)	101.275
C(364)-P(400)-C(344)	100.171
C(353)-P(400)-C(344)	104.139
C(329)-P(399)-C(318)	104.064
C(329)-P(399)-C(309)	102.769
C(318)-P(399)-C(309)	102.647
C(271)-P(398)-C(260)	101.645
C(271)-P(398)-C(251)	102.261
C(260)-P(398)-C(251)	103.371
C(236)-P(397)-C(225)	104.683
C(236)-P(397)-C(216)	100.646
C(225)-P(397)-C(216)	105.293
C(82)-P(396)-C(71)	102.004
C(82)-P(396)-C(60)	102.122
C(71)-P(396)-C(60)	102.302
C(143)-P(395)-C(132)	103.468
C(143)-P(395)-C(123)	98.739
C(132)-P(395)-C(123)	105.171
C(178)-P(394)-C(167)	102.993
C(178)-P(394)-C(158)	103.892
C(167)-P(394)-C(158)	102.234
C(48)-P(393)-C(37)	101.665
C(48)-P(393)-C(28)	104.047
C(37)-P(393)-C(28)	104.388
C(340)-N(380)-C(290)	117.667
C(340)-N(380)-C(282)	121.094
C(290)-N(380)-C(282)	120.64
C(305)-N(379)-C(283)	117.417
C(305)-N(379)-C(282)	116.478
C(283)-N(379)-C(282)	123.581
C(247)-N(378)-C(197)	116.29
C(247)-N(378)-C(189)	122.544
C(197)-N(378)-C(189)	120.988
C(212)-N(377)-C(190)	119.035
C(212)-N(377)-C(189)	117.479
C(190)-N(377)-C(189)	121.685
C(154)-N(376)-C(104)	117.168
C(154)-N(376)-C(96)	121.748
C(104)-N(376)-C(96)	119.885
C(119)-N(375)-C(97)	115.942
C(119)-N(375)-C(96)	119.034
C(97)-N(375)-C(96)	123.939
C(83)-N(374)-C(9)	116.013
C(83)-N(374)-C(1)	122.731
C(9)-N(374)-C(1)	120.697

C(24)-N(373)-C(2)	116.979
C(24)-N(373)-C(1)	116.999
C(2)-N(373)-C(1)	123.483
H(372)-C(371)-C(369)	120.175
H(372)-C(371)-C(61)	120.307
C(369)-C(371)-C(61)	119.518
H(370)-C(369)-C(371)	120.13
H(370)-C(369)-C(367)	120.333
C(371)-C(369)-C(367)	119.536
H(368)-C(367)-C(369)	119.076
H(368)-C(367)-C(365)	119.204
C(369)-C(367)-C(365)	121.72
H(366)-C(365)-C(367)	119.909
H(366)-C(365)-C(364)	120.123
C(367)-C(365)-C(364)	119.968
P(400)-C(364)-C(365)	124.286
P(400)-C(364)-C(61)	117.226
C(365)-C(364)-C(61)	118.487
H(363)-C(362)-C(360)	119.411
H(363)-C(362)-C(353)	119.285
C(360)-C(362)-C(353)	121.304
H(361)-C(360)-C(362)	119.438
H(361)-C(360)-C(358)	119.569
C(362)-C(360)-C(358)	120.994
H(359)-C(358)-C(360)	120.146
H(359)-C(358)-C(356)	120.015
C(360)-C(358)-C(356)	119.839
H(357)-C(356)-C(358)	120.834
H(357)-C(356)-C(354)	120.823
C(358)-C(356)-C(354)	118.343
H(355)-C(354)-C(356)	118.215
H(355)-C(354)-C(353)	118.507
C(356)-C(354)-C(353)	123.278
P(400)-C(353)-C(362)	126.115
P(400)-C(353)-C(354)	117.551
C(362)-C(353)-C(354)	116.205
H(352)-C(351)-C(349)	119.21
H(352)-C(351)-C(343)	119.204
C(349)-C(351)-C(343)	121.586
H(350)-C(349)-C(351)	120.28
H(350)-C(349)-C(347)	120.378
C(351)-C(349)-C(347)	119.342
H(348)-C(347)-C(349)	120.04
H(348)-C(347)-C(345)	120.016
C(349)-C(347)-C(345)	119.944
H(346)-C(345)-C(347)	119.796
H(346)-C(345)-C(344)	119.59
C(347)-C(345)-C(344)	120.614
P(400)-C(344)-C(345)	121.208
P(400)-C(344)-C(343)	119.343
C(345)-C(344)-C(343)	119.348
C(351)-C(343)-C(344)	119.113
C(351)-C(343)-C(340)	118.22
C(344)-C(343)-C(340)	122.602
H(342)-C(340)-H(341)	107.657
H(342)-C(340)-C(343)	108.882
H(342)-C(340)-N(380)	108.697
H(341)-C(340)-C(343)	108.797
H(341)-C(340)-N(380)	108.731
C(343)-C(340)-N(380)	113.9
H(339)-C(338)-C(336)	119.792
H(339)-C(338)-C(329)	119.846
C(336)-C(338)-C(329)	120.362
H(337)-C(336)-C(338)	119.855
H(337)-C(336)-C(334)	119.898
C(338)-C(336)-C(334)	120.247
H(335)-C(334)-C(336)	119.737
H(335)-C(334)-C(332)	119.696
C(336)-C(334)-C(332)	120.568
H(333)-C(332)-C(334)	119.69
H(333)-C(332)-C(330)	119.629
C(334)-C(332)-C(330)	120.681
H(331)-C(330)-C(332)	120.345
H(331)-C(330)-C(329)	120.337
C(332)-C(330)-C(329)	119.318
P(399)-C(329)-C(338)	116.972
P(399)-C(329)-C(330)	124
C(338)-C(329)-C(330)	118.694
H(328)-C(327)-C(325)	119.837
H(328)-C(327)-C(318)	119.705
C(325)-C(327)-C(318)	120.458
H(326)-C(325)-C(327)	119.421
H(326)-C(325)-C(323)	119.433
C(327)-C(325)-C(323)	121.145
H(324)-C(323)-C(325)	119.975
H(324)-C(323)-C(321)	119.877
C(325)-C(323)-C(321)	120.148
H(322)-C(321)-C(323)	120.684
H(322)-C(321)-C(319)	120.505
C(323)-C(321)-C(319)	118.811
H(320)-C(319)-C(321)	119.002
H(320)-C(319)-C(318)	119.097
C(321)-C(319)-C(318)	121.901
P(399)-C(318)-C(327)	125.11
P(399)-C(318)-C(319)	117.368
C(327)-C(318)-C(319)	117.522

H(317)-C(316)-C(314)	119.515
H(317)-C(316)-C(308)	119.506
C(314)-C(316)-C(308)	120.979
H(315)-C(314)-C(316)	120.523
H(315)-C(314)-C(312)	120.493
C(316)-C(314)-C(312)	118.984
H(313)-C(312)-C(314)	119.961
H(313)-C(312)-C(310)	119.81
C(314)-C(312)-C(310)	120.23
H(311)-C(310)-C(312)	118.923
H(311)-C(310)-C(309)	118.775
C(312)-C(310)-C(309)	122.302
P(399)-C(309)-C(310)	123.219
P(399)-C(309)-C(308)	117.92
C(310)-C(309)-C(308)	118.522
C(309)-C(308)-C(316)	118.958
C(309)-C(308)-C(305)	118.629
C(316)-C(308)-C(305)	122.323
H(307)-C(305)-H(306)	107.431
H(307)-C(305)-C(308)	108.226
H(307)-C(305)-N(379)	108.09
H(306)-C(305)-C(308)	108.374
H(306)-C(305)-N(379)	108.155
C(308)-C(305)-N(379)	116.246
H(304)-C(301)-H(303)	109.58
H(304)-C(301)-H(302)	109.336
H(304)-C(301)-C(292)	109.493
H(303)-C(301)-H(302)	109.457
H(303)-C(301)-C(292)	109.588
H(302)-C(301)-C(292)	109.372
H(300)-C(297)-H(299)	109.429
H(300)-C(297)-H(298)	109.522
H(300)-C(297)-C(292)	109.442
H(299)-C(297)-H(298)	109.537
H(299)-C(297)-C(292)	109.423
H(298)-C(297)-C(292)	109.475
H(296)-C(293)-H(295)	109.531
H(296)-C(293)-H(294)	109.493
H(296)-C(293)-C(283)	109.366
H(295)-C(293)-H(294)	109.425
H(295)-C(293)-C(283)	109.456
H(294)-C(293)-C(283)	109.556
C(297)-C(292)-C(301)	108.561
C(297)-C(292)-C(290)	109.459
C(297)-C(292)-C(283)	110.729
C(301)-C(292)-C(290)	115.883
C(301)-C(292)-C(283)	114.853
C(290)-C(292)-C(283)	96.912
H(291)-C(290)-C(292)	110.653
H(291)-C(290)-N(380)	110.712
H(291)-C(290)-C(287)	110.652
C(292)-C(290)-N(380)	107.521
C(292)-C(290)-C(287)	106.195
N(380)-C(290)-C(287)	110.971
H(289)-C(287)-H(288)	108.545
H(289)-C(287)-C(290)	110.443
H(289)-C(287)-C(284)	110.419
H(288)-C(287)-C(290)	110.432
H(288)-C(287)-C(284)	110.376
C(290)-C(287)-C(284)	106.627
H(286)-C(284)-H(285)	109.41
H(286)-C(284)-C(287)	111.83
H(286)-C(284)-C(283)	111.856
H(285)-C(284)-C(287)	111.77
H(285)-C(284)-C(283)	111.713
C(287)-C(284)-C(283)	100.04
C(284)-C(283)-N(379)	105.966
C(284)-C(283)-C(292)	106.275
C(284)-C(283)-C(293)	114.09
N(379)-C(283)-C(292)	105.926
N(379)-C(283)-C(293)	108.841
C(292)-C(283)-C(293)	115.072
Au(404)-C(282)-N(380)	122.639
Au(404)-C(282)-N(379)	119.664
N(380)-C(282)-N(379)	116.546
H(281)-C(280)-C(278)	118.322
H(281)-C(280)-C(271)	118.444
C(278)-C(280)-C(271)	123.233
H(279)-C(278)-C(280)	120.46
H(279)-C(278)-C(276)	120.516
C(280)-C(278)-C(276)	119.024
H(277)-C(276)-C(278)	120.549
H(277)-C(276)-C(274)	120.404
C(278)-C(276)-C(274)	119.046
H(275)-C(274)-C(276)	119.261
H(275)-C(274)-C(272)	119.273
C(276)-C(274)-C(272)	121.466
H(273)-C(272)-C(274)	119.449
H(273)-C(272)-C(271)	119.307
C(274)-C(272)-C(271)	121.244
P(398)-C(271)-C(272)	125.347
P(398)-C(271)-C(280)	118.718
C(272)-C(271)-C(280)	115.864
H(270)-C(269)-C(267)	119.641
H(270)-C(269)-C(260)	119.737
C(267)-C(269)-C(260)	120.622

H(268)-C(267)-C(269)	119.611
H(268)-C(267)-C(265)	119.559
C(269)-C(267)-C(265)	120.829
H(266)-C(265)-C(267)	120.76
H(266)-C(265)-C(263)	120.781
C(267)-C(265)-C(263)	118.459
H(264)-C(263)-C(265)	119.569
H(264)-C(263)-C(261)	119.525
C(265)-C(263)-C(261)	120.906
H(262)-C(261)-C(263)	119.506
H(262)-C(261)-C(260)	119.294
C(263)-C(261)-C(260)	121.199
P(398)-C(260)-C(269)	125.579
P(398)-C(260)-C(261)	116.475
C(269)-C(260)-C(261)	117.928
H(259)-C(258)-C(256)	118.85
H(259)-C(258)-C(250)	118.962
C(256)-C(258)-C(250)	122.189
H(257)-C(256)-C(258)	120.603
H(257)-C(256)-C(254)	120.446
C(258)-C(256)-C(254)	118.951
H(255)-C(254)-C(256)	120.332
H(255)-C(254)-C(252)	120.419
C(256)-C(254)-C(252)	119.248
H(253)-C(252)-C(254)	118.772
H(253)-C(252)-C(251)	119.01
C(254)-C(252)-C(251)	122.218
P(398)-C(251)-C(252)	121.398
P(398)-C(251)-C(250)	119.816
C(252)-C(251)-C(250)	118.715
C(258)-C(250)-C(251)	118.507
C(258)-C(250)-C(247)	119.463
C(251)-C(250)-C(247)	122.023
H(249)-C(247)-H(248)	107.837
H(249)-C(247)-C(250)	109.017
H(249)-C(247)-N(378)	108.999
H(248)-C(247)-C(250)	108.878
H(248)-C(247)-N(378)	108.829
C(250)-C(247)-N(378)	113.146
H(246)-C(245)-C(243)	118.947
H(246)-C(245)-C(236)	119.143
C(243)-C(245)-C(236)	121.909
H(244)-C(243)-C(245)	121.376
H(244)-C(243)-C(241)	121.291
C(245)-C(243)-C(241)	117.333
H(242)-C(241)-C(243)	118.152
H(242)-C(241)-C(239)	118.261
C(243)-C(241)-C(239)	123.587
H(240)-C(239)-C(241)	120.954
H(240)-C(239)-C(237)	120.934
C(241)-C(239)-C(237)	118.111
H(238)-C(237)-C(239)	119.525
H(238)-C(237)-C(236)	119.621
C(239)-C(237)-C(236)	120.853
P(397)-C(236)-C(245)	124.134
P(397)-C(236)-C(237)	117.704
C(245)-C(236)-C(237)	118.136
H(235)-C(234)-C(232)	119.146
H(235)-C(234)-C(225)	119.248
C(232)-C(234)-C(225)	121.606
H(233)-C(232)-C(234)	119.67
H(233)-C(232)-C(230)	119.708
C(234)-C(232)-C(230)	120.621
H(231)-C(230)-C(232)	120.587
H(231)-C(230)-C(228)	120.524
C(232)-C(230)-C(228)	118.889
H(229)-C(228)-C(230)	119.397
H(229)-C(228)-C(226)	119.327
C(230)-C(228)-C(226)	121.276
H(227)-C(226)-C(228)	119.155
H(227)-C(226)-C(225)	119.117
C(228)-C(226)-C(225)	121.728
P(397)-C(225)-C(226)	125.114
P(397)-C(225)-C(234)	118.202
C(226)-C(225)-C(234)	115.863
H(224)-C(223)-C(221)	119.7
H(224)-C(223)-C(215)	119.627
C(221)-C(223)-C(215)	120.673
H(222)-C(221)-C(223)	119.783
H(222)-C(221)-C(219)	119.859
C(223)-C(221)-C(219)	120.358
H(220)-C(219)-C(221)	120.284
H(220)-C(219)-C(217)	120.259
C(221)-C(219)-C(217)	119.457
H(218)-C(217)-C(219)	119.524
H(218)-C(217)-C(216)	119.59
C(219)-C(217)-C(216)	120.885
P(397)-C(216)-C(217)	122.404
P(397)-C(216)-C(215)	116.829
C(217)-C(216)-C(215)	120.767
C(223)-C(215)-C(216)	117.838
C(223)-C(215)-C(212)	120.951
C(216)-C(215)-C(212)	120.854
H(214)-C(212)-H(213)	107.292
H(214)-C(212)-C(215)	107.99
H(214)-C(212)-N(377)	108.173

H(213)-C(212)-C(215)	108.032	C(199)-C(190)-C(200)	115.524
H(213)-C(212)-N(377)	108.074	C(199)-C(190)-N(377)	106.554
C(215)-C(212)-N(377)	116.907	C(200)-C(190)-N(377)	109.905
H(211)-C(208)-H(210)	109.445	Au(404)-C(189)-N(377)	118.484
H(211)-C(208)-H(209)	109.372	Au(404)-C(189)-N(378)	121.756
H(211)-C(208)-C(199)	109.518	N(377)-C(189)-N(378)	118.214
H(210)-C(208)-H(209)	109.514	H(188)-C(187)-C(185)	119.224
H(210)-C(208)-C(199)	109.455	H(188)-C(187)-C(178)	119.186
H(209)-C(208)-C(199)	109.523	C(185)-C(187)-C(178)	121.589
H(207)-C(204)-H(206)	109.374	H(186)-C(185)-C(187)	119.121
H(207)-C(204)-H(205)	109.352	H(186)-C(185)-C(183)	119.259
H(207)-C(204)-C(199)	109.522	C(187)-C(185)-C(183)	121.619
H(206)-C(204)-H(205)	109.527	H(184)-C(183)-C(185)	122.127
H(206)-C(204)-C(199)	109.531	H(184)-C(183)-C(181)	121.451
H(205)-C(204)-C(199)	109.521	C(185)-C(183)-C(181)	116.421
H(203)-C(200)-H(202)	109.619	H(182)-C(181)-C(183)	117.487
H(203)-C(200)-H(201)	109.469	H(182)-C(181)-C(179)	117.476
H(203)-C(200)-C(190)	109.431	C(183)-C(181)-C(179)	125.036
H(202)-C(200)-H(201)	109.5	H(180)-C(179)-C(181)	120.46
H(202)-C(200)-C(190)	109.334	H(180)-C(179)-C(178)	120.616
H(201)-C(200)-C(190)	109.475	C(181)-C(179)-C(178)	118.924
C(208)-C(199)-C(204)	104.995	P(394)-C(178)-C(179)	120.818
C(208)-C(199)-C(197)	115.955	P(394)-C(178)-C(187)	121.602
C(208)-C(199)-C(190)	114.95	C(179)-C(178)-C(187)	116.362
C(204)-C(199)-C(197)	109.182	H(177)-C(176)-C(174)	119.322
C(204)-C(199)-C(190)	113.941	H(177)-C(176)-C(167)	119.334
C(197)-C(199)-C(190)	98.008	C(174)-C(176)-C(167)	121.344
H(198)-C(197)-C(199)	111.213	H(175)-C(174)-C(176)	120.156
H(198)-C(197)-N(378)	111.165	H(175)-C(174)-C(172)	120.196
H(198)-C(197)-C(194)	111.226	C(176)-C(174)-C(172)	119.648
C(199)-C(197)-N(378)	107.591	H(173)-C(172)-C(174)	120.239
C(199)-C(197)-C(194)	104.729	H(173)-C(172)-C(170)	120.245
N(378)-C(197)-C(194)	110.678	C(174)-C(172)-C(170)	119.516
H(196)-C(194)-H(195)	108.586	H(171)-C(170)-C(172)	119.527
H(196)-C(194)-C(197)	110.51	H(171)-C(170)-C(168)	119.428
H(196)-C(194)-C(191)	110.558	C(172)-C(170)-C(168)	121.045
H(195)-C(194)-C(197)	110.444	H(169)-C(168)-C(170)	120.206
H(195)-C(194)-C(191)	110.423	H(169)-C(168)-C(167)	120.086
C(197)-C(194)-C(191)	106.319	C(170)-C(168)-C(167)	119.707
H(193)-C(191)-H(192)	109.144	P(394)-C(167)-C(168)	115.93
H(193)-C(191)-C(194)	111.218	P(394)-C(167)-C(176)	125.449
H(193)-C(191)-C(190)	111.231	C(168)-C(167)-C(176)	118.617
H(192)-C(191)-C(194)	111.306	H(166)-C(165)-C(163)	118.189
H(192)-C(191)-C(190)	111.352	H(166)-C(165)-C(157)	118.334
C(194)-C(191)-C(190)	102.49	C(163)-C(165)-C(157)	123.477
C(191)-C(190)-C(199)	103.985	H(164)-C(163)-C(165)	120.789
C(191)-C(190)-C(200)	114.022	H(164)-C(163)-C(161)	120.645
C(191)-C(190)-N(377)	106.147	C(165)-C(163)-C(161)	118.566

H(162)-C(161)-C(163)	120.814
H(162)-C(161)-C(159)	120.934
C(163)-C(161)-C(159)	118.251
H(160)-C(159)-C(161)	118.467
H(160)-C(159)-C(158)	118.266
C(161)-C(159)-C(158)	123.267
P(394)-C(158)-C(159)	123.833
P(394)-C(158)-C(157)	118.14
C(159)-C(158)-C(157)	117.985
C(158)-C(157)-C(165)	118.428
C(158)-C(157)-C(154)	120.786
C(165)-C(157)-C(154)	120.786
H(156)-C(154)-H(155)	107.78
H(156)-C(154)-C(157)	108.959
H(156)-C(154)-N(376)	108.926
H(155)-C(154)-C(157)	108.844
H(155)-C(154)-N(376)	108.701
C(157)-C(154)-N(376)	113.48
H(153)-C(152)-C(150)	118.828
H(153)-C(152)-C(143)	118.765
C(150)-C(152)-C(143)	122.407
H(151)-C(150)-C(152)	120.105
H(151)-C(150)-C(148)	119.941
C(152)-C(150)-C(148)	119.954
H(149)-C(148)-C(150)	119.185
H(149)-C(148)-C(146)	119.146
C(150)-C(148)-C(146)	121.669
H(147)-C(146)-C(148)	120.85
H(147)-C(146)-C(144)	120.924
C(148)-C(146)-C(144)	118.225
H(145)-C(144)-C(146)	119.816
H(145)-C(144)-C(143)	119.719
C(146)-C(144)-C(143)	120.464
P(395)-C(143)-C(144)	117.567
P(395)-C(143)-C(152)	125.085
C(144)-C(143)-C(152)	117.258
H(142)-C(141)-C(139)	119.839
H(142)-C(141)-C(132)	119.77
C(139)-C(141)-C(132)	120.39
H(140)-C(139)-C(141)	120.989
H(140)-C(139)-C(137)	120.295
C(141)-C(139)-C(137)	118.704
H(138)-C(137)-C(139)	118.945
H(138)-C(137)-C(135)	118.546
C(139)-C(137)-C(135)	122.507
H(136)-C(135)-C(137)	121.258
H(136)-C(135)-C(133)	121.163
C(137)-C(135)-C(133)	117.58
H(134)-C(133)-C(135)	118.88
H(134)-C(133)-C(132)	118.941
C(135)-C(133)-C(132)	122.178
P(395)-C(132)-C(133)	116.771
P(395)-C(132)-C(141)	124.518
C(133)-C(132)-C(141)	118.56
H(131)-C(130)-C(128)	119.685
H(131)-C(130)-C(122)	119.671
C(128)-C(130)-C(122)	120.643
H(129)-C(128)-C(130)	120.192
H(129)-C(128)-C(126)	120.22
C(130)-C(128)-C(126)	119.588
H(127)-C(126)-C(128)	119.41
H(127)-C(126)-C(124)	119.394
C(128)-C(126)-C(124)	121.196
H(125)-C(124)-C(126)	119.284
H(125)-C(124)-C(123)	119.217
C(126)-C(124)-C(123)	121.499
P(395)-C(123)-C(124)	124.507
P(395)-C(123)-C(122)	118.365
C(124)-C(123)-C(122)	117.122
C(123)-C(122)-C(130)	119.911
C(123)-C(122)-C(119)	120.218
C(130)-C(122)-C(119)	119.744
H(121)-C(119)-H(120)	106.932
H(121)-C(119)-C(122)	107.737
H(121)-C(119)-N(375)	107.771
H(120)-C(119)-C(122)	107.788
H(120)-C(119)-N(375)	107.781
C(122)-C(119)-N(375)	118.318
H(118)-C(115)-H(117)	109.524
H(118)-C(115)-H(116)	109.505
H(118)-C(115)-C(106)	109.398
H(117)-C(115)-H(116)	109.54
H(117)-C(115)-C(106)	109.47
H(116)-C(115)-C(106)	109.39
H(114)-C(111)-H(113)	109.442
H(114)-C(111)-H(112)	109.532
H(114)-C(111)-C(106)	109.493
H(113)-C(111)-H(112)	109.425
H(113)-C(111)-C(106)	109.418
H(112)-C(111)-C(106)	109.517
H(110)-C(107)-H(109)	109.288
H(110)-C(107)-H(108)	109.512
H(110)-C(107)-C(97)	109.346
H(109)-C(107)-H(108)	109.549
H(109)-C(107)-C(97)	109.498
H(108)-C(107)-C(97)	109.633

C(115)-C(106)-C(111)	109.604
C(115)-C(106)-C(104)	108.602
C(115)-C(106)-C(97)	109.682
C(111)-C(106)-C(104)	114.841
C(111)-C(106)-C(97)	115.801
C(104)-C(106)-C(97)	97.649
H(105)-C(104)-C(106)	111.11
H(105)-C(104)-N(376)	111.196
H(105)-C(104)-C(101)	111.139
C(106)-C(104)-N(376)	107.445
C(106)-C(104)-C(101)	105.448
N(376)-C(104)-C(101)	110.291
H(103)-C(101)-H(102)	108.796
H(103)-C(101)-C(104)	110.693
H(103)-C(101)-C(98)	110.905
H(102)-C(101)-C(104)	110.776
H(102)-C(101)-C(98)	110.834
C(104)-C(101)-C(98)	104.815
H(100)-C(98)-H(99)	108.829
H(100)-C(98)-C(101)	110.836
H(100)-C(98)-C(97)	110.74
H(99)-C(98)-C(101)	110.703
H(99)-C(98)-C(97)	110.66
C(101)-C(98)-C(97)	105.052
C(106)-C(97)-N(375)	105.064
C(106)-C(97)-C(98)	103.138
C(106)-C(97)-C(107)	111.851
N(375)-C(97)-C(98)	106.824
N(375)-C(97)-C(107)	112.163
C(98)-C(97)-C(107)	116.793
Au(403)-C(96)-N(376)	123.37
Au(403)-C(96)-N(375)	118.602
N(376)-C(96)-N(375)	117.705
H(95)-C(94)-C(92)	118.614
H(95)-C(94)-C(82)	118.757
C(92)-C(94)-C(82)	122.628
H(93)-C(92)-C(94)	120.623
H(93)-C(92)-C(90)	120.735
C(94)-C(92)-C(90)	118.642
H(91)-C(90)-C(92)	119.255
H(91)-C(90)-C(88)	119.34
C(92)-C(90)-C(88)	121.405
H(89)-C(88)-C(90)	120.518
H(89)-C(88)-C(86)	120.573
C(90)-C(88)-C(86)	118.909
H(87)-C(86)-C(88)	119.312
H(87)-C(86)-C(82)	119.304
C(88)-C(86)-C(82)	121.384
H(85)-C(83)-H(84)	107.817
H(85)-C(83)-N(374)	109.122
H(85)-C(83)-C(59)	109.053
H(84)-C(83)-N(374)	109.032
H(84)-C(83)-C(59)	109.199
N(374)-C(83)-C(59)	112.506
P(396)-C(82)-C(86)	124.081
P(396)-C(82)-C(94)	118.867
C(86)-C(82)-C(94)	117.031
H(81)-C(80)-C(78)	118.96
H(81)-C(80)-C(71)	118.725
C(78)-C(80)-C(71)	122.315
H(79)-C(78)-C(80)	120.725
H(79)-C(78)-C(76)	120.857
C(80)-C(78)-C(76)	118.418
H(77)-C(76)-C(78)	119.968
H(77)-C(76)-C(74)	120.04
C(78)-C(76)-C(74)	119.992
H(75)-C(74)-C(76)	119.583
H(75)-C(74)-C(72)	119.781
C(76)-C(74)-C(72)	120.636
H(73)-C(72)-C(74)	119.697
H(73)-C(72)-C(71)	119.768
C(74)-C(72)-C(71)	120.535
P(396)-C(71)-C(72)	115.642
P(396)-C(71)-C(80)	126.264
C(72)-C(71)-C(80)	118.043
H(70)-C(69)-C(67)	120.34
H(70)-C(69)-C(59)	120.55
C(67)-C(69)-C(59)	119.11
H(68)-C(67)-C(69)	119.31
H(68)-C(67)-C(65)	119.306
C(69)-C(67)-C(65)	121.383
H(66)-C(65)-C(67)	120.927
H(66)-C(65)-C(63)	121.002
C(67)-C(65)-C(63)	118.07
H(64)-C(63)-C(65)	118.33
H(64)-C(63)-C(60)	118.449
C(65)-C(63)-C(60)	123.22
H(62)-C(61)-C(371)	119.605
H(62)-C(61)-C(364)	119.73
C(371)-C(61)-C(364)	120.665
P(396)-C(60)-C(63)	122.793
P(396)-C(60)-C(59)	119.171
C(63)-C(60)-C(59)	117.892
C(83)-C(59)-C(69)	116.913
C(83)-C(59)-C(60)	122.552
C(69)-C(59)-C(60)	120.319

H(58)-C(57)-C(55)	119.627
H(58)-C(57)-C(48)	119.472
C(55)-C(57)-C(48)	120.901
H(56)-C(55)-C(57)	120.539
H(56)-C(55)-C(53)	120.613
C(57)-C(55)-C(53)	118.847
H(54)-C(53)-C(55)	119.35
H(54)-C(53)-C(51)	119.44
C(55)-C(53)-C(51)	121.21
H(52)-C(51)-C(53)	120.549
H(52)-C(51)-C(49)	120.591
C(53)-C(51)-C(49)	118.86
H(50)-C(49)-C(51)	119.748
H(50)-C(49)-C(48)	119.605
C(51)-C(49)-C(48)	120.647
P(393)-C(48)-C(49)	116.53
P(393)-C(48)-C(57)	123.735
C(49)-C(48)-C(57)	119.522
H(47)-C(46)-C(44)	119.402
H(47)-C(46)-C(37)	119.382
C(44)-C(46)-C(37)	121.217
H(45)-C(44)-C(46)	120.093
H(45)-C(44)-C(42)	120.118
C(46)-C(44)-C(42)	119.789
H(43)-C(42)-C(44)	120.013
H(43)-C(42)-C(40)	119.8
C(44)-C(42)-C(40)	120.187
H(41)-C(40)-C(42)	119.853
H(41)-C(40)-C(38)	119.631
C(42)-C(40)-C(38)	120.515
H(39)-C(38)-C(40)	119.738
H(39)-C(38)-C(37)	119.488
C(40)-C(38)-C(37)	120.774
P(393)-C(37)-C(46)	118.505
P(393)-C(37)-C(38)	123.975
C(46)-C(37)-C(38)	117.499
H(36)-C(35)-C(33)	119.497
H(36)-C(35)-C(27)	119.455
C(33)-C(35)-C(27)	121.049
H(34)-C(33)-C(35)	120.566
H(34)-C(33)-C(31)	120.562
C(35)-C(33)-C(31)	118.872
H(32)-C(31)-C(33)	119.507
H(32)-C(31)-C(29)	119.472
C(33)-C(31)-C(29)	121.021
H(30)-C(29)-C(31)	119.686
H(30)-C(29)-C(28)	120.025
C(31)-C(29)-C(28)	120.289
P(393)-C(28)-C(29)	122.472
P(393)-C(28)-C(27)	117.597
C(29)-C(28)-C(27)	119.655
C(28)-C(27)-C(35)	119.014
C(28)-C(27)-C(24)	118.857
C(35)-C(27)-C(24)	122.018
H(26)-C(24)-H(25)	107.112
H(26)-C(24)-C(27)	107.783
H(26)-C(24)-N(373)	107.862
H(25)-C(24)-C(27)	107.832
H(25)-C(24)-N(373)	107.805
C(27)-C(24)-N(373)	117.981
H(23)-C(20)-H(22)	109.434
H(23)-C(20)-H(21)	109.504
H(23)-C(20)-C(11)	109.483
H(22)-C(20)-H(21)	109.46
H(22)-C(20)-C(11)	109.498
H(21)-C(20)-C(11)	109.447
H(19)-C(16)-H(18)	109.474
H(19)-C(16)-H(17)	109.378
H(19)-C(16)-C(11)	109.458
H(18)-C(16)-H(17)	109.596
H(18)-C(16)-C(11)	109.516
H(17)-C(16)-C(11)	109.407
H(15)-C(12)-H(14)	109.549
H(15)-C(12)-H(13)	109.413
H(15)-C(12)-C(2)	109.457
H(14)-C(12)-H(13)	109.442
H(14)-C(12)-C(2)	109.465
H(13)-C(12)-C(2)	109.501
C(16)-C(11)-C(20)	107.827
C(16)-C(11)-C(9)	109.176
C(16)-C(11)-C(2)	111.976
C(20)-C(11)-C(9)	114.338
C(20)-C(11)-C(2)	115.514
C(9)-C(11)-C(2)	97.729
H(10)-C(9)-C(11)	111.181
H(10)-C(9)-N(374)	111.214
H(10)-C(9)-C(6)	111.356
C(11)-C(9)-N(374)	107.651
C(11)-C(9)-C(6)	104.805
N(374)-C(9)-C(6)	110.39
H(8)-C(6)-H(7)	108.821
H(8)-C(6)-C(9)	110.88
H(8)-C(6)-C(3)	110.869
H(7)-C(6)-C(9)	110.818
H(7)-C(6)-C(3)	110.859
C(9)-C(6)-C(3)	104.567

H(5)-C(3)-H(4)	108.975
H(5)-C(3)-C(6)	110.998
H(5)-C(3)-C(2)	110.938
H(4)-C(3)-C(6)	110.956
H(4)-C(3)-C(2)	110.91
C(6)-C(3)-C(2)	104.016
C(11)-C(2)-C(3)	103.985
C(11)-C(2)-C(12)	113.59
C(11)-C(2)-N(373)	106.296
C(3)-C(2)-C(12)	113.996
C(3)-C(2)-N(373)	107.27
C(12)-C(2)-N(373)	111.097
Au(403)-C(1)-N(373)	118.522
Au(403)-C(1)-N(374)	122.751
N(373)-C(1)-N(374)	117.244

***Bis*((1*R*,5*S*)-2,4-bis(pyridine-2-ylmethyl)-1,8,8-trimethyl-2,4-diazabicyclo[3.2.1]octan-3-ylidene)) gold(I) tetrafluoroborate**

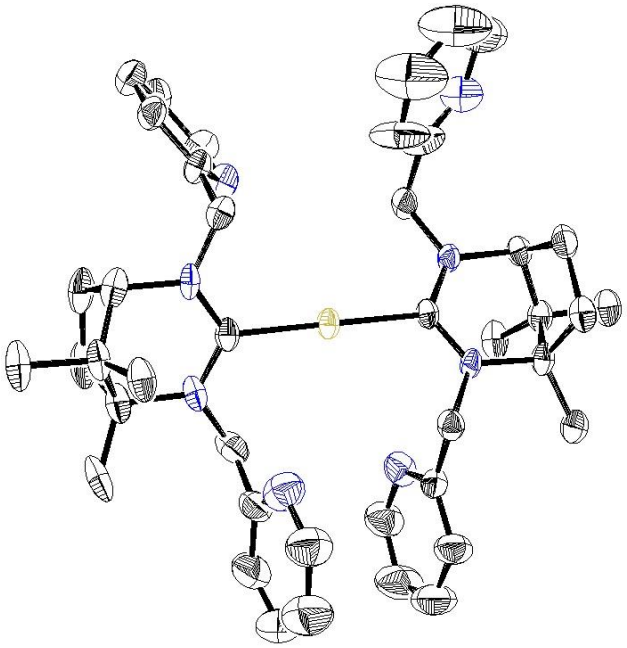

Figure 4: Molecular structure of bis(dipyridyl carbene) gold complex, pdn1505

Identification code	**pdn1505**	
Empirical formula	$C_{45}H_{58}AuBF_4N_8O$	
Formula weight	1743.53	
Temperature	298(2) K	
Wavelength	1.54184 Å	
Crystal system	monoclinic	
Space group	$P2_1$	
Unit cell dimensions	a = 16.7838(2) Å	$\alpha = 90$ °
	b = 13.04800(10) Å	$\beta = 91.259$ °
	c = 20.4063(2) Å	$\gamma = 90$ °
Volume	4467.8 Å^3	
Z	4	
Density (calculated)	1.503 Mg / m^3	
Absorption coefficient	6.688 mm^{-1}	
F(000)	2048	
Crystal size	0.414 × 0.233 × 0.141 mm^3	
Θ Range for data collection	3.373 – 74.030°	
Index ranges	$-14 \leq \eta \leq 20$, $-16 \leq \kappa \leq 16$, $-25 \leq \lambda \leq 25$	
Reflections collected	17626	
Independent reflections	17021	
Absorption correction	Semi–empirical from equivalents	
Max. and min. transmission	0.920 and 0.678	
Refinement method	Full-matrix least-squares on F^2	
Data / restraints / parameters	17626 / 2016 / 1353	
Goodness-of-fit on F^2	1.041	
Final *R* indices [$F^2 > 2\sigma(F^2)$]	*R1* = 0.0347, *wR2* = 0.0895	

***R* indices (all data)**	*R1* = 0.0367, *wR2* = 0.0917
Extinction coefficient	n/a

Table 10:Bond lengths (Å)

Atom1	Atom2	Length
C1	C2	1.31(2)
C1	C6	1.49(1)
C1	N1	1.37(2)
C2	H2	0.93
C2	C3	1.32(2)
C3	H3	0.93
C3	C4	1.37(3)
C4	H4	0.93
C4	C5	1.38(3)
C5	H5	0.93
C5	N1	1.46(2)
C6	H6A	0.969
C6	H6B	0.97
C6	N2	1.47(1)
C7	N2	1.33(1)
C7	N3	1.33(1)
C7	Au1	2.062(8)
C8	H8	0.98
C8	C9	1.52(1)
C8	C12	1.53(1)
C8	N2	1.50(1)
C9	H9A	0.97
C9	H9B	0.97
C9	C10	1.54(1)
C10	H10A	0.97
C10	H10B	0.97
C10	C11	1.54(1)
C11	C12	1.54(1)
C11	C13	1.52(1)
C11	N3	1.53(1)
C12	C14	1.51(1)
C12	C15	1.54(1)
C13	H13A	0.96
C13	H13B	0.96
C13	H13C	0.96
C14	H14A	0.96
C14	H14B	0.96
C14	H14C	0.959
C15	H15A	0.96
C15	H15B	0.96
C15	H15C	0.96
C16	H16A	0.97
C16	H16B	0.97
C16	C17	1.51(1)
C16	N3	1.46(1)
C17	C18	1.39(1)
C17	N4	1.33(1)
C18	H18	0.93
C18	C19	1.39(2)
C19	H19	0.93
C19	C20	1.37(2)
C20	H20	0.93
C20	C21	1.35(2)
C21	H21	0.93
C21	N4	1.35(1)
C22	H22	0.93
C22	C23	1.34(2)
C22	N5	1.34(2)
C23	H23	0.93
C23	C24	1.37(3)
C24	H24	0.93
C24	C25	1.43(2)
C25	H25	0.93
C25	C26	1.38(2)
C26	C27	1.51(1)
C26	N5	1.34(1)
C27	H27A	0.97
C27	H27B	0.97
C27	N6	1.46(1)
C28	N6	1.35(1)
C28	N7	1.34(1)
C28	Au1	2.051(8)
C29	C30	1.55(2)
C29	C33	1.55(1)
C29	C34	1.51(1)
C29	N6	1.53(1)
C30	H30A	0.97
C30	H30B	0.97
C30	C31	1.53(1)
C31	H31A	0.97
C31	H31B	0.97
C31	C32	1.53(1)
C32	H32	0.981
C32	C33	1.52(1)
C32	N7	1.47(1)
C33	C35	1.54(1)

C33	C36	1.54(1)
C34	H34A	0.96
C34	H34B	0.96
C34	H34C	0.96
C35	H35A	0.959
C35	H35B	0.96
C35	H35C	0.96
C36	H36A	0.96
C36	H36B	0.96
C36	H36C	0.96
C37	H37A	0.971
C37	H37B	0.97
C37	C38	1.50(1)
C37	N7	1.47(1)
C38	C39	1.39(1)
C38	N8	1.34(1)
C39	H39	0.93
C39	C40	1.38(1)
C40	H40	0.93
C40	C41	1.40(1)
C41	H41	0.93
C41	C42	1.40(1)
C42	H42	0.929
C42	N8	1.34(1)
N9	C43	1.390(9)
N9	C47	1.391(9)
C43	H43	0.929
C43	C44	1.390(9)
C44	H44	0.93
C44	C45	1.390(9)
C45	H45	0.93
C45	C46	1.390(9)
C46	H46	0.929
C46	C47	1.390(9)
C47	C48	1.50(1)
C48	H48A	0.97
C48	H48B	0.97
C48	N10	1.50(1)
C49	N10	1.35(3)
C49	N11	1.34(3)
C49	Au2	2.06(2)
C50	C51	1.54(2)
C50	C54	1.55(2)
C50	C55	1.52(2)
C50	N10	1.48(2)
C51	H51A	0.97
C51	H51B	0.97
C51	C52	1.56(2)
C52	H52A	0.97
C52	H52B	0.97
C52	C53	1.54(2)
C53	H53	0.98
C53	C54	1.53(2)
C53	N11	1.46(2)
C54	C56	1.56(2)
C54	C57	1.54(2)
C55	H55A	0.96
C55	H55B	0.96
C55	H55C	0.96
C56	H56A	0.96
C56	H56B	0.96
C56	H56C	0.96
C57	H57A	0.96
C57	H57B	0.96
C57	H57C	0.96
C58	H58A	0.97
C58	H58B	0.97
C58	N11	1.38(2)
C58	C59	1.48(2)
N12	C59	1.39(1)
N12	C63	1.39(1)
C59	C60	1.39(1)
C60	H60	0.93
C60	C61	1.39(1)
C61	H61	0.929
C61	C62	1.39(1)
C62	H62	0.93
C62	C63	1.39(1)
C63	H63	0.93
C64	H64	0.93
C64	C65	1.35(2)
C64	N13	1.34(1)
C65	H65	0.93
C65	C66	1.40(2)
C66	H66	0.93
C66	C67	1.37(2)
C67	H67	0.93
C67	C68	1.39(1)
C68	C69	1.52(1)
C68	N13	1.35(1)
C69	H69A	0.969
C69	H69B	0.97
C69	N14	1.47(1)
C70	N14	1.35(2)
C70	N15	1.36(2)
C70	Au2	2.01(2)

C71	C72	1.55(2)
C71	C75	1.55(2)
C71	C76	1.54(2)
C71	N14	1.50(1)
C72	H72A	0.97
C72	H72B	0.97
C72	C73	1.54(2)
C73	H73A	0.97
C73	H73B	0.97
C73	C74	1.54(2)
C74	H74	0.98
C74	C75	1.53(2)
C74	N15	1.51(1)
C75	C77	1.54(2)
C75	C78	1.52(2)
C76	H76A	0.96
C76	H76B	0.96
C76	H76C	0.96
C77	H77A	0.96
C77	H77B	0.96
C77	H77C	0.96
C78	H78A	0.96
C78	H78B	0.96
C78	H78C	0.96
C79	H79A	0.97
C79	H79B	0.97
C79	N15	1.42(1)
C79	C80	1.39(2)
C80	C81	1.39(1)
C80	N16	1.39(1)
C81	H81	0.931
C81	C82	1.39(1)
C82	H82	0.932
C82	C83	1.39(1)
C83	H83	0.93
C83	C84	1.39(1)
C84	H84	0.93
C84	N16	1.39(1)
F1	B1	1.32(2)
F2	B1	1.28(2)
F3	B1	1.35(2)
F4	B1	1.31(2)
F5	B2	1.32(2)
F6	B2	1.35(2)
F7	B2	1.36(2)
F8	B2	1.34(2)
O1	C85	1.22(4)
C85	C86	1.49(3)
C85	C87	1.39(4)
C86	H86A	0.96
C86	H86B	0.96
C86	H86C	0.96
C87	H87A	0.96
C87	H87B	0.96
C87	H87C	0.97
O2	C88	1.23(3)
C88	C89	1.49(3)
C88	C90	1.49(3)
C89	H89A	0.96
C89	H89B	0.96
C89	H89C	0.96
C90	H90A	0.96
C90	H90B	0.96
C90	H90C	0.96

Table 11: Bond angles (°)

H(325)-C(322)-H(324)	108.95
H(325)-C(322)-H(323)	109.449
H(325)-C(322)-C(317)	109.926
H(324)-C(322)-H(323)	109.015
H(324)-C(322)-C(317)	109.608
H(323)-C(322)-C(317)	109.871
H(321)-C(318)-H(320)	109.281
H(321)-C(318)-H(319)	109.409
H(321)-C(318)-C(317)	109.375
H(320)-C(318)-H(319)	109.606

H(320)-C(318)-C(317)	109.622
H(319)-C(318)-C(317)	109.533
C(322)-C(317)-C(318)	109.199
C(322)-C(317)-O(316)	119.718
C(318)-C(317)-O(316)	128.472
H(315)-C(312)-H(314)	108.918
H(315)-C(312)-H(313)	109.212
H(315)-C(312)-C(307)	109.444
H(314)-C(312)-H(313)	109.571
H(314)-C(312)-C(307)	109.752
H(313)-C(312)-C(307)	109.924
H(311)-C(308)-H(310)	109.762
H(311)-C(308)-H(309)	109.286
H(311)-C(308)-C(307)	109.594
H(310)-C(308)-H(309)	109.372
H(310)-C(308)-C(307)	109.554
H(309)-C(308)-C(307)	109.257
C(308)-C(307)-C(312)	127.313
C(308)-C(307)-O(306)	104.038
C(312)-C(307)-O(306)	128.649
F(301)-B(305)-F(300)	104.358
F(301)-B(305)-F(299)	103.518
F(301)-B(305)-F(298)	103.993
F(300)-B(305)-F(299)	118.283
F(300)-B(305)-F(298)	114.362
F(299)-B(305)-F(298)	110.423
F(297)-B(304)-F(296)	115.691
F(297)-B(304)-F(295)	112.607
F(297)-B(304)-F(294)	106.301
F(296)-B(304)-F(295)	114.234
F(296)-B(304)-F(294)	102.696
F(295)-B(304)-F(294)	103.637
H(252)-C(251)-C(253)	120.037
H(252)-C(251)-C(249)	119.966
C(253)-C(251)-C(249)	119.997
H(250)-C(249)-C(251)	119.983
H(250)-C(249)-C(247)	120.053
C(251)-C(249)-C(247)	119.964
H(248)-C(247)-C(249)	119.957
H(248)-C(247)-N(256)	120.045
C(249)-C(247)-N(256)	119.998
C(255)-N(256)-C(247)	120.023
H(254)-C(253)-C(255)	120.14
H(254)-C(253)-C(251)	119.889
C(255)-C(253)-C(251)	119.971
C(257)-C(255)-N(256)	119.958
C(257)-C(255)-C(253)	119.995
N(256)-C(255)-C(253)	120.048

H(259)-C(257)-H(258)	111.192
H(259)-C(257)-N(283)	113.598
H(259)-C(257)-C(255)	113.25
H(258)-C(257)-N(283)	113.638
H(258)-C(257)-C(255)	113.124
N(283)-C(257)-C(255)	90.667
H(282)-C(279)-H(281)	109.821
H(282)-C(279)-H(280)	109.792
H(282)-C(279)-C(270)	109.755
H(281)-C(279)-H(280)	108.937
H(281)-C(279)-C(270)	109.328
H(280)-C(279)-C(270)	109.189
H(278)-C(275)-H(277)	109.568
H(278)-C(275)-H(276)	109.521
H(278)-C(275)-C(270)	109.481
H(277)-C(275)-H(276)	109.364
H(277)-C(275)-C(270)	109.487
H(276)-C(275)-C(270)	109.407
H(274)-C(271)-H(273)	109.586
H(274)-C(271)-H(272)	109.481
H(274)-C(271)-C(261)	109.334
H(273)-C(271)-H(272)	109.579
H(273)-C(271)-C(261)	109.449
H(272)-C(271)-C(261)	109.398
H(269)-C(268)-C(270)	112.284
H(269)-C(268)-C(265)	112.202
C(270)-C(268)-C(265)	105.564
H(267)-C(265)-H(266)	109.386
H(267)-C(265)-C(268)	111.344
H(267)-C(265)-C(262)	111.373
H(266)-C(265)-C(268)	111.613
H(266)-C(265)-C(262)	111.544
C(268)-C(265)-C(262)	101.418
C(275)-C(270)-C(279)	107.193
C(275)-C(270)-C(268)	108.844
C(275)-C(270)-C(261)	111.661
C(279)-C(270)-C(268)	115.964
C(279)-C(270)-C(261)	115.975
C(268)-C(270)-C(261)	96.921
H(264)-C(262)-H(263)	108.836
H(264)-C(262)-C(265)	110.86
H(264)-C(262)-C(261)	110.889
H(263)-C(262)-C(265)	110.908
H(263)-C(262)-C(261)	110.781
C(265)-C(262)-C(261)	104.538
C(271)-C(261)-C(270)	114.229
C(271)-C(261)-C(262)	116.755
C(271)-C(261)-N(283)	104.971

C(270)-C(261)-C(262)	109.581
C(270)-C(261)-N(283)	105.518
C(262)-C(261)-N(283)	104.564
C(261)-N(283)-C(260)	115.488
C(261)-N(283)-C(257)	106.829
C(260)-N(283)-C(257)	136.86
Au(303)-C(260)-N(283)	123.912
H(245)-C(244)-N(246)	120.058
H(245)-C(244)-C(242)	119.936
N(246)-C(244)-C(242)	120.006
H(243)-C(242)-C(244)	119.946
H(243)-C(242)-C(240)	120.111
C(244)-C(242)-C(240)	119.943
H(241)-C(240)-C(242)	119.922
H(241)-C(240)-C(238)	119.975
C(242)-C(240)-C(238)	120.102
C(244)-N(246)-C(237)	119.88
H(239)-C(238)-C(240)	120.052
H(239)-C(238)-C(237)	120.016
C(240)-C(238)-C(237)	119.931
C(238)-C(237)-N(246)	120.138
C(238)-C(237)-C(232)	121.444
N(246)-C(237)-C(232)	118.274
H(234)-C(232)-H(233)	108.51
H(234)-C(232)-N(236)	110.313
H(234)-C(232)-C(237)	110.195
H(233)-C(232)-N(236)	110.289
H(233)-C(232)-C(237)	110.273
N(236)-C(232)-C(237)	107.263
H(231)-C(228)-H(230)	109.473
H(231)-C(228)-H(229)	109.44
H(231)-C(228)-C(219)	109.402
H(230)-C(228)-H(229)	109.513
H(230)-C(228)-C(219)	109.484
H(229)-C(228)-C(219)	109.514
H(227)-C(224)-H(226)	109.438
H(227)-C(224)-H(225)	109.63
H(227)-C(224)-C(219)	109.411
H(226)-C(224)-H(225)	109.497
H(226)-C(224)-C(219)	109.347
H(225)-C(224)-C(219)	109.503
H(202)-C(201)-C(203)	120.87
H(202)-C(201)-C(199)	120.73
C(203)-C(201)-C(199)	118.4
H(200)-C(199)-C(201)	120.779
H(200)-C(199)-C(197)	120.713
C(201)-C(199)-C(197)	118.507
H(198)-C(197)-C(199)	117.647

H(198)-C(197)-N(293)	117.675
C(199)-C(197)-N(293)	124.678
C(205)-N(293)-C(197)	116.433
H(204)-C(203)-C(205)	120.42
H(204)-C(203)-C(201)	120.311
C(205)-C(203)-C(201)	119.269
C(206)-C(205)-N(293)	117.211
C(206)-C(205)-C(203)	119.873
N(293)-C(205)-C(203)	122.689
H(208)-C(206)-H(207)	107.482
H(208)-C(206)-N(235)	108.581
H(208)-C(206)-C(205)	108.702
H(207)-C(206)-N(235)	108.549
H(207)-C(206)-C(205)	108.753
N(235)-C(206)-C(205)	114.551
H(186)-C(185)-C(183)	119.982
H(186)-C(185)-N(177)	119.929
C(183)-C(185)-N(177)	120.089
H(184)-C(183)-C(185)	120.044
H(184)-C(183)-C(181)	120.042
C(185)-C(183)-C(181)	119.913
H(182)-C(181)-C(183)	119.994
H(182)-C(181)-C(179)	119.908
C(183)-C(181)-C(179)	120.098
H(180)-C(179)-C(181)	120.04
H(180)-C(179)-C(178)	120.007
C(181)-C(179)-C(178)	119.953
C(185)-N(177)-C(178)	119.954
C(179)-C(178)-N(177)	119.992
C(179)-C(178)-C(172)	109.654
N(177)-C(178)-C(172)	130.352
H(174)-C(172)-H(173)	109.149
H(174)-C(172)-C(178)	111.466
H(174)-C(172)-N(176)	111.504
H(173)-C(172)-C(178)	111.466
H(173)-C(172)-N(176)	111.527
C(178)-C(172)-N(176)	101.6
H(171)-C(168)-H(170)	110.123
H(171)-C(168)-H(169)	108.899
H(171)-C(168)-C(159)	109.216
H(170)-C(168)-H(169)	109.826
H(170)-C(168)-C(159)	109.779
H(169)-C(168)-C(159)	108.973
H(167)-C(164)-H(166)	109.831
H(167)-C(164)-H(165)	109.602
H(167)-C(164)-C(159)	109.239
H(166)-C(164)-H(165)	109.77
H(166)-C(164)-C(159)	109.263

H(165)-C(164)-C(159)	109.118
H(193)-C(192)-C(194)	120.063
H(193)-C(192)-C(190)	119.946
C(194)-C(192)-C(190)	119.991
H(191)-C(190)-C(192)	120.038
H(191)-C(190)-C(188)	119.952
C(192)-C(190)-C(188)	120.01
H(189)-C(188)-C(190)	120.055
H(189)-C(188)-N(187)	119.954
C(190)-C(188)-N(187)	119.992
H(195)-C(194)-C(196)	119.915
H(195)-C(194)-C(192)	120.074
C(196)-C(194)-C(192)	120.011
C(196)-N(187)-C(188)	119.998
C(194)-C(196)-N(187)	119.998
C(194)-C(196)-C(146)	133.376
N(187)-C(196)-C(146)	106.489
H(148)-C(146)-H(147)	105.868
H(148)-C(146)-C(196)	105.801
H(148)-C(146)-N(175)	105.941
H(147)-C(146)-C(196)	106.04
H(147)-C(146)-N(175)	106.161
C(196)-C(146)-N(175)	125.623
H(223)-C(220)-H(222)	109.356
H(223)-C(220)-H(221)	109.412
H(223)-C(220)-C(210)	109.482
H(222)-C(220)-H(221)	109.537
H(222)-C(220)-C(210)	109.439
H(221)-C(220)-C(210)	109.601
H(163)-C(160)-H(162)	109.143
H(163)-C(160)-H(161)	109.323
H(163)-C(160)-C(150)	109.051
H(162)-C(160)-H(161)	110
H(162)-C(160)-C(150)	109.658
H(161)-C(160)-C(150)	109.648
H(216)-C(214)-H(215)	109.019
H(216)-C(214)-C(217)	111.033
H(216)-C(214)-C(211)	111.016
H(215)-C(214)-C(217)	111.03
H(215)-C(214)-C(211)	111.125
C(217)-C(214)-C(211)	103.557
C(224)-C(219)-C(228)	101.39
C(224)-C(219)-C(217)	111.107
C(224)-C(219)-C(210)	113.414
C(228)-C(219)-C(217)	117.994
C(228)-C(219)-C(210)	116.024
C(217)-C(219)-C(210)	97.529
H(213)-C(211)-H(212)	108.711

H(213)-C(211)-C(214)	110.755
H(213)-C(211)-C(210)	110.737
H(212)-C(211)-C(214)	110.677
H(212)-C(211)-C(210)	110.689
C(214)-C(211)-C(210)	105.259
H(218)-C(217)-C(219)	110.872
H(218)-C(217)-N(236)	110.921
H(218)-C(217)-C(214)	110.995
C(219)-C(217)-N(236)	110.428
C(219)-C(217)-C(214)	102.879
N(236)-C(217)-C(214)	110.49
C(232)-N(236)-C(217)	117.965
C(232)-N(236)-C(209)	123.162
C(217)-N(236)-C(209)	118.801
C(211)-C(210)-C(219)	102.325
C(211)-C(210)-C(220)	113.378
C(211)-C(210)-N(235)	112.866
C(219)-C(210)-C(220)	112.967
C(219)-C(210)-N(235)	106.593
C(220)-C(210)-N(235)	108.482
C(210)-N(235)-C(209)	120.372
C(210)-N(235)-C(206)	121.496
C(209)-N(235)-C(206)	117.659
H(156)-C(154)-H(155)	109.165
H(156)-C(154)-C(157)	110.576
H(156)-C(154)-C(151)	110.648
H(155)-C(154)-C(157)	110.893
H(155)-C(154)-C(151)	110.977
C(157)-C(154)-C(151)	104.53
C(164)-C(159)-C(168)	104.934
C(164)-C(159)-C(157)	109.815
C(164)-C(159)-C(150)	111.328
C(168)-C(159)-C(157)	122.806
C(168)-C(159)-C(150)	105.526
C(157)-C(159)-C(150)	102.267
H(153)-C(151)-H(152)	108.566
H(153)-C(151)-C(154)	110.36
H(153)-C(151)-C(150)	110.139
H(152)-C(151)-C(154)	110.288
H(152)-C(151)-C(150)	110.318
C(154)-C(151)-C(150)	107.171
H(158)-C(157)-C(159)	112.751
H(158)-C(157)-N(176)	112.671
H(158)-C(157)-C(154)	112.454
C(159)-C(157)-N(176)	107.588
C(159)-C(157)-C(154)	99.472
N(176)-C(157)-C(154)	111.089
C(172)-N(176)-C(157)	96.297

C(172)-N(176)-C(149)	143.757
C(157)-N(176)-C(149)	119.844
C(159)-C(150)-C(151)	99.864
C(159)-C(150)-C(160)	114.965
C(159)-C(150)-N(175)	107.837
C(151)-C(150)-C(160)	113.903
C(151)-C(150)-N(175)	108.423
C(160)-C(150)-N(175)	111.105
C(150)-N(175)-C(149)	119.544
C(150)-N(175)-C(146)	127.31
C(149)-N(175)-C(146)	113.01
Au(303)-C(209)-N(236)	117.345
Au(303)-C(209)-N(235)	122.831
N(236)-C(209)-N(235)	119.341
Au(303)-C(149)-N(176)	115.911
Au(303)-C(149)-N(175)	121.591
N(176)-C(149)-N(175)	122.002
C(260)-Au(303)-C(209)	3.618
C(260)-Au(303)-C(149)	177.968
C(260)-Au(303)-C(108)	175.735
C(209)-Au(303)-C(149)	176.001
C(209)-Au(303)-C(108)	172.134
C(149)-Au(303)-C(108)	5.094
H(145)-C(144)-C(142)	120.065
H(145)-C(144)-N(136)	119.97
C(142)-C(144)-N(136)	119.965
H(143)-C(142)-C(144)	119.948
H(143)-C(142)-C(140)	120.038
C(144)-C(142)-C(140)	120.013
H(141)-C(140)-C(142)	120.078
H(141)-C(140)-C(138)	119.865
C(142)-C(140)-C(138)	120.057
H(139)-C(138)-C(140)	120.118
H(139)-C(138)-C(137)	119.891
C(140)-C(138)-C(137)	119.991
C(144)-N(136)-C(137)	120.009
C(138)-C(137)-N(136)	119.964
C(138)-C(137)-C(131)	117.809
N(136)-C(137)-C(131)	122.226
H(133)-C(131)-H(132)	107.742
H(133)-C(131)-C(137)	108.985
H(133)-C(131)-N(135)	108.823
H(132)-C(131)-C(137)	108.877
H(132)-C(131)-N(135)	108.89
C(137)-C(131)-N(135)	113.376
H(130)-C(127)-H(129)	109.405
H(130)-C(127)-H(128)	109.51
H(130)-C(127)-C(118)	109.525

H(129)-C(127)-H(128)	109.477
H(129)-C(127)-C(118)	109.406
H(128)-C(127)-C(118)	109.504
H(126)-C(123)-H(125)	109.467
H(126)-C(123)-H(124)	109.565
H(126)-C(123)-C(118)	109.415
H(125)-C(123)-H(124)	109.412
H(125)-C(123)-C(118)	109.474
H(124)-C(123)-C(118)	109.495
H(122)-C(119)-H(121)	109.516
H(122)-C(119)-H(120)	109.399
H(122)-C(119)-C(109)	109.437
H(121)-C(119)-H(120)	109.544
H(121)-C(119)-C(109)	109.51
H(120)-C(119)-C(109)	109.42
C(131)-N(135)-C(116)	107.447
C(131)-N(135)-C(108)	128.51
C(116)-N(135)-C(108)	123.916
H(115)-C(113)-H(114)	108.655
H(115)-C(113)-C(116)	110.338
H(115)-C(113)-C(110)	110.394
H(114)-C(113)-C(116)	110.445
H(114)-C(113)-C(110)	110.407
C(116)-C(113)-C(110)	106.6
H(117)-C(116)-C(118)	113.246
H(117)-C(116)-N(135)	113.341
H(117)-C(116)-C(113)	113.346
C(118)-C(116)-N(135)	106.135
C(118)-C(116)-C(113)	101.713
N(135)-C(116)-C(113)	108.177
C(123)-C(118)-C(127)	109.841
C(123)-C(118)-C(116)	108.235
C(123)-C(118)-C(109)	111.353
C(127)-C(118)-C(116)	113.61
C(127)-C(118)-C(109)	113.401
C(116)-C(118)-C(109)	100.003
H(112)-C(110)-H(111)	108.98
H(112)-C(110)-C(113)	111.075
H(112)-C(110)-C(109)	111.093
H(111)-C(110)-C(113)	111.092
H(111)-C(110)-C(109)	111.154
C(113)-C(110)-C(109)	103.385
Au(303)-C(108)-N(134)	123.93
Au(303)-C(108)-N(135)	118.444
N(134)-C(108)-N(135)	117.478
C(118)-C(109)-C(110)	104.673
C(118)-C(109)-C(119)	114.446
C(118)-C(109)-N(134)	106.617

C(110)-C(109)-C(119)	110.641
C(110)-C(109)-N(134)	107.232
C(119)-C(109)-N(134)	112.673
C(109)-N(134)-C(108)	120.92
C(109)-N(134)-C(105)	124.616
C(108)-N(134)-C(105)	113.967
H(107)-C(105)-H(106)	107.632
H(107)-C(105)-N(134)	108.624
H(107)-C(105)-C(104)	108.64
H(106)-C(105)-N(134)	108.64
H(106)-C(105)-C(104)	108.627
N(134)-C(105)-C(104)	114.472
H(103)-C(102)-C(104)	119.953
H(103)-C(102)-C(100)	119.998
C(104)-C(102)-C(100)	120.049
H(101)-C(100)-C(102)	120.003
H(101)-C(100)-C(98)	119.984
C(102)-C(100)-C(98)	120.012
H(99)-C(98)-C(100)	120.004
H(99)-C(98)-C(96)	119.959
C(100)-C(98)-C(96)	120.037
H(97)-C(96)-C(98)	120.113
H(97)-C(96)-N(95)	119.919
C(98)-C(96)-N(95)	119.967
C(104)-N(95)-C(96)	119.988
C(105)-C(104)-C(102)	127.955
C(105)-C(104)-N(95)	112.098
C(102)-C(104)-N(95)	119.946
H(94)-C(93)-N(292)	118.827
H(94)-C(93)-C(91)	118.697
N(292)-C(93)-C(91)	122.477
H(92)-C(91)-C(93)	120.626
H(92)-C(91)-C(89)	120.571
C(93)-C(91)-C(89)	118.803
H(90)-C(89)-C(91)	120.903
H(90)-C(89)-C(87)	120.935
C(91)-C(89)-C(87)	118.162
C(93)-N(292)-C(86)	118.287
H(88)-C(87)-C(89)	120.314
H(88)-C(87)-C(86)	120.48
C(89)-C(87)-C(86)	119.206
C(87)-C(86)-N(292)	122.994
C(87)-C(86)-C(83)	121.833
N(292)-C(86)-C(83)	115.153
H(85)-C(83)-H(84)	107.866
H(85)-C(83)-C(86)	109.377
H(85)-C(83)-N(291)	109.4
H(84)-C(83)-C(86)	109.373

H(84)-C(83)-N(291)	109.462
C(86)-C(83)-N(291)	111.296
H(82)-C(79)-H(81)	109.406
H(82)-C(79)-H(80)	109.389
H(82)-C(79)-C(70)	109.503
H(81)-C(79)-H(80)	109.59
H(81)-C(79)-C(70)	109.439
H(80)-C(79)-C(70)	109.501
H(78)-C(75)-H(77)	109.566
H(78)-C(75)-H(76)	109.538
H(78)-C(75)-C(70)	109.444
H(77)-C(75)-H(76)	109.561
H(77)-C(75)-C(70)	109.339
H(76)-C(75)-C(70)	109.378
H(53)-C(52)-C(54)	119.057
H(53)-C(52)-C(50)	118.987
C(54)-C(52)-C(50)	121.955
H(51)-C(50)-C(52)	121.78
H(51)-C(50)-C(48)	121.698
C(52)-C(50)-C(48)	116.522
H(49)-C(48)-N(289)	117.186
H(49)-C(48)-C(50)	117.243
N(289)-C(48)-C(50)	125.57
C(56)-N(289)-C(48)	117.145
H(55)-C(54)-C(56)	122.542
H(55)-C(54)-C(52)	122.444
C(56)-C(54)-C(52)	115.014
C(57)-C(56)-N(289)	117.209
C(57)-C(56)-C(54)	118.914
N(289)-C(56)-C(54)	123.759
H(59)-C(57)-H(58)	107.472
H(59)-C(57)-N(290)	108.371
H(59)-C(57)-C(56)	108.543
H(58)-C(57)-N(290)	108.293
H(58)-C(57)-C(56)	108.421
N(290)-C(57)-C(56)	115.471
H(74)-C(71)-H(73)	109.547
H(74)-C(71)-H(72)	109.579
H(74)-C(71)-C(61)	109.353
H(73)-C(71)-H(72)	109.394
H(73)-C(71)-C(61)	109.529
H(72)-C(71)-C(61)	109.426
H(67)-C(65)-H(66)	108.816
H(67)-C(65)-C(68)	110.844
H(67)-C(65)-C(62)	110.687
H(66)-C(65)-C(68)	110.702
H(66)-C(65)-C(62)	110.646
C(68)-C(65)-C(62)	105.126

C(79)-C(70)-C(75)	108.714
C(79)-C(70)-C(68)	108.835
C(79)-C(70)-C(61)	111.236
C(75)-C(70)-C(68)	114.537
C(75)-C(70)-C(61)	114.316
C(68)-C(70)-C(61)	98.873
H(64)-C(62)-H(63)	108.792
H(64)-C(62)-C(65)	110.729
H(64)-C(62)-C(61)	110.618
H(63)-C(62)-C(65)	110.664
H(63)-C(62)-C(61)	110.756
C(65)-C(62)-C(61)	105.266
H(69)-C(68)-C(70)	111.52
H(69)-C(68)-N(291)	111.514
H(69)-C(68)-C(65)	111.543
C(70)-C(68)-N(291)	107.724
C(70)-C(68)-C(65)	104.367
N(291)-C(68)-C(65)	109.877
C(83)-N(291)-C(68)	117.666
C(83)-N(291)-C(60)	120.897
C(68)-N(291)-C(60)	120.994
C(70)-C(61)-C(62)	103.057
C(70)-C(61)-N(290)	105.798
C(70)-C(61)-C(71)	114.727
C(62)-C(61)-N(290)	106.067
C(62)-C(61)-C(71)	114.451
N(290)-C(61)-C(71)	111.839
C(61)-N(290)-C(60)	122.214
C(61)-N(290)-C(57)	118.426
C(60)-N(290)-C(57)	119.17
Au(302)-C(60)-N(290)	120.963
Au(302)-C(60)-N(291)	121.209
N(290)-C(60)-N(291)	117.824
C(60)-Au(302)-C(13)	179.195
H(47)-C(46)-N(288)	117.964
H(47)-C(46)-C(44)	117.952
N(288)-C(46)-C(44)	124.085
H(45)-C(44)-C(46)	120.367
H(45)-C(44)-C(42)	120.162
C(46)-C(44)-C(42)	119.471
H(43)-C(42)-C(44)	120.664
H(43)-C(42)-C(40)	120.72
C(44)-C(42)-C(40)	118.615
C(46)-N(288)-C(39)	116.258
H(41)-C(40)-C(42)	120.94
H(41)-C(40)-C(39)	120.895
C(42)-C(40)-C(39)	118.165
C(40)-C(39)-N(288)	123.399

C(40)-C(39)-C(36)	119.863
N(288)-C(39)-C(36)	116.692
H(38)-C(36)-H(37)	107.546
H(38)-C(36)-C(39)	108.321
H(38)-C(36)-N(287)	108.43
H(37)-C(36)-C(39)	108.399
H(37)-C(36)-N(287)	108.441
C(39)-C(36)-N(287)	115.442
H(35)-C(32)-H(34)	109.498
H(35)-C(32)-H(33)	109.409
H(35)-C(32)-C(23)	109.549
H(34)-C(32)-H(33)	109.362
H(34)-C(32)-C(23)	109.539
H(33)-C(32)-C(23)	109.471
H(31)-C(28)-H(30)	109.454
H(31)-C(28)-H(29)	109.474
H(31)-C(28)-C(23)	109.538
H(30)-C(28)-H(29)	109.322
H(30)-C(28)-C(23)	109.497
H(29)-C(28)-C(23)	109.542
H(9)-C(8)-N(285)	121.841
H(9)-C(8)-C(6)	121.835
N(285)-C(8)-C(6)	116.323
H(7)-C(6)-C(8)	119.981
H(7)-C(6)-C(4)	119.971
C(8)-C(6)-C(4)	120.048
H(5)-C(4)-C(6)	118.569
H(5)-C(4)-C(2)	118.432
C(6)-C(4)-C(2)	122.999
C(8)-N(285)-C(1)	117.236
H(3)-C(2)-C(4)	120.699
H(3)-C(2)-C(1)	120.86
C(4)-C(2)-C(1)	118.441
C(10)-C(1)-N(285)	121.535
C(10)-C(1)-C(2)	114.072
N(285)-C(1)-C(2)	124.376
H(12)-C(10)-H(11)	107.943
H(12)-C(10)-N(286)	109.111
H(12)-C(10)-C(1)	109.32
H(11)-C(10)-N(286)	109.304
H(11)-C(10)-C(1)	109.297
N(286)-C(10)-C(1)	111.786
H(27)-C(24)-H(26)	109.493
H(27)-C(24)-H(25)	109.538
H(27)-C(24)-C(22)	109.453
H(26)-C(24)-H(25)	109.451
H(26)-C(24)-C(22)	109.416
H(25)-C(24)-C(22)	109.477

Au(302)-C(13)-N(286)	120.581
Au(302)-C(13)-N(287)	120.548
N(286)-C(13)-N(287)	118.871
C(36)-N(287)-C(22)	117.566
C(36)-N(287)-C(13)	119.908
C(22)-N(287)-C(13)	122.356
H(21)-C(19)-H(20)	108.769
H(21)-C(19)-C(22)	110.82
H(21)-C(19)-C(16)	111.048
H(20)-C(19)-C(22)	110.698
H(20)-C(19)-C(16)	111.003
C(22)-C(19)-C(16)	104.477
C(14)-N(286)-C(13)	120.17
C(14)-N(286)-C(10)	117.632
C(13)-N(286)-C(10)	122.198
C(23)-C(22)-N(287)	106.113
C(23)-C(22)-C(24)	113.907
C(23)-C(22)-C(19)	103.327
N(287)-C(22)-C(24)	112.409
N(287)-C(22)-C(19)	106.633
C(24)-C(22)-C(19)	113.667
C(32)-C(23)-C(28)	108.856
C(32)-C(23)-C(22)	111.348
C(32)-C(23)-C(14)	108.469
C(28)-C(23)-C(22)	115.146
C(28)-C(23)-C(14)	114.099
C(22)-C(23)-C(14)	98.5
H(18)-C(16)-H(17)	108.723
H(18)-C(16)-C(19)	110.75
H(18)-C(16)-C(14)	110.67
H(17)-C(16)-C(19)	110.651
H(17)-C(16)-C(14)	110.671
C(19)-C(16)-C(14)	105.365
H(15)-C(14)-C(23)	111.786
H(15)-C(14)-C(16)	111.647
H(15)-C(14)-N(286)	111.599
C(23)-C(14)-C(16)	104.764
C(23)-C(14)-N(286)	107.024
C(16)-C(14)-N(286)	109.706